Report No. FHWA-RD-78-69

STUDENT WORKBOOK – FRACTURE MECHANICS FOR BRIDGE DESIGN

July 1977
Final Report

Prepared for
FEDERAL HIGHWAY ADMINISTRATION
Offices of Research & Development
Washington, D. C. 20590

FOREWORD

This report, FHWA-RD-78-69, prepared under the general direction of Professor Richard Roberts, Lehigh University, Bethlehem, Pennsylvania is intended as a workbook to supplement the accompanying report FHWA-RD-78-68. Together they provide the highway bridge engineer with examples and applications of fracture mechanics criteria in order to develop an understanding and working knowledge of the subject.

Sufficient copies of the report are being distributed to provide a minimum of one copy to each Regional office, one copy to each Division office, and two copies to each State highway agency. Direct distribution is being made to the Division offices.

Charles F. Scheffey
Director, Office of Research
Federal Highway Administration

NOTICE

ACKNOWLEDGMENTS

The assistance and guidance of Mr. Charles McGogney and Mr. Jerar Nishanian of the Office of Research of the Federal Highway Administration is gratefully acknowledged. The able assistance of Ms. Jone Svirzofsky in the preparation of the manuscript is also noted.

Technical Report Documentation Page

1. Report No.	2. Government Accession No.	3. Recipient's Catalog No.
FHWA-RD-78-69		PB298186

4. Title and Subtitle	5. Report Date
Student Workbook - Fracture Mechanics for Bridge Design	July 1977
	6. Performing Organization Code
	8. Performing Organization Report No.

7. Author(s)
R. Roberts, J. M. Barsom, S. T. Rolfe, J. W. Fisher

9. Performing Organization Name and Address	10. Work Unit No. (TRAIS)
Coxe Lab., #32 Lehigh University Bethlehem, Pennsylvania 18015	FCP 35F2143
	11. Contract or Grant No. P.O. No. 5-3-0209
	13. Type of Report and Period Covered

12. Sponsoring Agency Name and Address	13. Type of Report and Period Covered
Department of Transportation Federal Highway Administration Washington, D.C. 20590	Final Report
	14. Sponsoring Agency Code S0872

15. Supplementary Notes

Federal Highway Administration Contract Manager: C. H. McGogney (HRS-11)

16. Abstract

This workbook is a companion to the volume Fracture Mechanics for Bridge Design which provides an introduction to the elements of fracture mechanics for bridge design. Fracture mechanics are introduced and used as the basis for understanding fatigue and fracture in bridge structures. Various applications are cited.

17. Key Words	18. Distribution Statement
Fracture, Fatigue, Bridges, Bridge Safety, Bridge Design, Bridge Failure	No restrictions. This document is available to the public through the National Technical Information Service, Springfield, Virginia 22161

19. Security Classif. (of this report)	20. Security Classif. (of this page)	21. No. of Pages	22. Price
Unclassified	Unclassified	241	PA13 / MF A01

Form DOT F 1700.7 (8-72)

PREFACE

This student workbook is a companion volume to the report entitled "Fracture Mechanics for Bridge Design." The purpose of the workbook is to provide the reader with a copy of the figures and tables used in the development of a basic understanding of Fracture Mechanics as applied to Bridge Design. These figures and their accompanying captions will greatly assist the reader in following the material presented in the accompanying volume. Furthermore, the workbook provides a convenient method for working problems and examples presented in the accompanying volume.

TABLE OF CONTENTS

FIGURES - SESSION 1

INTRODUCTION AND OVERVIEW OF

FRACTURE MECHANICS AS RELATED TO BRIDGE STRUCTURES

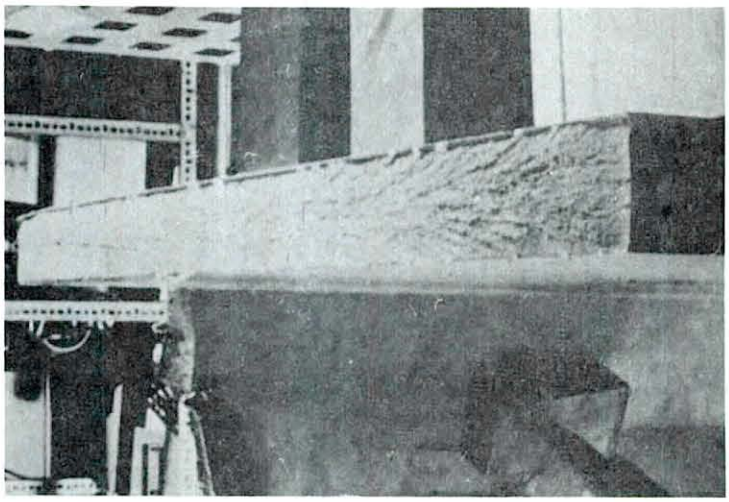

I-1. Brittle Fracture Surface

a) sudden type of failure
b) no warning
c) nil ductility

NOTES:

I-2. Pt. Pleasant Bridge after Brittle Fracture

NOTES:

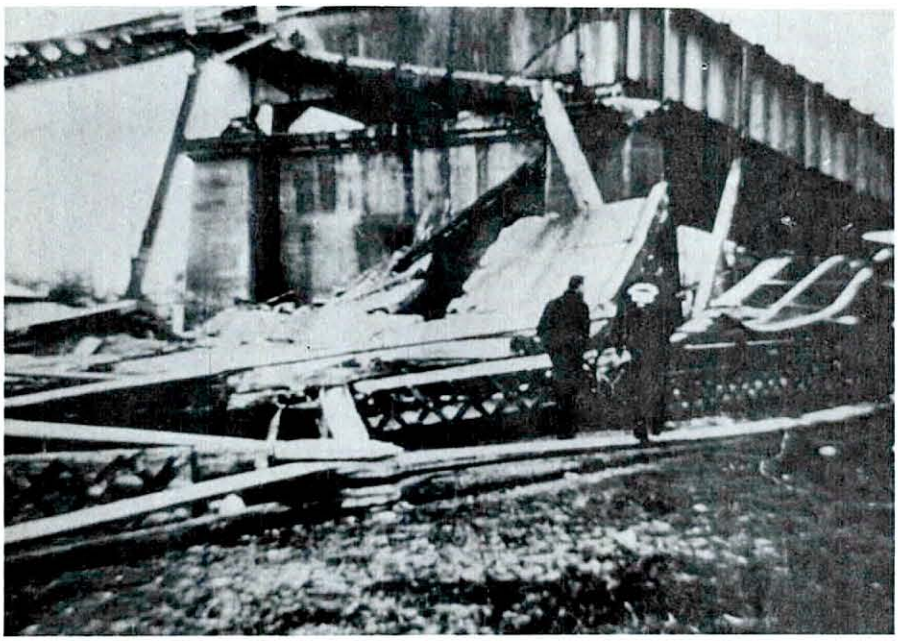

I-3. Closeup of Eyebar in Pt. Pleasant Bridge

NOTES:

I-4. Failed Eyebar

a) brittle behavior
b) ductile behavior
c) yielding and elastic core

NOTES:

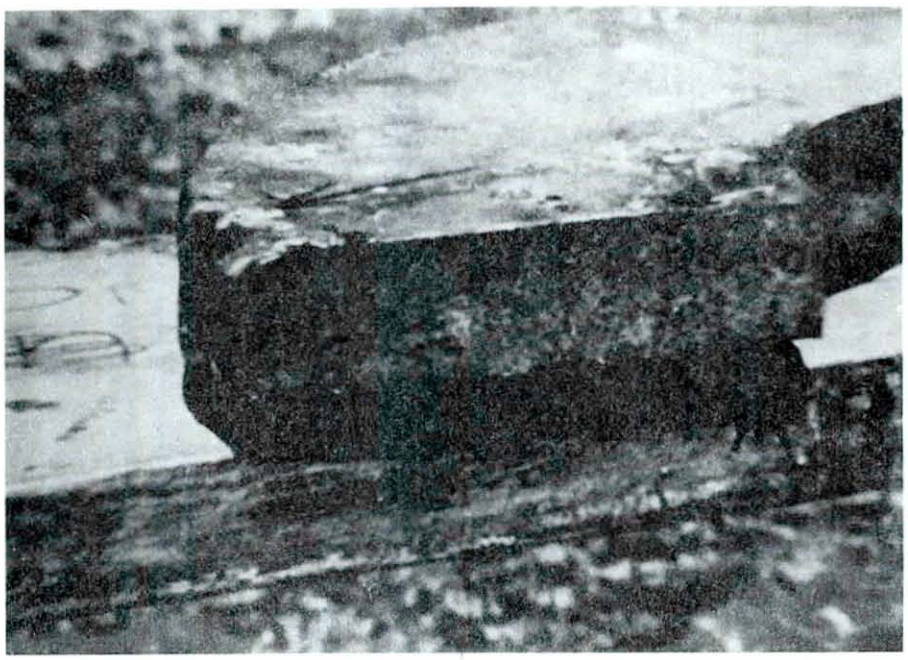

Figure 1-5. Fracture surface of Point Pleasant Bridge Eyebar

a) flat fracture
b) very small shear lips

NOTES:

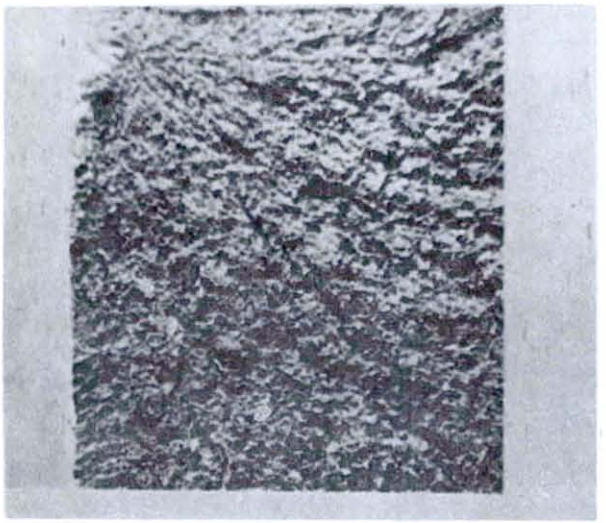

I-6. Critical crack size ∿ 1/8-inch

a) stress corrosion or corrosion fatigue
b) non-inspectable

NOTES:

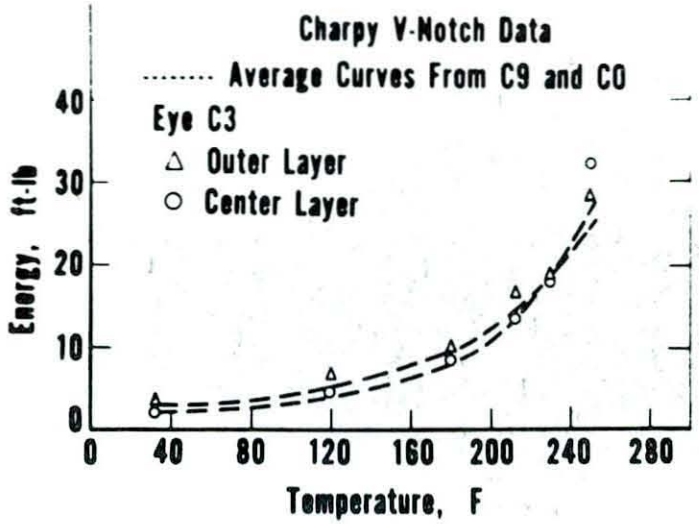

I-7. Very Low Notch Toughness

a) $K_{Ic} \sim 40$ ksi$\sqrt{in.}$ at +32°F

b) CVN ~ 2 ft lbs.

NOTES:

1943

I-8. Historical - World War II Ships

a) Major Problem

NOTES:

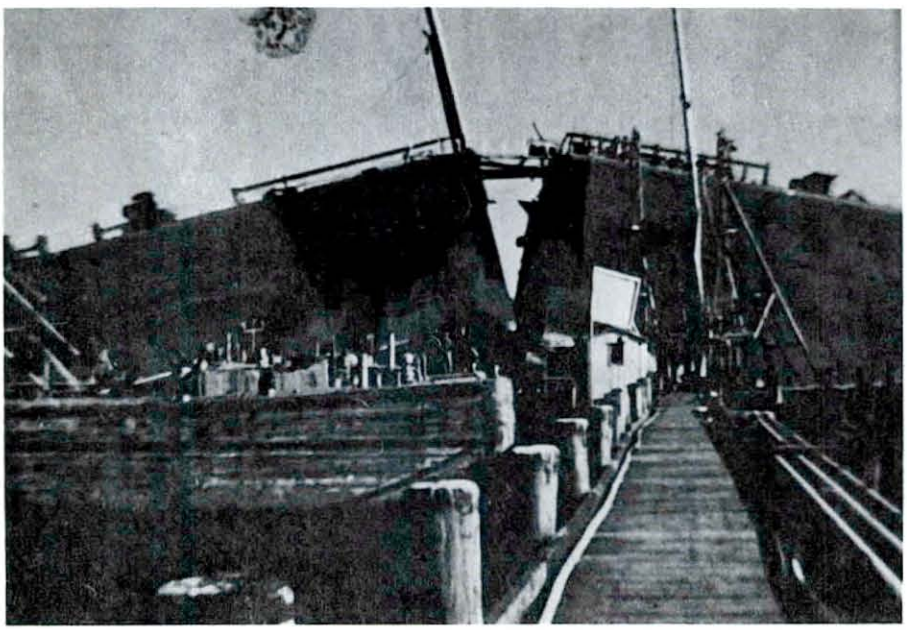

1-9. Recent 1972 Brittle Fracture

NOTES:

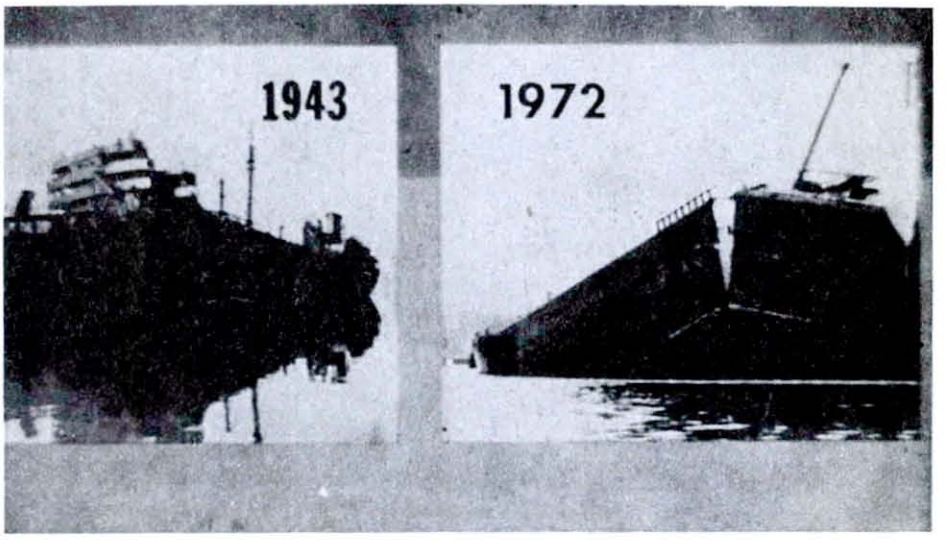

I-10. Comparison of 1943 and 1972 Failures
a) distinct differences in materials and loadings
b) resistance factors improved
c) for this failure, load factor very high

NOTES:

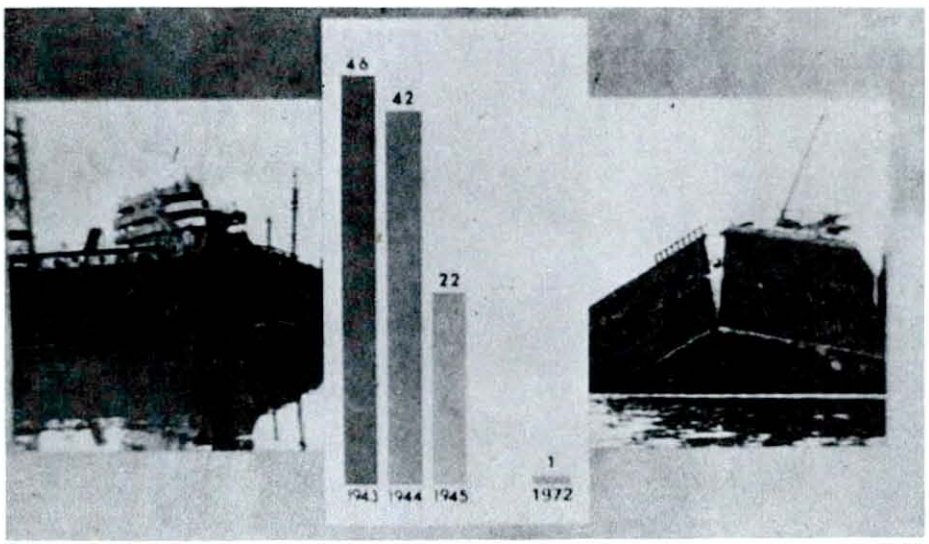

I-II. Significant reduction in number of failures but occasionally failures still do occur

a) 1967 - Pt. Pleasant Bridge
b) 1970 - Bryte Bend Bridge
c) 1971 - Fremont St. Bridge
d) 1972 - Ingram Barge
e) 1975 - Lafayette St. Bridge

NOTES:

MATERIAL TOUGHNESS

STRESS

TEMPERATURE

LOADING RATE

CONSTRAINT

REDUNDANCY

RESIDUAL STRESSES

PLATE THICKNESS

FLAWS

INSPECTION

STRESS CORROSION

1-12. Many Factors Affect Brittle Fracture

a) material toughness
b) stress
c) temperature
d) loading rate
e) restraint
f) redundancy
g) residual stresses
h) plate thickness
i) flaws
j) inspection
k) stress-corrosion crack growth
l) fatigue crack growth

NOTES:

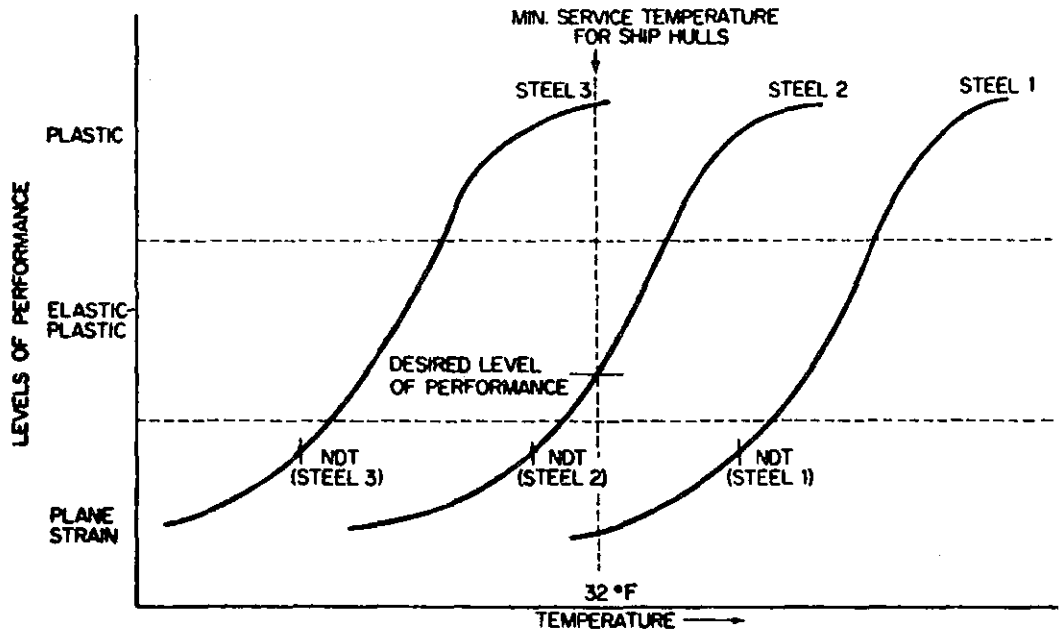

I-13. Basic Transition Temperature Approach

a) some level of toughness at service temp. (ft lb, L.E., or % shear)
b) impact loading only
c) small scale CVN specimens (or others)
d) no effect of thickness
e) NDT reference point

NOTES:

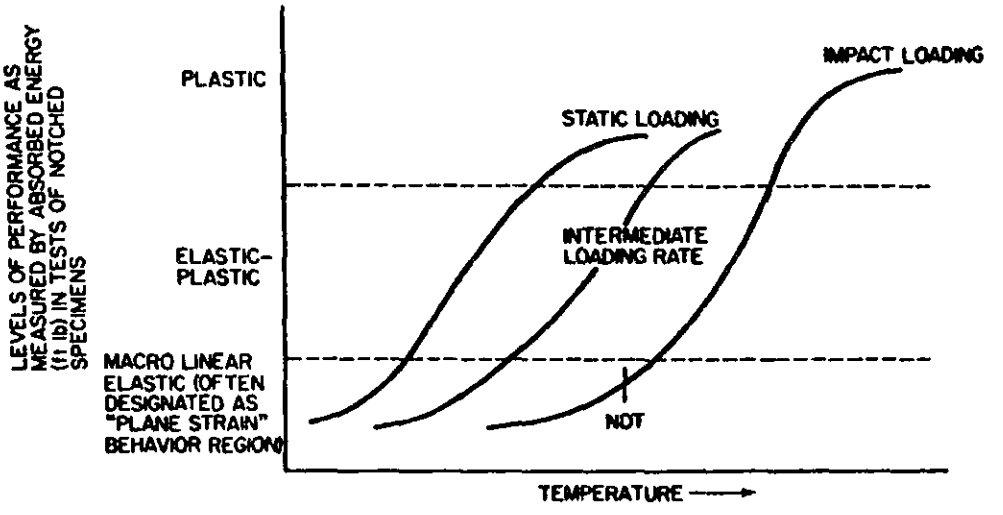

I-14. Effect of Loading Rate

a) dynamic
b) intermediate
c) slow

NOTES:

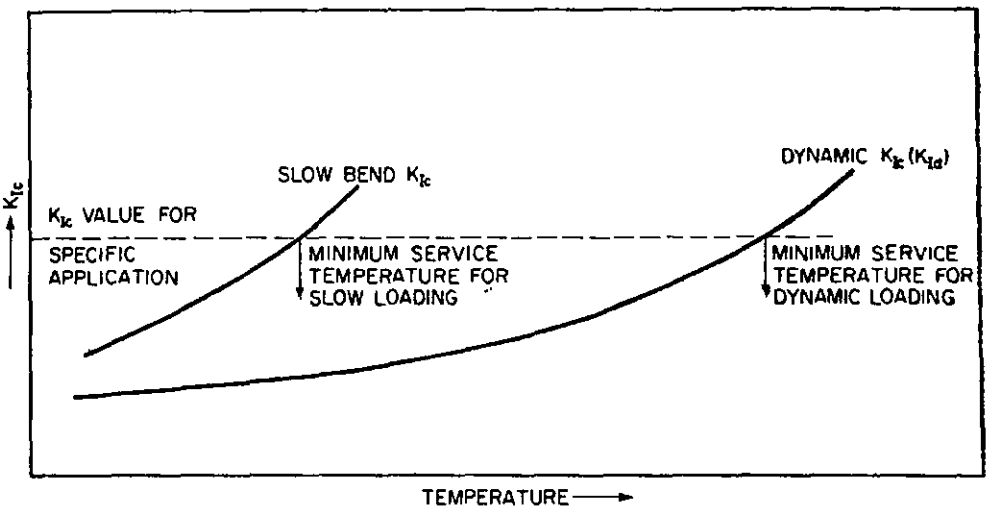

I-15. Design Significance of Loading Rate

NOTES:

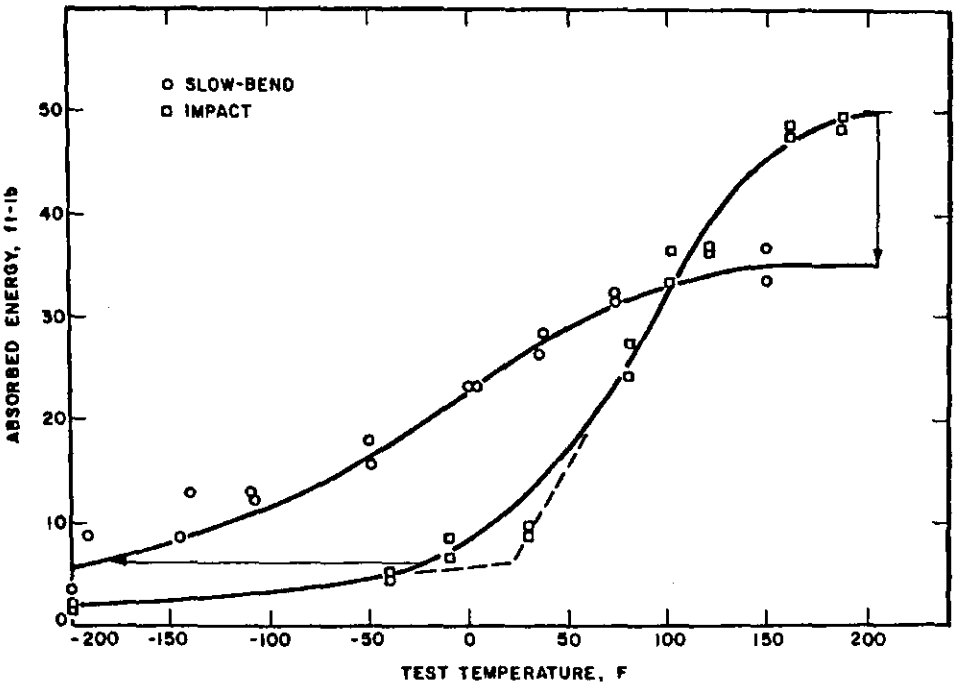

I-16. Example of CVN Shift for A36 Steel

NOTES:

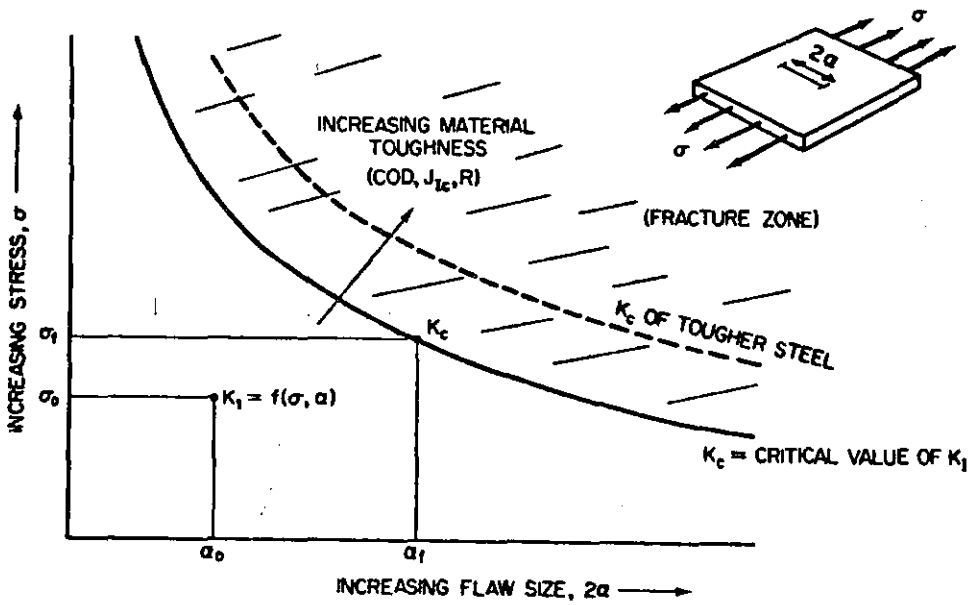

I-17. Fracture Mechanics Framework

a) stress or loading at service temperature and loading rate
b) material toughness at service temperature and loading rate
c) severity of discontinuity or flaw size (sub-critical crack growth)
d) brittle fracture is not just a material problem
e) fracture mechanics accounts for factors other than just material toughness

NOTES:

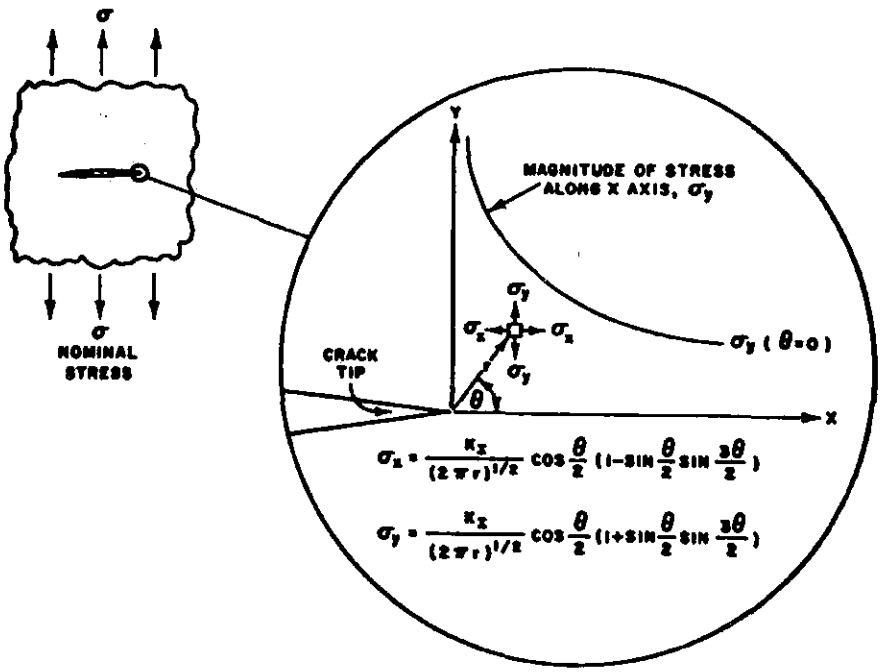

1-18. Stress intensity, K_I, ahead of sharp crack

a) K_I
b) comparison of plastic zone size to size of elastic stress field
c) specimen size requirements

NOTES:

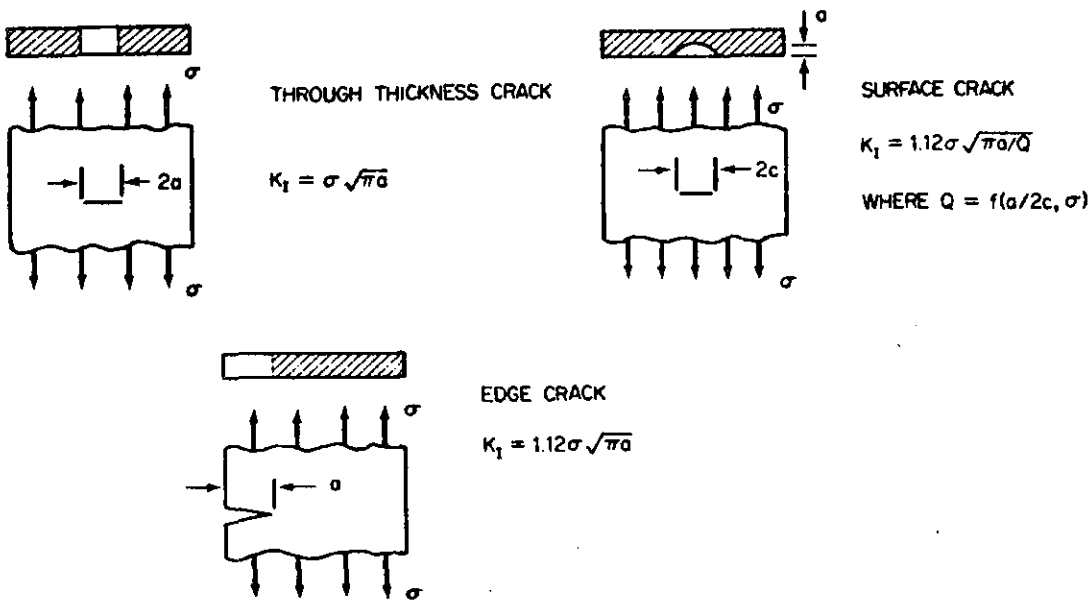

I-19. K_I Relations for Various Crack Geometries

a) Interaction between σ and a
b) K_I and K_{Ic}

NOTES:

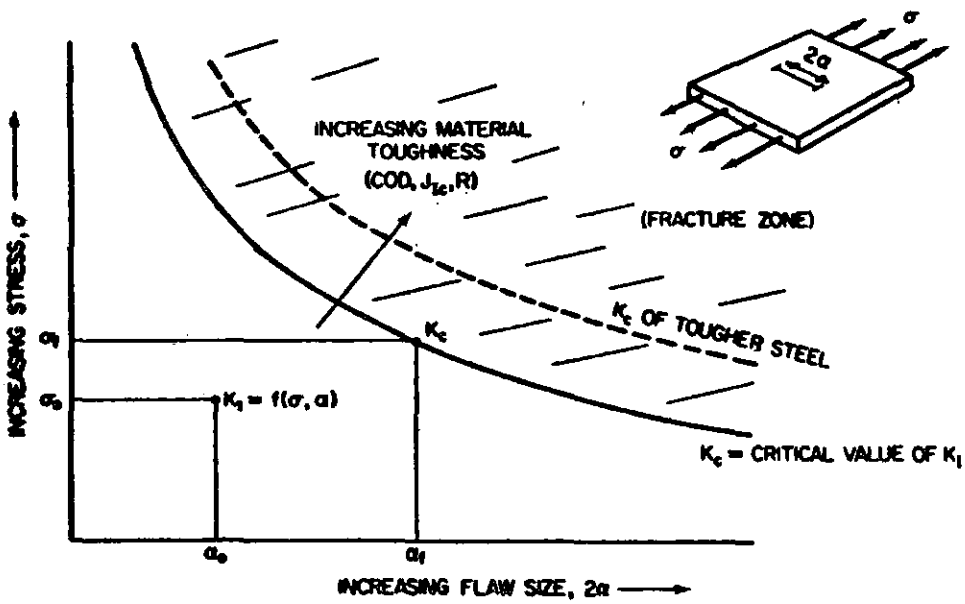

1-20. Interrelation Between K_I, K_{Ic}, σ , a

a) Effect of improved toughness
b) Effect of Lower stress
c) Effect of Improved fabrication

NOTES:

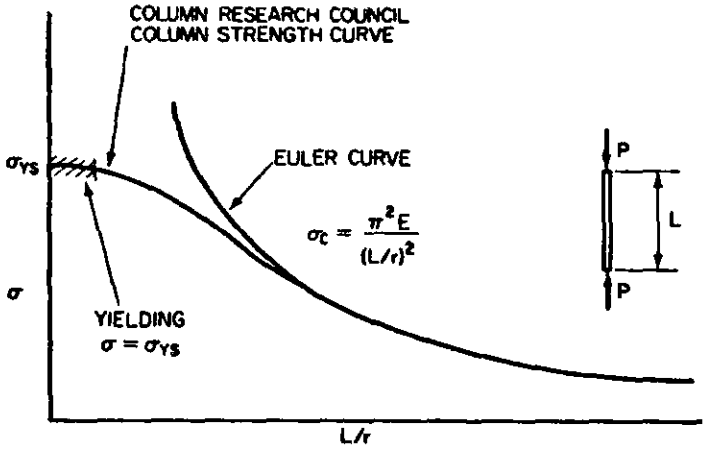

(a) COLUMN INSTABILITY

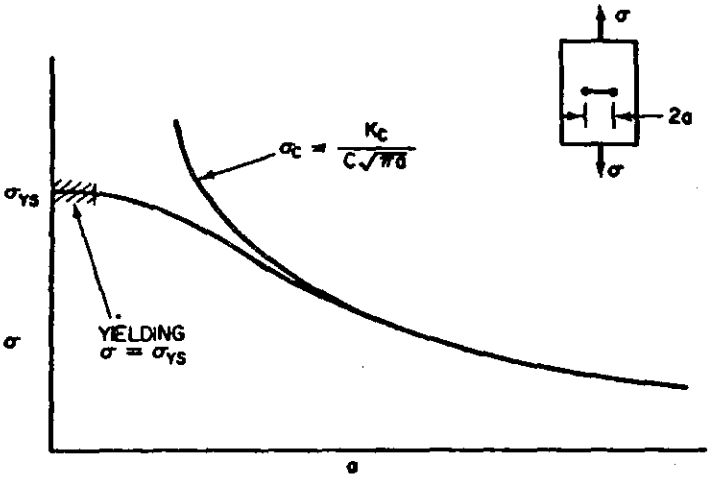

(b) CRACK INSTABILITY

I-21. Analogy with Euler Curve

a) Design to stay below Euler and K_{Ic} curves
b) Effect of yielding

NOTES:

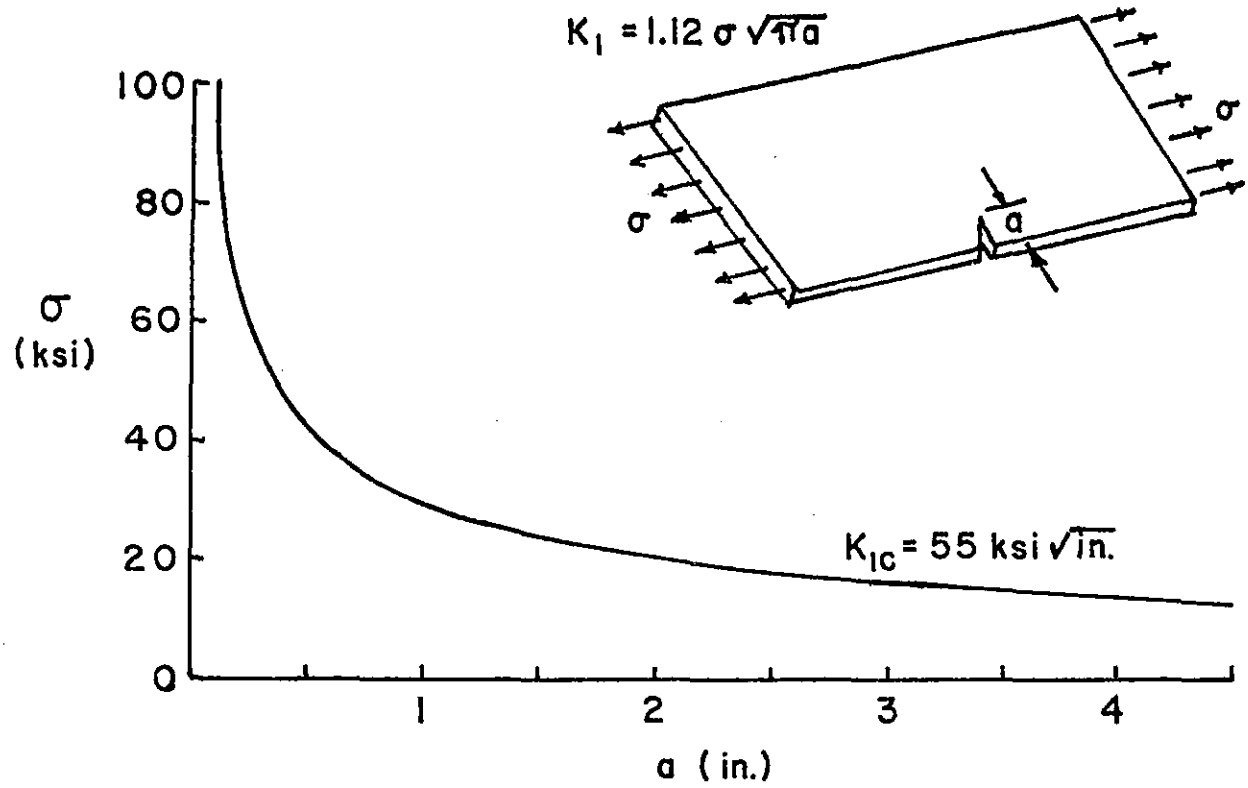

I-22. K_{Ic} Relation for Edge Crack

a) Comparison of "critical crack sizes at different stress levels

NOTES:

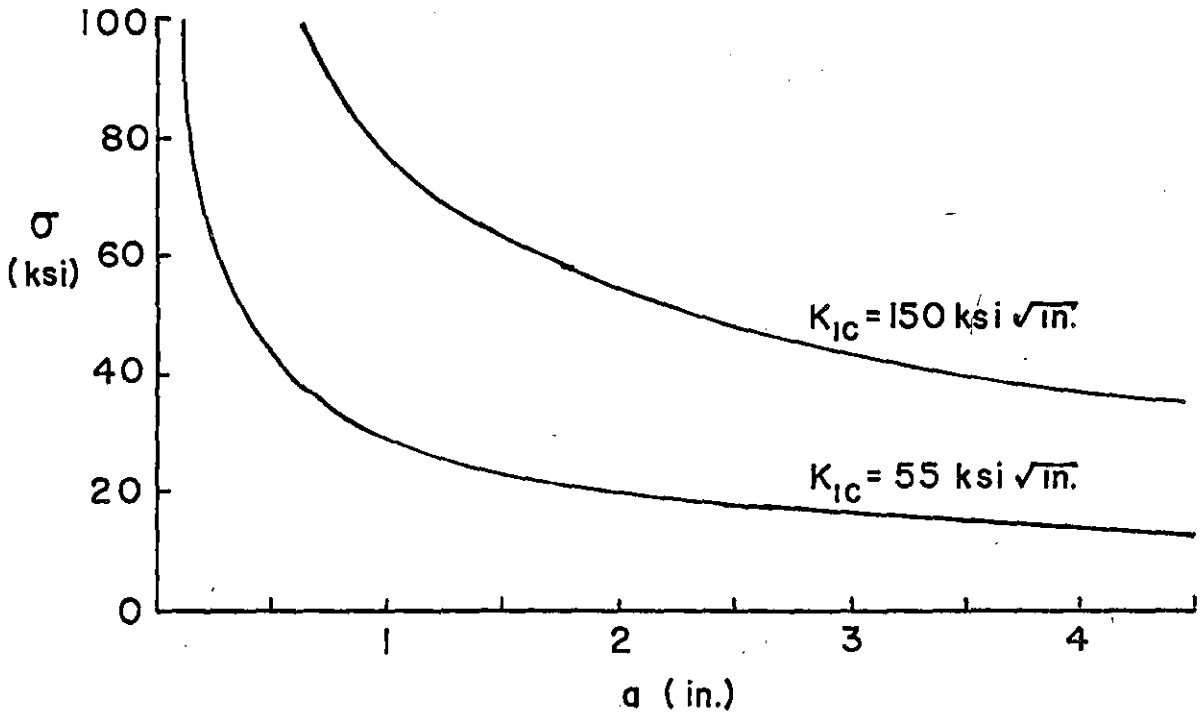

I-23. K_{Ic} = 55 and 150

a) Effect of Improved toughness on a_{cr}
b) At higher toughness levels, correlations are needed but approximations are meaningful
c) e.g. - $a_{cr} \sim .1$ or 1.0.

NOTES:

σ = APPLIED STRESS, KSI

a = CRACK LENGTH, INCHES

K_I = STRESS INTENSITY FACTOR AHEAD OF A SHARP CRACK, KSI$\sqrt{\text{INCH}}$

K_{Ic} = CRITICAL STRESS INTENSITY FACTOR, KSI$\sqrt{\text{INCH}}$, AT WHICH UNSTABLE CRACK GROWTH OCCURS

PLANE STRAIN = STATE-OF-STRESS UNDER MAXIMUM CONSTRAINT (THICK PLATES—$\sigma_z = \mu(\sigma_x + \sigma_y)$

PLANE STRESS = STATE-OF-STRESS UNDER MINIMUM CONSTRAINT (THIN PLATES—$\sigma_z = 0$)

I-24. Summary of Terms

NOTES:

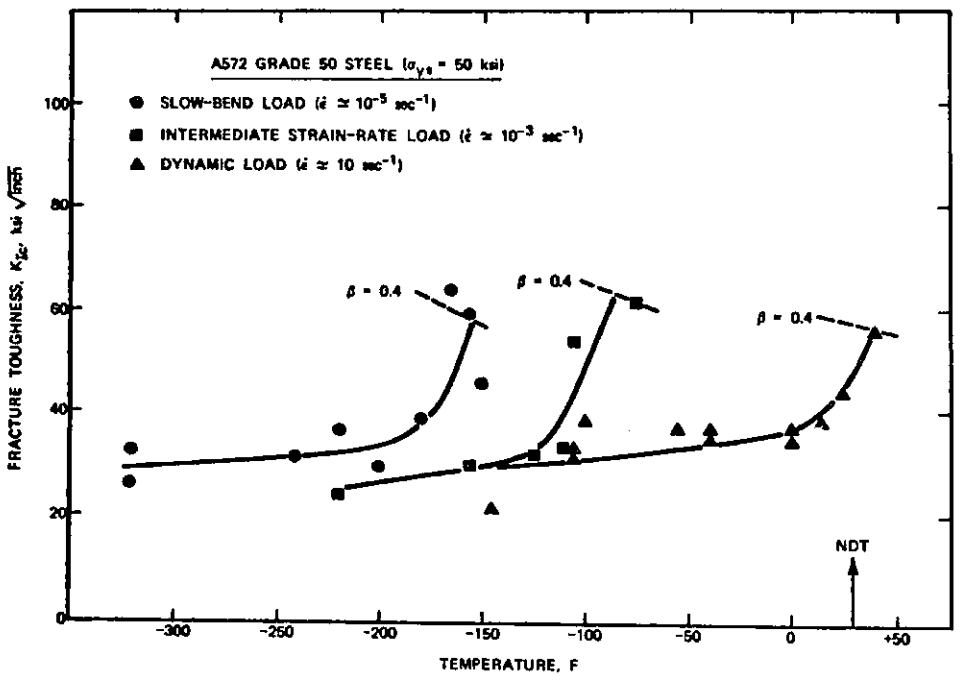

I-25. K_{Ic} is a function of Temperature and Loading Rate

a) similar to σ_y but effect is greater

NOTES:

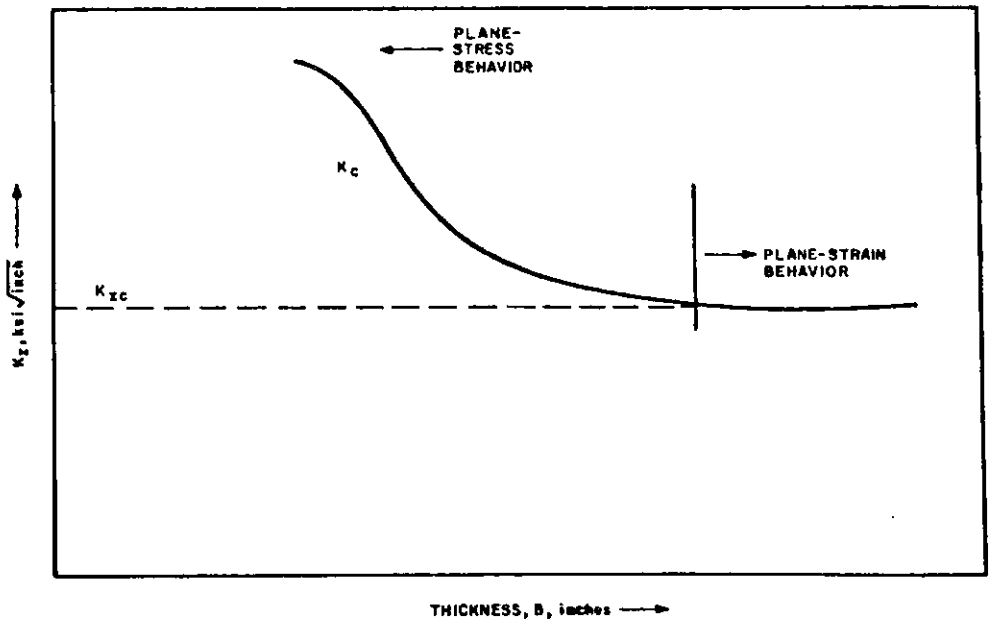

I-26. Critical K (K_c or K_{Ic}) is a function of thickness

a) plane stress
b) plane strain
c) thickness vs. constraint

NOTES:

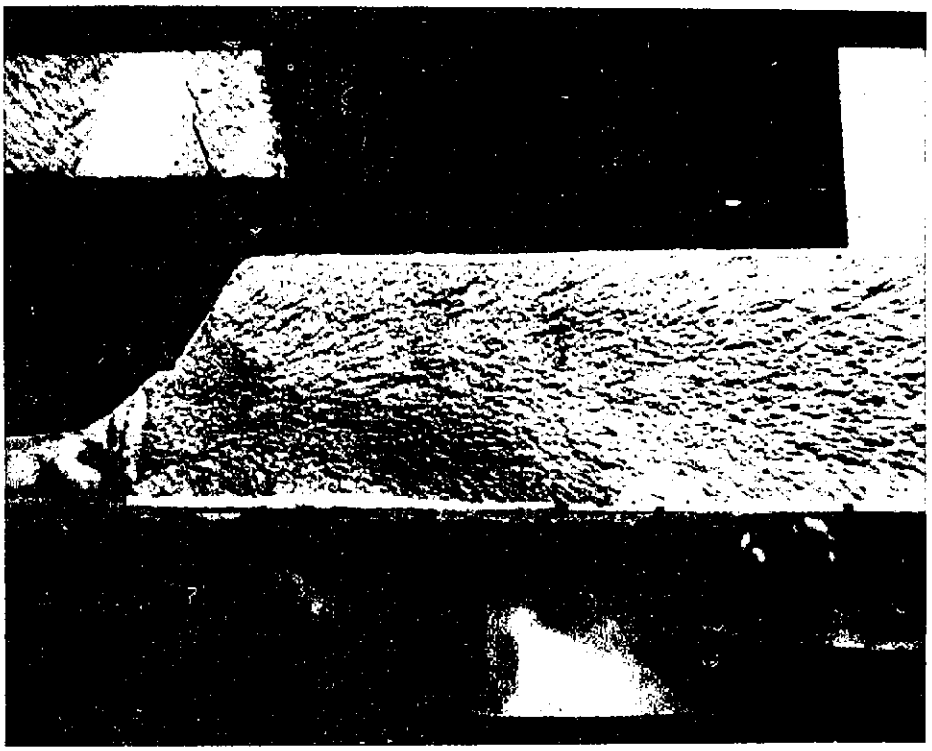

1-27. Actual Flaw Size compared with theoretical flaw size

NOTES:

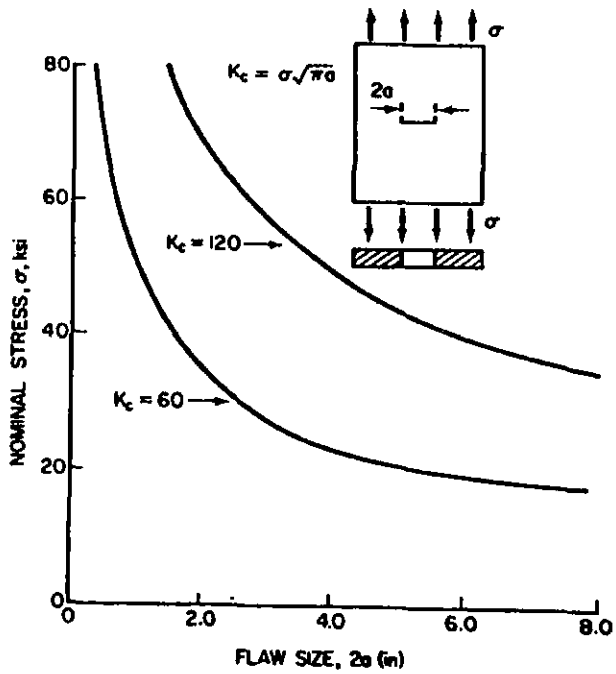

I-28. Design Use of K_{Ic}

a) $K_{Ic} = 60$
b) $K_{Ic} = 120$
c) for K_{Ic} values at service temperature and loading rate

NOTES:

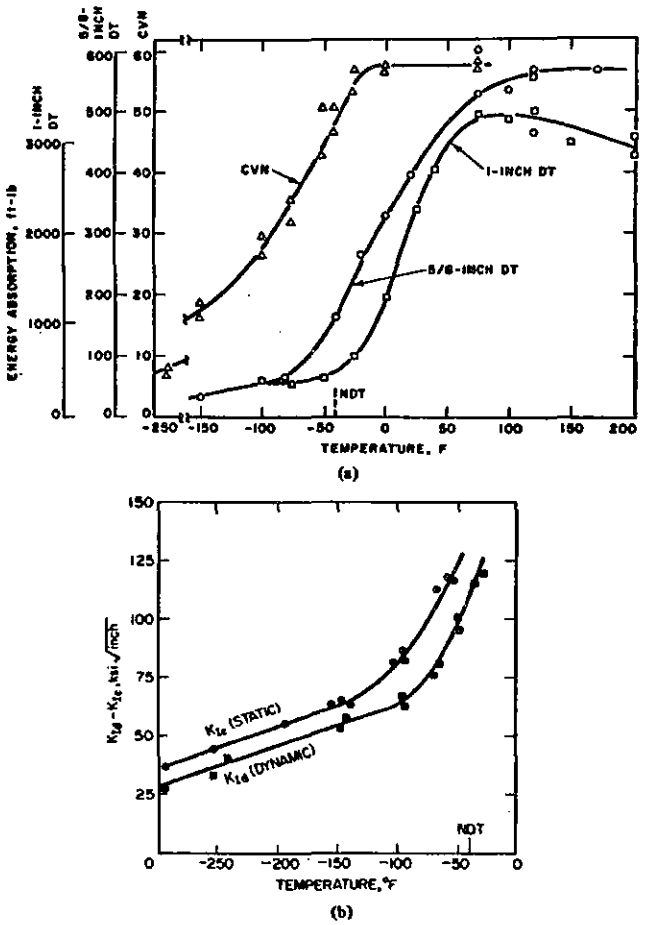

I-29. Temperature Effect on K_{Ic} and K_{Id} similar for Other Notch Toughness Tests

a) K_{Ic} and K_{Id}
b) CVN
c) DT (notch acuity and cold work)

NOTES:

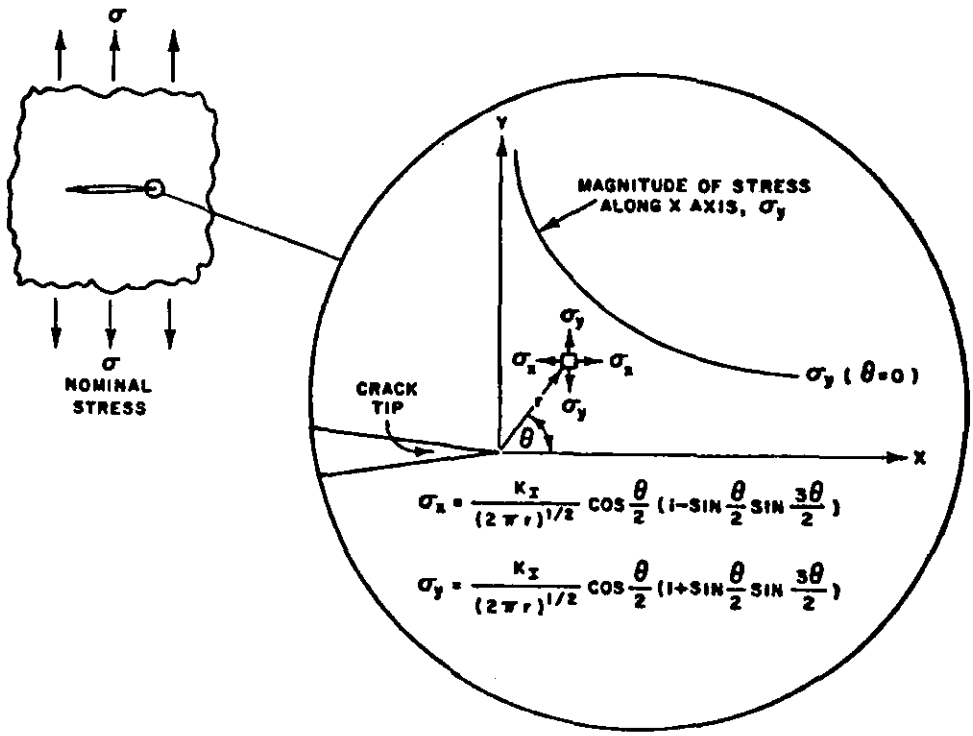

I-30. Stress-Intensity ahead of Crack

a) behavior for K_{Ic} as CVN and DT
b) advantages of K_{Ic} = stress, flaw size rather than energy
c) analysis valid for many geometries

NOTES:

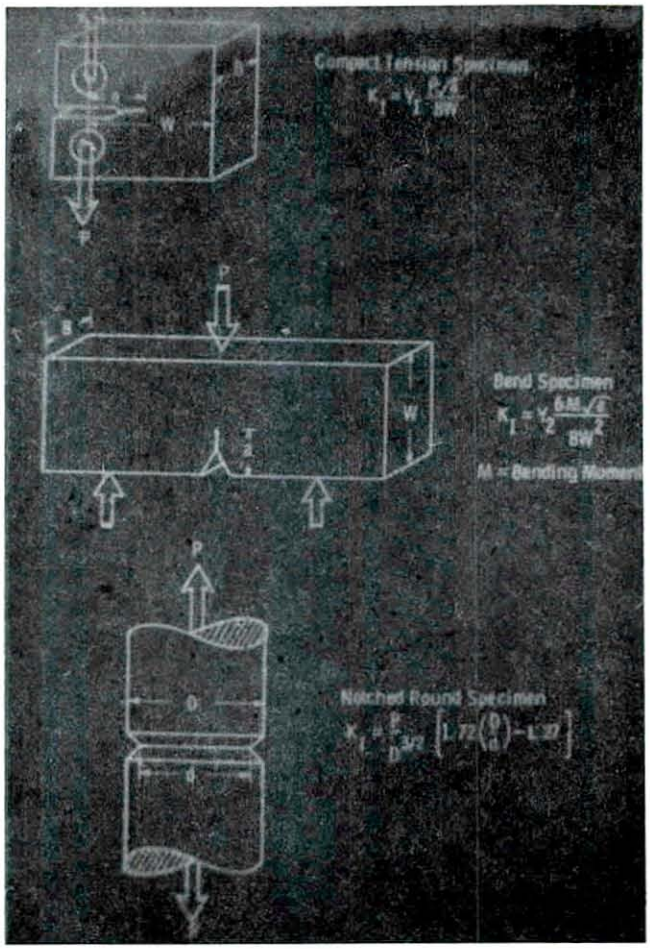

I-31. Various K_{Ic} Test Specimen

a) CTS
b) Bend
c) Notched Round
d) K_{Ic} Value can be used in design

NOTES:

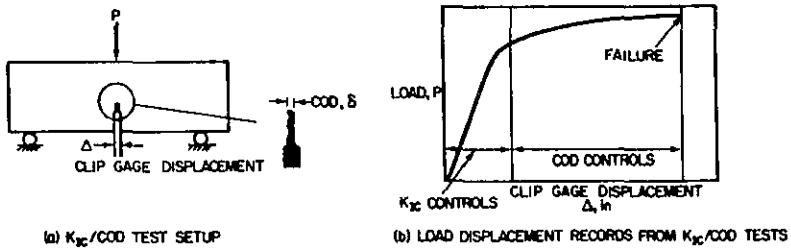

(a) K_{Ic}/COD TEST SETUP

(b) LOAD DISPLACEMENT RECORDS FROM K_{Ic}/COD TESTS

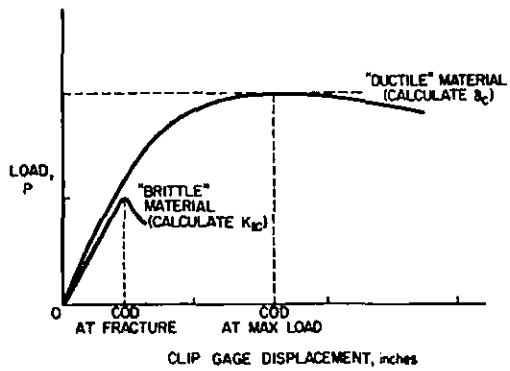

I-32. Slow-Bend Test Setup

a) K_{Ic} - elastic
c) COD - inelastic

NOTES:

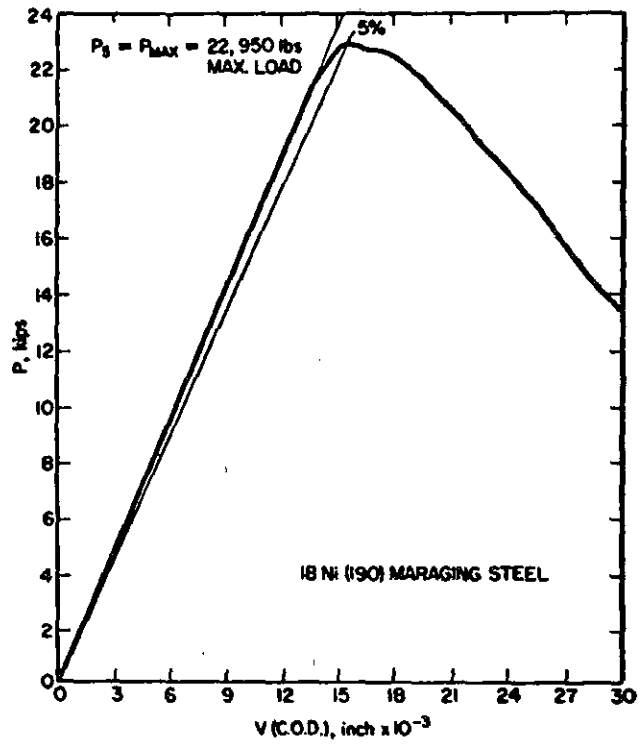

I-33. P-Δ Record for Elastic Behavior

a) Linear
b) Clear instability

NOTES:

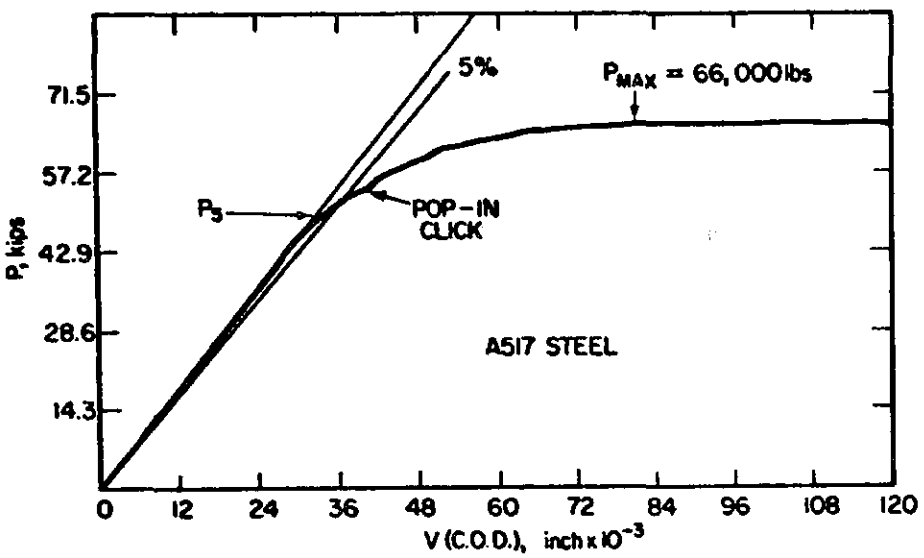

1-34. P-Δ Record for inelastic behavior

a) non-linear
b) ductile crack extension
c) K_I analysis invalid
d) typical of bridge steels at service temperatures and loading rates - fortunately

NOTES:

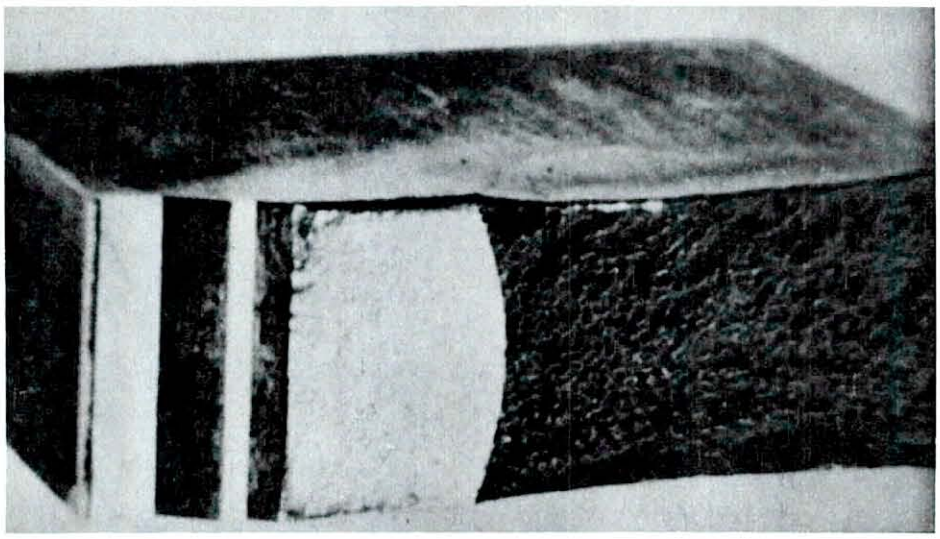

I-35. Fracture-surface of K_{Ic} Test Specimen

a) inelastic behavior
b) shear lips suppressed artifically
c) lateral contraction

NOTES:

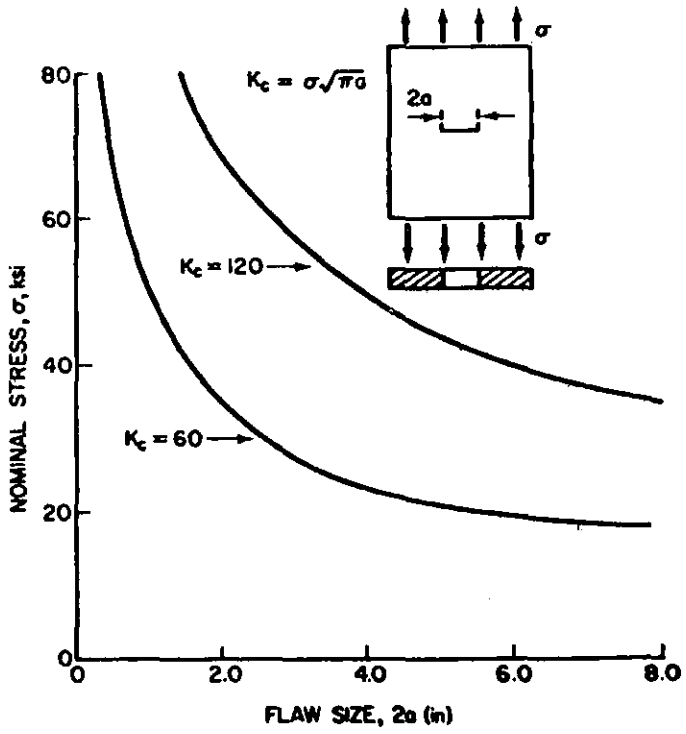

I-36. Design Use of K_{Ic} Values

a) exact
b) approximate
c) correlations

NOTES:

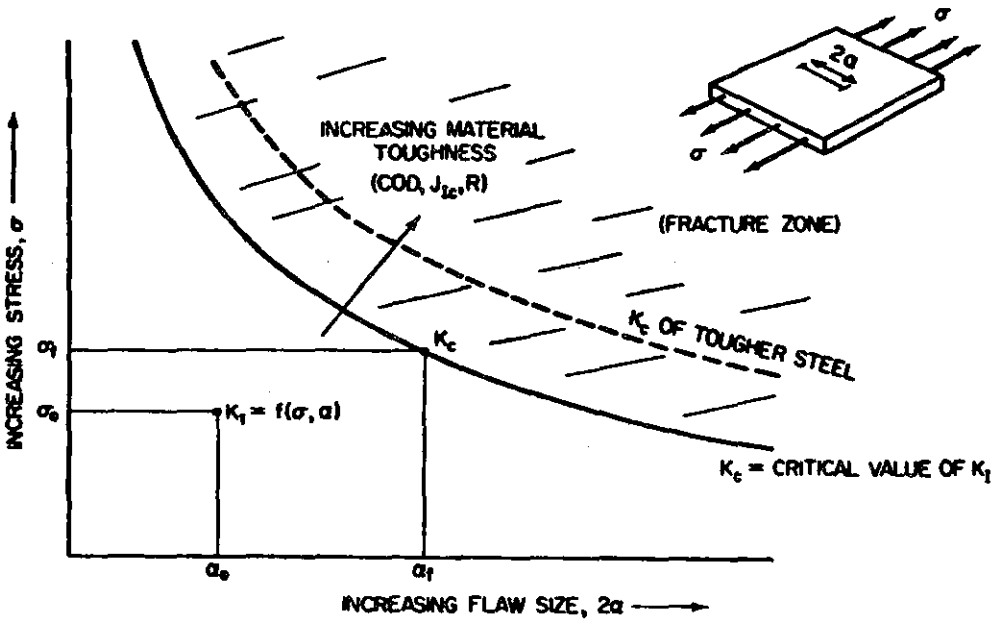

I-37. Fundamental fracture-resistant design approach

a) lower stress
b) improve fabrication
c) use tougher materials
d) engineers knew this, but fracture mechanics defines trade-offs

NOTES:

K_{IC} VALUES FOR BRIDGE STEELS

$$K_{IC} = f \begin{pmatrix} \text{TEMPERATURE,} \\ \text{LOADING RATE,} \\ \text{PLATE THICKNESS} \end{pmatrix}$$

I-38. K_{IC} Values depend on Temperature, Loading Rate, Thickness (constraint)

NOTES:

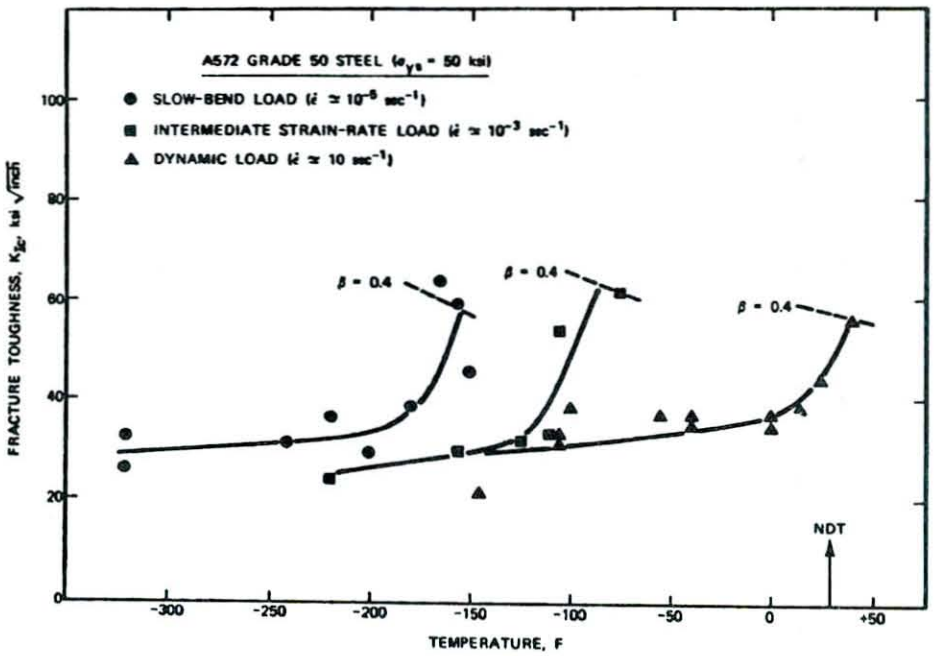

I-39. Effect of Temperature and Loading Rate on K_{Ic} for A572 Steel

a) slow
b) intermediate (Ottawa bridge test results plus others for bridges
c) dynamic

NOTES:

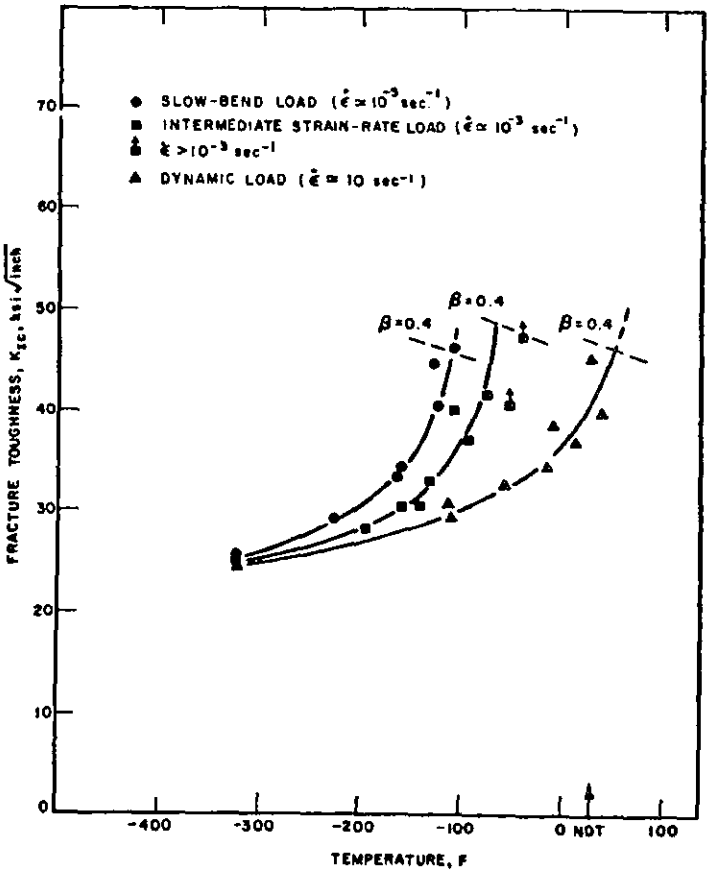

I-40. Effect of Temperature and Loading Rate on K_{Ic} for A36 Steel

a) Note metallurgical effect as limiting temperature is reached
b) significant improvement in toughness
c) basis of AASHTO for intermediate loading rate

NOTES:

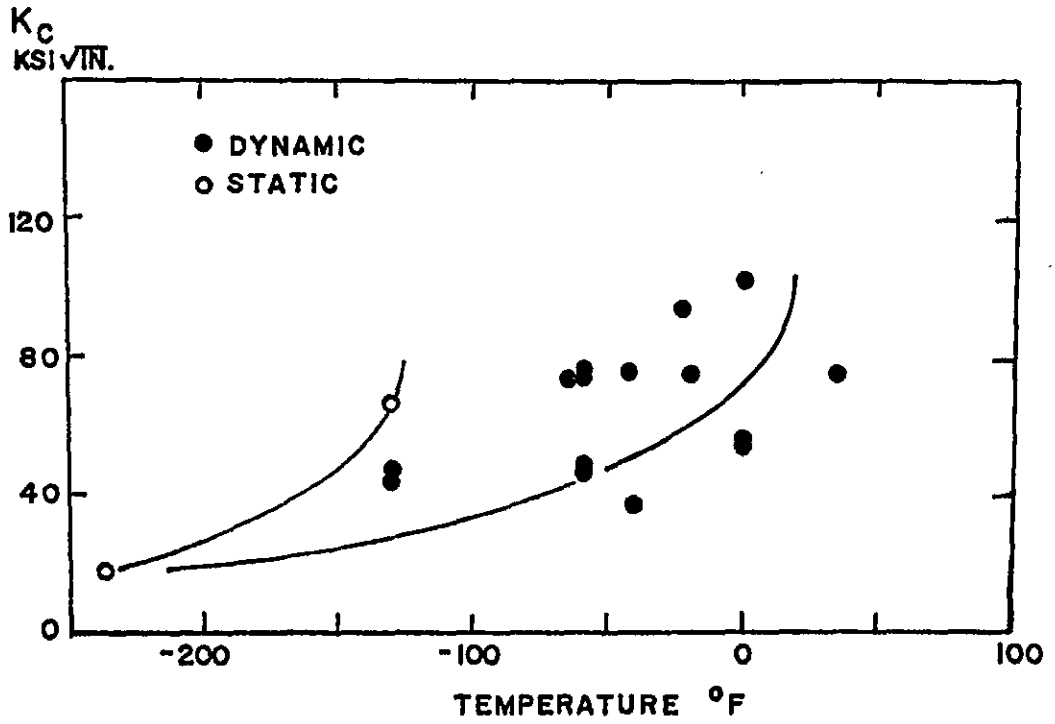

I-41. Test Results for A588

a) scatter
b) effect of loading rate
c) actual behavior better than guaranteed minimum

NOTES:

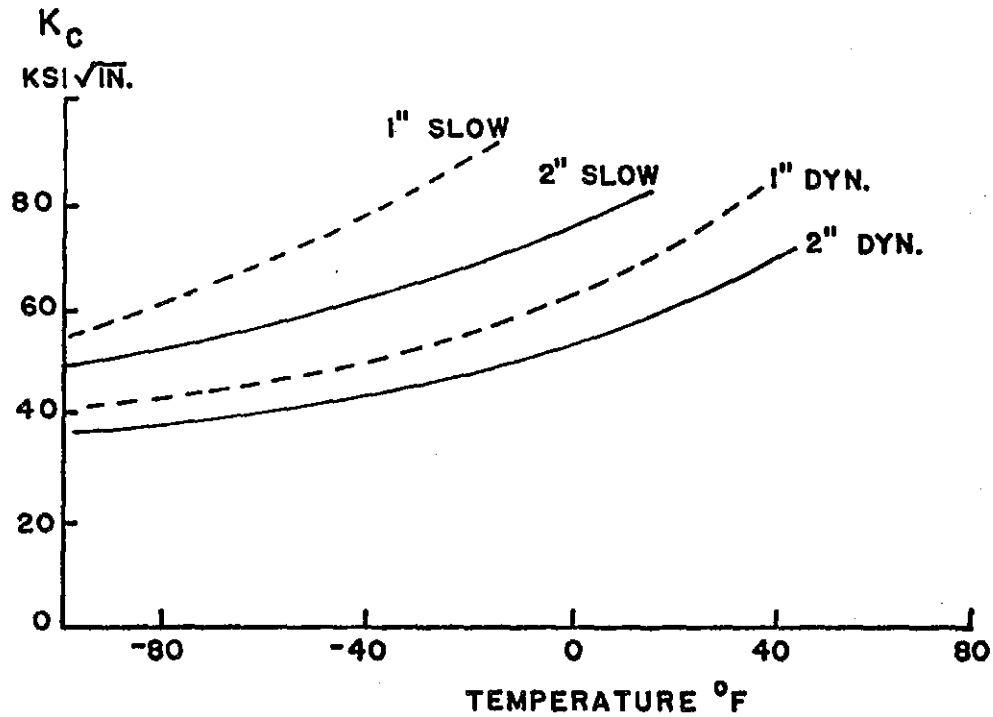

I-42. A441 Test Results from Lehigh

a) thickness
b) loading rate
c) temperature

NOTES:

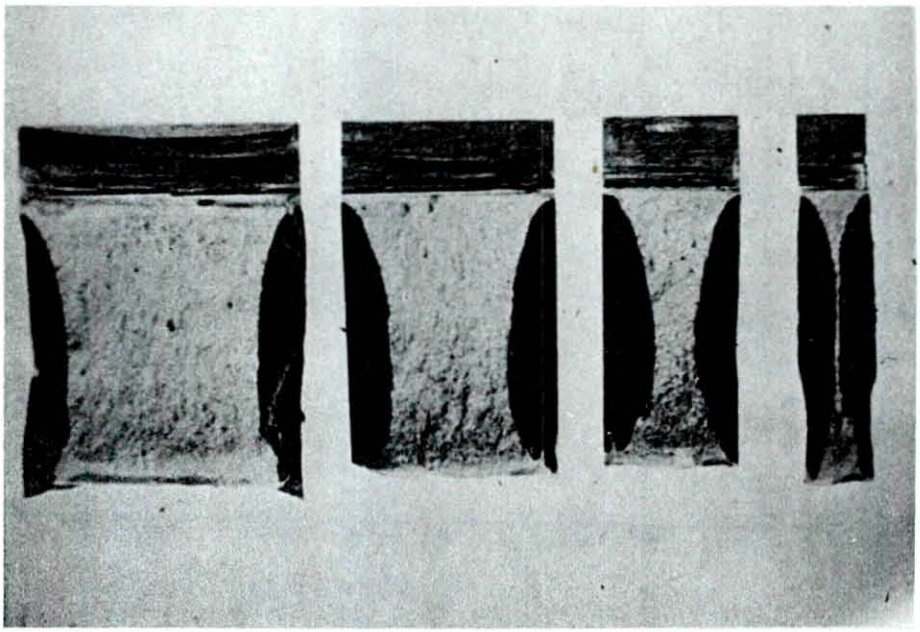

I-43. Fracture Surfaces Showing Effect of Thickness

a) original 2-inch thick plate
b) specimens from center-line (no metallurgical effect)
c) shear lip size similar

NOTES:

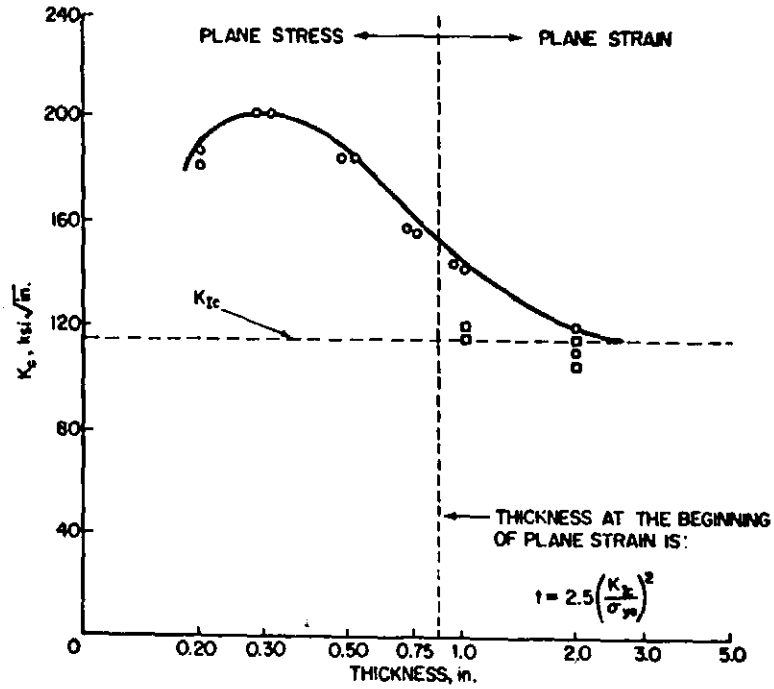

I-44. Test Results showing effect of Thickness

a) plane stress is function of thickness
b) plane strain is minimum value
c) constraint similar to thickness

NOTES:

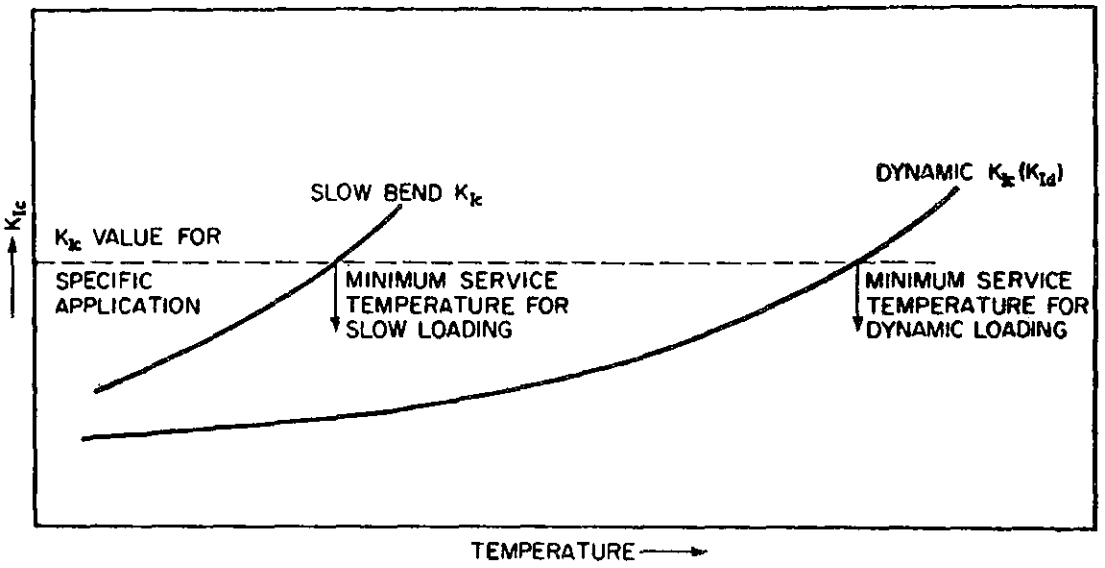

I-45. Design Significance of Loading Rate

a) basis of AASHTO toughness requirements

NOTES:

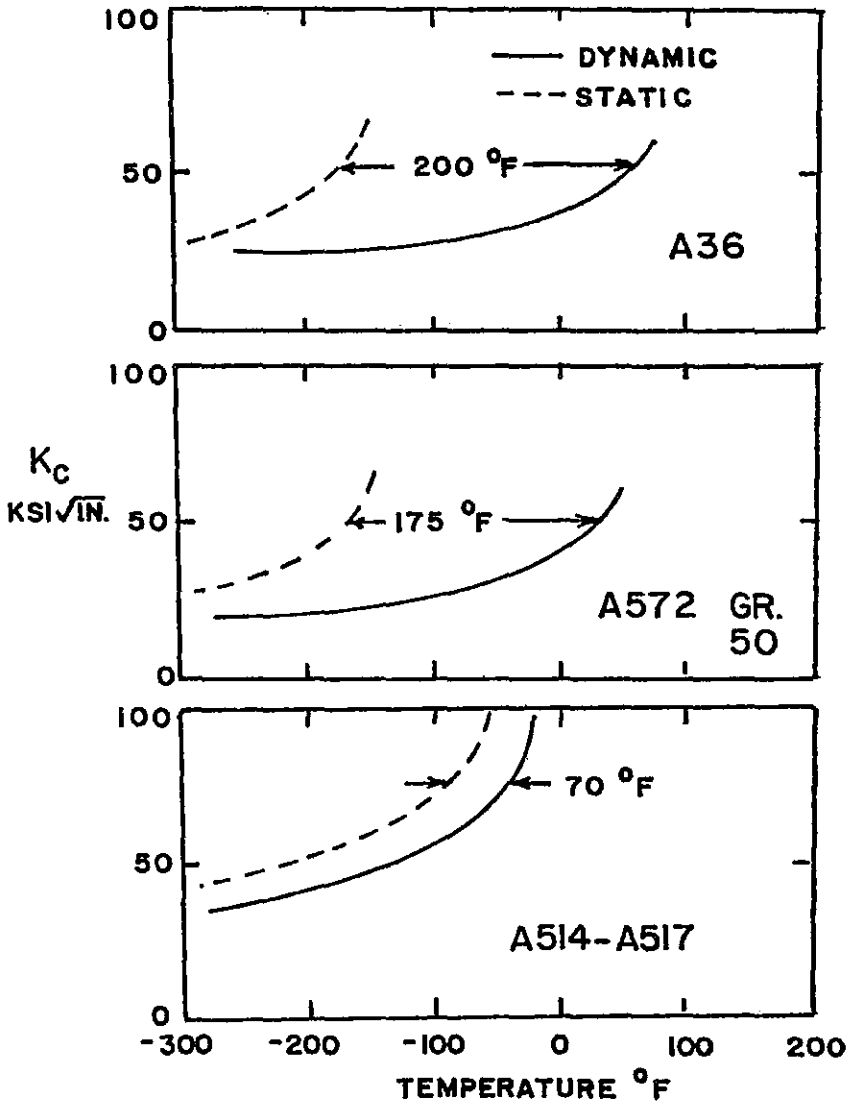

I-46. Loading Rate Shift for A36, A572, A514

a) measured by several investigators
b) depends on yield strength

NOTES:

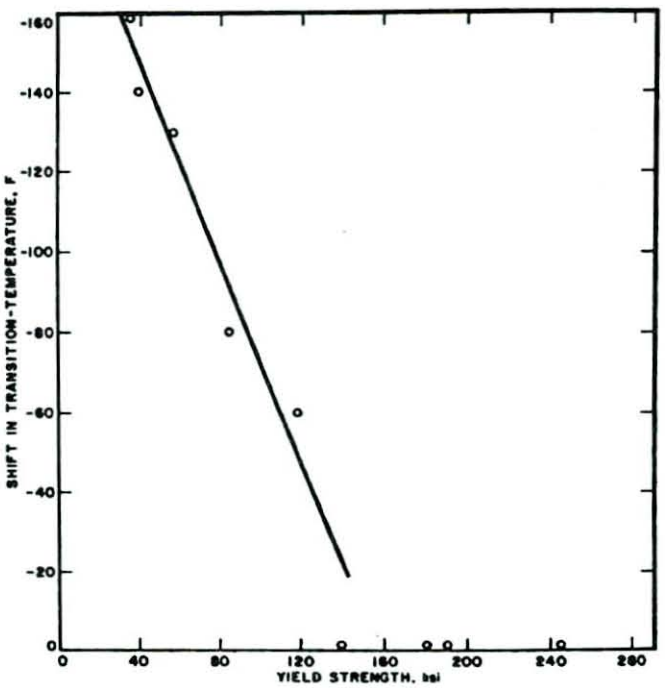

I-47. Loading Rate Shift is a function of Yield Strength

a) $T_S = 215 - 1.5\ \sigma_{ys}$ $(\sigma_{ys} < 140)$

b) $T_S = 0$ $(\sigma_{ys} > 140)$

NOTES:

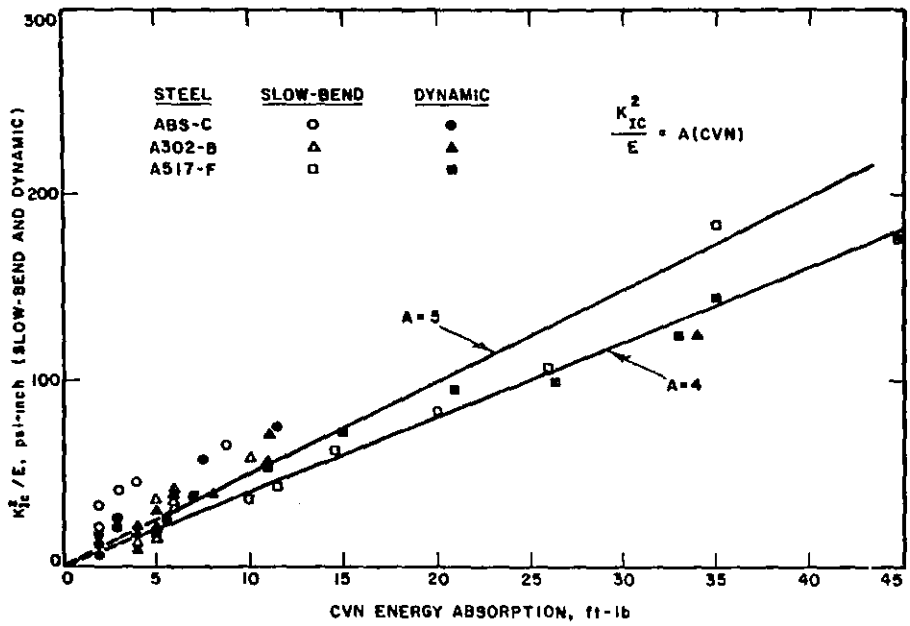

I-48. K_{Ic} - CVN Correlation

a) static CVN - static K_{Ic}
b) impact CVN - dynamic K_{Ic}
c) fatigue cracked
d) A = 5 for regular CVN impact

NOTES:

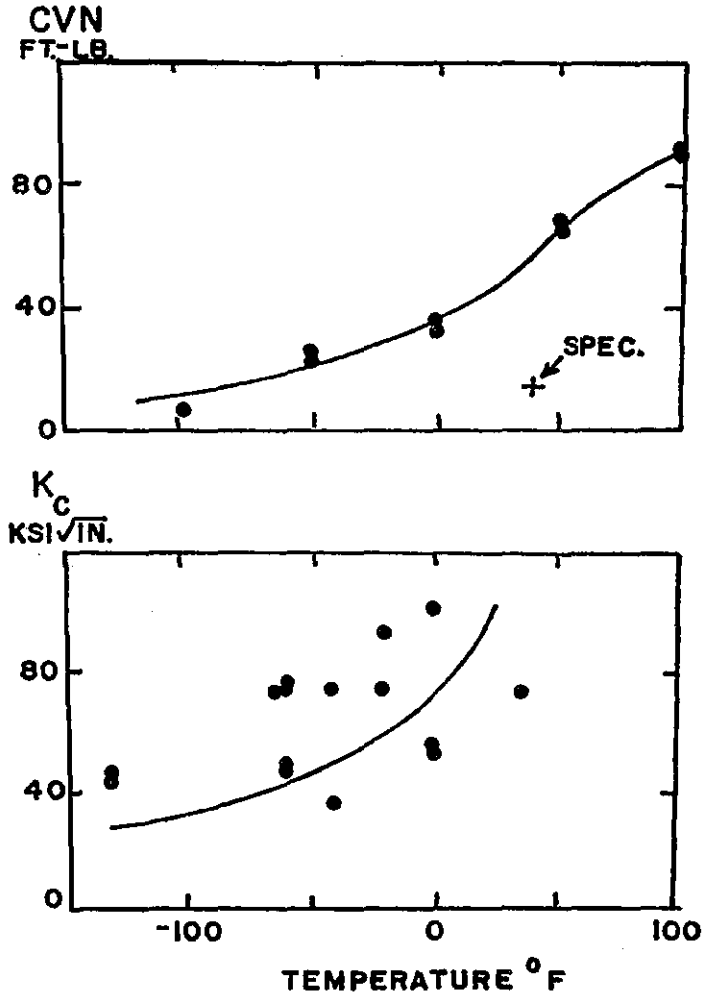

I-49. AASHTO Specification Based on CVN

a) Quality Control Test
b) Minimum Value in impact test
c) Loading Rate Shift

NOTES:

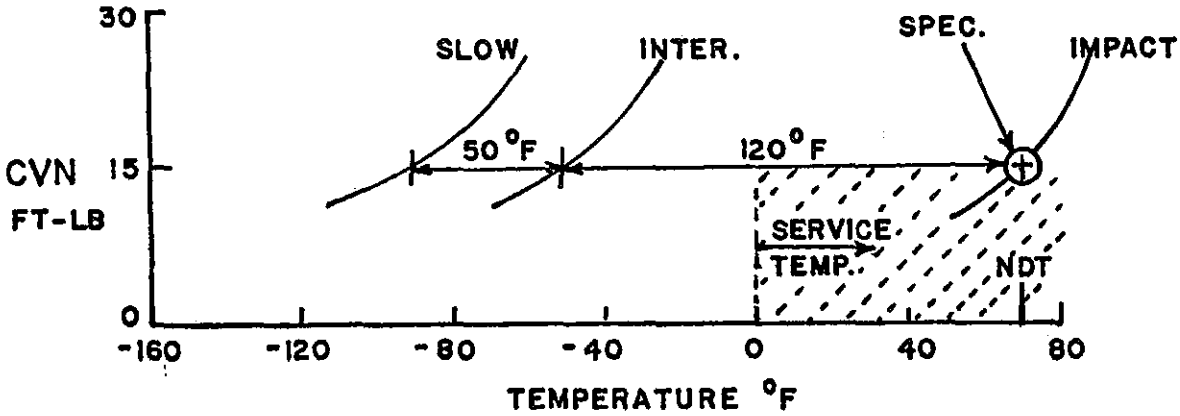

I-50. Class I AASHTO Toughness Specification

a) Service Temperature = 0°F
b) CVN impact - 15 ft lb at +70°F
c) Loading Rate Shift
d) Intermediate loading rate behavior

NOTES:

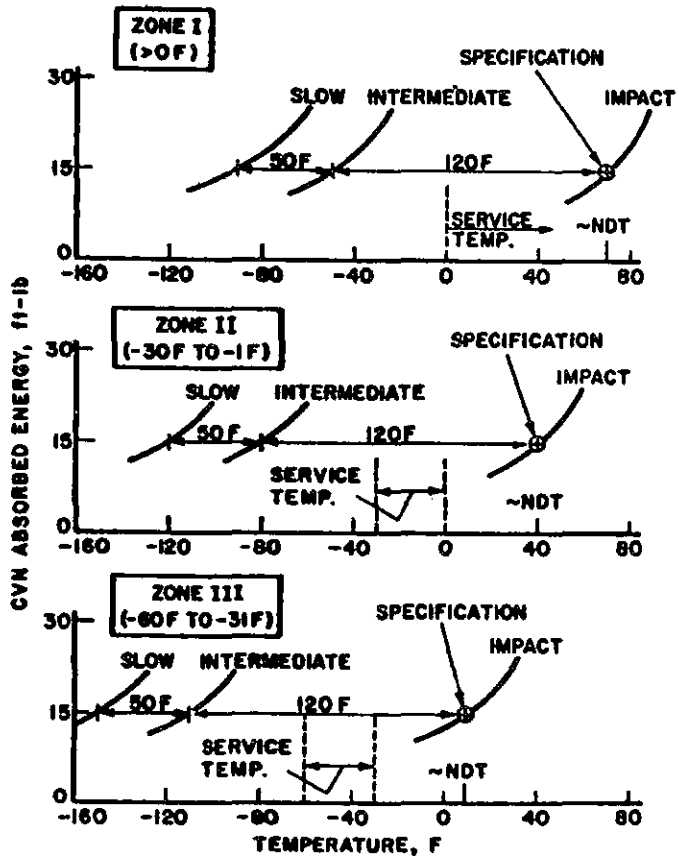

I-51. AASHTO - 3 zones

a) > 0°F
b) -30 to 0°F
c) -60 to -30°F

NOTES:

ASTM Designation	*Thickness (in.)*	*CVN Impact Value, ft lb*		
		*Zone 1**	*Zone 2**	*Zone 3**
A36		15 @ 70°F	15 @ 40°F	15 @ 10°F
A572	Up to 4 in. mechanically fastened	15 @ 70°F	15 @ 40°F	15 @ 10°F
	Up to 2 in. welded	15 @ 70°F	15 @ 40°F	15 @ 10°F
A440		15 @ 70°F	15 @ 40°F	15 @ 10°F
A441		15 @ 70°F	15 @ 40°F	15 @ 10°F
A242		15 @ 70°F	15 @ 40°F	15 @ 10°F
A588**	Up to 4 in. mechanically fastened	15 @ 70°F	15 @ 40°F	15 @ 10°F
	Up to 2 in. welded	15 @ 70°F	15 @ 40°F	15 @ 10°F
	Over 2 in. welded	20 @ 70°F	20 @ 40°F	20 @ 10°F
A514	Up to 4 in. mechanically fastened	25 @ 30°F	25 @ 0°F	25 @ −30°F
	Up to 2½ in. welded	25 @ 30°F	25 @ 0°F	25 @ −30°F
	Between 2½–4 in. welded	35 @ 30°F	35 @ 0°F	35 @ −30°F

*Zone 1: minimum service temperature 0°F and above.
Zone 2: minimum service temperature from −1° to −30°F.
Zone 3: minimum service temperature from −31° to −60°F.
**If the yield point of the material exceeds 65 ksi, the temperature for the CVN value for acceptability shall be reduced by 15°F for each increment of 10 ksi above 65 ksi.

I-52. Table of AASHTO Toughness Requirements

a) Effect of σ_{ys}
b) Effect of thickness
c) Effect of stored elastic energy

NOTES:

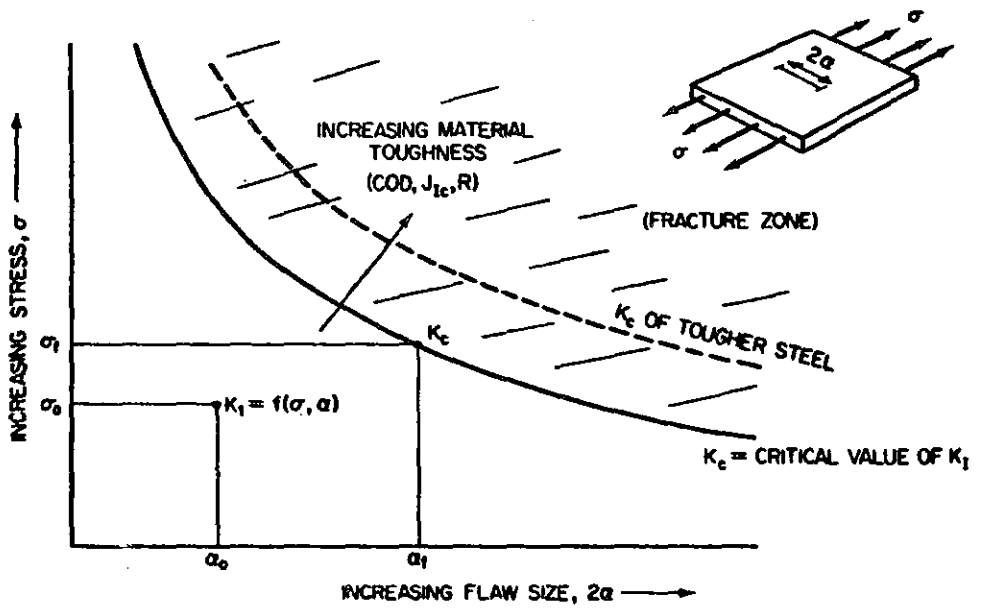

I-53. Overall Fracture Control Plan

a) Materials
b) Design
c) Fabrication
d) Loading
e) Sub-critical crack growth (fatigue, stress corrosion)

NOTES:

FRACTURE CONTROL PLAN

$$K_{IC} = f(\sigma, \sqrt{a})$$

K_{IC} = MATERIAL PROPERTY

σ = DESIGN

a = FABRICATION AND INSPECTION

I-54. Fracture Control Plan

a) Materials
b) Design
c) Fabrication
d) Brittle fracture problems will not be solved merely by AASHTO toughness requirements

NOTES:

INFORMATION REQUIRED FOR FRACTURE CONTROL PLAN FOR BRIDGES

1) TOUGHNESS VALUES OF BRIDGE STEELS

2) FLAW SIZES IN BRIDGE MEMBERS

3) FATIGUE CRACK GROWTH BEHAVIOR

4) FRACTURE TOUGHNESS CRITERIA

I-55. Information Required for Fracture Control

a) Toughness Values
b) Flaw Sizes
c) Fatigue Behavior
d) Criteria
e) Service experience

NOTES:

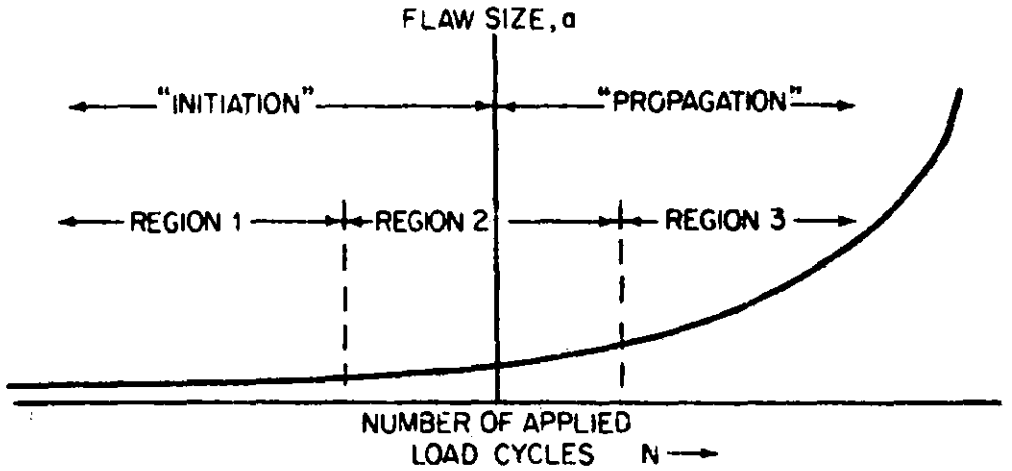

REGION 1 - DIFFICULTY IN DEFINING FLAW SIZE (DISLOCATION MICROCRACK, POROSITY, ETC.)

REGION 2 - FLAWS CAN FIRST BE OBSERVED IN AN ENGINEERING SENSE

REGION 3 - CRACK GROWTH CAN BE OBSERVED

I-56. General Fatigue Behavior

a) Initiation
b) Propagation
c) Unstable

NOTES:

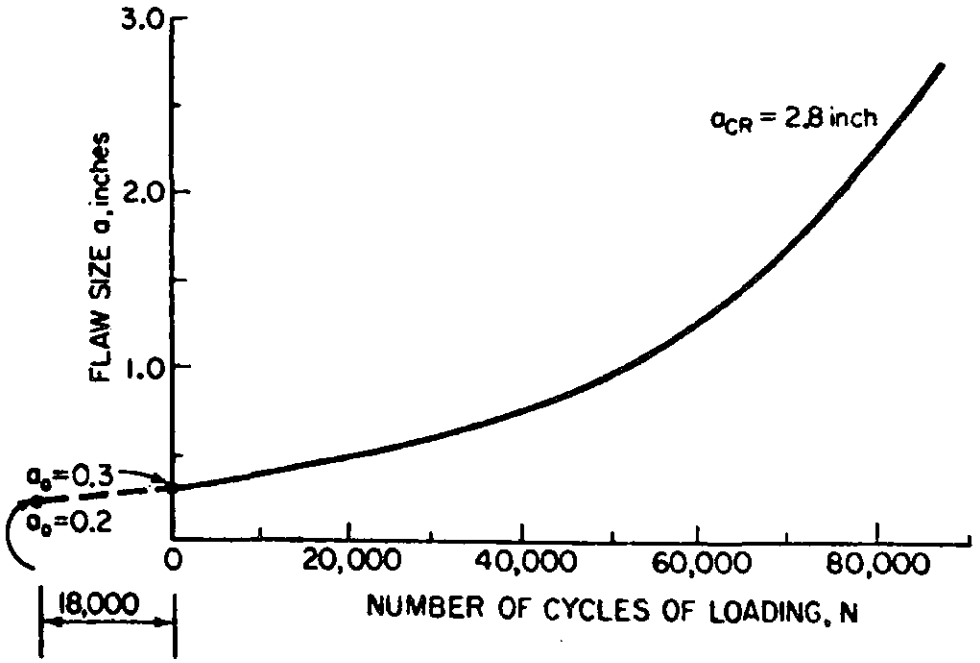

I-57. Fatigue Crack Growth Curve

a) $da/dN = A(\Delta K)^m$
b) growth is a power function of $\Delta\sigma$
c) rate increases
d) large effect of a_o

NOTES:

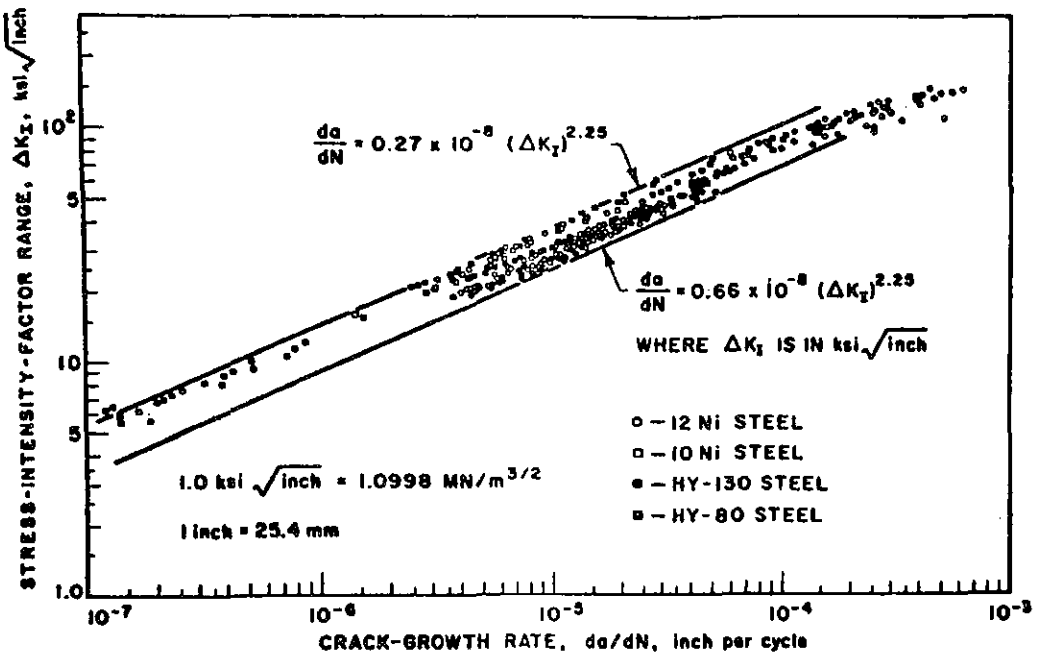

I-58. Fatigue Crack Growth Behavior

a) da/dN related to ΔK^m
b) general band for structural steels
c) ferrite pearlite steels $da/dN = 3.6 \times 10^{-10} (\Delta K_I)^{3.0}$
d) martensitic steels $da/dN = 0.66 \times 10^{-8} (\Delta K_I)^{2.25}$

NOTES:

$$\Delta N = \frac{\Delta a}{0.66 \times 10^{-8}[1.98(\Delta\sigma)\sqrt{\sigma_{avg}}]^{2.25}}$$

where $\Delta a = 0.10$ in. (2.54 mm)
$\Delta\sigma = 20$ ksi (138 MN/m²)

a_0 (in.)	a_f (in.)	a_{avg} (in.)	ΔK (ksi$\sqrt{in.}$)	ΔN (cycles)	$\sum N$ (cycles)
0.3	0.4	0.35	23.5	12,500	12,500
0.4	0.5	0.45	26.7	9,750	22,250
0.5	0.6	0.55	29.4	7,550	29,800
0.6	0.7	0.65	32.2	6,150	35,950
0.7	0.8	0.75	34.6	5,200	41,150
0.8	0.9	0.85	36.6	4,600	45,750
0.9	1.0	0.95	38.8	4,100	49,850
1.0	1.1	1.05	40.5	3,700	53,550

I-59. Table Showing Crack Growth Information

a) $\Delta N = \frac{\Delta a}{A(\Delta K)^m}$

b) $\Delta N = \frac{\Delta a}{A(C\ \Delta\sigma\sqrt{a_{avg}})^m}$

c) A, C, m are geometry and material constants

NOTES:

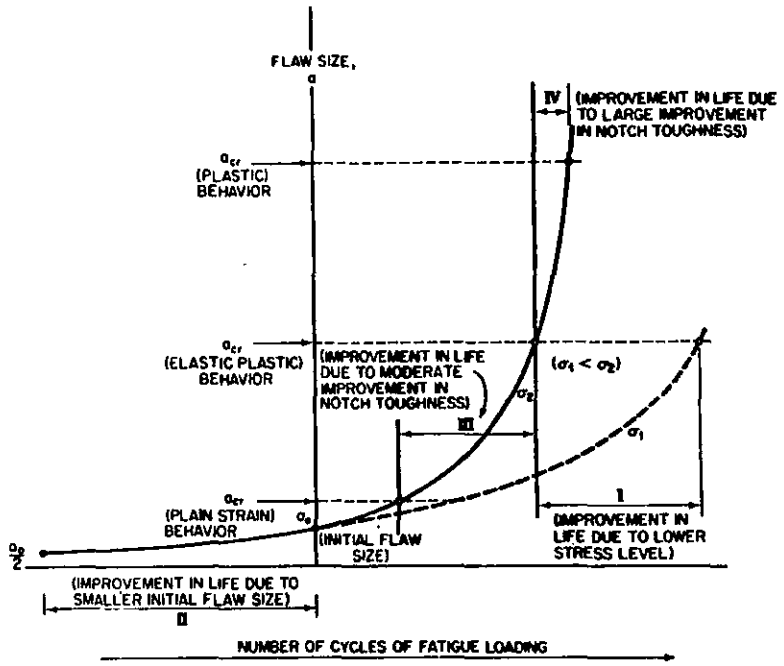

I-60. Effect of Fracture Resistant Design

a) Region I - effect of lower stress range
b) Region II - effect of better fabrication and inspection
c) Region III - effect of moderate level of notch toughness (AASHTO)
d) Region IV - effect of even higher toughness

NOTES:

FIGURES - SESSION 2

CONCEPTS OF FRACTURE MECHANICS -

FATIGUE CRACK GROWTH AND FRACTURE CONTROL

FATIGUE LIFE

CRACK INITIATION

CRACK PROPAGATION

FINAL FAILURE

2-1. Elements for a Fracture Control Plan

a) The life of structural components subjected to cyclic loading is governed by the initiation and propagation of cracks to critical dimensions.
b) The useful life of such components is equal to the sum of the initiation life and the subcritical propagation life.
c) One must be able to predict the initiation-, subcritical-crack-propagation-, and unstable-crack-propagation behavior to establish a Fracture Control Plan to ensure the safety and reliability of the structure.

NOTES:

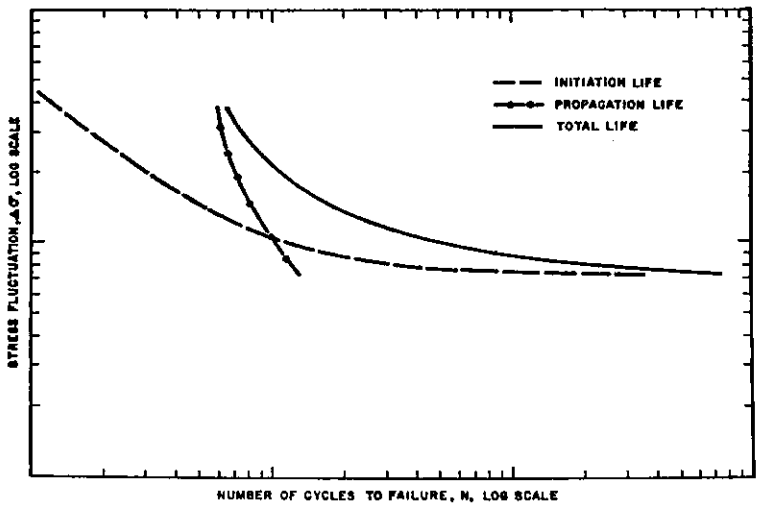

2-2. Schematic S-N Curve Divided into "Initiation" and "Propagation" Components

a) Small smooth-rotating-beam specimens.
b) Low-cycle (high-stress-fluctuation) life is primarily propagation.
c) High-cycle (low-stress-fluctuation) life is primarily initiation.
d) Endurance limit is fully initiation.
e) Change in surface roughness or in specimen geometry changes the S-N curve.
f) We must separate the initiation and propagation behavior.

NOTES:

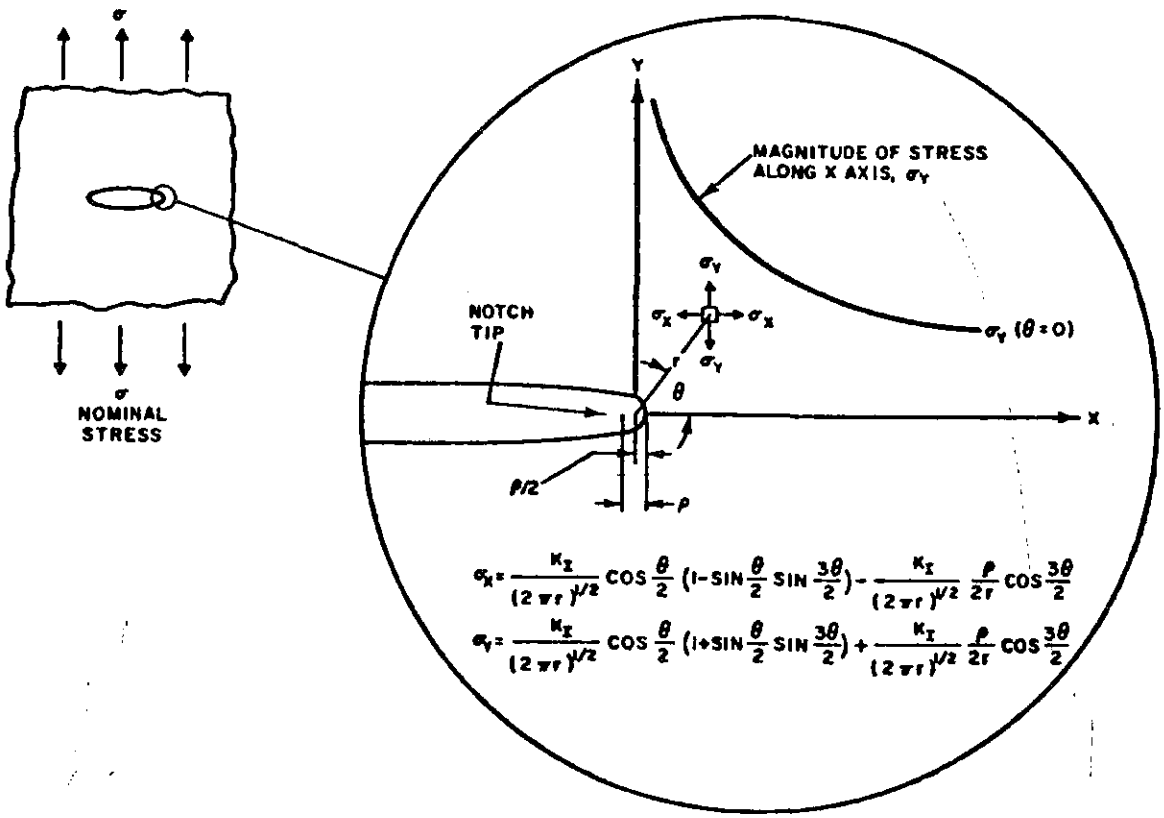

2-3. Schematic Illustration of the Elastic-Stress-Field Distribution Near the Tip of an Elliptical Notch (Mode I Deformation)

a) Most fatigue cracks initiate at regions of stress concentration.
b) Stress field in the vicinity of the notch depends on the stress-intensity-factor, K_I, and on the radius of the notch tip.

NOTES:

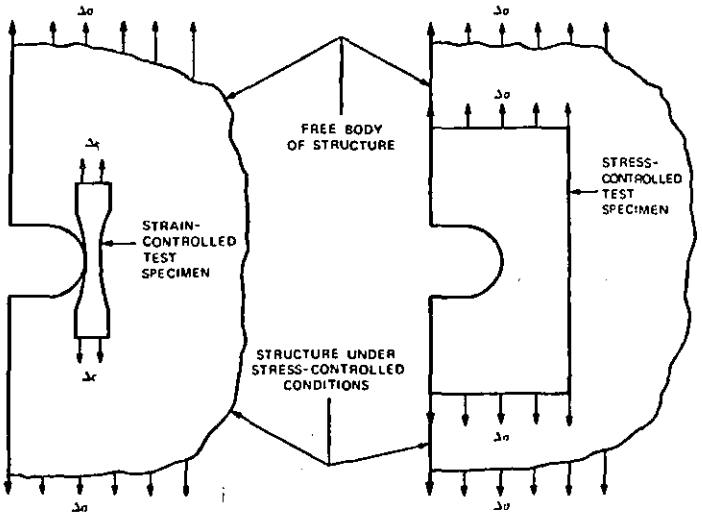

2-4. Test Specimen Simulation of Stress Concentrations in Structures (a) Strain-Controlled Specimen. (b) Stress-Controlled Specimen.

a) Smooth specimens tested under strain control are used to simulate the plastic damage at the tip of a notch.
b) A better procedure is to use a large specimen containing a notch and subjecting the specimen to the nominal elastic stress magnitudes and fluctuations that simulate those in the structural component of interest.

NOTES:

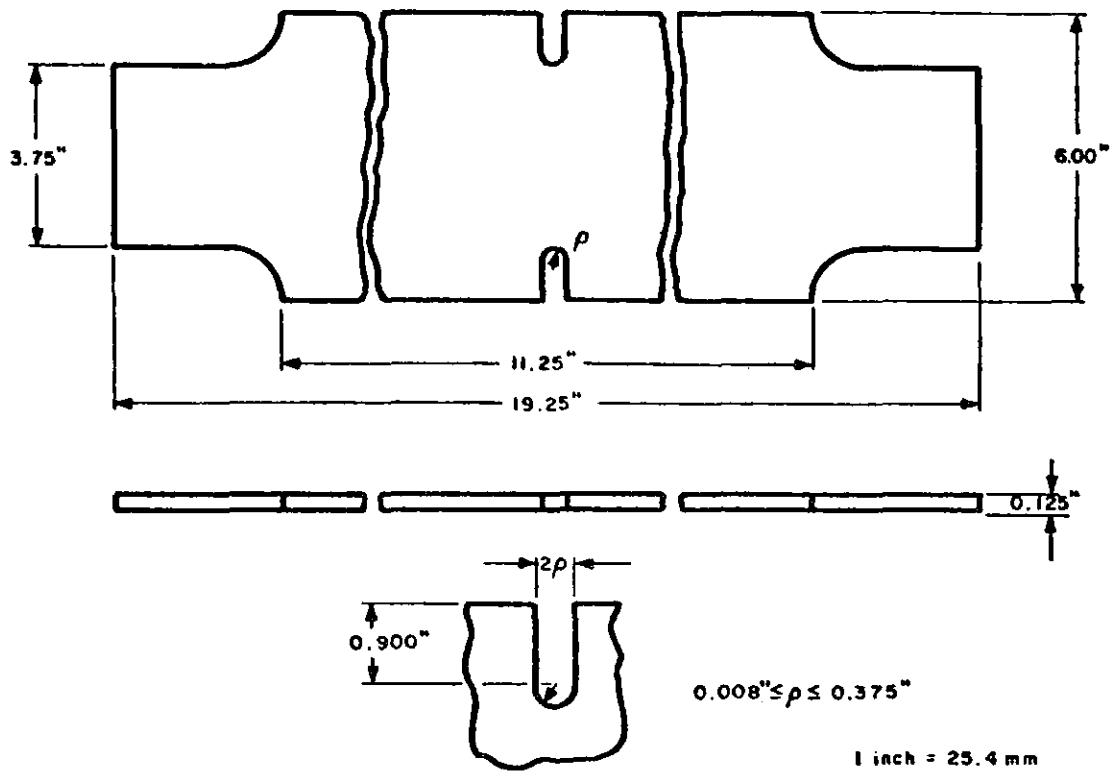

ENLARGED NOTCH DETAIL

2-5. Double-Edge-Notched Specimens

a) Specimens contain notches of various severities.
b) Specimens subjected to various stress fluctuations.

NOTES:

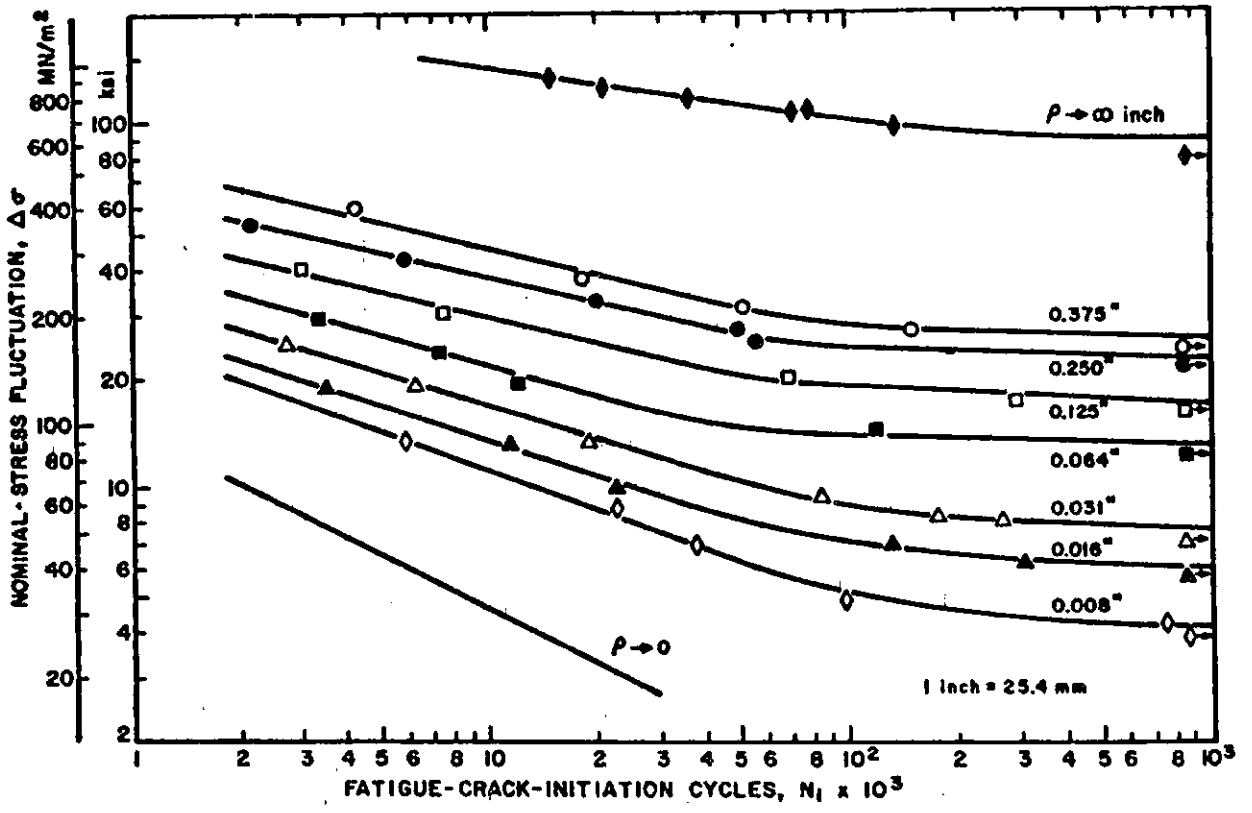

2-6. Dependence of Fatigue-Crack Initiation of HY-130 Steel on Nominal-Stress Fluctuations for Various Notch Geometries

a) Specimens containing same stress concentration (same notch geometry) give a curve that represents the life to initiate a small crack, N_i.
b) The crack-initiation life, N_i, decreases with increased stress-concentration factor, K_t.
c) For the same notch geometry (that is, same K_t), the initiation life decreases with increased magnitude of the stress range.

NOTES:

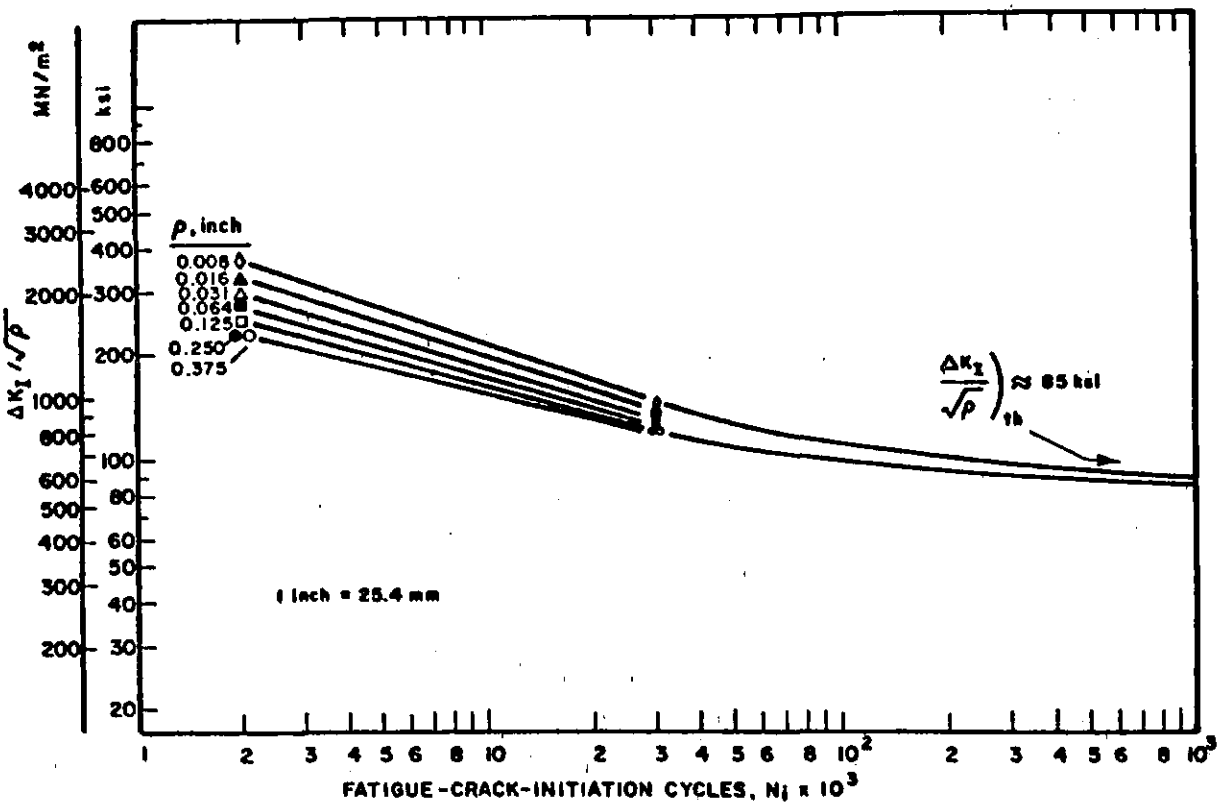

2-7. Correlation of Fatigue-Crack-Initiation Life with the Parameter $\Delta K_I/\sqrt{\rho}$ for HY-130 Steel.

a) The effect of specimen and notch geometry can be correlated using the fracture mechanics parameter, $\frac{\Delta K}{\sqrt{\rho}}$.

b) The parameter $\frac{\Delta K}{\sqrt{\rho}}$ times a constant equal to about 1.2 is equal to the maximum stress fluctuation in the region of the stress concentration.

c) The fatigue-crack-initiation threshold for various geometries occurs at the value that appears to be characteristic for the material tested.

NOTES:

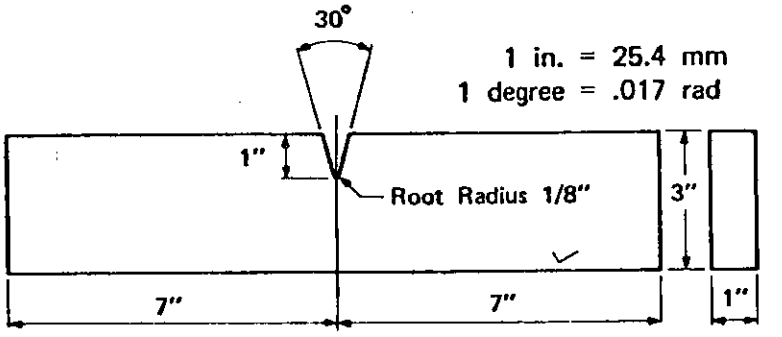

2-8. Single-Edge-Notched Bend Test Specimen

a) Any notched specimen can be used to study crack initiation.
b) The only requirement is to have a stress-field analysis or K_I for that specimen.

NOTES:

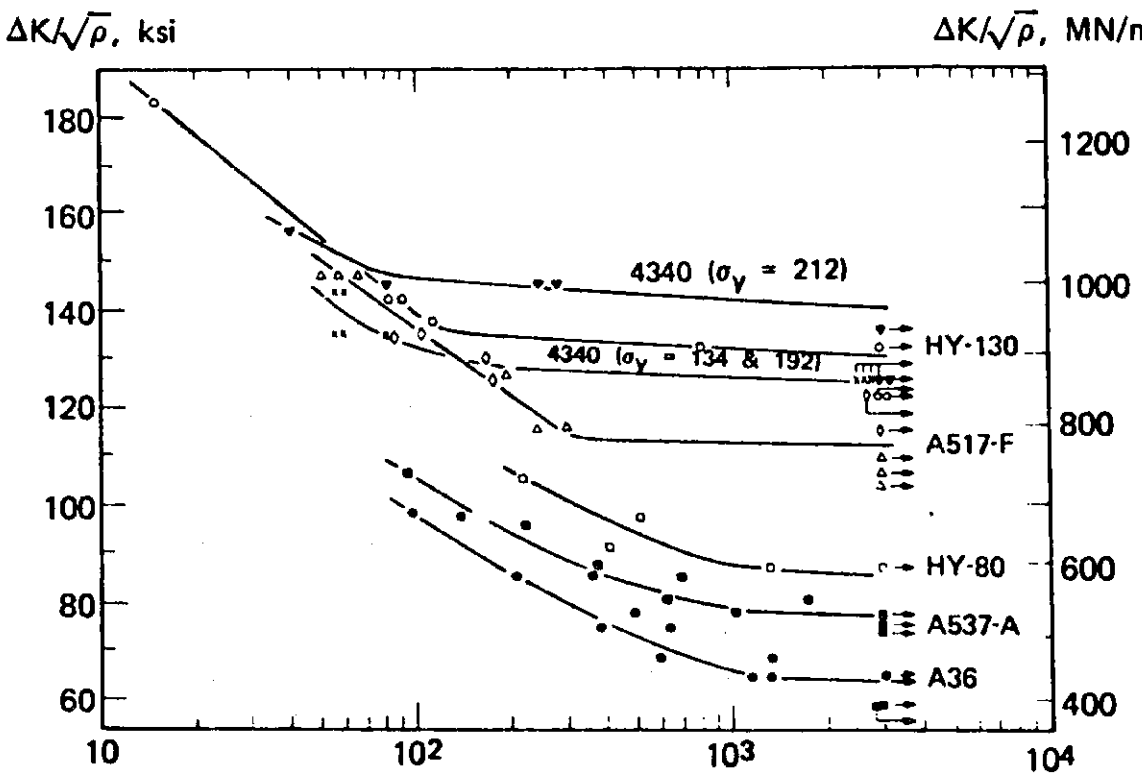

2-9. Fatigue-Crack-Initiation Behavior of Various Steels
a) Data obtained using a 3-point-bend loaded specimen under zero-to-tension loading.
b) The fatigue-crack-initiation threshold ∅ increases with steel strength.

NOTES:

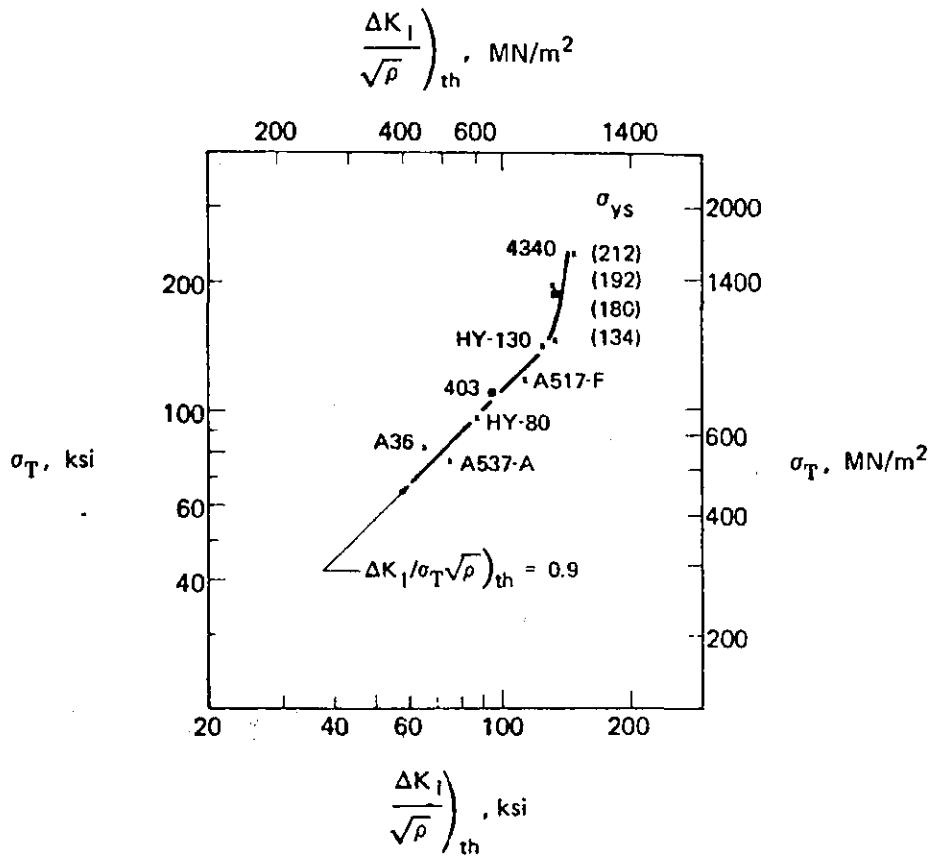

2-10. Dependence of Fatigue-Crack-Initiation Threshold on Tensile Strength

a) Fatigue-crack-initiation threshold appears to be related to tensile strength.
b) The data suggest that fatigue-crack initiation at a stress ratio of +0.1 occurs when the maximum stress range at the notch tip is equal to the tensile strength of the material.

NOTES:

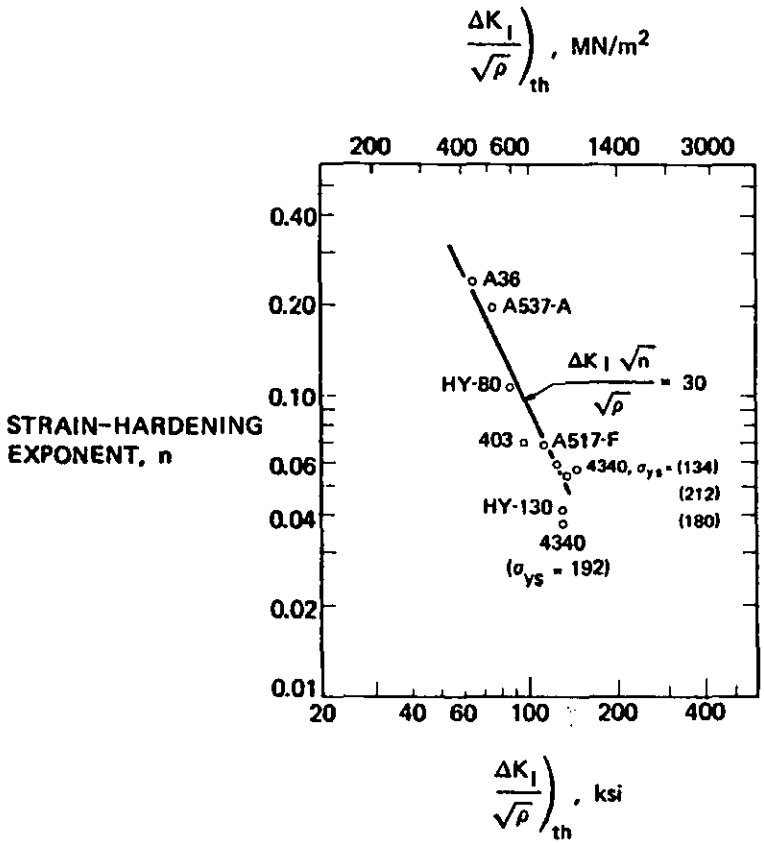

2-11. Dependence of Fatigue-Crack-Initiation Threshold on Strain-Hardening Exponent

a) Fatigue-crack-initiation threshold appears to be related to the strain-hardening exponent.
b) The scatter in the fatigue-crack-initiation-threshold data when correlated with the strain-hardening exponent is less than when correlated with the tensile strength.

NOTES:

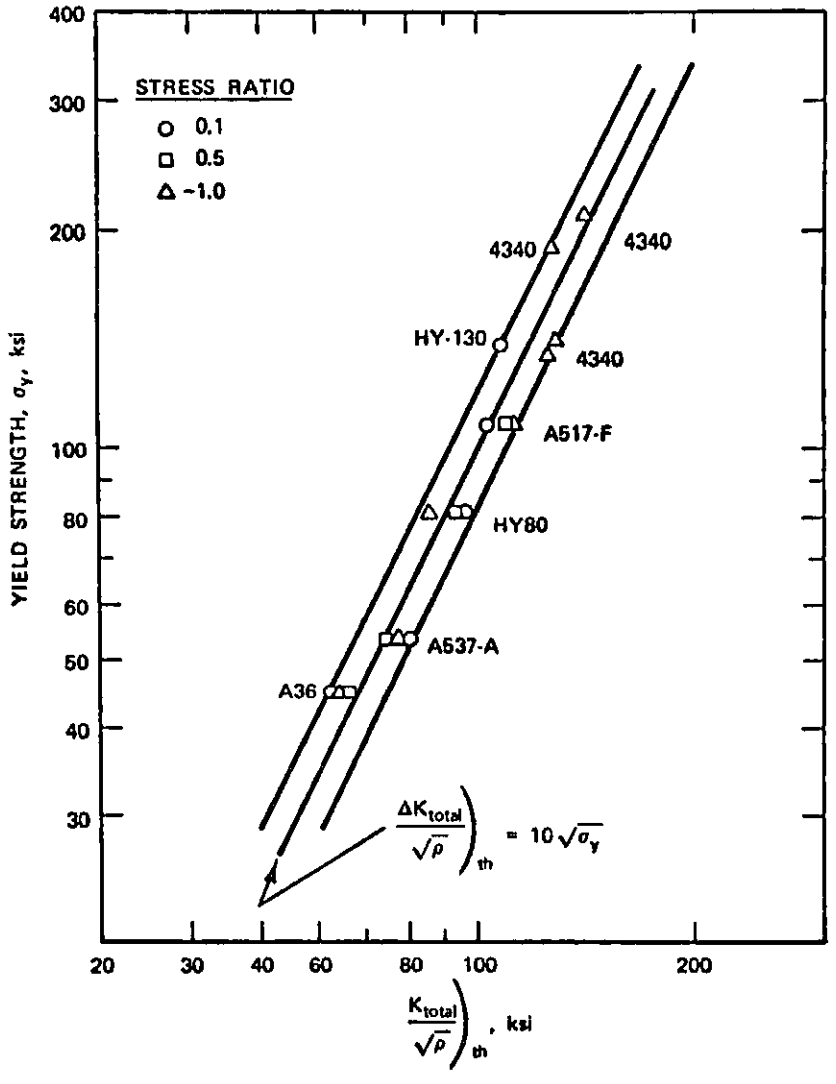

2-12. Dependence of Fatigue-Crack-Initiation Threshold on Yield Strength

a) The best correlation is obtained when the fatigue-crack-initiation threshold data is correlated with yield strength.

b) The slide also contains data obtained at various stress ratios.

c) The data show that the fatigue-crack-initiation threshold subjected to various stress ratios depend on the total stress range (tension and compression). Thus, the correlating parameter is $\frac{\Delta K_{total}}{\sqrt{\rho}}$.

NOTES:

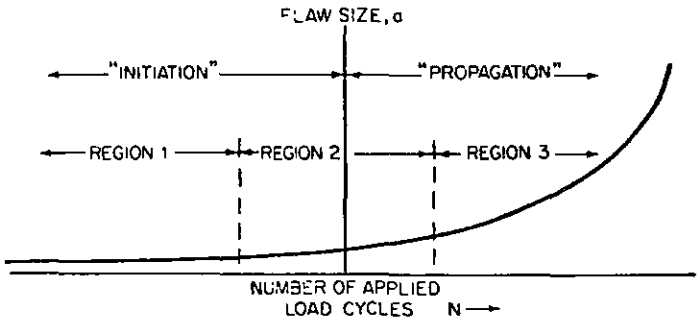

REGION 1 – DIFFICULTY IN DEFINING FLAW SIZE (DISLOCATION MICROCRACK, POROSITY, ETC.)

REGION 2 – FLAWS CAN FIRST BE OBSERVED IN AN ENGINEERING SENSE

REGION 3 – CRACK GROWTH CAN BE OBSERVED

2-13. General Fatigue Behavior

a) Initiation (very small discontinuities), Region 1.
b) Cracks can be first observed, Region 2.
c) Crack-growth rates can be measured, Region 3.

NOTES:

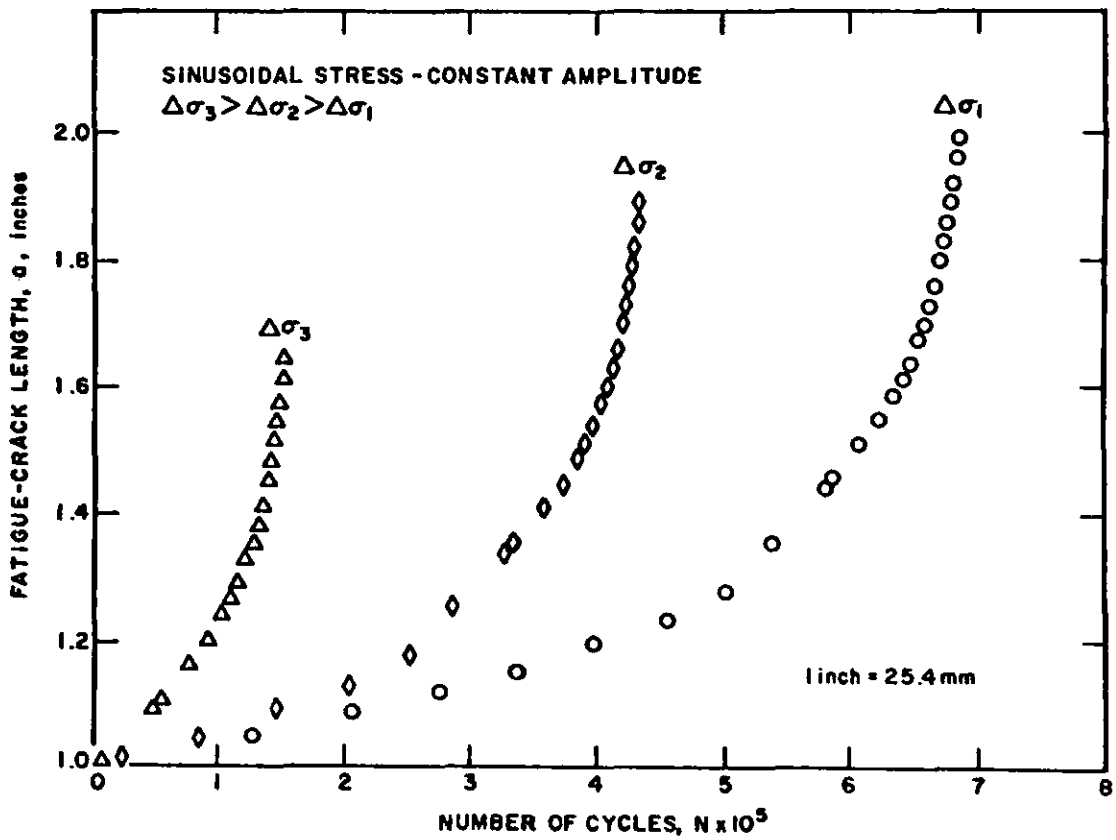

2-14. Effect of Cyclic-Stress Range on Crack Growth

a) Same specimen geometry—specimens subjected to various magnitude of stress fluctuation, $\Delta\sigma$.

b) The fatigue life decreased with increased $\Delta\sigma$.

NOTES:

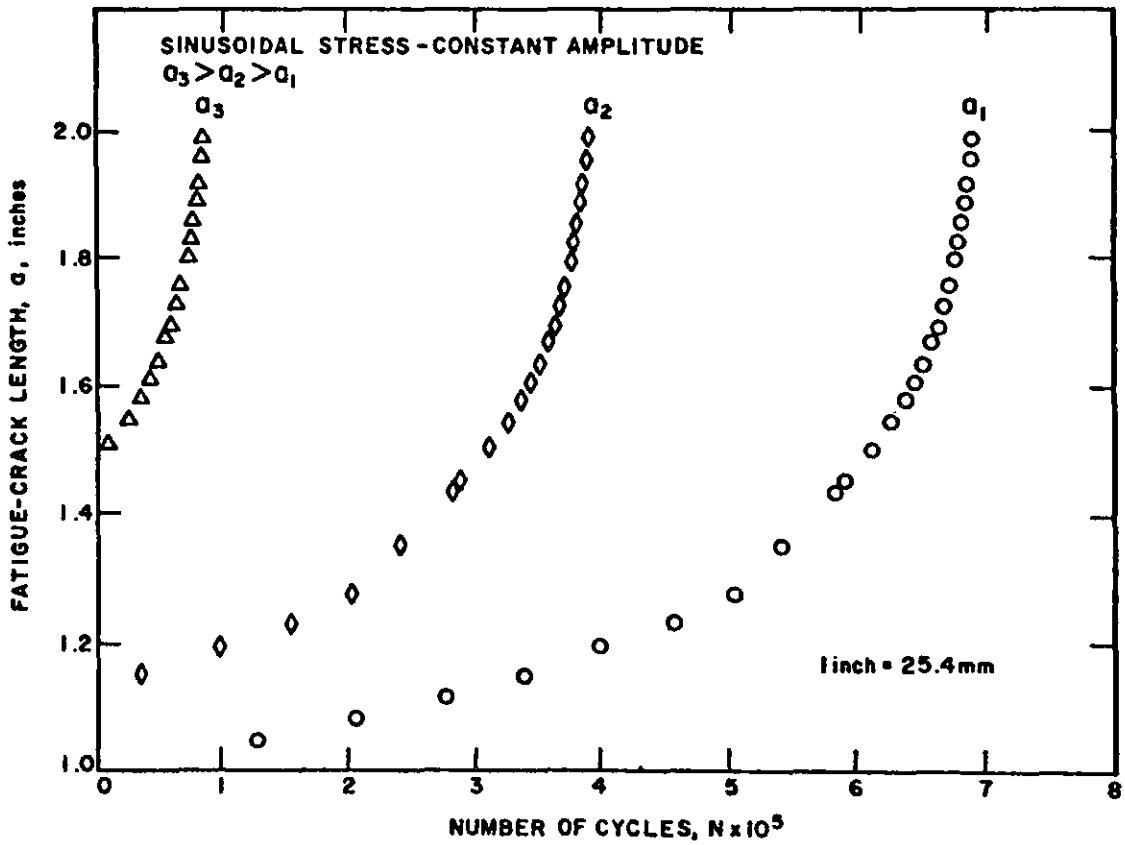

2-15. Effect of Initial Crack Length on Crack Growth

a) Same specimen geometry except for the initial crack size. Specimens subjected to identical $\Delta\sigma$ values.
b) The fatigue life decreases with increased size of the initial crack length.

NOTES:

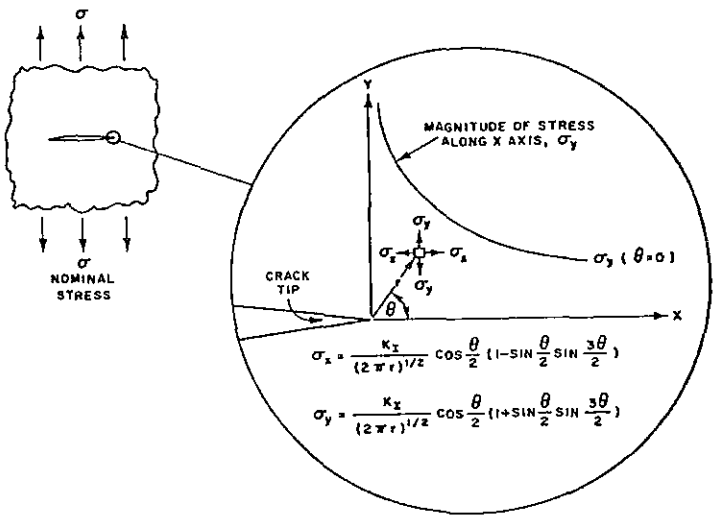

2-16. Schematic illustration of the Elastic-Stress-Field Distribution Near the Tip of a Fatigue Crack (Mode I Deformation)

a) The effect of applied stress and crack size can be combined using the stress-intensity-factor parameter K_I.
b) Thus, the effects of stress fluctuation and size of the crack on the fatigue life should be governed by the fluctuation in the stress-intensity factor.

NOTES:

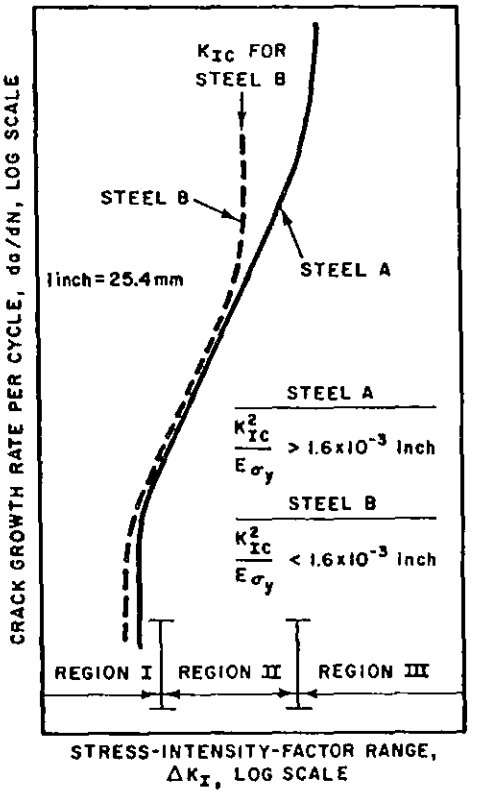

2-17. Schematic Representation of Fatigue-Crack Growth in Steel

a) Fatigue-crack-propagation behavior can be divided into three regions.
b) Region I, threshold behavior.
c) Region II, power-law relationship.
d) Region III, fast crack growth under cyclic loading.
e) Large effects of initial crack size.
f) Large effects of $\Delta\sigma$ because ΔK is raised to a power equal to or greater than 2.

NOTES:

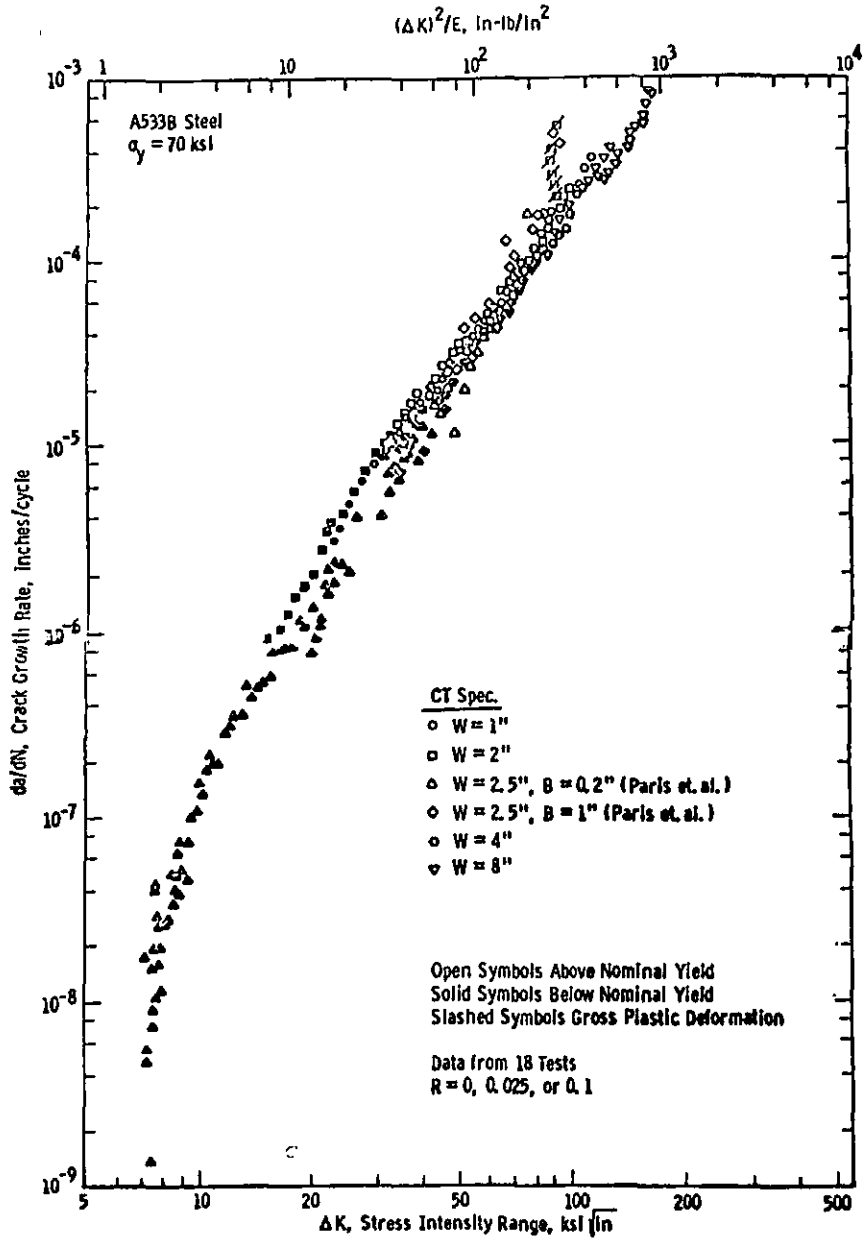

2-18. Example of Fatigue-Crack-Propagation Threshold

a) Test conducted at a stress ratio of about +0.1.
b) Fatigue-crack-propagation threshold at a stress ratio of about +0.1 occurs at a ΔK_I of about 7 ksi$\sqrt{inch}$.
c) The fatigue-crack-propagation threshold corresponds to growth rates that are below 10^{-8} inch per cycle.

NOTES:

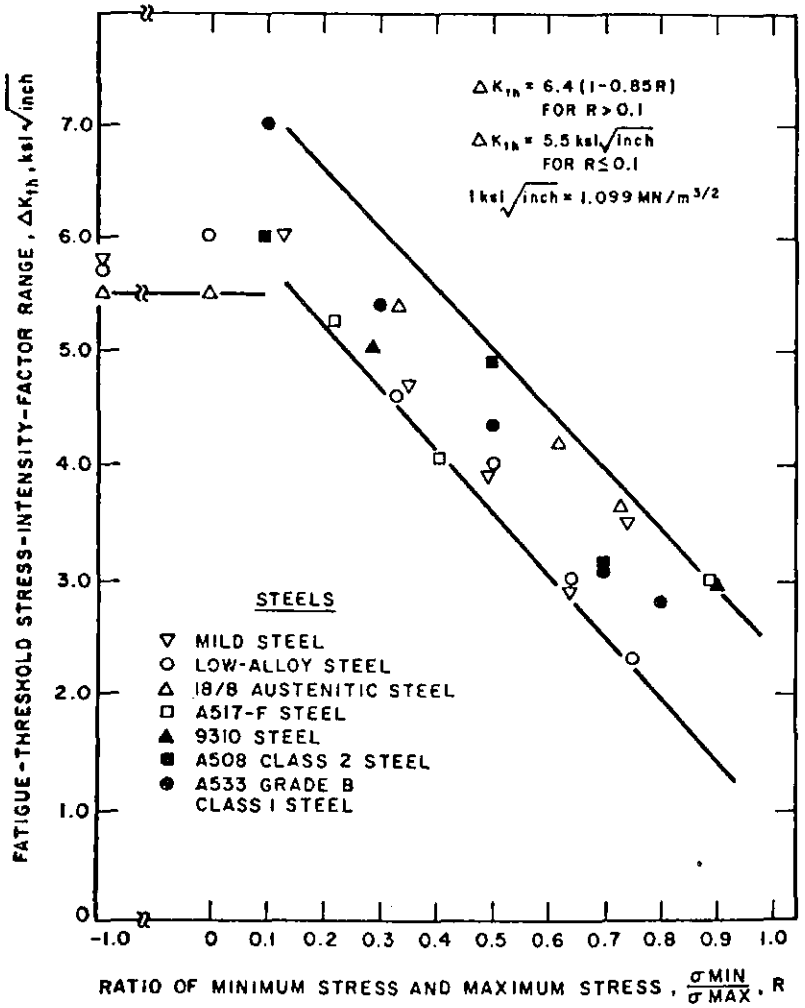

2-19. Dependence of Fatigue-Threshold Stress-Intensity-Factor Range on Stress Ratio

a) The fatigue-crack-propagation threshold, ΔK_{th}, is a function of stress ratio.

b) Within experimental scatter the chemical composition and mechanical properties of steels appear to have a very small effect on ΔK_{th}.

c) Conservative estimates of ΔK_{th} can be predicted for stress ratios less than about 0.9.

NOTES:

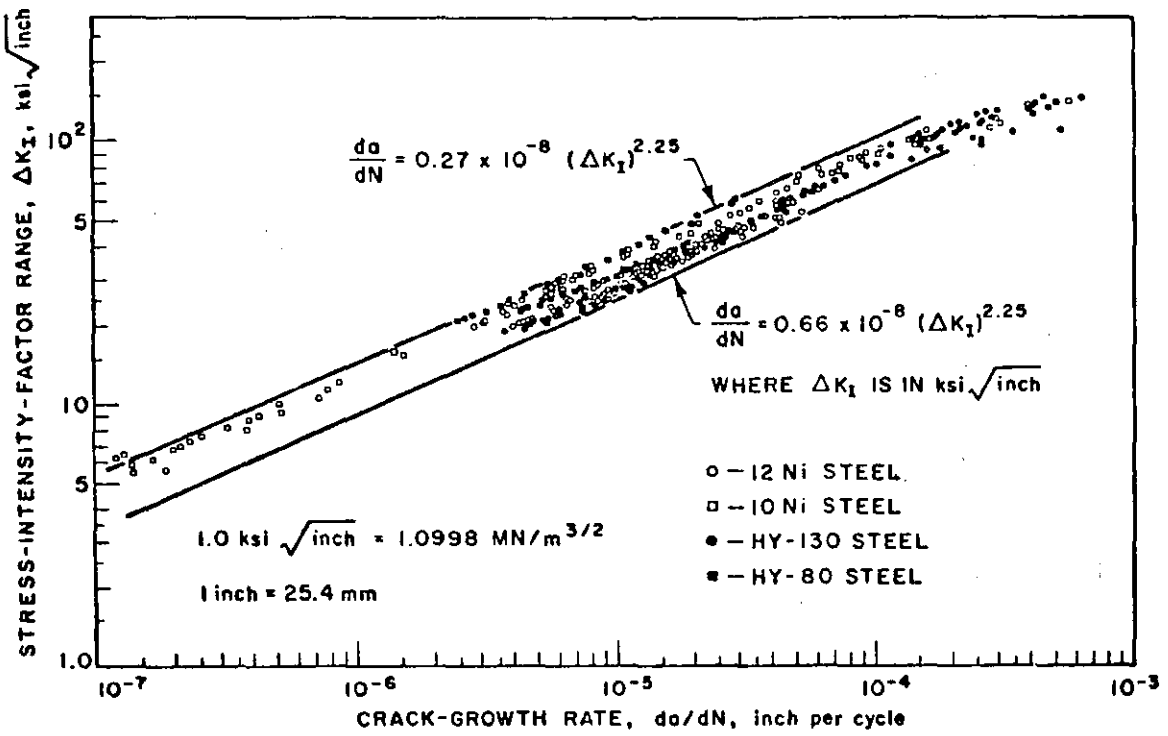

2-20. Summary of Fatigue-Crack-Propagation for Martensitic Steels

a) $\frac{da}{dN} = A(\Delta K^n)$

b) n for martensitic steels is equal to about 2.25.

c) Conservative estimates of growth rates in Region II can be obtained using the equation

$$\frac{da}{dN} = 0.66 \times 10^{-8} (\Delta K_I)^{2.25}$$

NOTES:

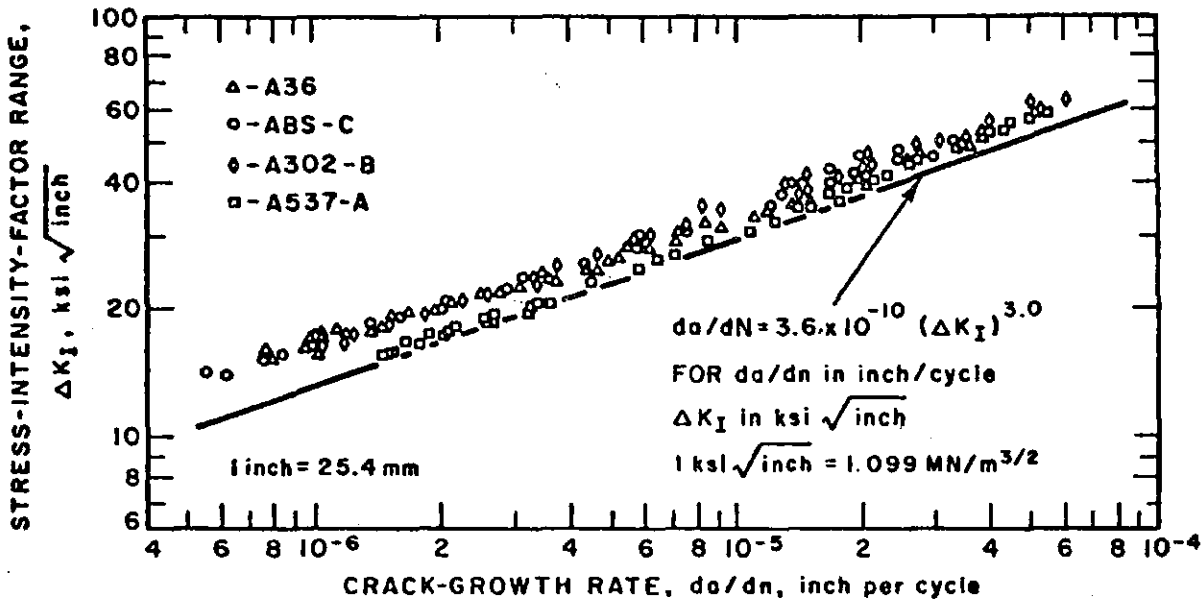

2-21. Summary of Fatigue-Crack-Growth Data for Ferrite-Pearlite Steels

a) $\frac{da}{dN} = a(\Delta K^n)$

b) n for ferrite-pearlite steels is equal to about 3.0.

c) Conservative estimates of growth rates in Region II can be obtained using the equation

$$\frac{da}{dN} = 3.6 \times 10^{-10} (\Delta K_I)^{3.0}$$

NOTES:

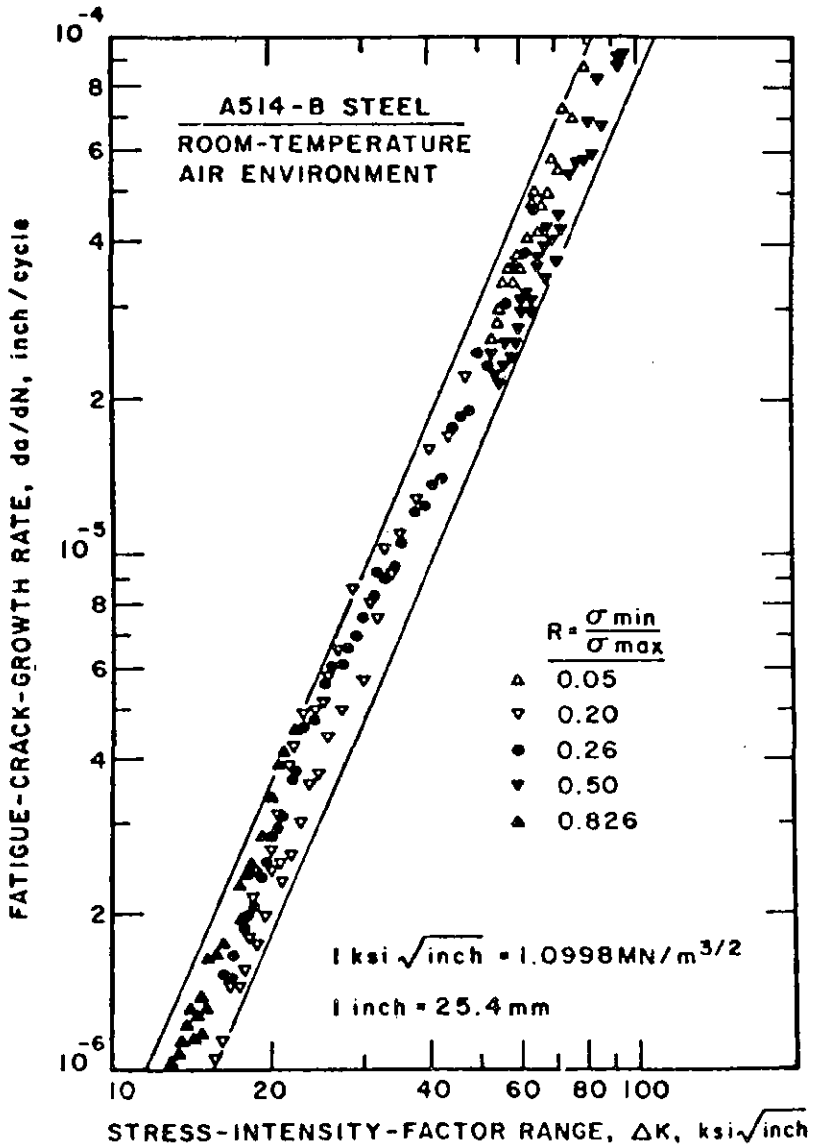

2-22. Crack-Growth Rate as a Function of Stress-Intensity Range for A514-B Steel

a) Unlike the behavior in Region I, the stress ratio has a negligible effect on the growth rate in Region II.

NOTES:

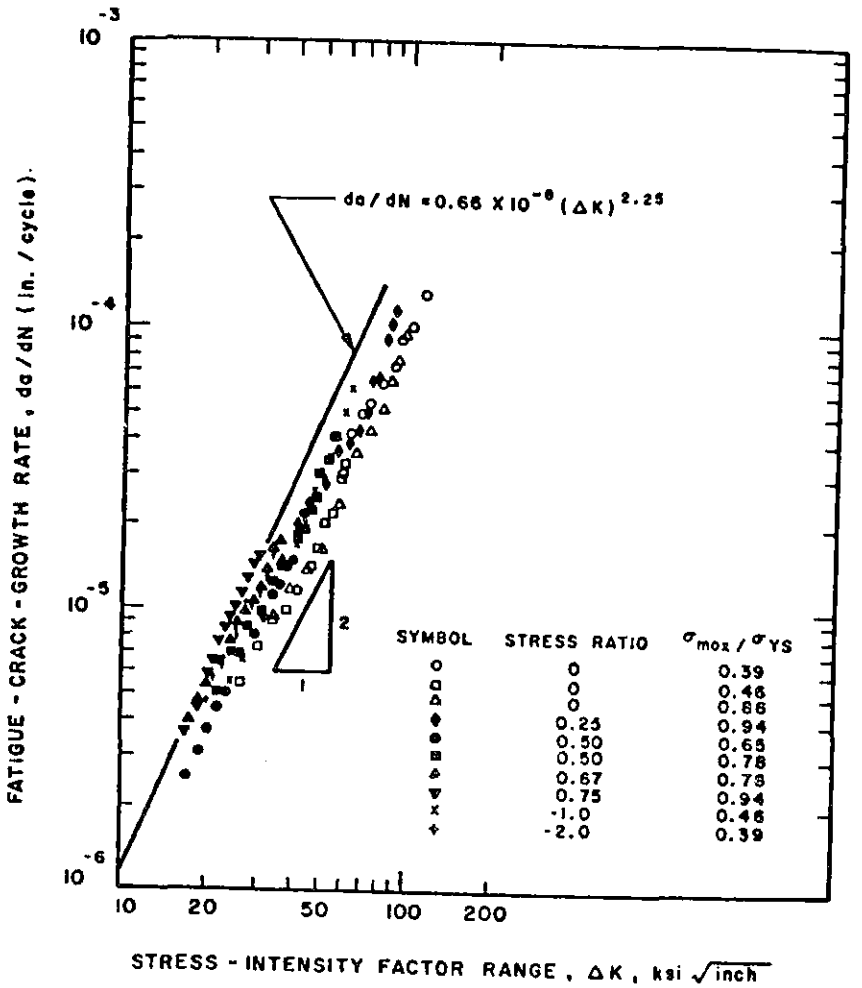

2-23. Effect of Stress Ratio on the Fatigue-Crack-Propagation Rate in a 140 ksi Yield Strength Martensitic Steel

a) Only the tension component of stress is used to calculate ΔK_I for crack propagation because compressive stresses do not generate a driving force at the crack tip.

b) Under those conditions the data in this slide show that stress ratio has a very small effect on growth rate in Region II.

c) The suggested conservative equation for martensitic steels appears to account for these small effects.

NOTES:

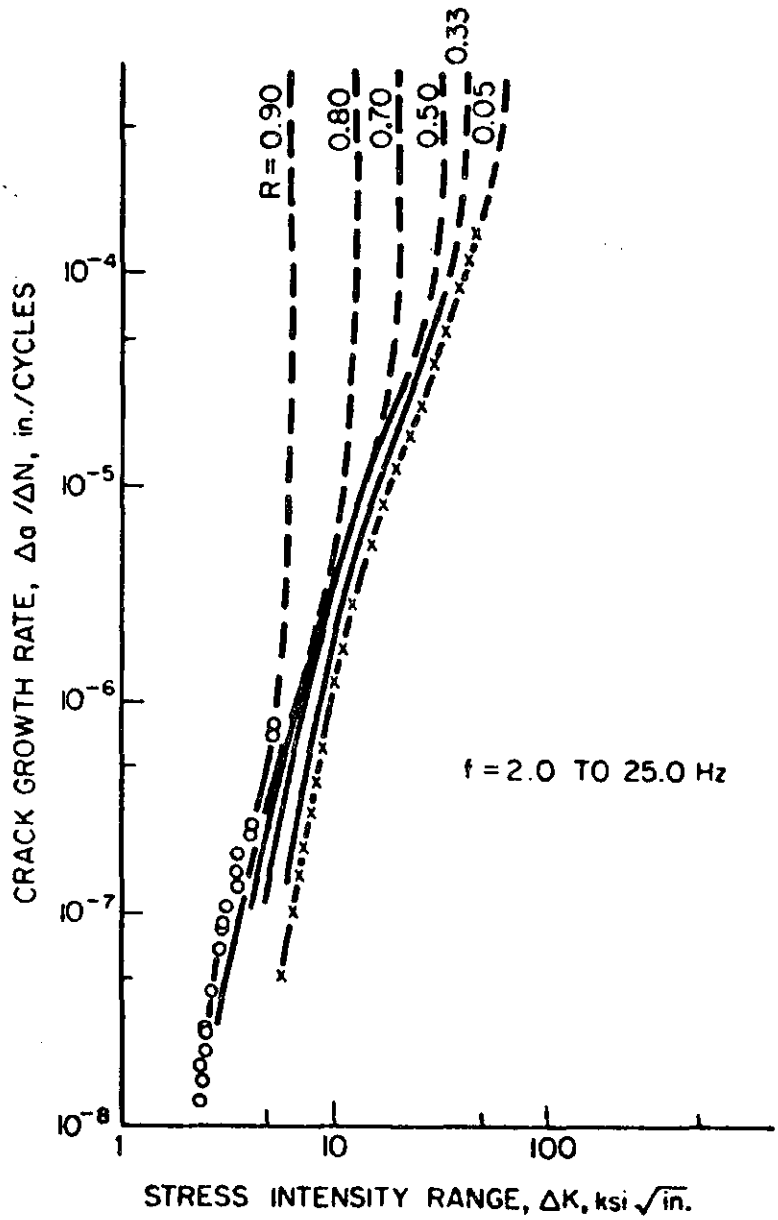

2-24. Effect of Stress Ratio, R, on Fatigue-Crack-Growth Upper Threshold

a) Stress ratio has a significant effect on acceleration in growth rate in Region III.
b) The reason for this effect in Region III is because the acceleration is governed by the value of the maximum stress applied to the specimen.

NOTES:

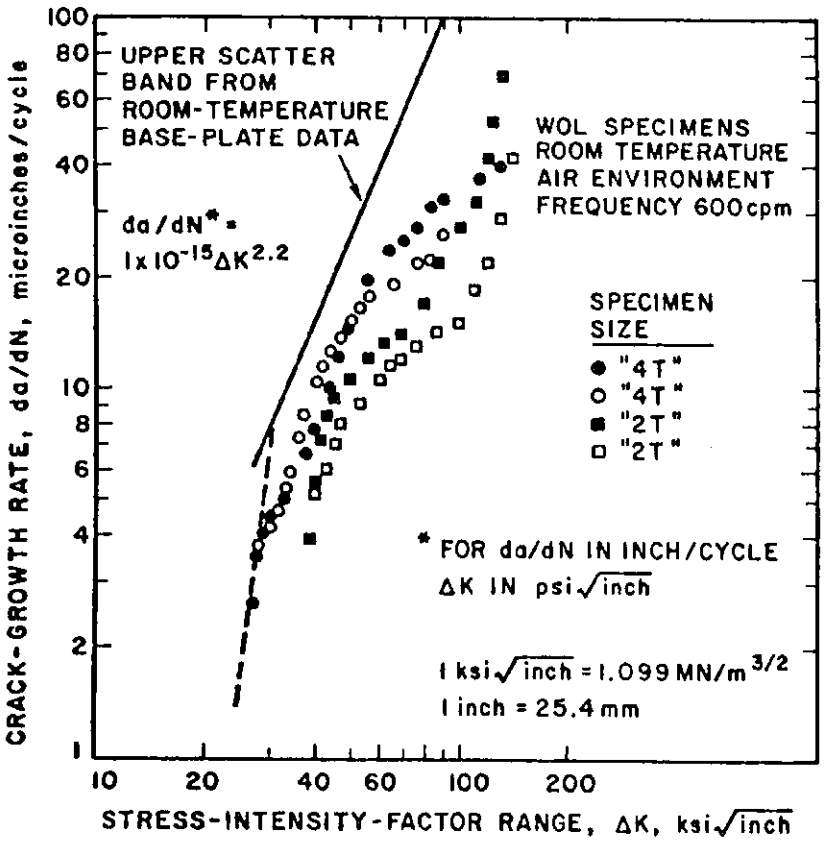

2-25. Effect of Specimen Size on the Crack-Growth-Rate Behavior of A533 GR.B, CL.1 Steel Weld Metal

a) Available data for weld metal indicate that the fatigue-crack-propagation rate in weld metal is equal to or less than in base metal.

NOTES:

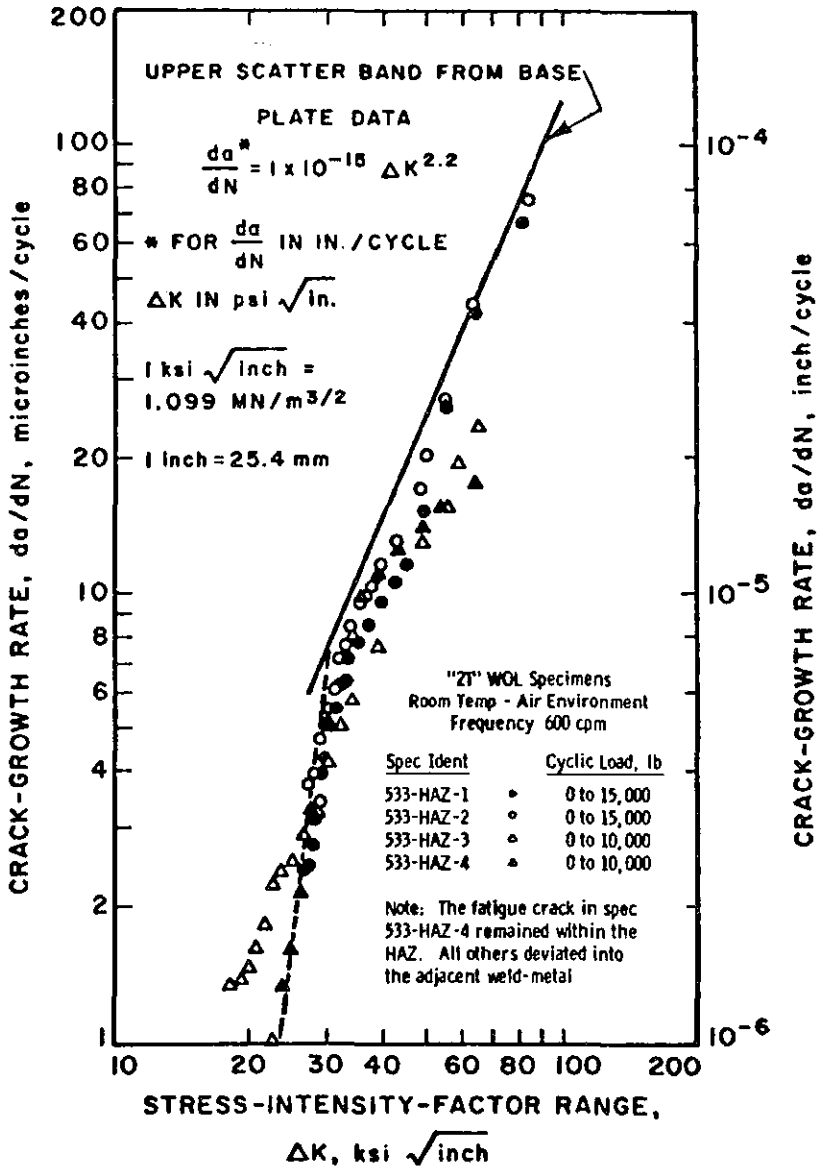

2-26. Fatigue-Crack Growth-Rate Behavior Observed in the Vicinity of the Heat-Affected Zone of an ASTM A533 Gr. B, CL.1 Weldment

a) Available data for heat-affected zone (HAZ) indicate that the fatigue-crack-growth rate in HAZ is equal to or less than for base metal.

b) The fatigue crack does not propagate in the HAZ. It invariably moves out of the HAZ into the base metal or weld metal. This behavior is caused by residual stresses and differences in the properties of the base metal and weld metal resulting in a skewed plastic zone.

NOTES:

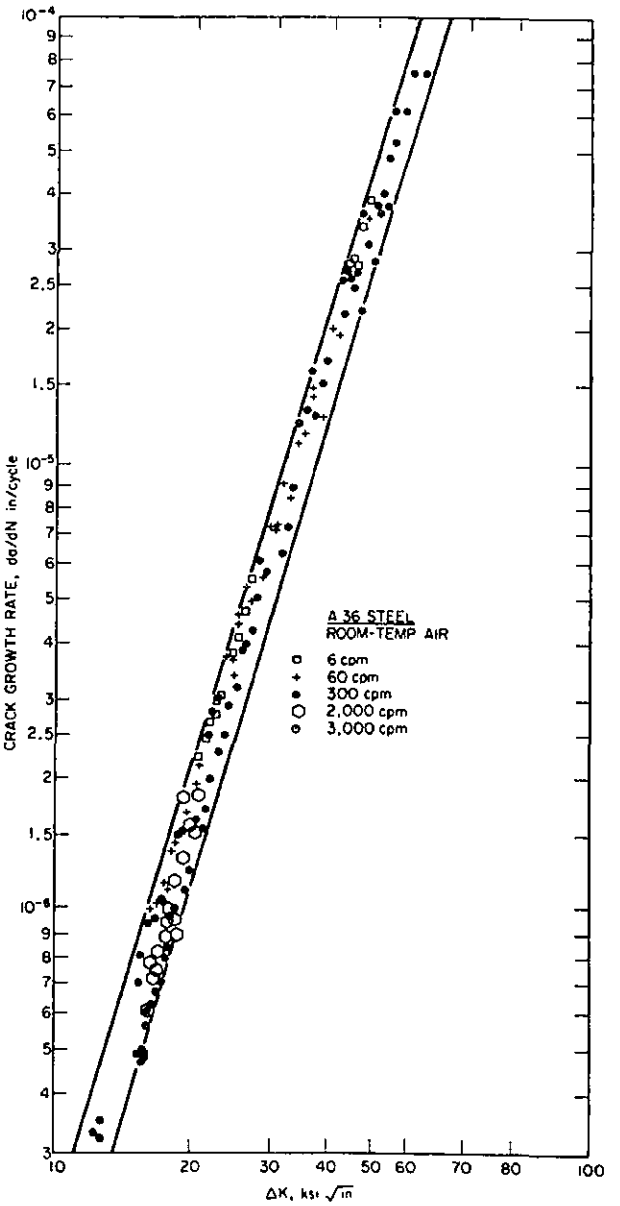

2-27. Effect of Cyclic Frequency on Crack Growth Rates in Benign Environment

a) Frequency of the applied cyclic load appears to have negligible effect on fatigue-crack-growth rate in low-strength steels tested in a benign environment.

b) Frequency could have a very significant effect on the corrosion-fatigue crack-growth rate in an aggressive environment.

NOTES:

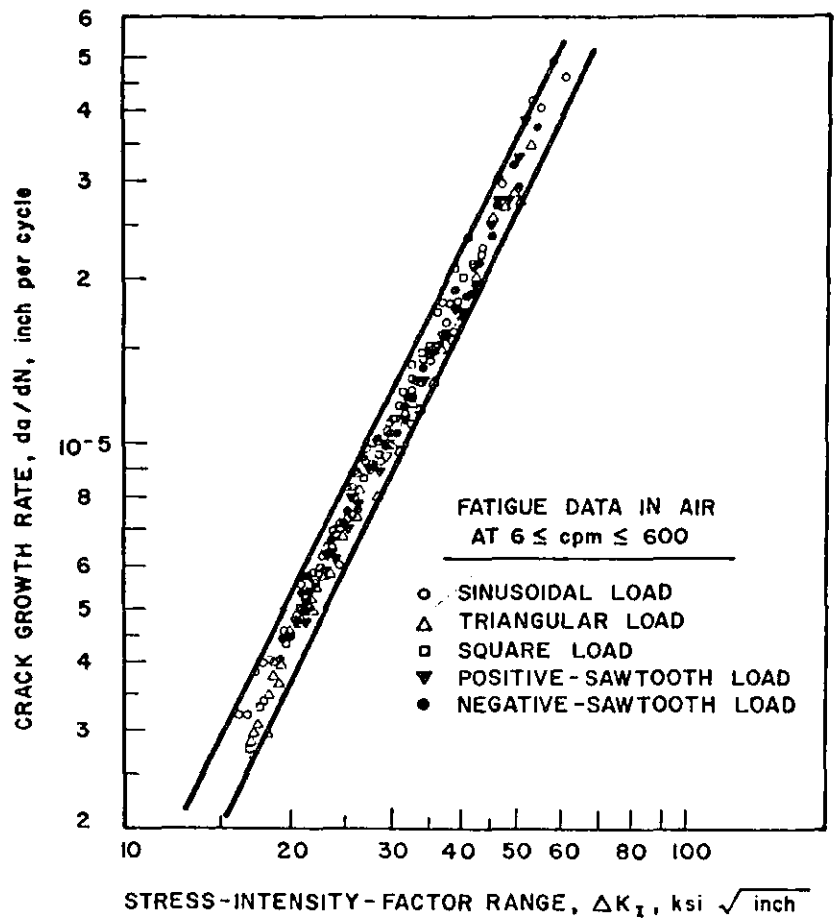

2-28. Fatigue-Crack-Growth Rates in 12Ni-5Cr-3Mo Steel Under Various Cyclic-Stress Fluctuations with Different Stress-Time Profiles

a) Frequency of the applied cyclic load appears to have negligible effect on fatigue-crack-growth rate in high-strength steels tested in a benign environment.

b) It can be concluded that frequency has a negligible effect on da/dN for all steels tested in benign environments.

NOTES:

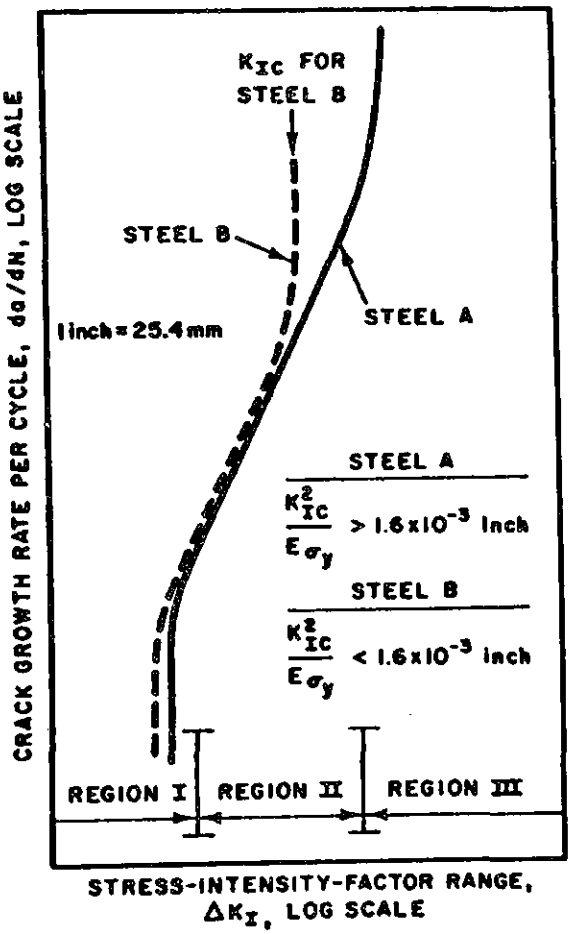

2-29. Schematic Representation of Fatigue-Crack Growth in Steel

a) Region III defines the region where acceleration in the rate of growth occurs.
b) Acceleration in the rate of fatigue-crack growth for brittle materials occurs when the maximum stress-intensity factor value approaches the critical stress-intensity factor value, K_{Ic}, for the material.
c) Acceleration in the rate of fatigue-crack growth for ductile materials occurs when the maximum stress-intensity-factor value satisfies the equation

$$K = 0.05 \sqrt{E\ \sigma_{ys}}$$

NOTES:

$$K = \sigma \sqrt{a}\, f(a/W)$$

$$\frac{da}{dN} = A(\Delta K)^n$$

$$\int_0^N dN = \int_{a_i}^{a_f} \frac{da}{A(\sigma \sqrt{a}\, f)^n}$$

$$N = \frac{1}{A \sigma^n} \int_{a_i}^{a_f} \frac{da}{a^{n/2} f^n}$$

2-30. Crack Propagation Laws and Integration

NOTES:

f = Constant

$$N = \frac{a_i\left[1 - (a_i/a_f)^{(n/2-1)}\right]}{(n/2-1)\,A(\sigma\sqrt{a_i}\,f)^n}$$

$$N = \frac{a_i\left[1 - (\dot{a}_i/\dot{a}_f)^{(1-2/n)}\right]}{(n/2-1)\,\dot{a}_i}$$

2-31. Crack Propagation Laws and Integration for f, a constant and A_i, A_f, $\dot{A}_i$, $\dot{A}_f$, are the initial and final crack lengths and the initial and final crack growth rates respectively.

NOTES:

K_{IC} VALUES FOR BRIDGE STEELS

$$K_{IC} = f \begin{pmatrix} \text{TEMPERATURE,} \\ \text{LOADING RATE,} \\ \text{PLATE THICKNESS} \end{pmatrix}$$

2-32. K_{IC} Values depend on Temperature, Loading Rate, Thickness (constraint)

NOTES:

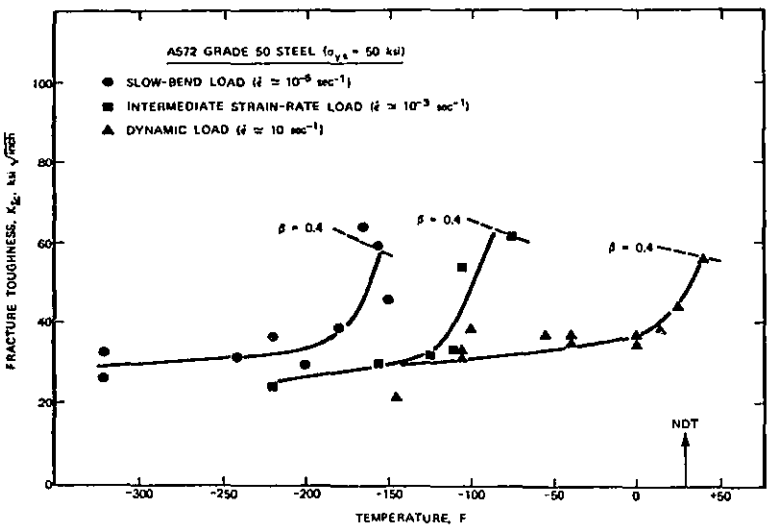

2-33. Effect of Temperature and Loading Rate on K_{Ic} for A572 Steel

a) slow
b) intermediate (Ottawa bridge test results plus others for bridges)
c) dynamic

NOTES:

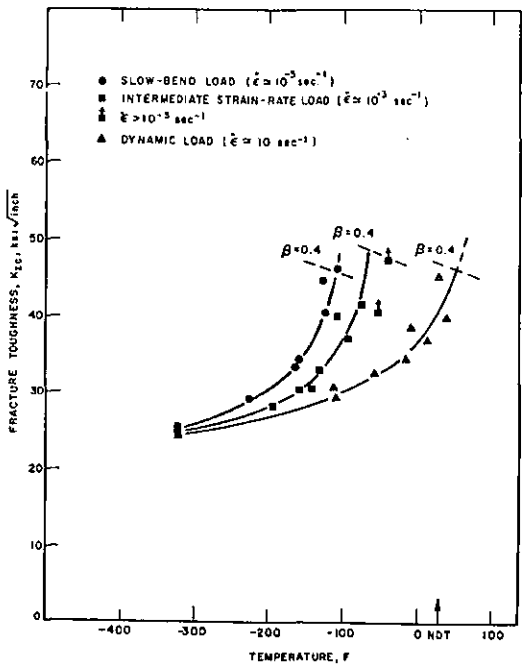

2-34. Effect of Temperature and Loading Rate on K_{Ic} for A36 Steel

a) Note metallurgical effect as limiting temperature is reached
b) significant improvement in toughness
c) basis of AASHTO for intermediate loading rate

NOTES:

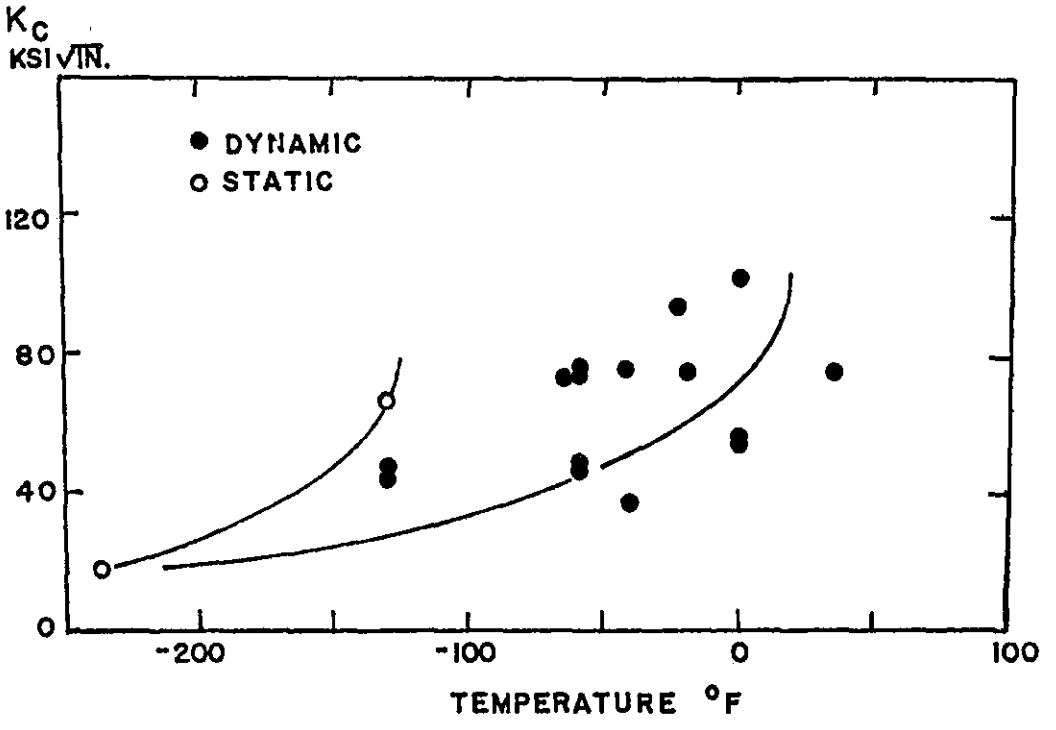

2-35. Test Results for A588

a) scatter
b) effect of loading rate
c) actual behavior better than guaranteed minimum

NOTES:

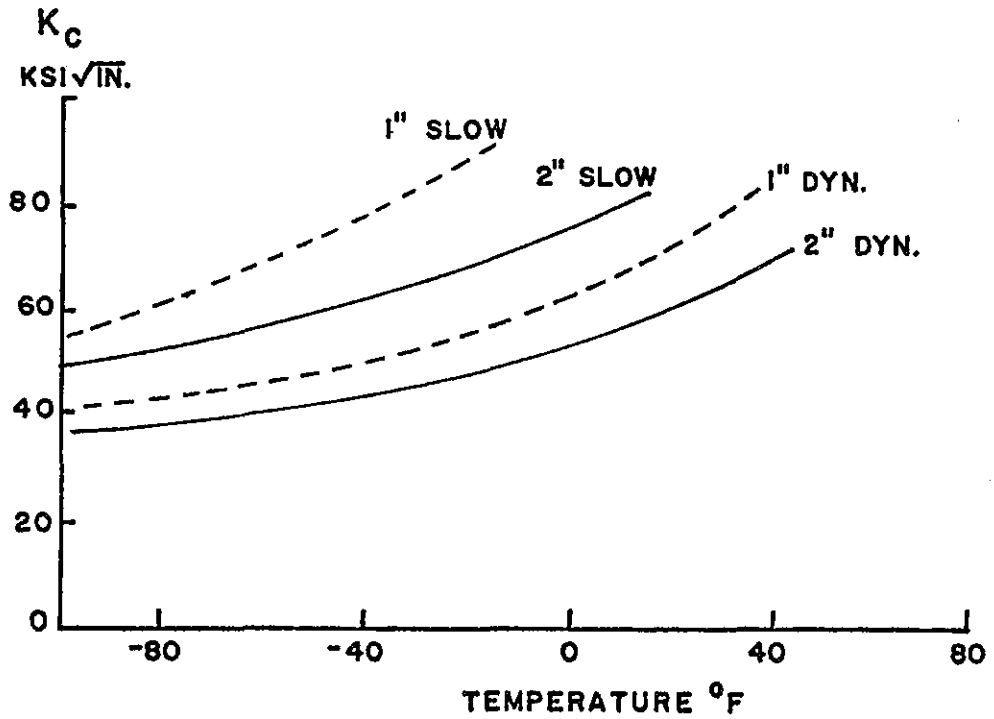

2-36. A441 Test Results from Lehigh

a) thickness
b) loading rate
c) temperature

NOTES:

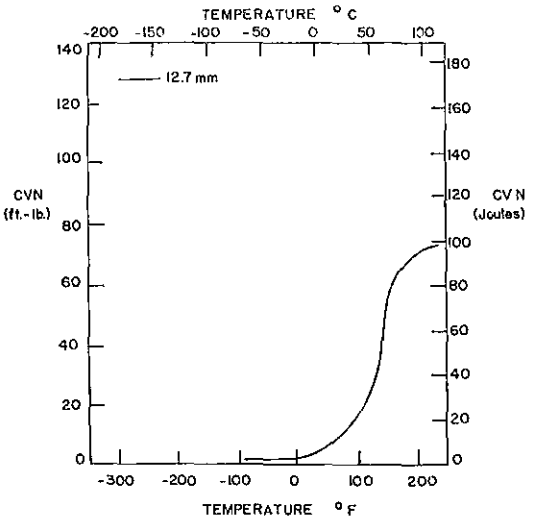

2-37. CVN Results A7 Steel. (Lehigh Data)

NOTES:

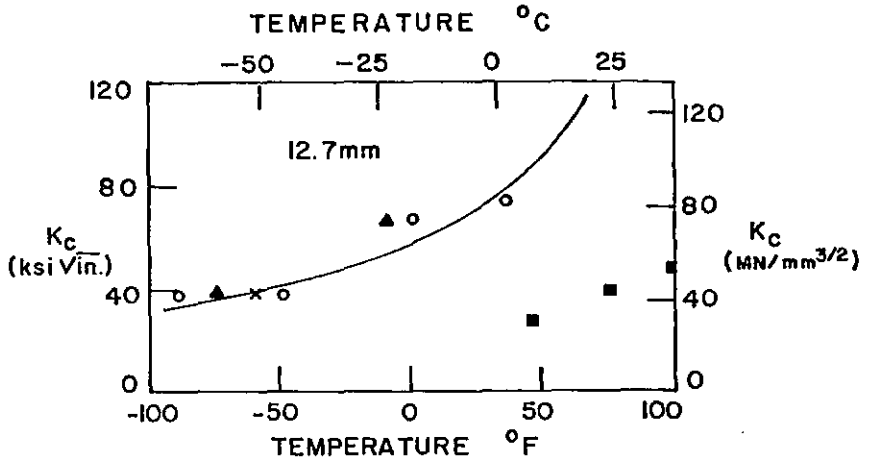

2-38. K Data A7 Steel --- "R" Values, o Dynamic K Values, ● Static K Values, ■ Estimate from Equation 4.5, x Point of Maximum Valid K. (Lehigh Data).

NOTES:

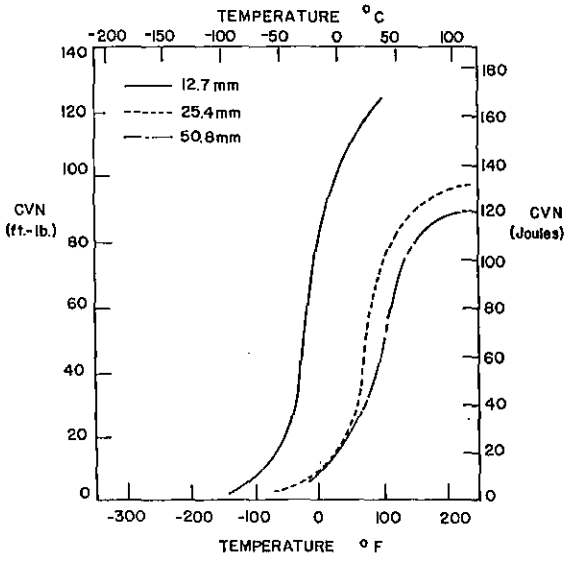

2-39. CVN Results A242 Steel. (Lehigh Data)

NOTES:

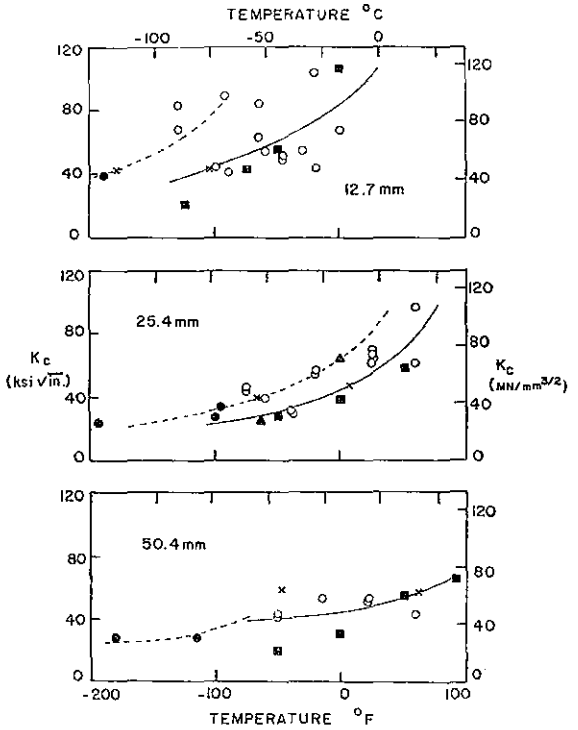

2-40. K Data A242 Steel --- "R" Values, o Dynamic K Values, ● Static K Values, ■ Estimate from Equation 4.5, x Point of Maximum Valid K. (Lehigh Data)

NOTES:

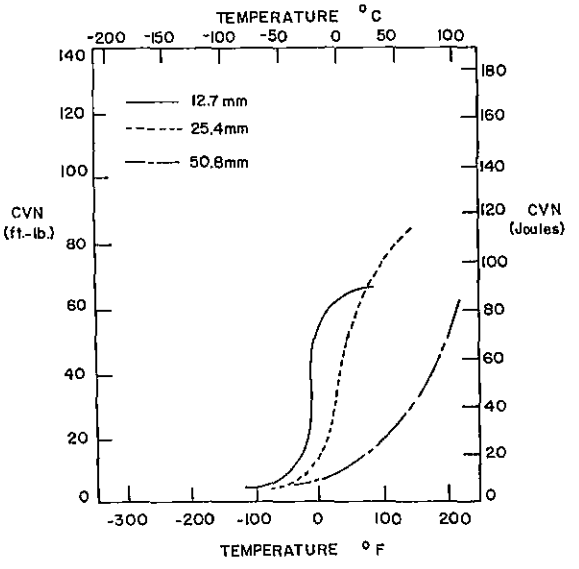

2-41. CVN Results A440 Steel. (Lehigh Data)

NOTES:

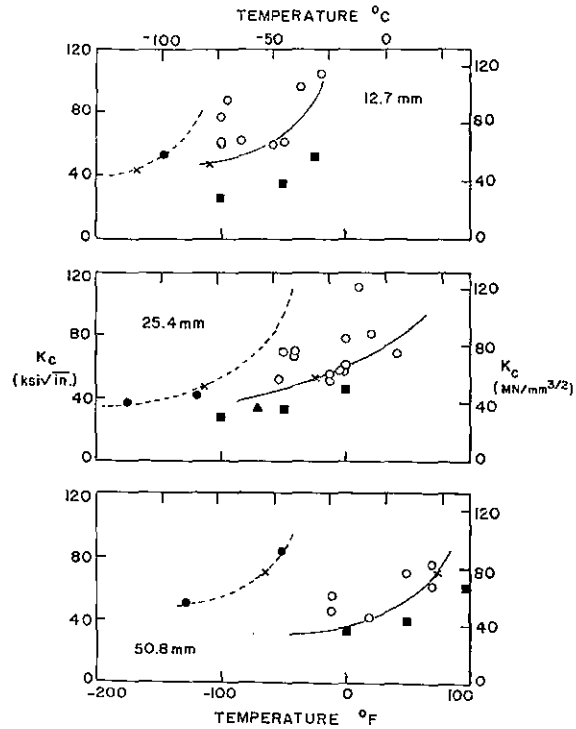

2-42. K Data A440 Steel --- "R" Values, o Dynamic K Values, • Static K Values, ■ Estimate from Equation 4.5, x Point of Maximum Valid K. (Lehigh Data)

NOTES:

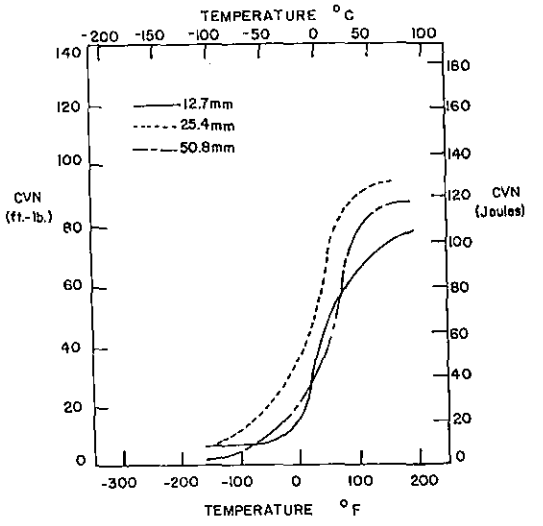

2-43. CVN Results A588 Steel. (Lehigh Data)

NOTES:

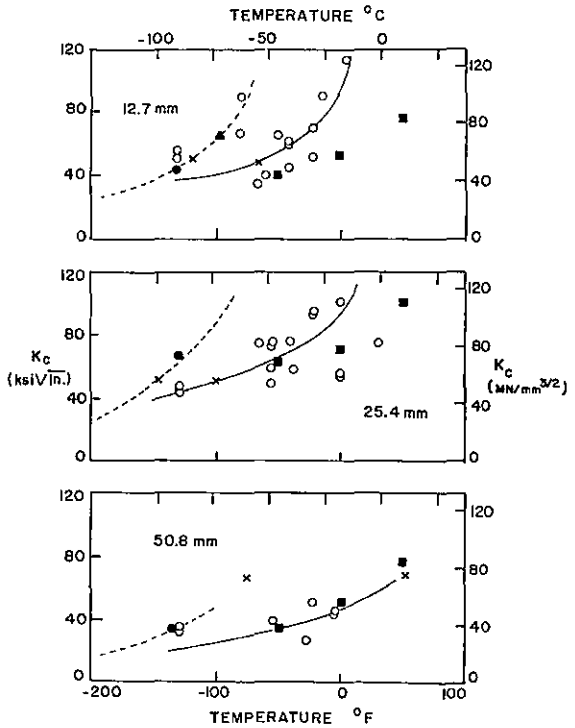

2-44. K Data A588 Steel --- "R" Values, o Dynamic K Values, ● Static K Values, ■ Estimate from Equation 4.5, x Point of Maximum Valid K. (Lehigh Data)

NOTES:

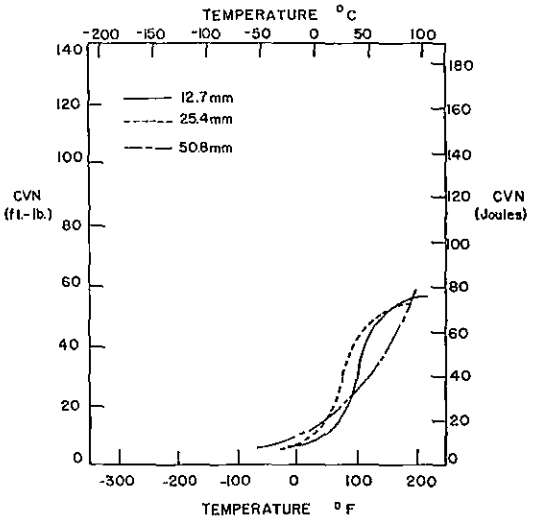

2-45. CVN Results SAE1035 Steel (Lehigh Data)

NOTES:

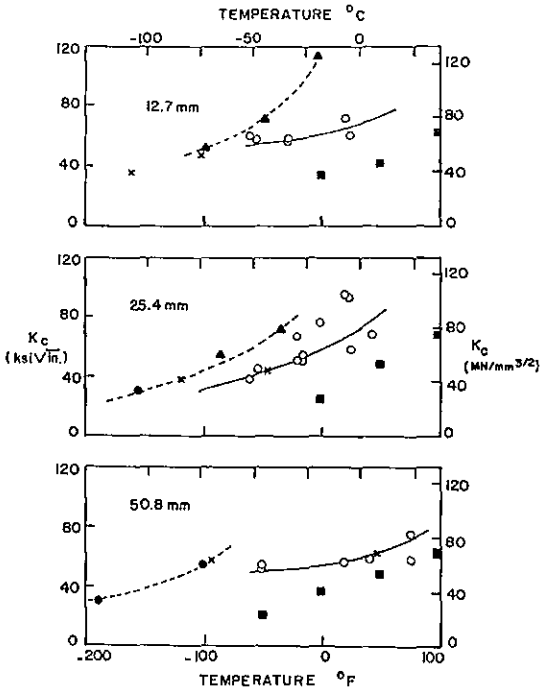

2-46. K Data SAE1035 Steel --- "R" Values, o Dynamic K Values, • Static K Values, ■ Estimate from Equation 4.5, x Point of Maximum Valid K. (Lehigh Data)

NOTES:

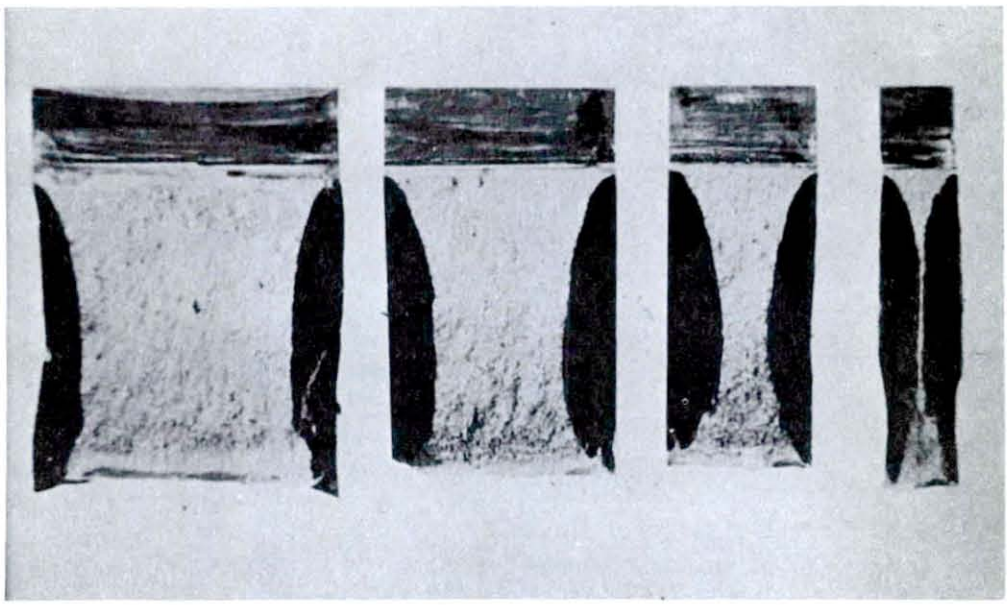

2-47. Fracture Surfaces Showing Effect of Thickness

a) original 2-inch thick plate
b) specimens from center-line (no metallurgical effect
c) shear lip size similar

NOTES:

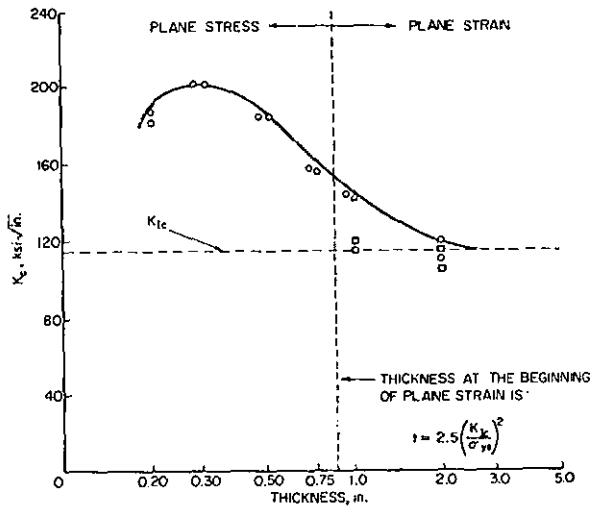

2-48. Test Results showing Effect of Thickness

a) plane stress is function of thickness
b) plane strain is minimum value
c) constraint similar to thickness

NOTES:

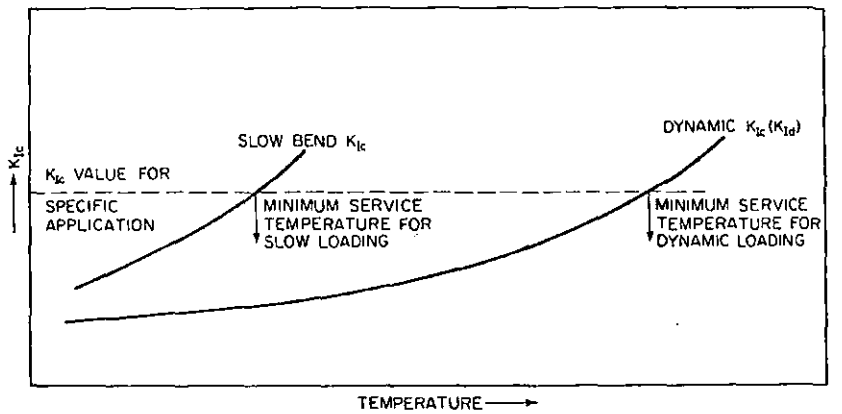

2-49. Design Significance of Loading Rate

a) basis of AASHTO toughness requirements

NOTES:

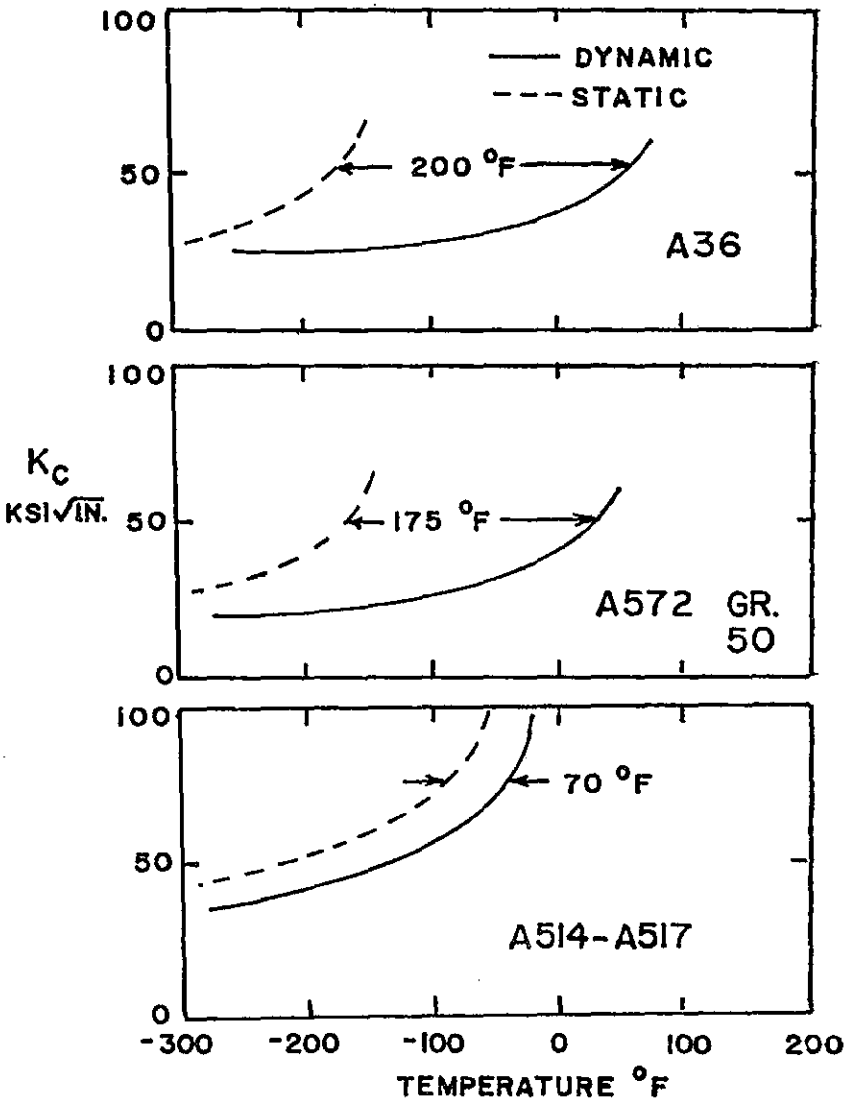

2-50. Loading Rate Shift for A36, A572, A514

a) measured by several investigators
b) depends on yield strength

NOTES:

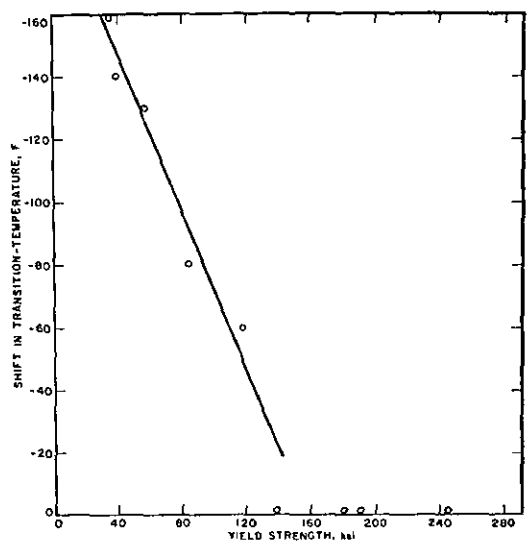

2-51. Loading Rate Shift is a function of Yield Strength

a) $T_S = 215 - 1.5\ \sigma_{ys}$ $(\sigma_{ys} < 140)$

b) $T_S = 0$ $(\sigma_{ys} > 140)$

NOTES:

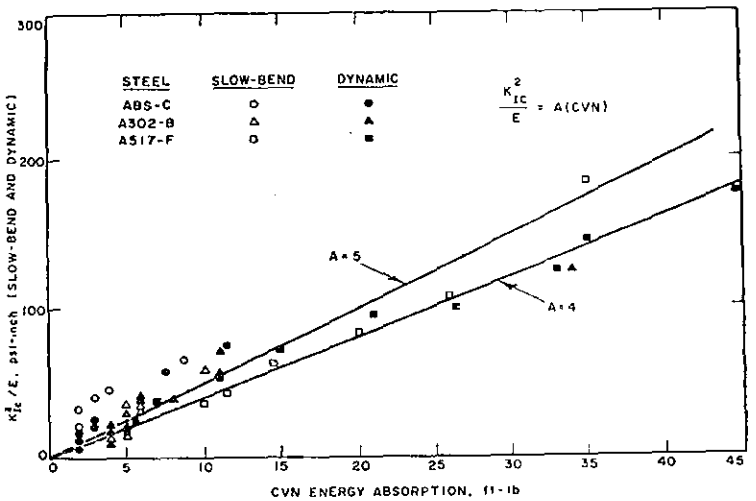

2-52. K_{Ic} - CVN Correlation

a) static CVN - static K_{Ic}
b) impact CVN - dyanmic K_{Ic}
c) fatigue cracked
d) A = 5 for regular CVN impact

NOTES:

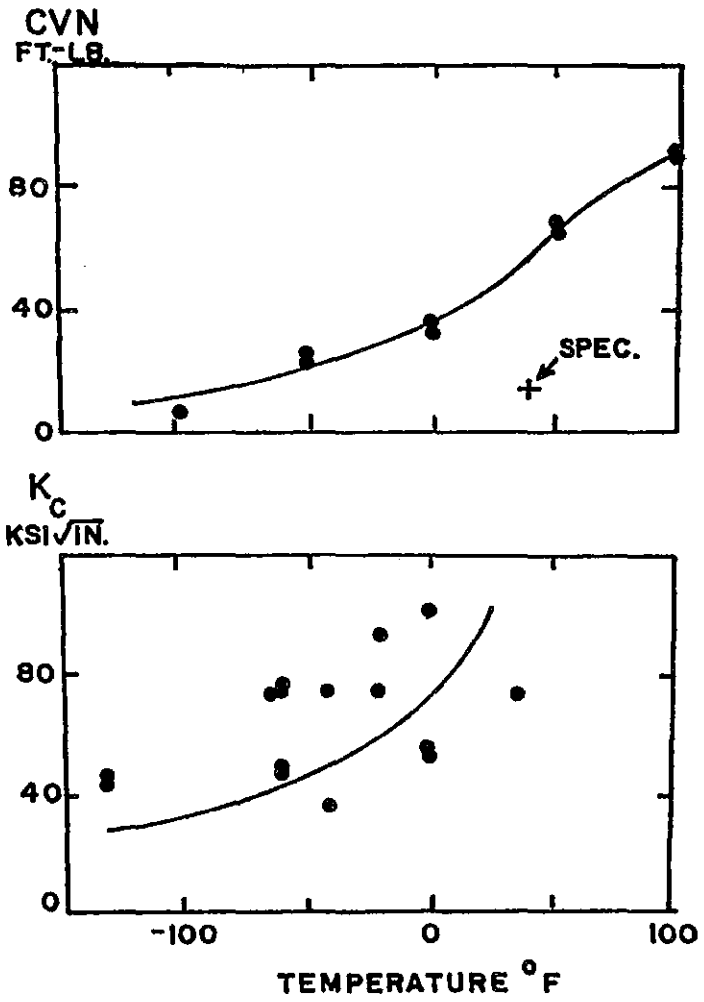

2-53. AASHTO Specification Based on CVN

a) Quality Control Test
b) Minimum Value in impact test
c) Loading Rate Shift

NOTES:

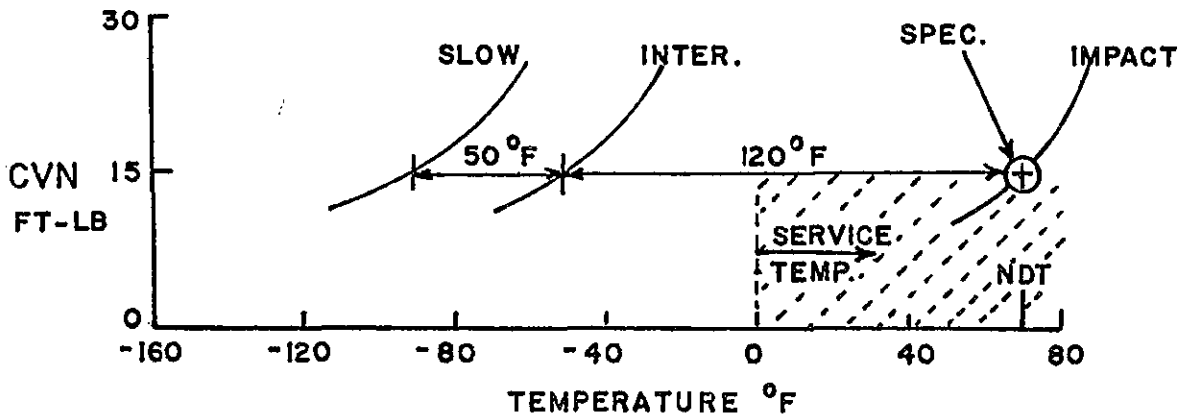

2-54. Class I AASHTO Toughness Specifications

a) Service Temperature - 0°F
b) CVN impact - 15 ft lb at +70°F
c) Loading Rate Shift
d) Intermediate loading rate behavior

NOTES:

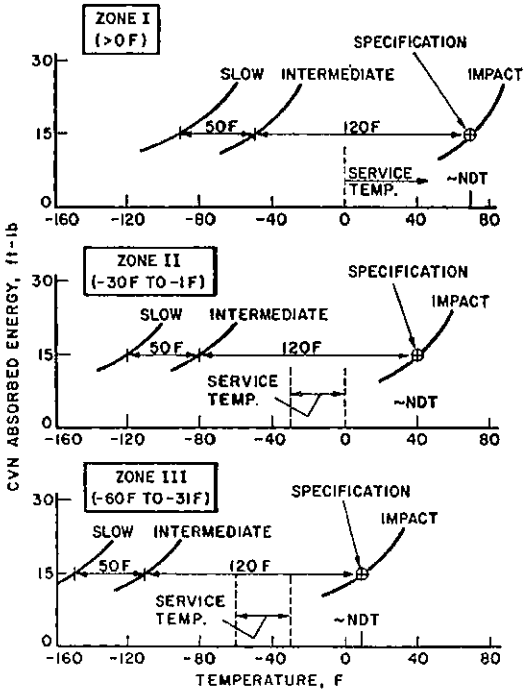

2-55. AASHTO - 3 zones

a) > 0°F

b) -30 to 0°F

c) -60 to -30°F

NOTES:

ASTM Designation	Thickness (in.)	CVN Impact Value, ft lb		
		Zone 1*	Zone 2*	Zone 3*
A36		15 @ 70°F	15 @ 40°F	15 @ 10°F
A572	Up to 4 in. mechanically fastened	15 @ 70°F	15 @ 40°F	15 @ 10°F
	Up to 2 in. welded	15 @ 70°F	15 @ 40°F	15 @ 10°F
A440		15 @ 70°F	15 @ 40°F	15 @ 10°F
A441		15 @ 70°F	15 @ 40°F	15 @ 10°F
A242		15 @ 70°F	15 @ 40°F	15 @ 10°F
A588**	Up to 4 in. mechanically fastened	15 @ 70°F	15 @ 40°F	15 @ 10°F
	Up to 2 in. welded	15 @ 70°F	15 @ 40°F	15 @ 10°F
	Over 2 in. welded	20 @ 70°F	20 @ 40°F	20 @ 10°F
A514	Up to 4 in. mechanically fastened	25 @ 30°F	25 @ 0°F	25 @ −30°F
	Up to 2½ in. welded	25 @ 30°F	25 @ 0°F	25 @ −30°F
	Between 2½–4 in. welded	35 @ 30°F	35 @ 0°F	35 @ −30°F

*Zone 1: minimum service temperature 0°F and above.
Zone 2: minimum service temperature from −1° to −30°F.
Zone 3: minimum service temperature from −31° to −60°F.
**If the yield point of the material exceeds 65 ksi, the temperature for the CVN value for acceptability shall be reduced by 15°F for each increment of 10 ksi above 65 ksi.

2-56. Table of AASHTO Toughness Requirements

a) Effect of σ_{ys}
b) Effect of thickness
c) Effect of stored elastic energy

NOTES:

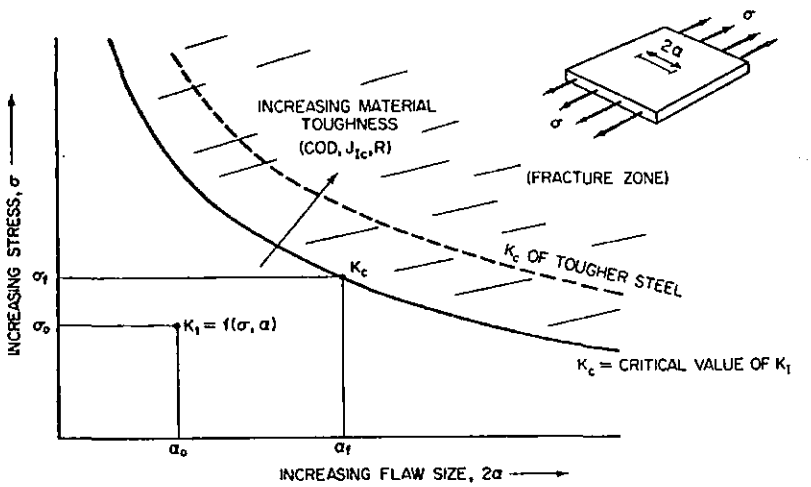

2-57. Overall Fracture Control Plan

a) Materials
b) Design
c) Fabrication
d) Loading
e) Sub-critical crack growth (fatigue, stress corrosion)

NOTES:

FRACTURE CONTROL PLAN

$K_{IC} = f(\sigma, \sqrt{a})$

K_{IC} = MATERIAL PROPERTY

σ = DESIGN

a = FABRICATION AND INSPECTION

2-58. Fracture Control Plan

a) Materials
b) Design
c) Fabrication
d) Brittle fracture problems will not be solved merely by AASHTO toughness requirements

NOTES:

INFORMATION REQUIRED FOR FRACTURE CONTROL PLAN FOR BRIDGES

1) TOUGHNESS VALUES OF BRIDGE STEELS

2) FLAW SIZES IN BRIDGE MEMBERS

3) FATIGUE CRACK GROWTH BEHAVIOR

4) FRACTURE TOUGHNESS CRITERIA

2-59. Information Required for Fracture Control

a) Toughness Values
b) Flaw Szies
c) Fatigue Behavior
d) Criteria
e) Service experience

NOTES:

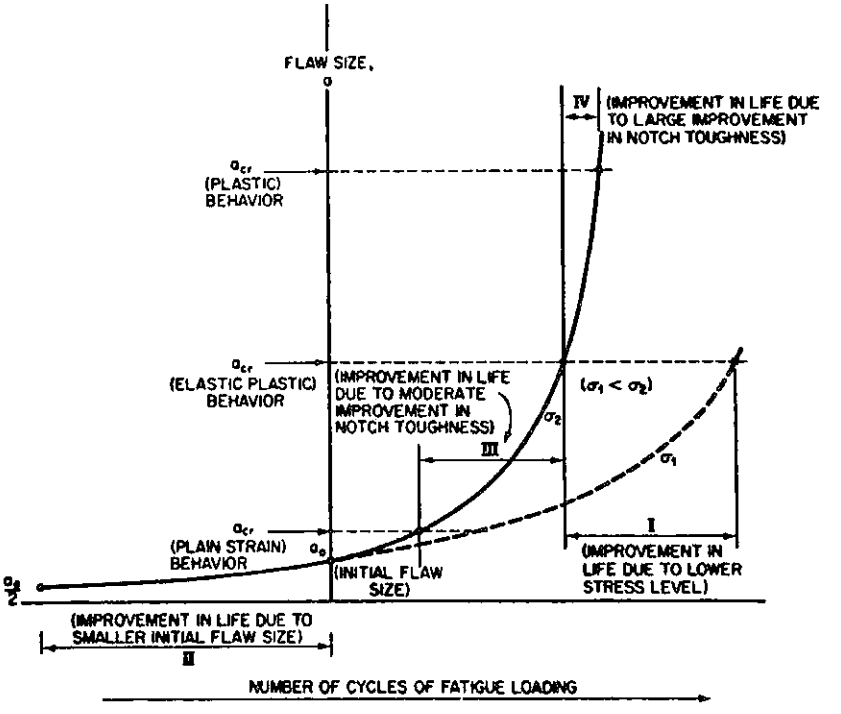

2-60. Effect of Fracture Resistant Design

a) Region I - effect of lower stress range
b) Region II - effect of better fabrication and inspection
c) Region III - effect of moderate level of notch toughness (AASHTO)
d) Region IV - effect of even higher toughness.

NOTES:

FATIGUE LIFE

CRACK INITIATION

CRACK PROPAGATION

FINAL FAILURE

2-61. Fracture Control

a) Crack Initiation
b) Subcritical-crack propagation
c) Unstable crack propagation

Fracture Control Plan

NOTES:

FIGURES - SESSION 3

FATIGUE CRACK PROPAGATION OF BRIDGE STEELS - SPECIMENS AND TESTS -

BASIS FOR CURRENT DESIGN RULES

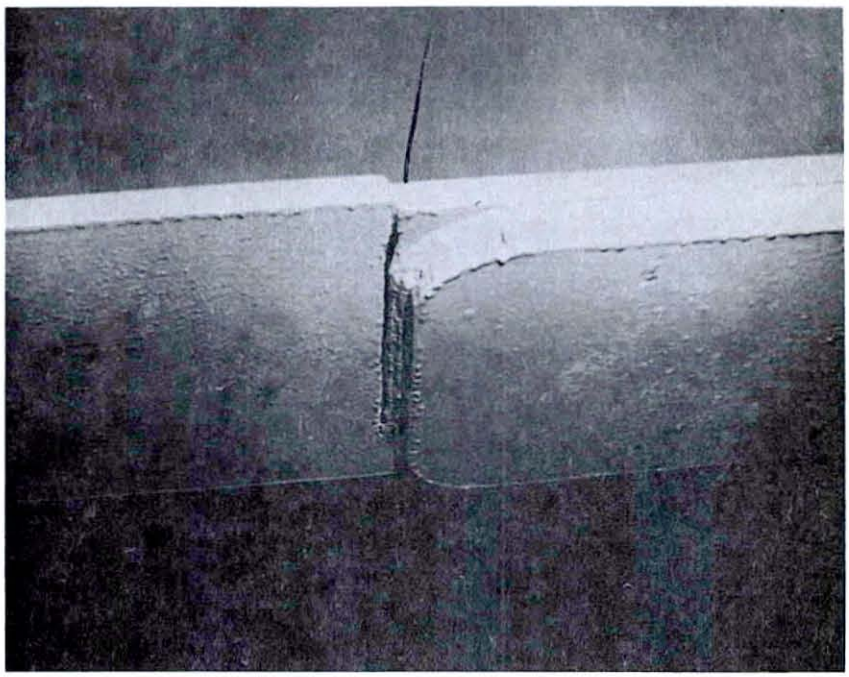

3-1. Fatigue crack that formed in the Yellow Mill Pond Bridge.

NOTES:

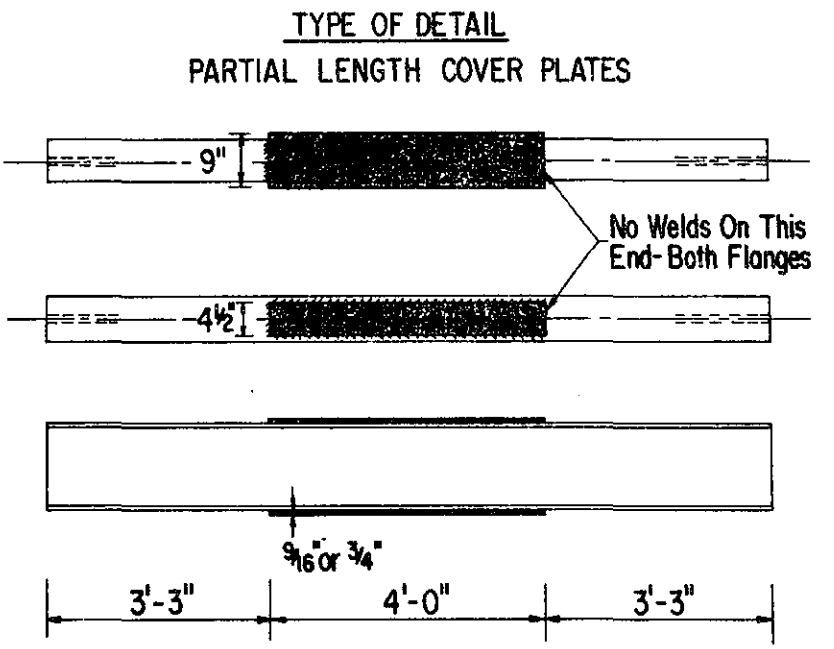

3-2. Schematic of simulated prototype connections that were tested to determine the basic fatigue strength.

NOTES:

3-3. Fatigue crack that has grown from an initial imperfection in the web-flange fillet weld.

NOTES:

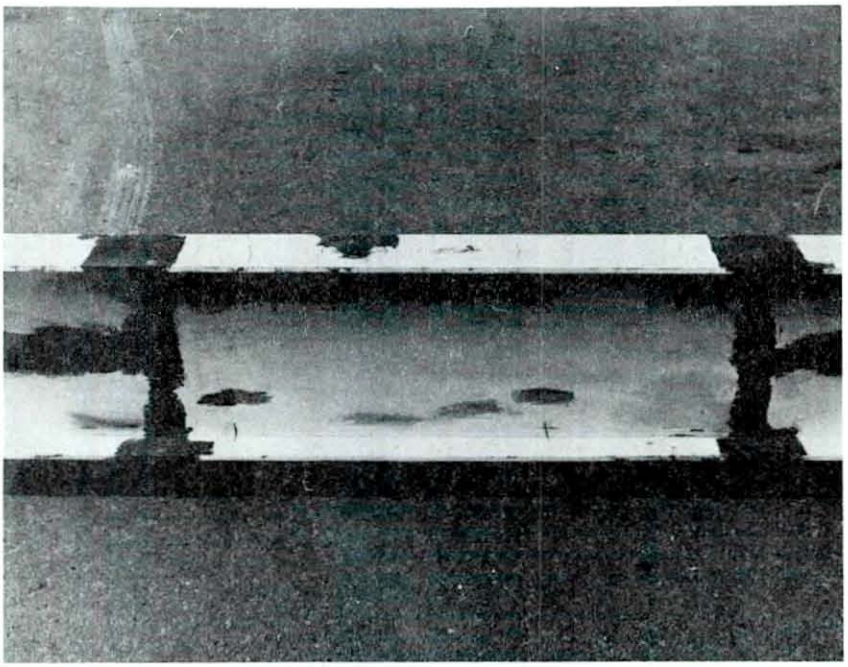

3-4. An overview of a fatigue cracked beam which shows fatigue cracks in both the tension and compression flanges.

NOTES:

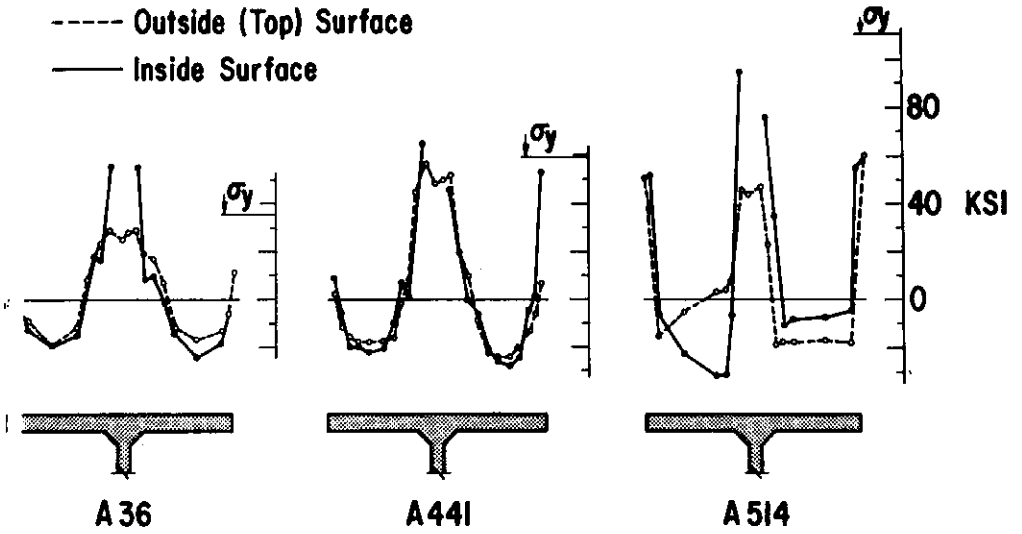

RESIDUAL STRESSES IN WELDED BEAMS

3-5. Welding residual tensial stresses for A36, A440 and A514 steel welded beams.

NOTES:

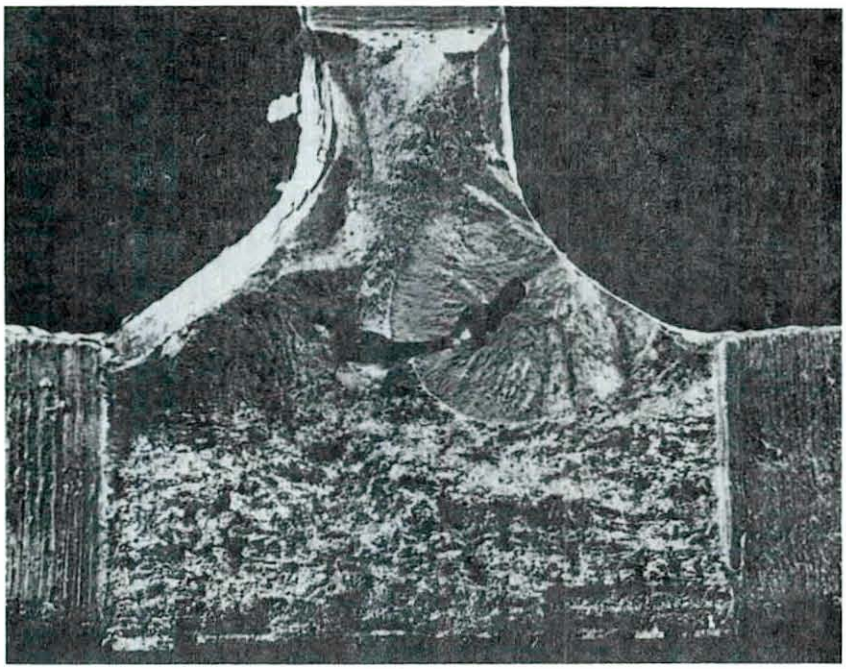

3-6. Small initial fatigue crack that has grown from an initial porosity or gas pocket. Crack diameter approximately .08 inches.

NOTES:

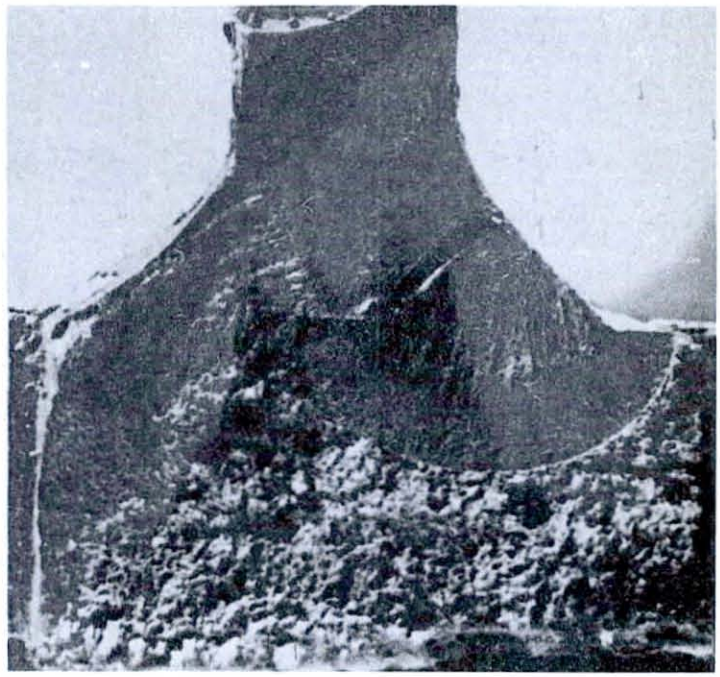

3-7. Growth of crack from porosity maintaining its penny shape.

NOTES:

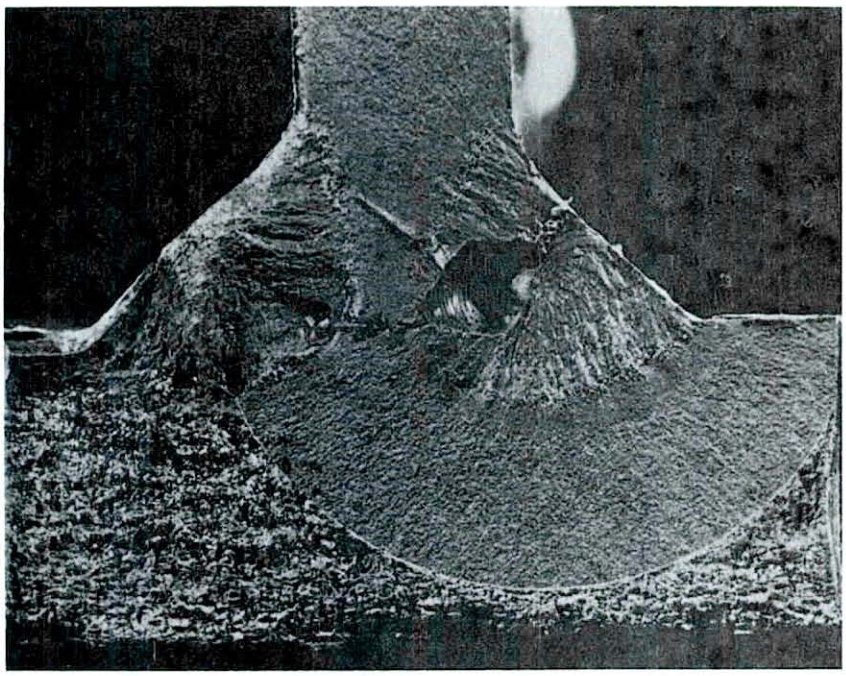

3-8. Penny shaped crack being maintained until crack has penetrated the bottom flange surface.

NOTES:

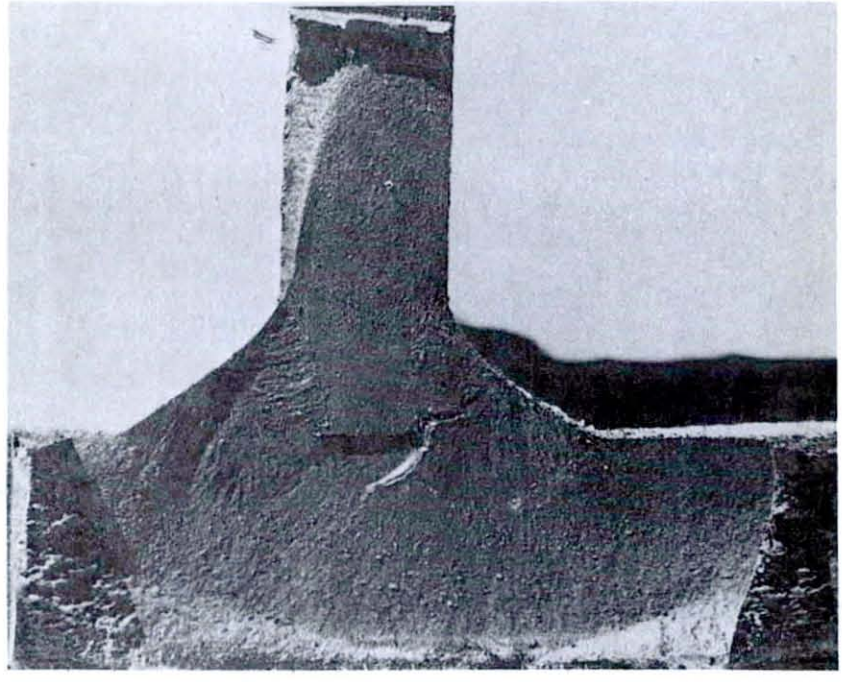

3-9. Final fracture exhibiting very high rates of crack growth near the edges of the flange.

NOTES:

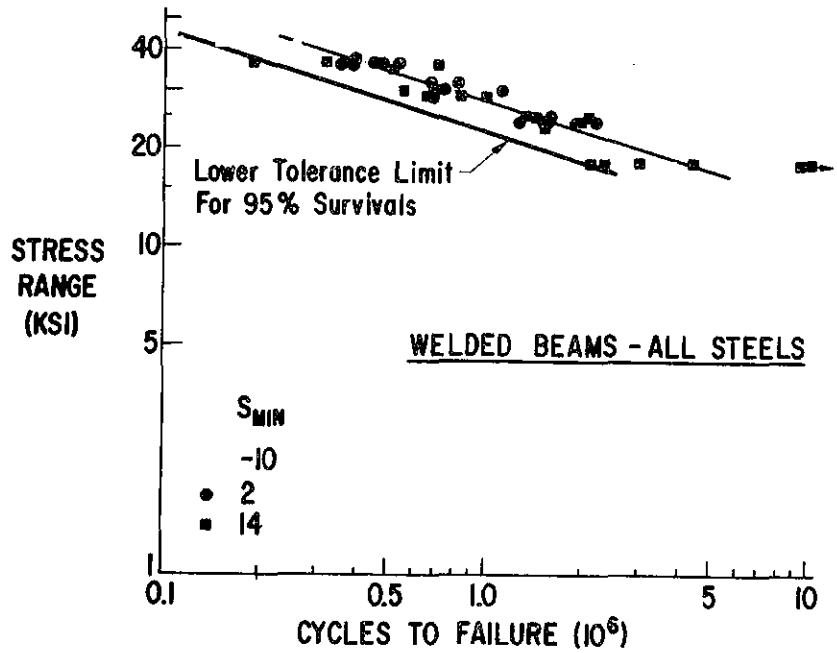

3-10. Stress range versus cycle life plot as a function of three levels of minimum stress. No influence of minimum stress or stress ratio.

NOTES:

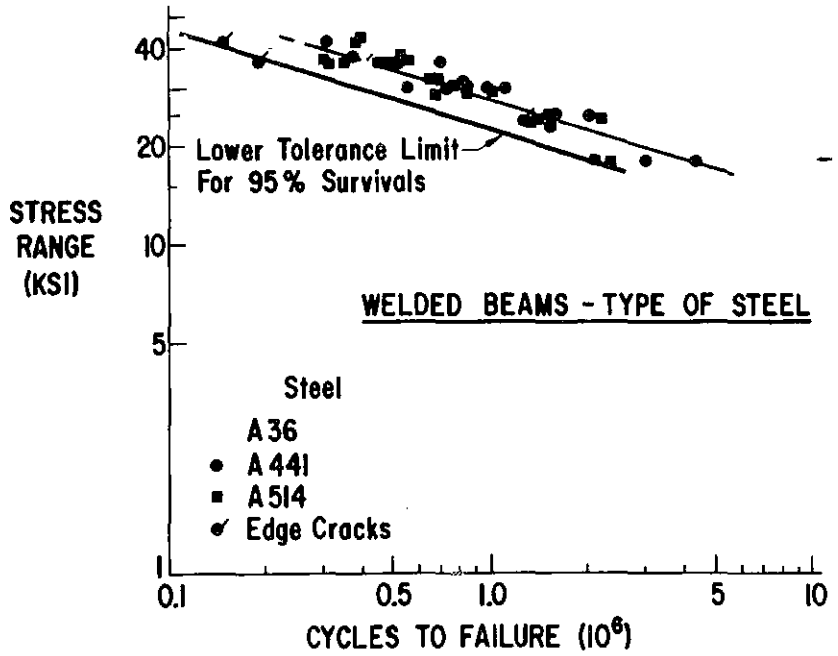

3-11. Stress range plotted as a function of cycle life for welded built-up beam as a function of the grade of steel. Yield point between 36 and 100 ksi shows no significance.

NOTES:

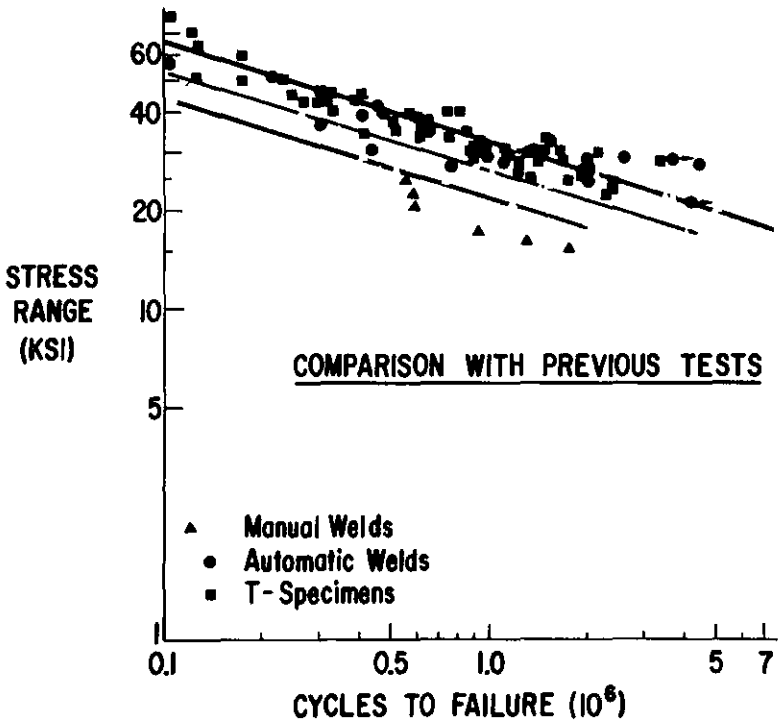

3-12. Comparison of results from the NCHRP Program with earlier studies that were undertaken since 1940. Good correlation, with small simulated specimens typically falling near the upper bound.

NOTES:

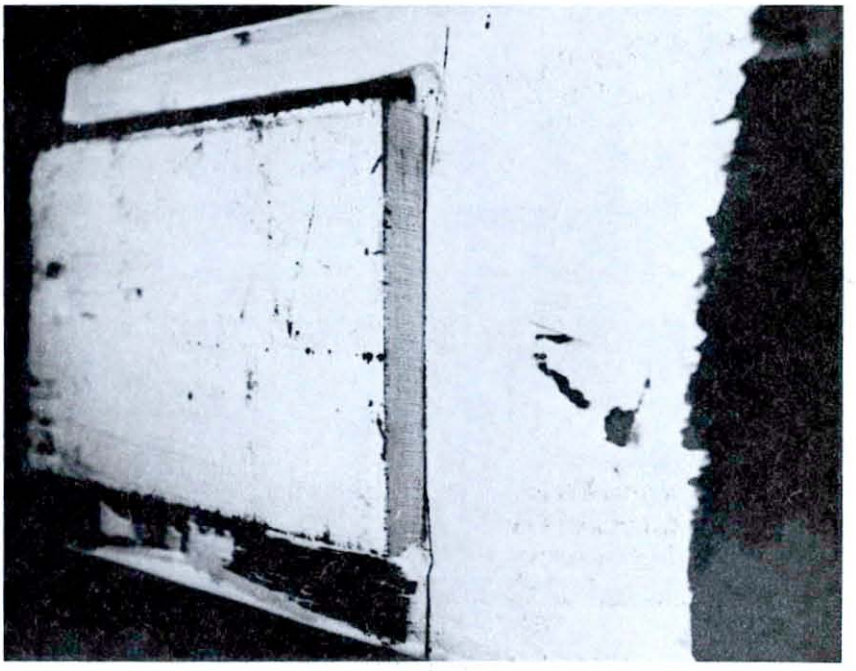

3-13. Fatigue crack formation at the termination of the weld toe of a longitudinal weld attaching a cover plate to a beam flange.

NOTES:

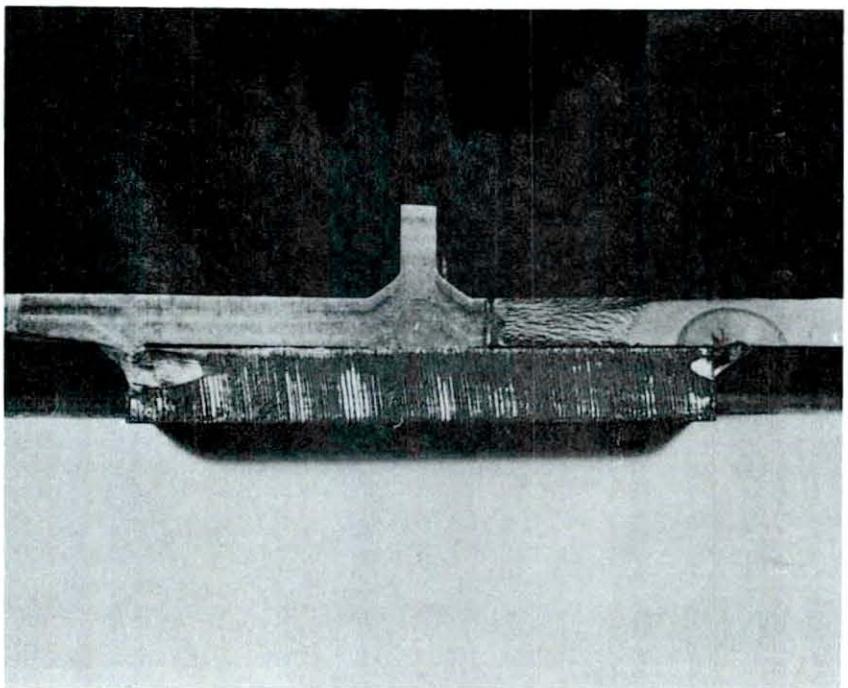

3-14. Fatigue fracture surface showing growth of crack from weld termination as a semi-eliptical crack until it has penetrated the flange thickness.

NOTES:

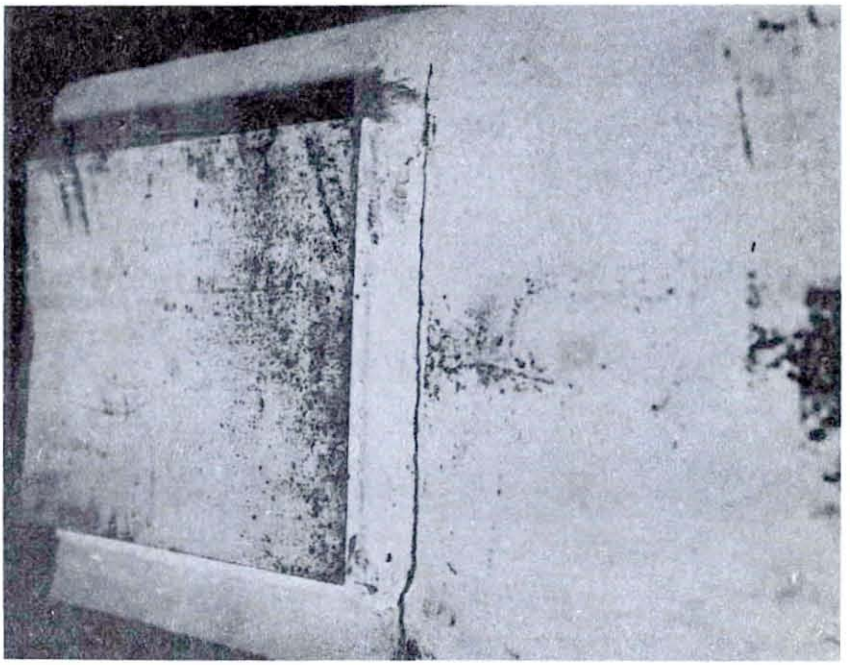

3-15. The formation of a fatigue crack at the end of a cover plate with transverse end welds.

NOTES:

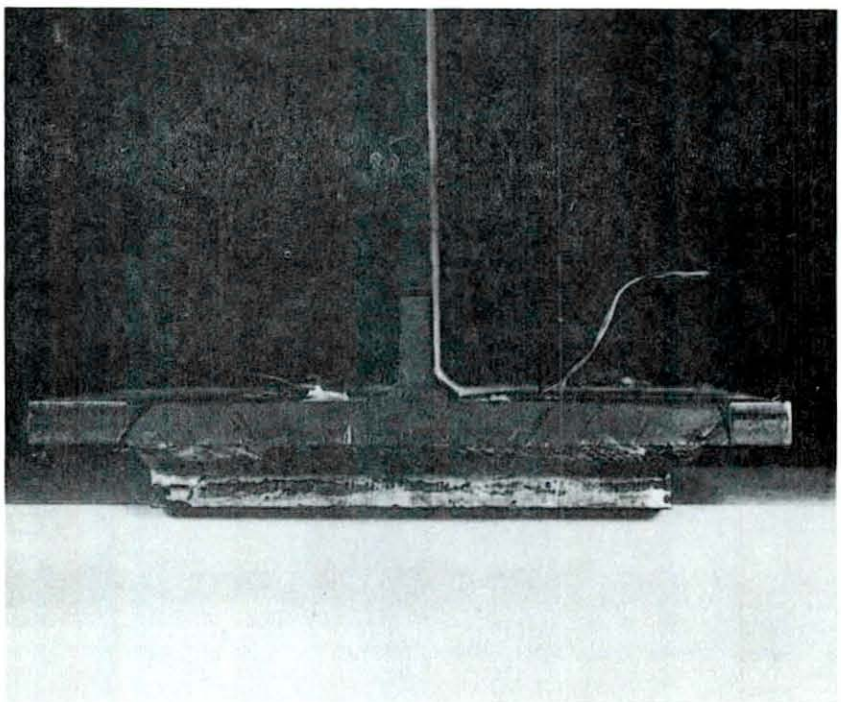

3-16. Fatigue fracture surface of transverse end welded cover plate showing semi-eliptical surface crack. Growth can be observed all along weld toe.

NOTES:

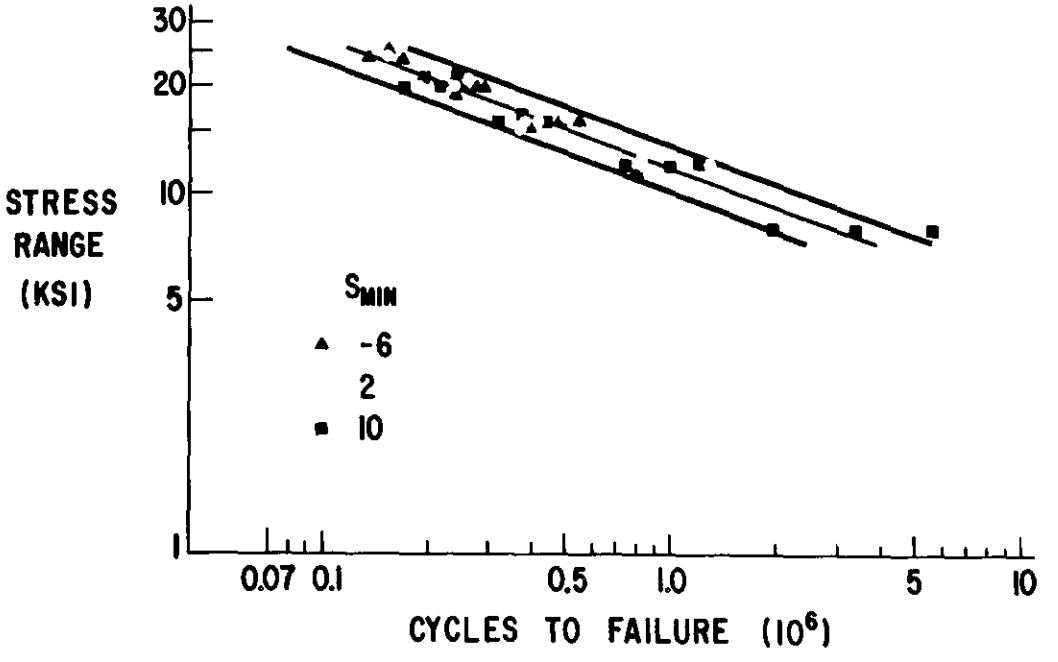

3-17. The test data for A36 steel cover-plated beams plotted with stress range as a function of cycle life. Several levels of minimum stress show no effect on the fatigue strength.

NOTES:

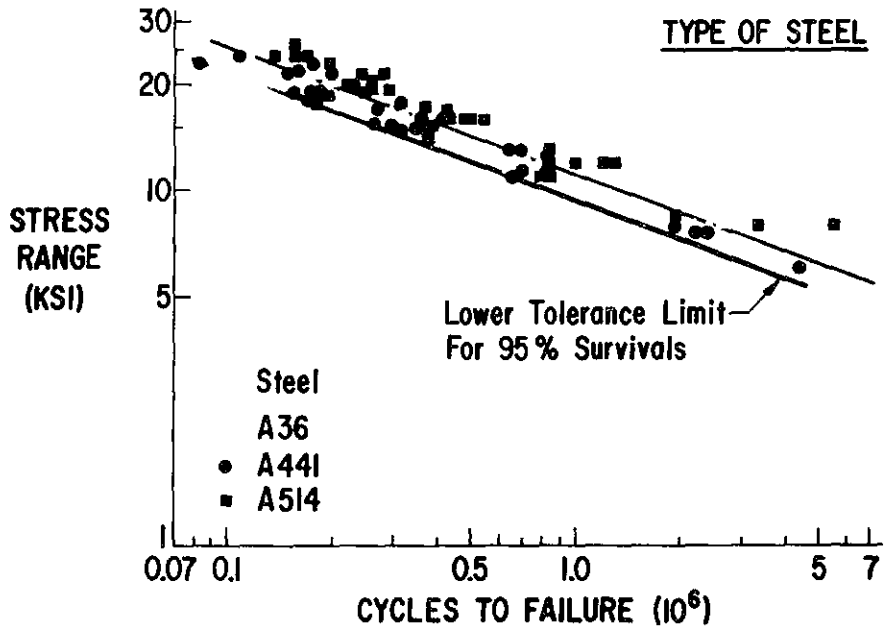

3-18. The test results for three grades of ferrite pearlite steel ranging in point from 36 to 100 ksi are compared with stress range as a function of cycle life. Type of steel does not influence fatigue strength.

NOTES:

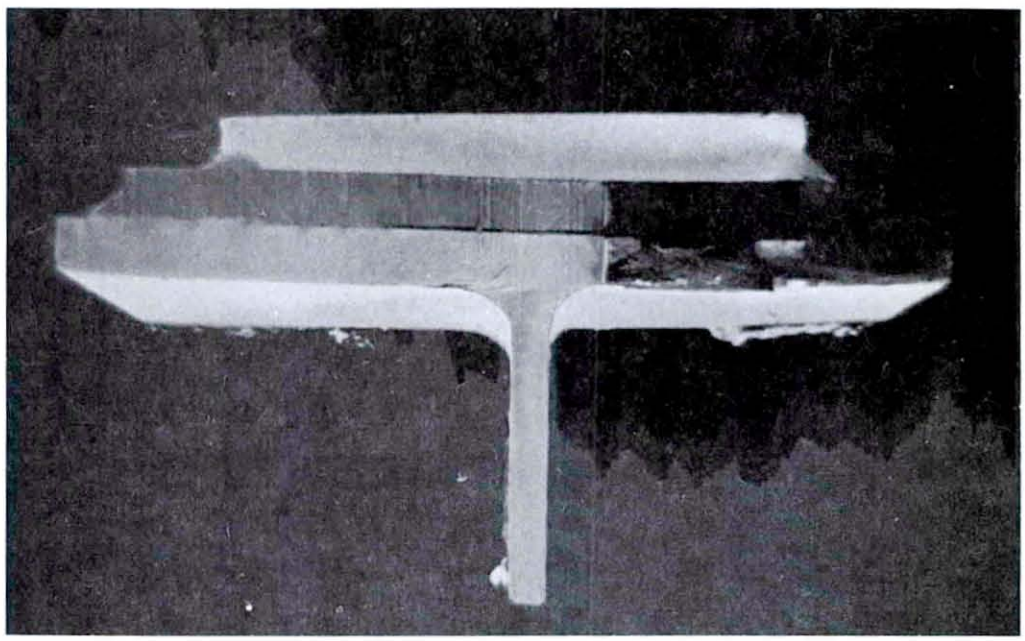

3-19. A multiple cover-plated beam where fatigue crack growth has penetrated the primary cover plate and entered into the beam flange via the continuous longitudinal weld.

NOTES:

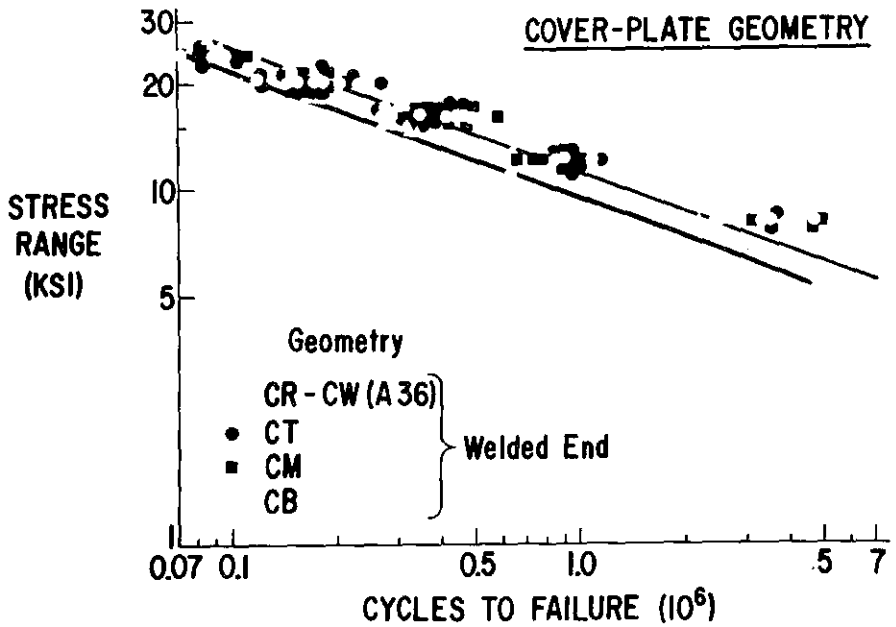

3-20. The stress range cycle life results for various types of welded cover-plated details. Large variations in cover plate geometry have only a negligible influence on the basic fatigue strength.

NOTES:

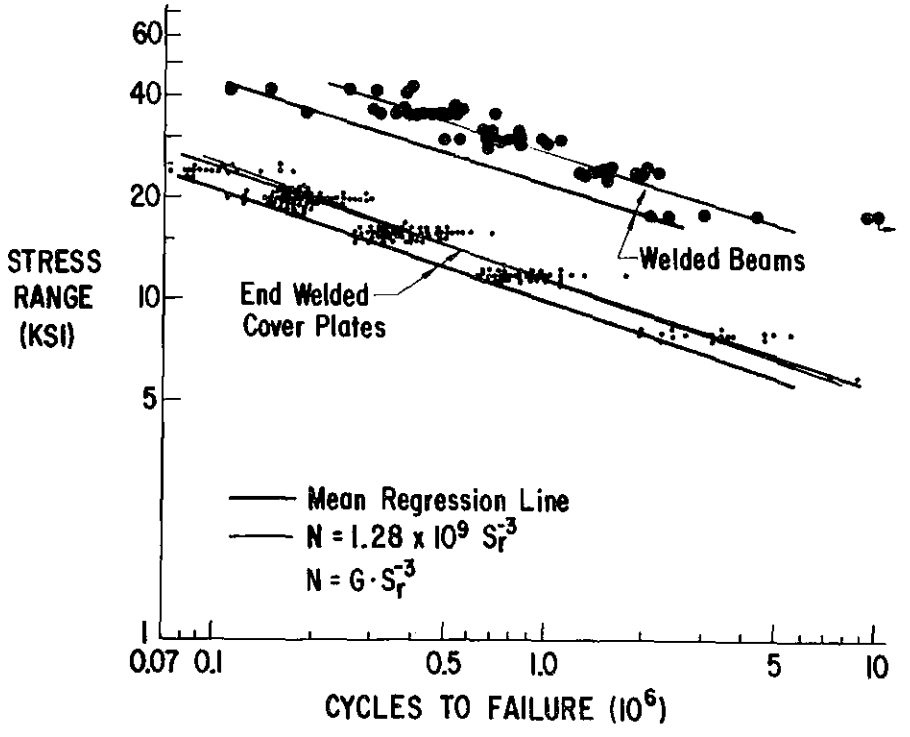

3-21. The stress range cycle like relationships for the welded and cover-plated beams are compared. Much higher fatigue resistance exists when cracks form from internal discontinuities as opposed to those that grow from the high stress concentration region at a weld termination. These details bound the fatigue strength of welded built-up beams.

NOTES:

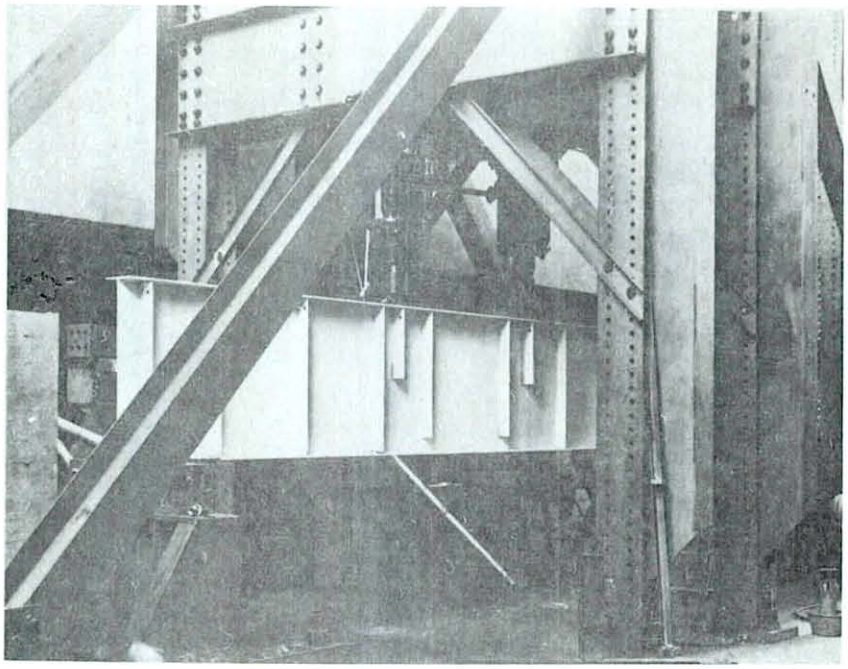

3-22. Test specimen used to examine the influence of stiffeners attached to the web or flange. These beams were fabricated 38 inches deep with half-inch flanges and 3/16 inch webs.

NOTES:

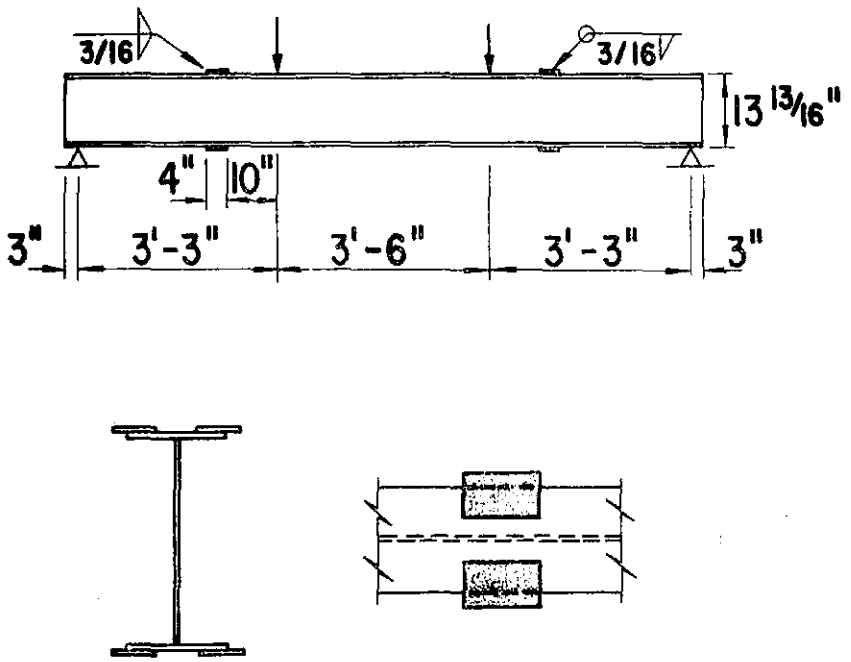

3-23. Smaller scale beams were also tested with a variety of welded attachments.

NOTES:

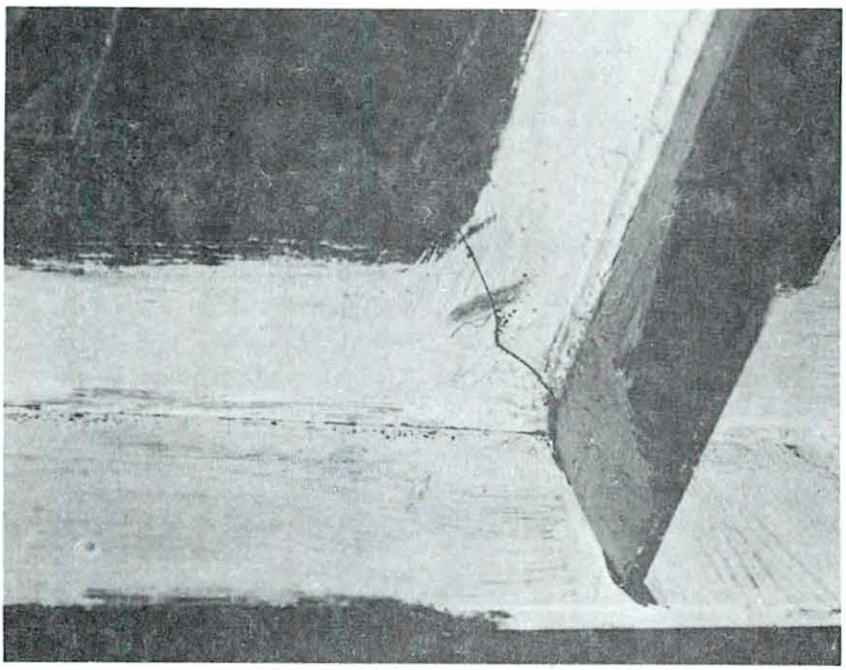

3-24. Crack growth occurred at the termination of the weld toe at the end of a transverse stiffener welded to the web alone.

NOTES:

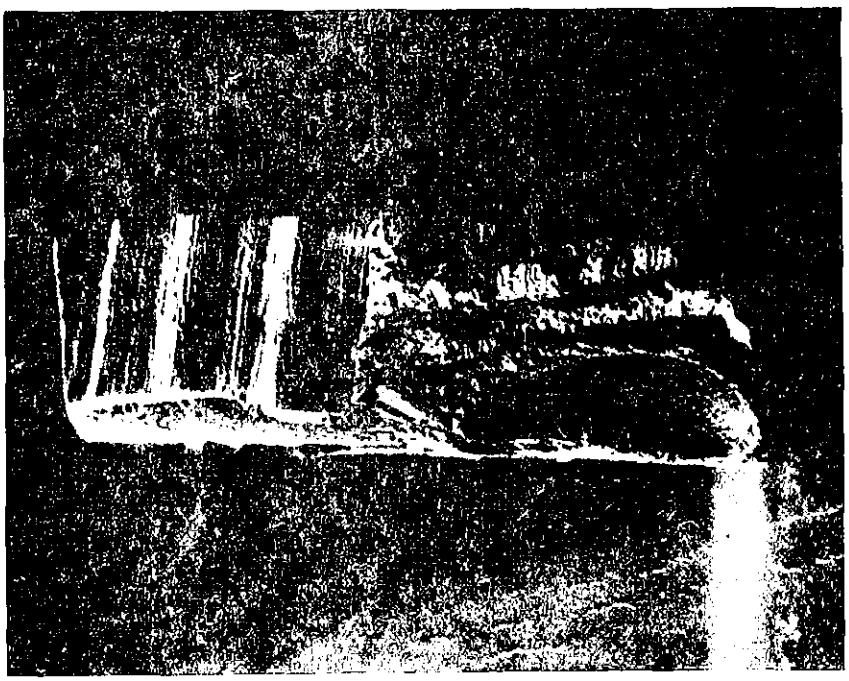

3-25. Fracture surface shows that crack penetrated through the web plate thickness at the weld toe as a semi-eliptical surface crack.

NOTES:

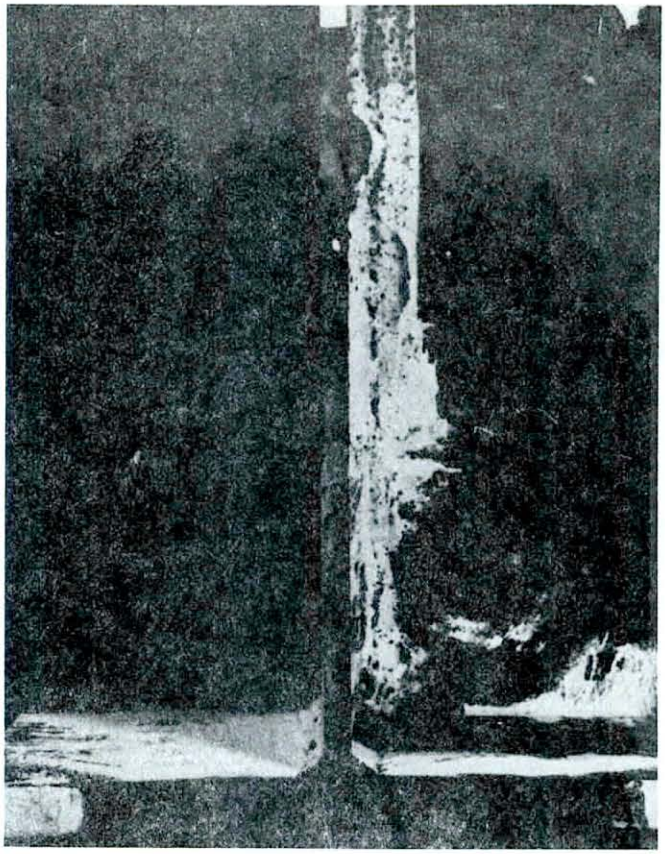

3-26. After the crack penetrated the beam web, it eventually destroyed most of the web and flange.

NOTES:

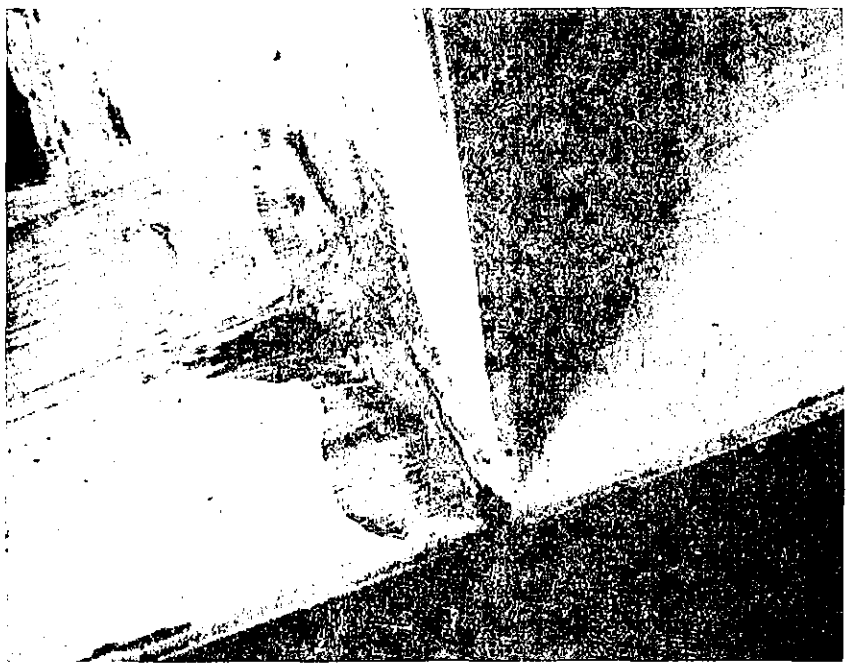

3-27. Stiffeners welded to flange experience crack growth from weld toe perpendicular to the stress field.

NOTES:

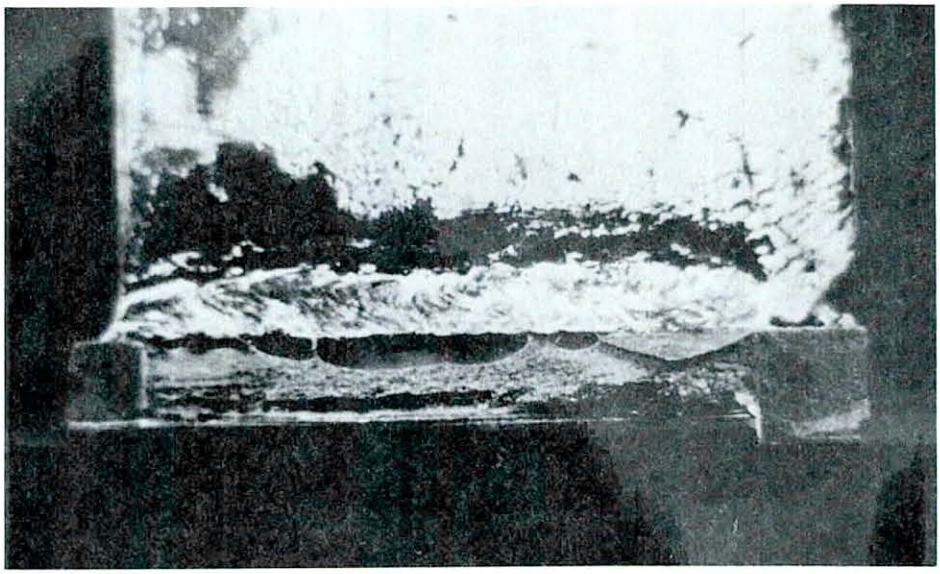

3-28. Crack observed to initiate at a number of points along the weld toe and grew as small semi-eliptical surface cracks.

NOTES:

3-29. Continued growth caused crack coalescense.

NOTES:

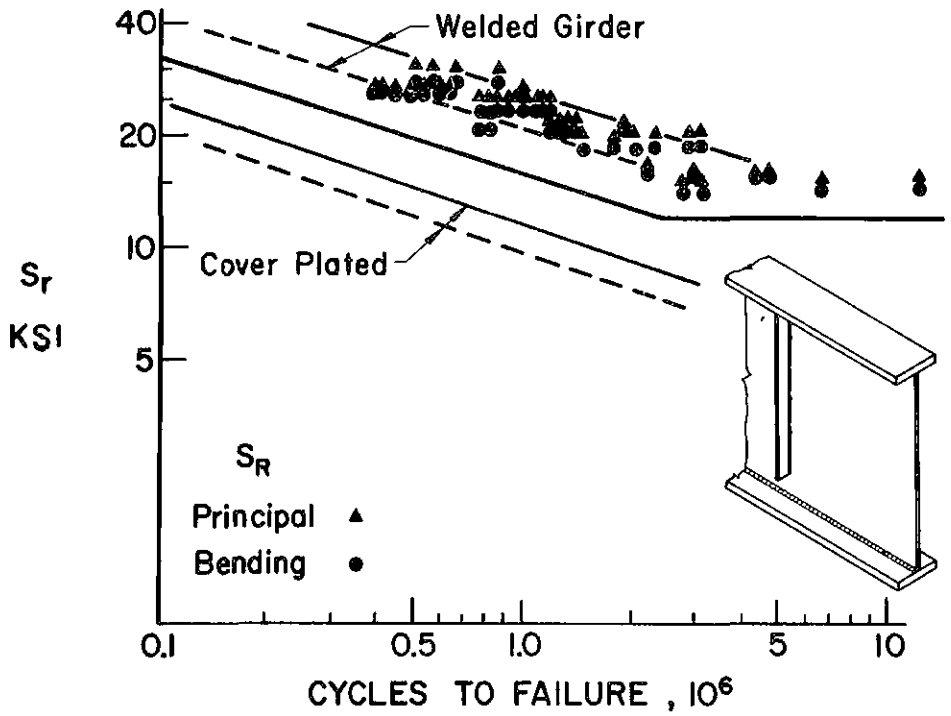

3-30. Stress range due to bending along and principal stress, are compared as a function of cycle life for stiffeners attached to the web alone. Under normal combinations of bending and shear, bending alone describes fatigue strength.

NOTES:

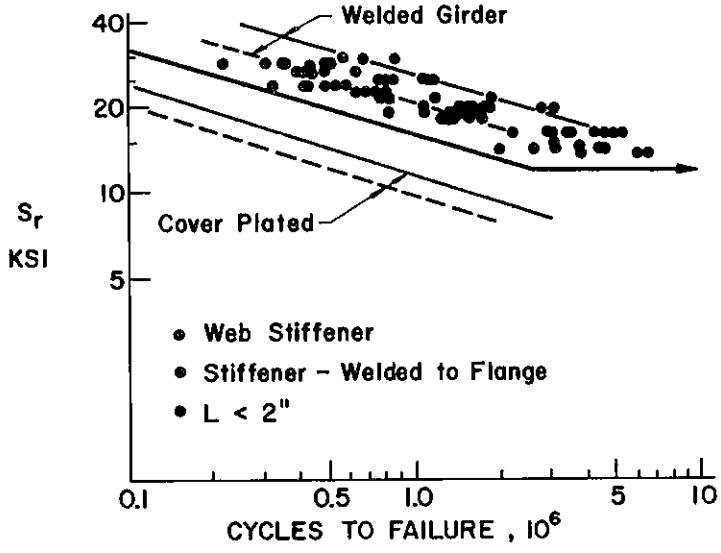

3-31. Stress range is plotted as a function of cycle life for stiffeners attached to web and flange. Fatigue strength is close to the upper bound provided by plane welded beams.

NOTES:

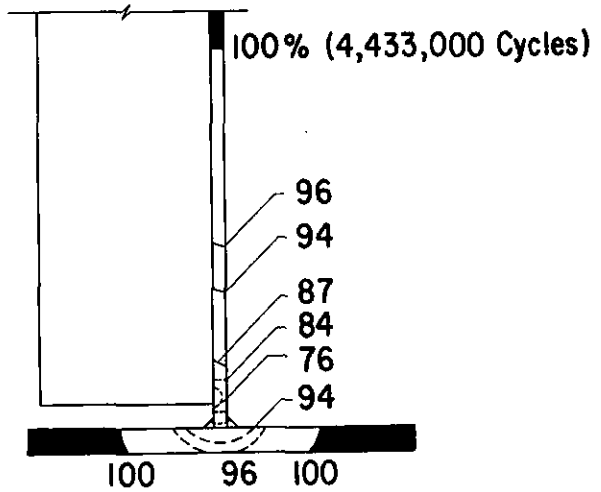

PHASES OF CRACK GROWTH AT STIFFENER TYPE I

3-32. Schematic of phases of crack growth for a stiffener attached to the web alone. Eighty percent of life is exhausted propagating the crack through the web.

NOTES:

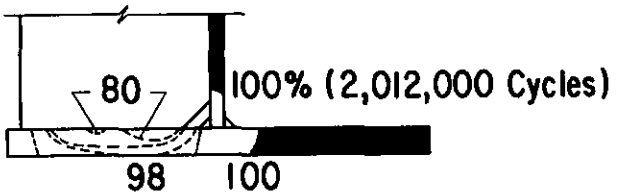

PHASES OF CRACK GROWTH AT STIFFENER TYPE 3

3-33. Schematic showing crack propagation into the web and flange for stiffeners welded to web and flange.

NOTES:

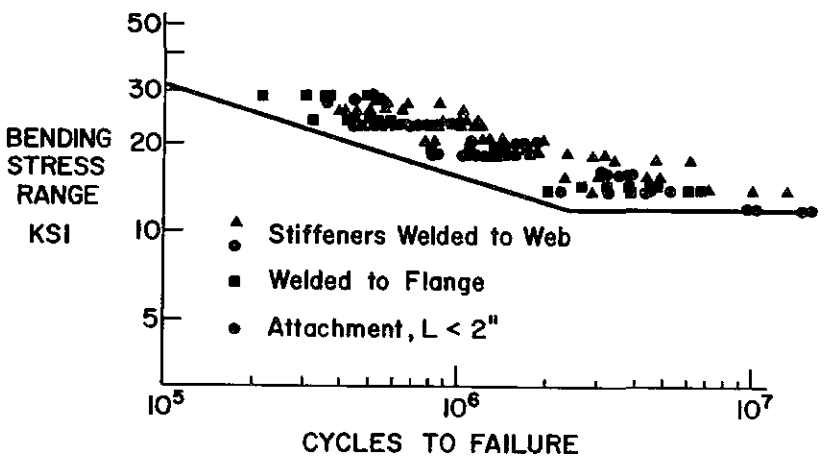

3-34. The stress range-cycle life relationship is compared for various types of stiffeners. Demonstrates no difference in the fatigue strength.

NOTES:

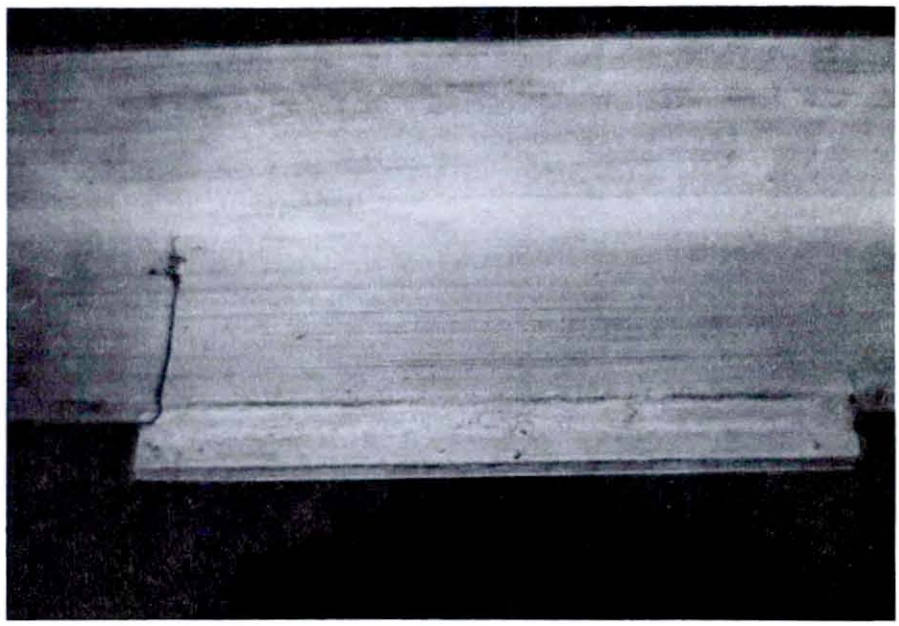

3-35. A crack growing from the weld toe of an eight-inch long attachment.

NOTES:

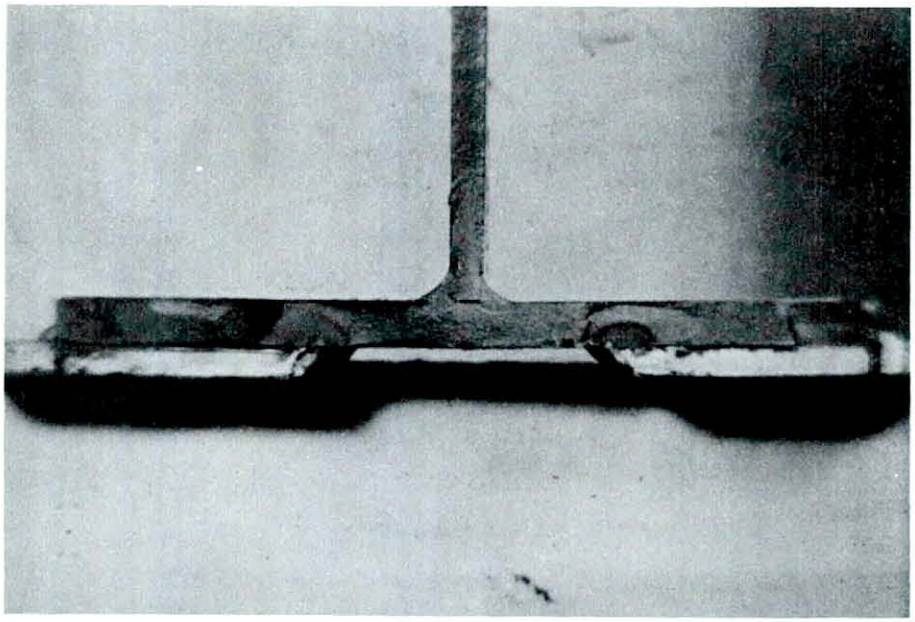

3-36. The crack surface showing cracks propagating from the longitudinal weld toe at the flange edge and at the interior surface.

NOTES:

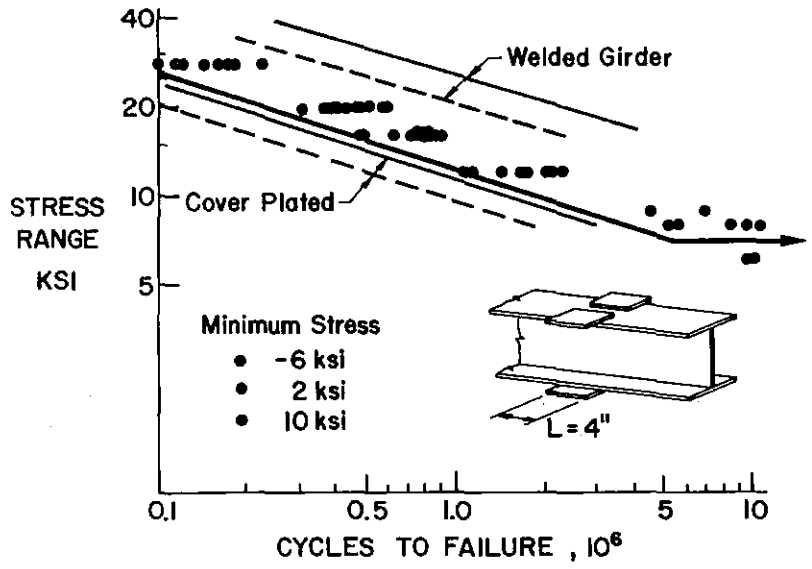

3-37. Stress range-cycle life relationship for beams with four-inch attachments. The test data falls between the upper and lower bound provided by the plane welded and cover-plated beams.

NOTES:

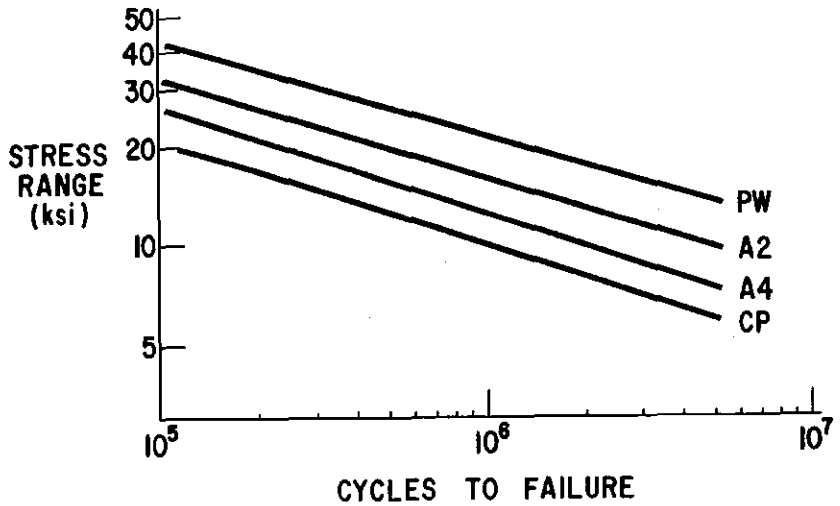

3-38. The stress range-cycle life relationships of welded details provide a series of parallel curves. The stress concentration effect causes a decrease in fatigue strength.

NOTES:

CATEGORY	STRESS RANGE (ksi)			
	100,000 Cycles	500,000 Cycles	2,000,000 Cycles	Over 2,000,000 Cycles
A	60	36	24	24
B	45	27.5	18	16
C	32	19	13	10
D	27	16	10	7
E	21	12.5	8	5
F	15	12	9	8

3-39. Table of stress ranges corresponding to discrete numbers of stress cycles - 100,000, 500,000, 2,000,000 and more than 2,000,000 for categories A & B.

NOTES:

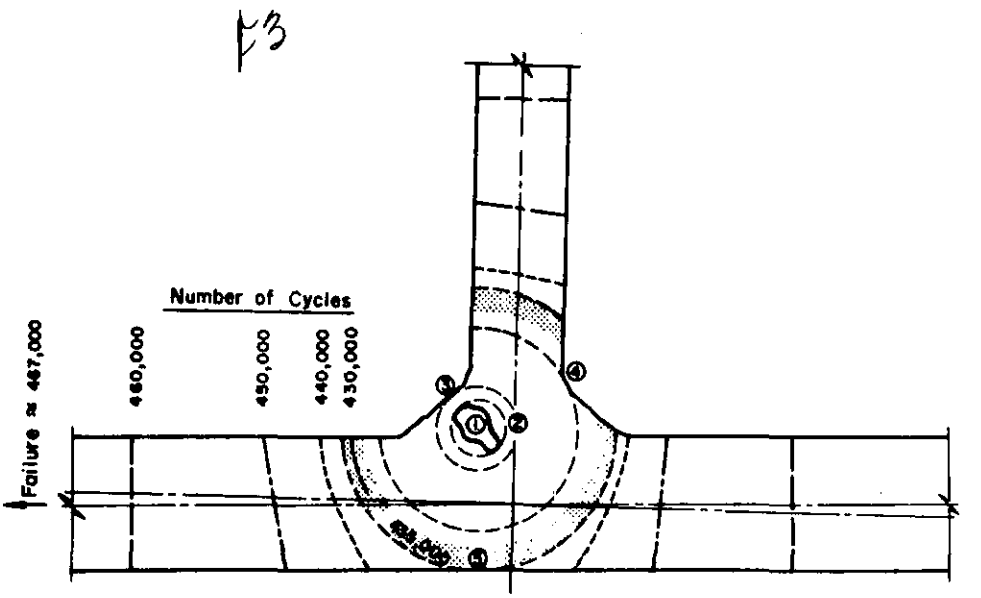

3-40. Fatigue fracture surface showing penny shaped crack in a plane welded beam. The stress intensity factor for the penny shaped crack $\Delta K = S_r \frac{2}{\Pi}\sqrt{\Pi a}$

NOTES:

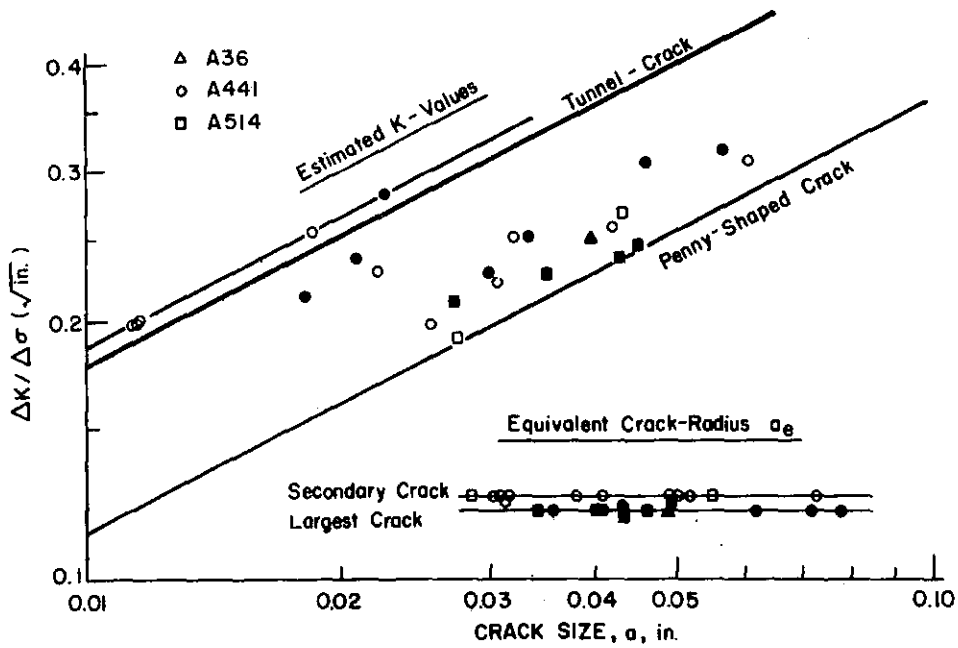

3-41. Plot of the measured initial discontinuities observed in welded beams and K value estimated for the equivalent penny shaped crack.

NOTES:

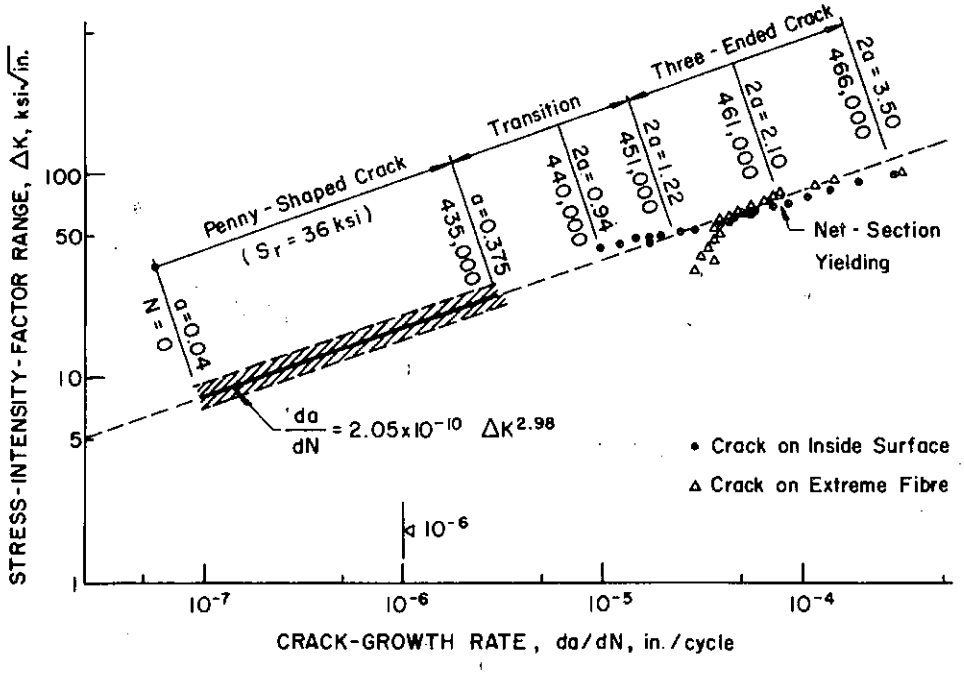

3-42. Plot of the crack growth rate measured during test of plane welded beam.

NOTES:

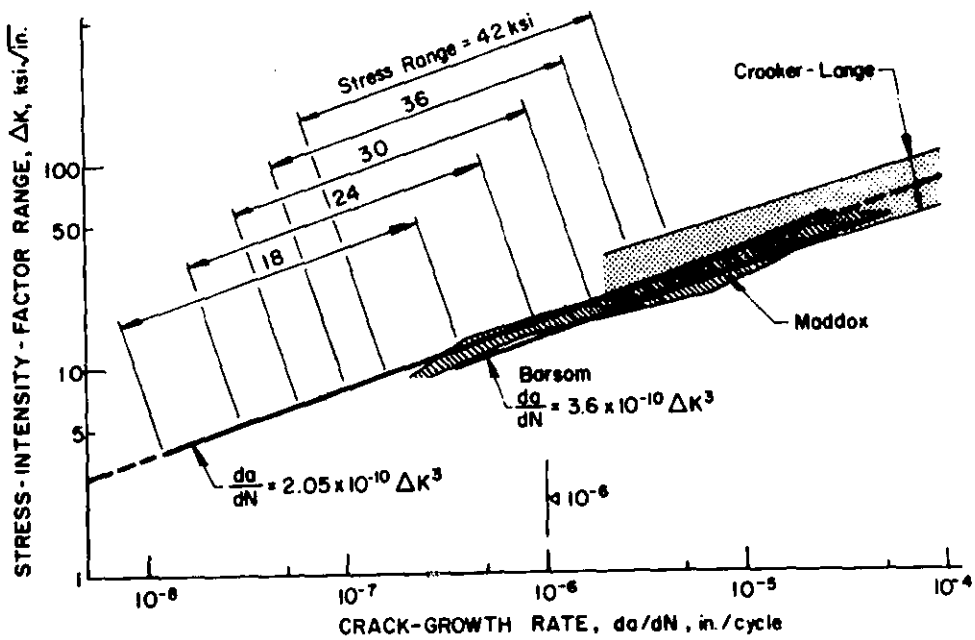

3-43. Predicted ΔK-crack growth relationship using penny shaped crack model. Most fatigue life occurs below 10^{-6} inches per cycle in a beam.

NOTES:

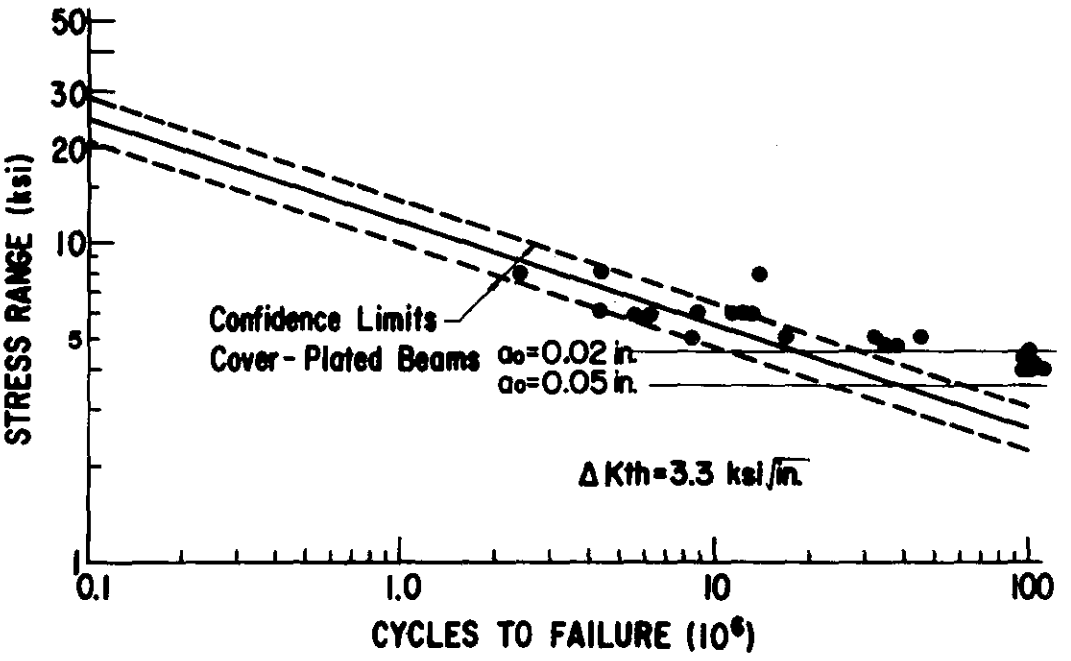

3-44. Predicted crack growth threshold for cover-plated beams with ΔK_{TH} = 3 ksi$\sqrt{in}$.

NOTES:

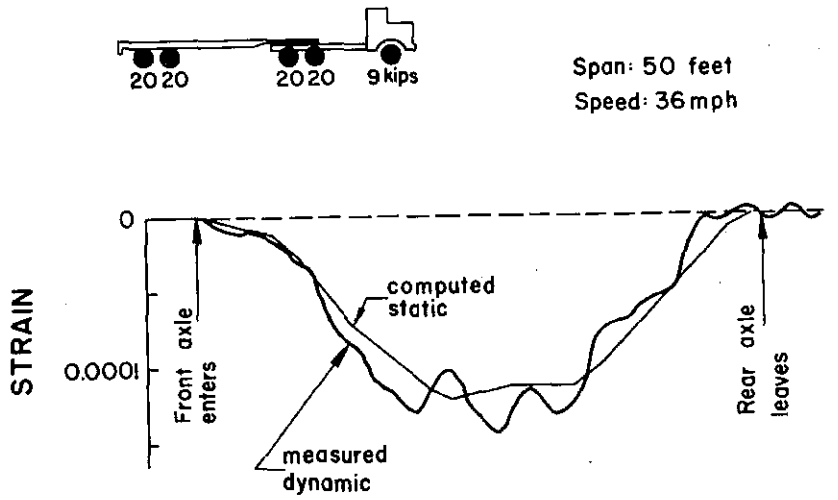

3-45. Stress-time response for a typical bridge member.

NOTES:

MINER'S HYPOTHESIS

$$\sum \frac{n_x}{N_x} = 1.0$$

3-46. Miner's Rule Σ n/N

NOTES:

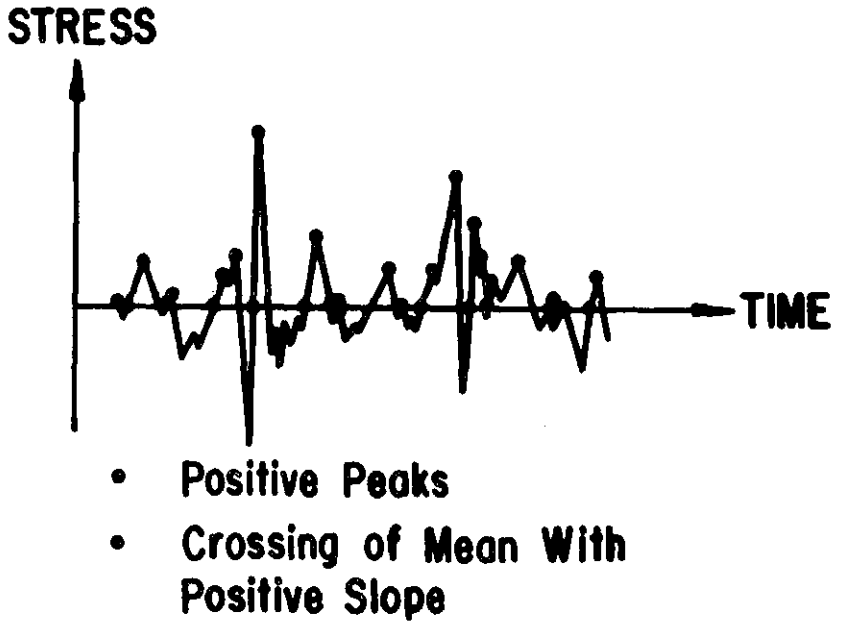

3-47. Random variable stress spectrum.

NOTES:

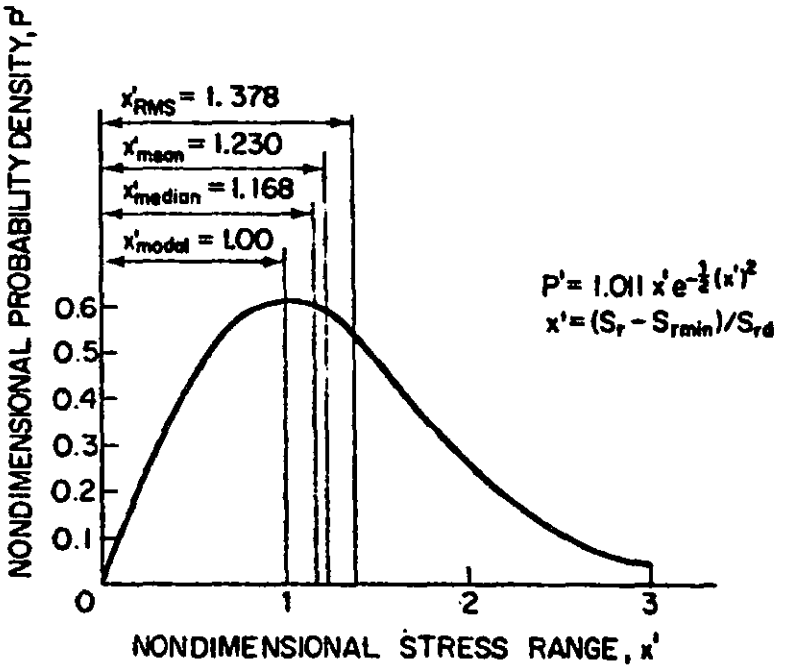

3-48. Raliegh probability density curve describing variable stress spectrum.

NOTES:

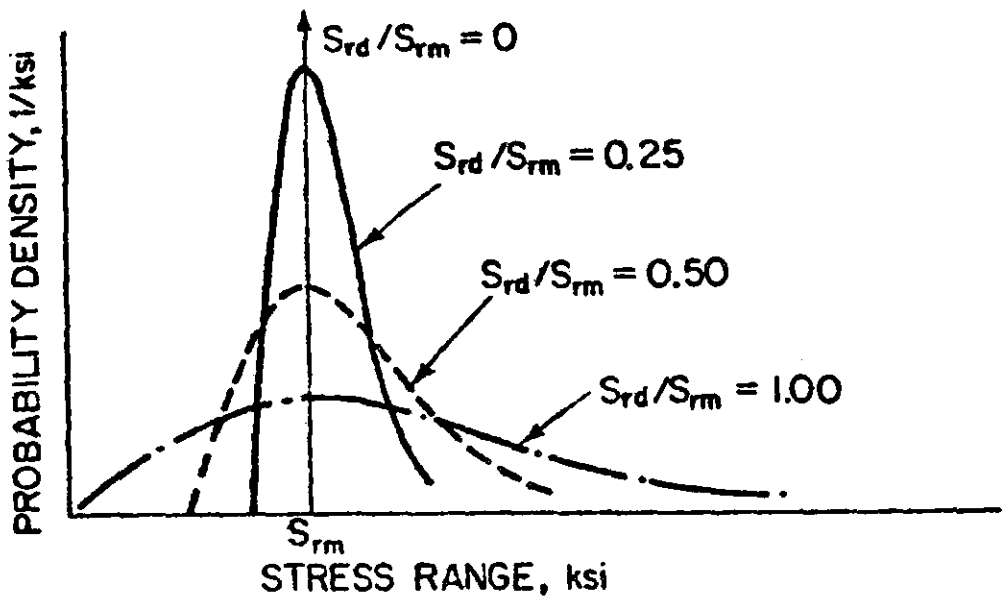

3-49. Ratio of S_{rd}/S_{rm} varied from 0 to 1.0. 0 corresponds to constant cycle stresses. An increase in the ratio increases the difference between the minimum and maximum stress ranges in the spectrum.

NOTES:

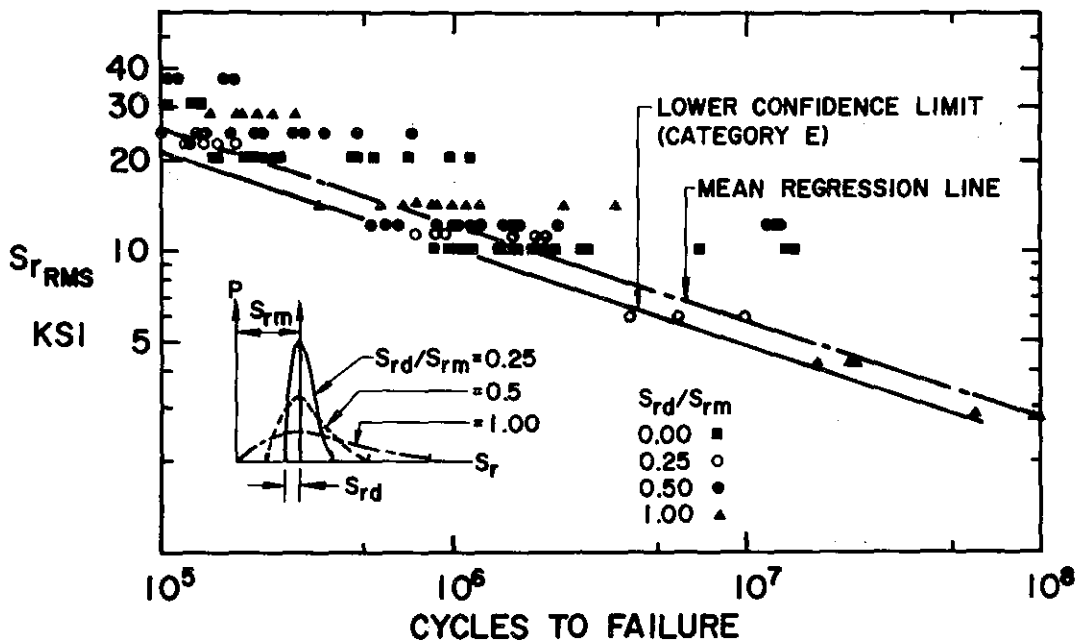

3-50. The results of variable and constant amplitude tests of cover plated beams. Effective stress range ($S_{r\ RMS}$) provides good correlation with constant cycle data.

NOTES:

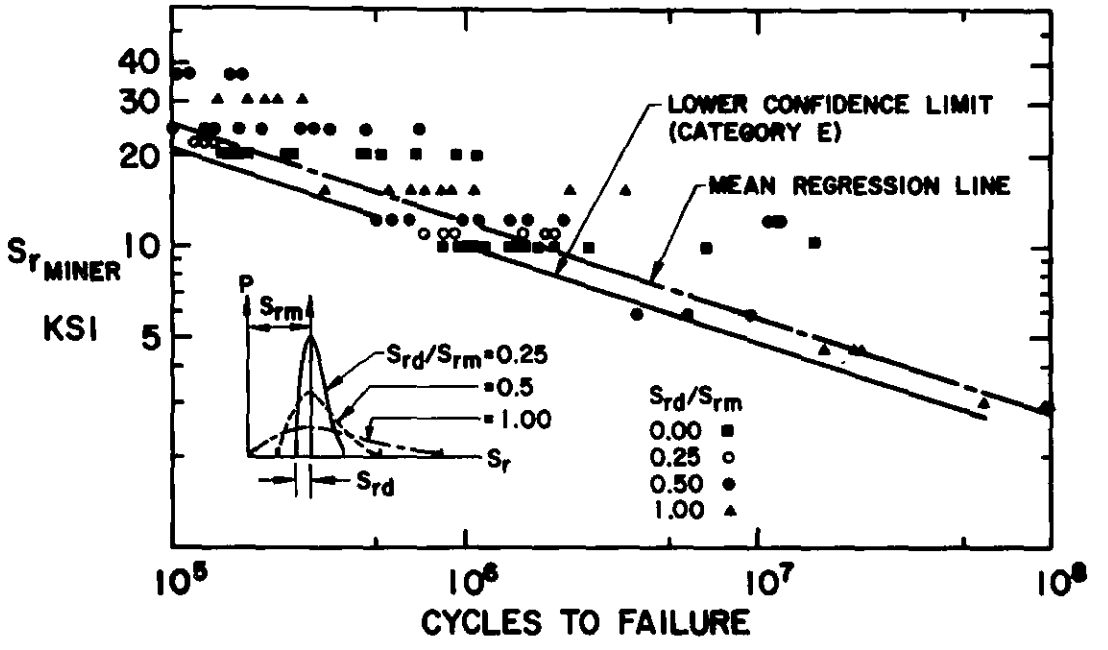

3-51. A comparable result was also obtained using Miner's Law to derive an equivalent stress range. Both Miner's Law and RMS were found to provide a satisfactory link between variable stress cycles and constant cycle fatigue data.

NOTES:

$$N_D \sim S_r^D$$

$$N_V \sim S_{rRMS} \text{ OR } S_{rMINER}$$

$$\therefore N_D = \left(\frac{S_{rMINER}}{S_r^D} \right)^3 N_V$$

3-52. Design
$S_r^D \rightarrow N_D$

Actual Stresses
$S_{Ri} \rightarrow N_A$

NOTES:

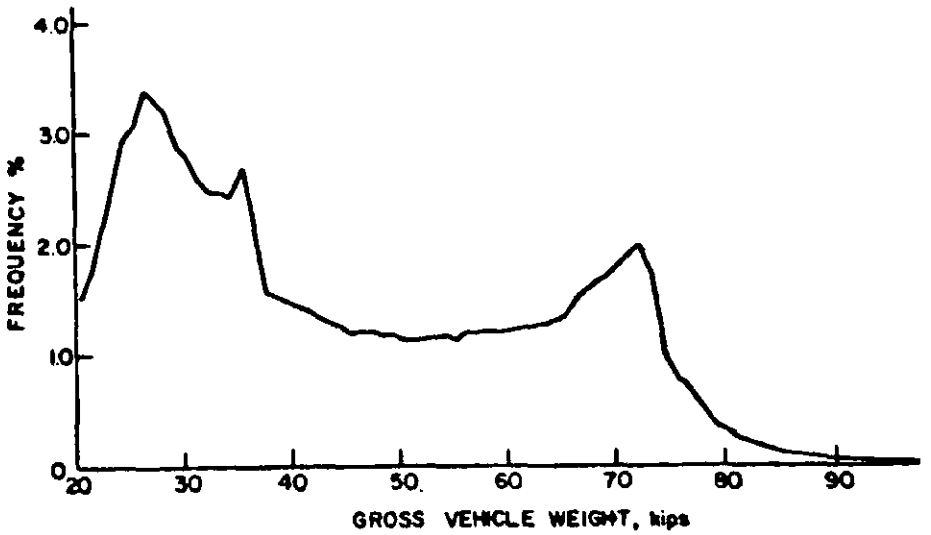

3-53. 1970 FHWA nationwide gross vehicle weight distribution.

NOTES:

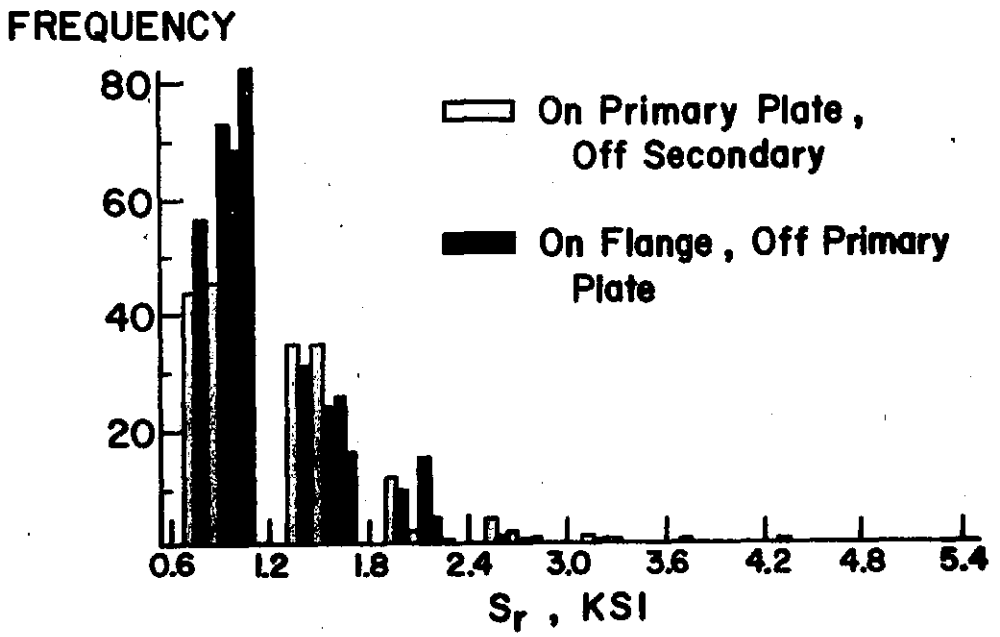

3-54. Typical stress range distribution determined from measured stresses on a bridge showing the same general shape and trend as the gross vehicle weight distribution.

NOTES:

BRIDGE	MAX. S_r (KSI)	SPAN (FT.)	$S_r^D(S/5.5)$ (KSI)	$S_r^D(S/7)$ (KSI)
MICH. 1	6.3	95	9.5	7.45
MICH. 2	5.1	79.5	6.3	4.95
MICH. 3	5.6	66	6.84	5.37
MICH. 5	4.2	72	6.14	4.82
MICH. 6	3.9	58.7	7.1	5.58
MICH. 7	5.1	78.5	6.2	4.86
MICH. 8	6.9	128.7	8.2	6.45
VIR. 1	3.5	74.5	7.74	6.08
MARY. 1	5.4	42-52-42	6.2	4.87
CONN. 1	3.5-5.7	113.5	6.5	5.17

3-55. Tabular summary showing the maximum design stress range and its relationship to maximum measured stress for several bridges.

NOTES:

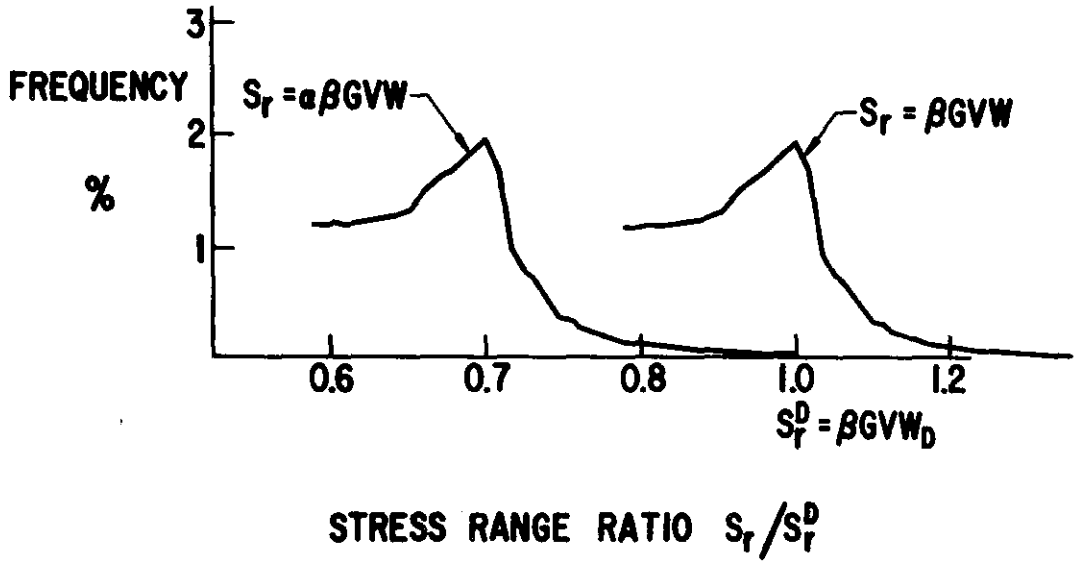

3-56. Schematic showing that the stresses predicted from the gross vehicle weight distribution exceed measured stresses due to variation in impact, load distribution and design idealization.

NOTES:

$$\Sigma^{n}/N = 1$$

$$\alpha^{3} \frac{(\beta GVW_D)^3}{A} (ADTT)(D_L) \Sigma \gamma_i \phi_i^3 = 1$$

OR

$$\alpha^{3} \times ADTT \times D_L \times 0.35 = N_D$$

3-57. Miner's Rule used to derive AASHTO design stress table. $N_D = ADTT \times D_L \times o^3/2.85$.

NOTES:

MAIN (LONGITUDINAL) LOAD CARRYING MEMBERS

TYPE OF ROAD	CASE	ADTT *	TRUCK LOADING	LANE LOADING+
Freeways, Expressways, Major Highways and Streets	I**	2500 or more	over 2,000,000	500,000
	II	less than 2500	500,000	100,000
Other Highways and Streets not included in Case I or II	III	———	100,000	100,000

3-58. Tabulation provided for longitudinal members showing roadway classification truck volume, and required equivalent design stress cycles.

NOTES:

FIGURES - SESSION 4

FRACTURE BEHAVIOR OF BRIDGE STEELS - SPECIMENS AND TESTS - BASIS FOR CURRENT DESIGN RULES

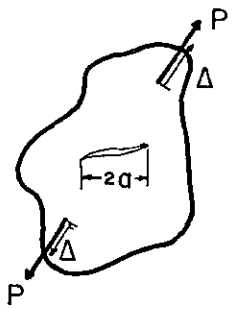

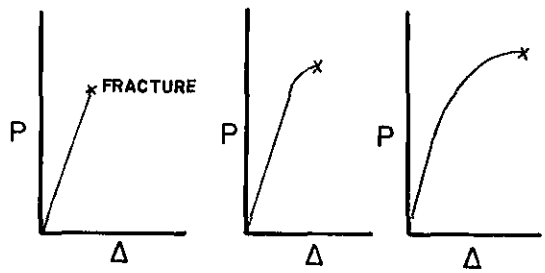

4-1. Fracture behavior can be dramatically changed by just changing the crack size in a specimen. This behavior can be

a) linear
b) slightly non-linear
c) highly non-linear

NOTES:

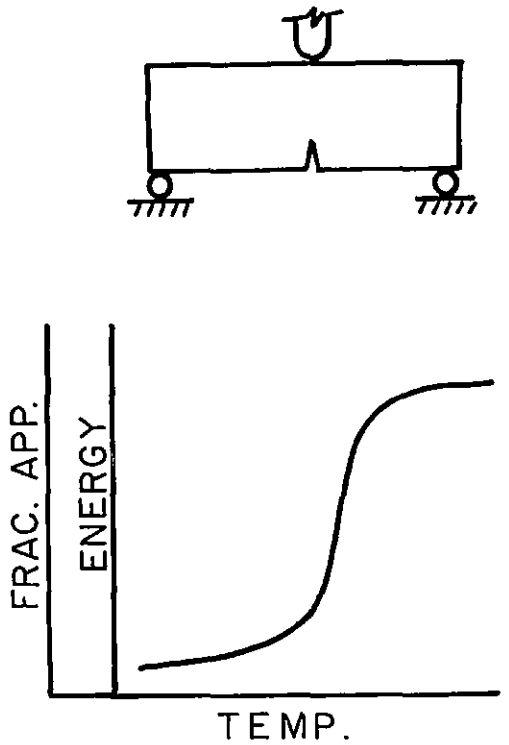

4-2. Typical impact specimen behavior as a function of temperature.

NOTES:

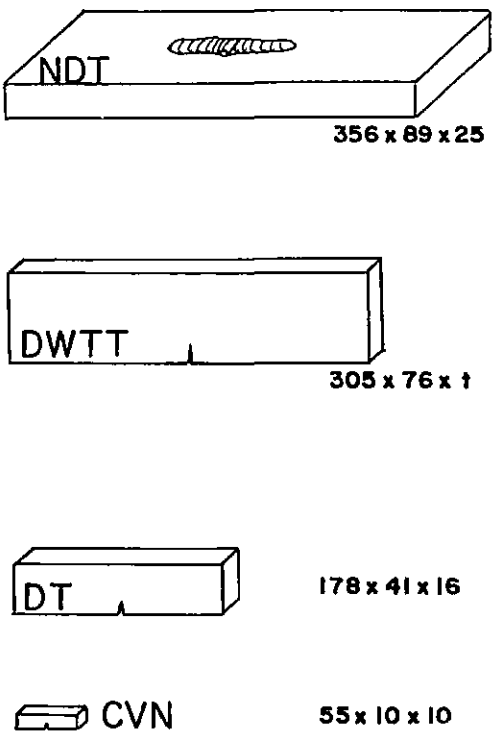

4-3. Relative size of the NDT, DWTT, DT and CVN specimens. All dimensions in millimeters.

NOTES:

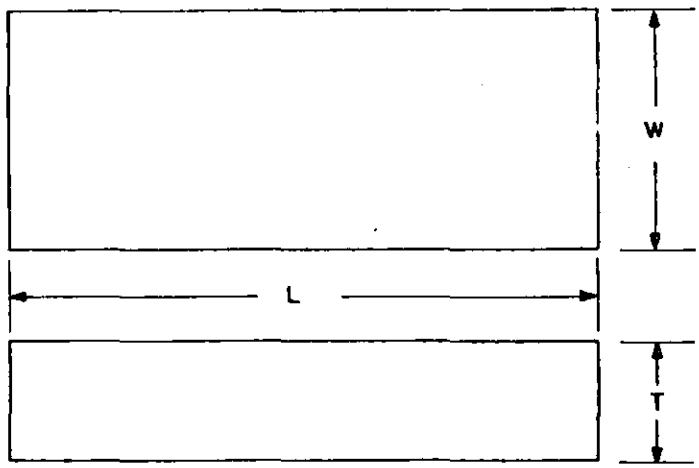

Dimension	Units	Specimen Type					
		P-1		P-2		P-3	
		Dimension	Tolerance	Dimension	Tolerance	Dimension	Tolerance
T, Thickness	in.	1.0	±0.12	0.75	±0.04	0.62	±0.02
	mm	25	±2.5	19	±1.0	16	±0.5
L, Length	in.	14.0	±0.5	5.0	±0.5	5.0	±0.5
	mm	360	±10	130	±10	130	±10
W, Width	in.	3.5	±0.1	2.0	±0.04	2.0	±0.04
	mm	90	±2.0	50	±1.0	50	±1.0

4-4. Specimen dimensions for the NDT test.

NOTES:

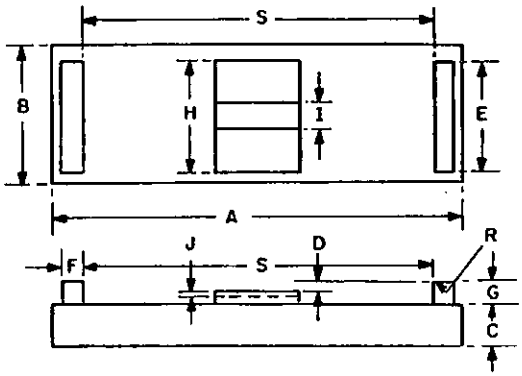

Anvil Dimension	Units	Specimen Type			Tolerance
		P-1	P-2	P-3	
S, Span	in.	12.0	4.0	4.0	±0.05
	mm	305	100	100	±1.5
D, Deflection stop	in.	0.30	0.060	0.075	±0.002
	mm	7.60	1.50	1.90	±0.05
A, Anvil length	← not critical →				
B, Anvil width	← not critical →				
C, Anvil thickness	in.	1.5 min	1.5 min	1.5 min	
	mm	38 min	38 min	38 min	
E, Support length	in.	3.5 min	2.0 min	2.0 min	
	mm	90 min	50 min	50 min	
F, Support width	← not less than *G* →				
G, Support height	in.	2.0	2.0	2.0	±1
	mm	50	50	50	±25
R, Support radius	in.	0.075	0.075	0.075	±0.025
	mm	1.0	1.0	1.0	±0.1
H, Stop width	in.	3.5 min	2.0 min	2.0 min	±2
	mm	90 min	50 min	50 min	±50
I, Weld clearance	in.	0.9	0.9	0.9	±0.1
	mm	22	22	22	±3
J, Weld clearance depth	in.	0.4 min	0.4 min	0.4 min	
	mm	10 min	10 min	10 min	

4-5. Typical test fixture for NDT tests.

NOTES:

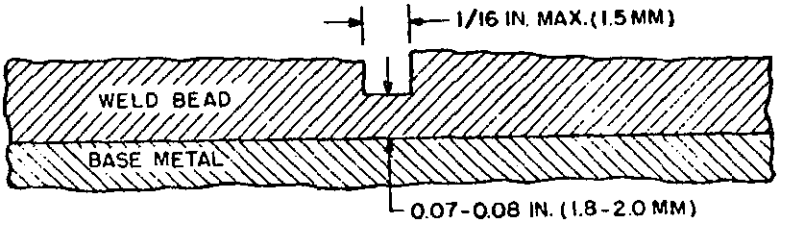

4-6. Typical notch detail for NDT test.

NOTES:

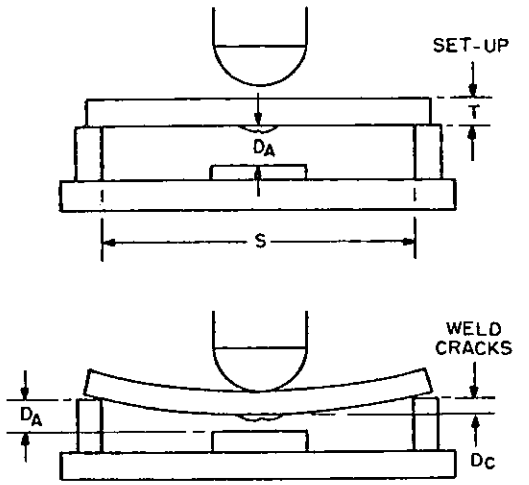

YIELD POINT LOADING IN PRESENCE OF SMALL CRACK IS TERMINATED BY CONTACT WITH STOP

4-7. View of NDT specimen being deflected to yield point strain. The engineering yield point is a strain derived quantity. Strain and deflection are directly related in the test procedure.

NOTES:

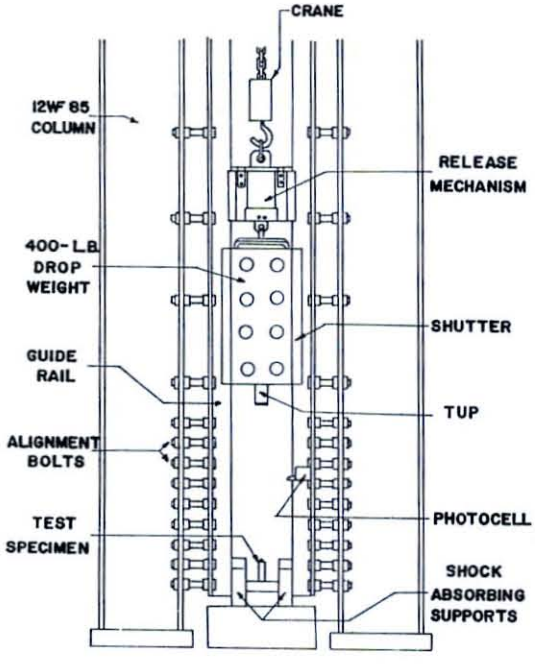

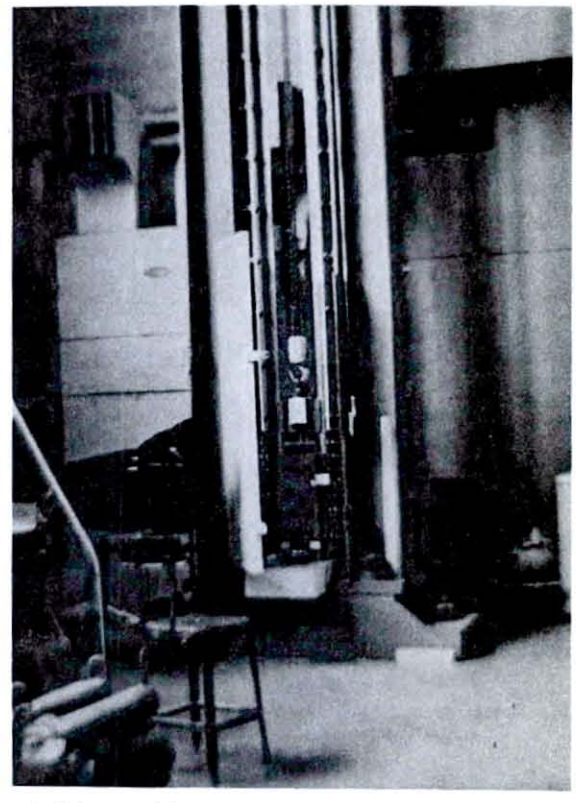

4-8. View of typical drop weight machine.

NOTES:

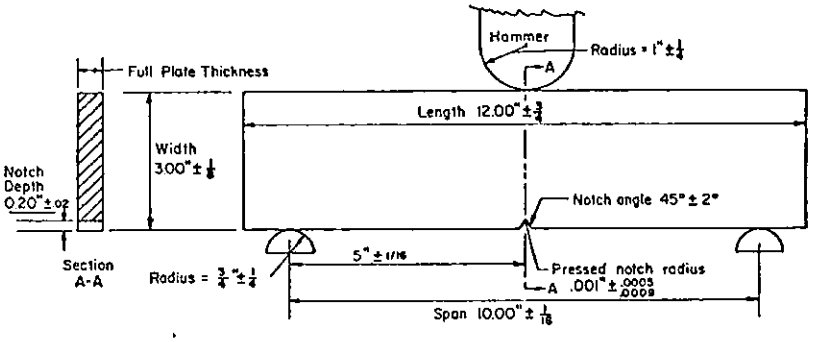

4-9. DWTT test specimen and fixtures.

NOTES:

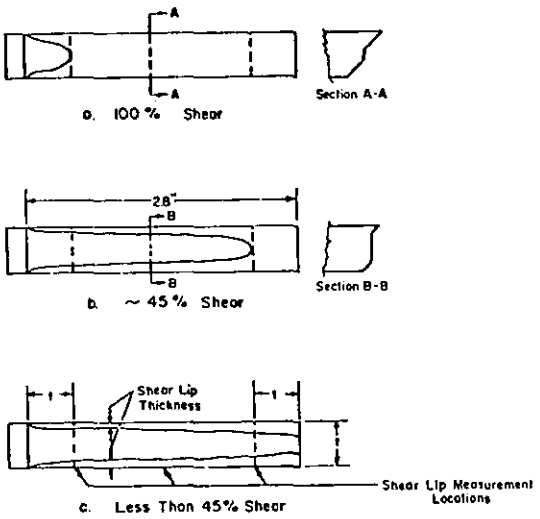

4-10. Procedure for determining shear area.

NOTES:

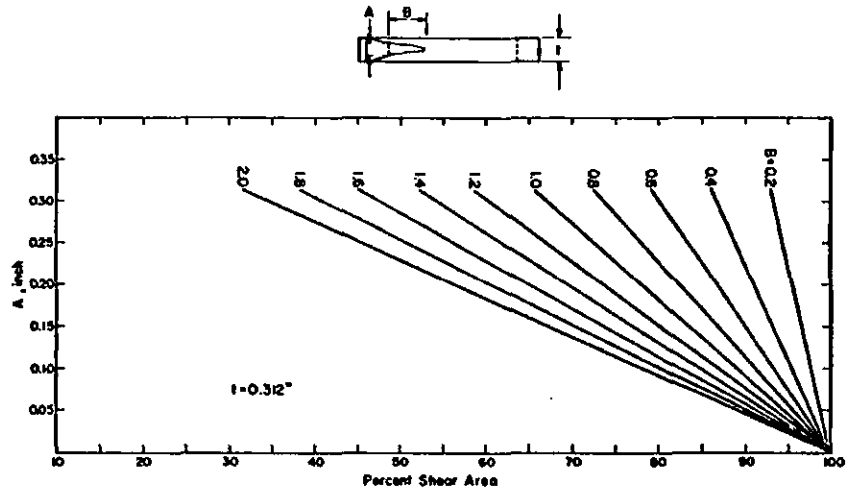

FIG. A2 Chart for Determining Percent Shear for 0.312-in. Material.

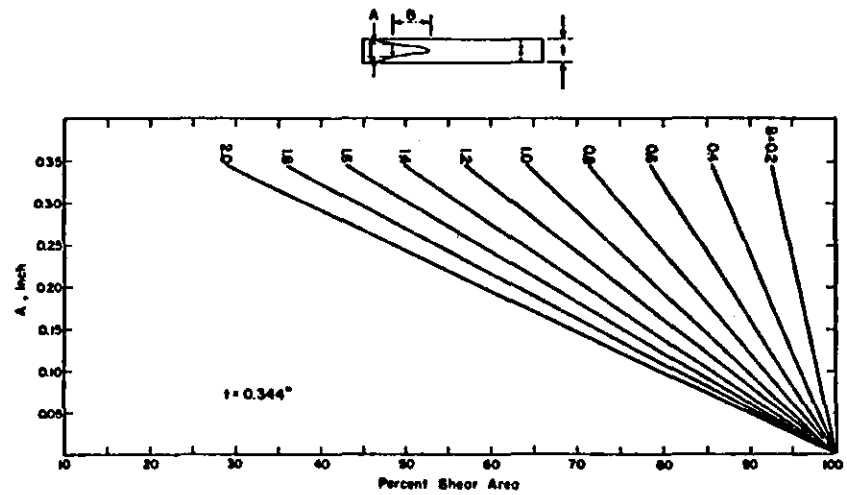

Fig. A3 Chart for Determining Percent Shear for 0.344-in. Material.

4-11. Procedure for determining shear area.

NOTES:

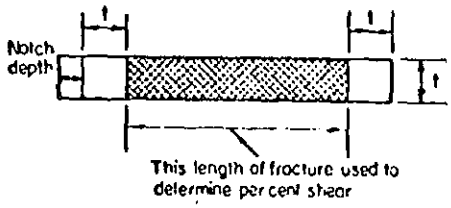

Fracture Surface Included in Shear-Area Determination.

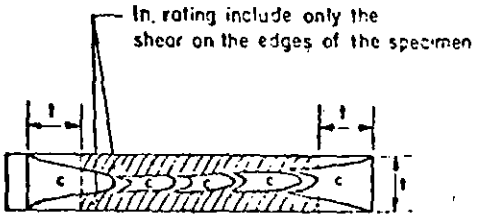

c denotes the cleavage appearing regions

Alternative Shear-Cleavage Fracture Appearance.

4-12. Procedure for determining shear area.

NOTES:

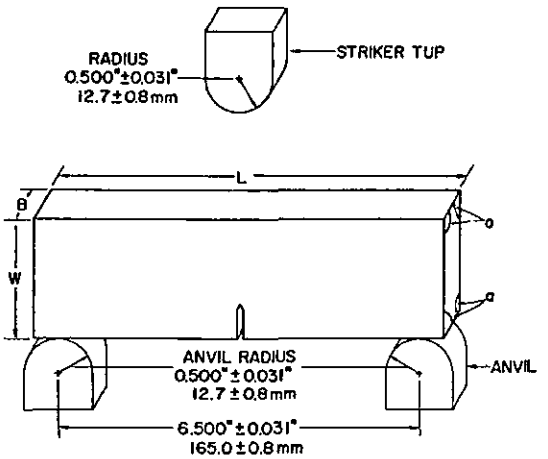

Dimensions and Tolerance for Specimen Blank

Parameter	Units	Dimension	Tolerance
Length, L	in.	7.125	±0.125
	mm	181.0	±3.2
Width, W	in.	1.60	±0.10
	mm	38.0	±2.5
Thickness, B	in.	0.625	±0.033
	mm	15.8	±0.8
Angularity, α	deg	90	±2

4-13. DT specimen and fixturing.

NOTES:

MACHINING DIMENSIONS

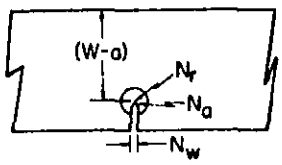

PRESSED TIP DETAILS

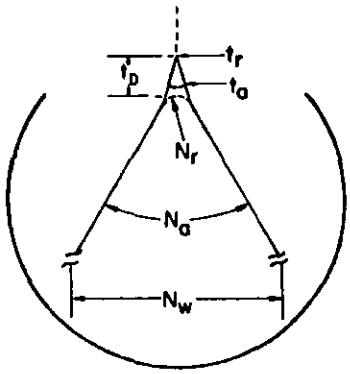

Dimensions and Tolerances for Notch Tip

Parameter	Units	Dimension	Tolerance
Net width, $(W-a)$	in.	1.125	±0.020
	mm	28.5	±0.5
Machined notch width, N_w	in.	0.0625	±0.005
	mm	1.60	±0.12
Machined notch root angle, N_a	deg	60	±2
Machined notch root radius, N_r	in.	0.005	max
	mm	0.13	max
Pressed tip depth, t_D	in.	0.009	±0.002
	mm	0.20	±0.05
Pressed tip angle, t_a	deg	40	±5
Pressed tip root radius, t_r	in.	0.001	max
	mm	0.025	max

4-14. DT specimen machining and notch details.

NOTES:

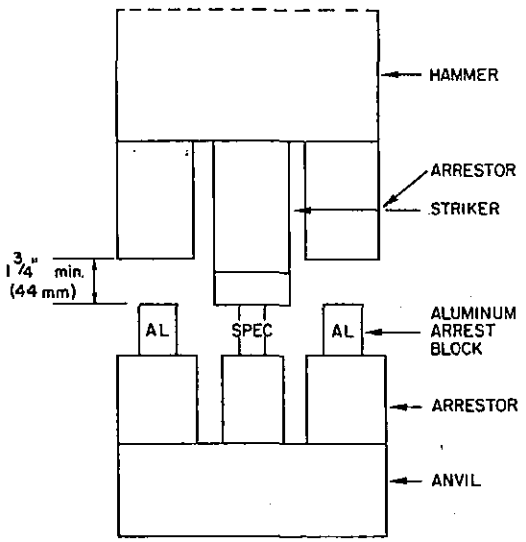

4-15. DT energy absorbing system.

NOTES:

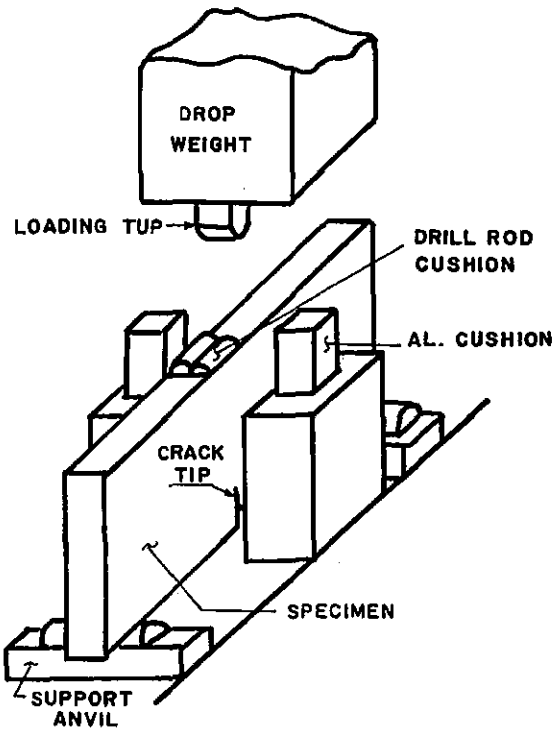

4-16. Lehigh DT energy absorbing system

NOTES:

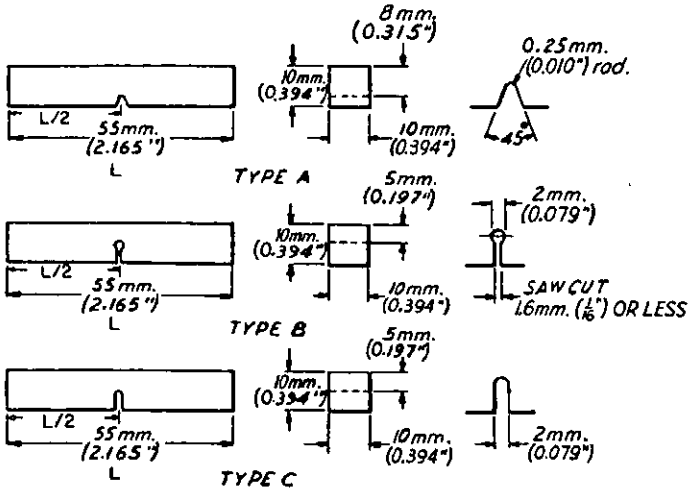

NOTE—Permissible variations shall be as follows:

Adjacent sides shall be at	90 deg ± 10 min
Cross-section dimensions	±0.001 in. (±0.025 mm)
Length of specimen (*L*)	+0, −0.100 in. (2.5 mm)
Centering of notch (*L*/2)	±0.039 in. (1 mm): When an end-centering device is necessary to center the specimen in the anvil, see 8.3, it is necessary that the notch be accurately centered to ensure compliance with 4.2.1.
Angle of notch	±1 deg
Radius of notch	±0.001 in. (0.025 mm)
Dimensions to bottom of notch:	
Type A specimen	0.315 ± 0.001 in. (8 ± 0.025 mm)
Types B and C specimen	0.197 ± 0.002 in. (5 ± 0.05 mm)
Finish requirements	63 μin. (2 μm) on notched surface and opposite face; 125 μin. (4 μm) on other two surfaces

4-17. CVN specimens

NOTES:

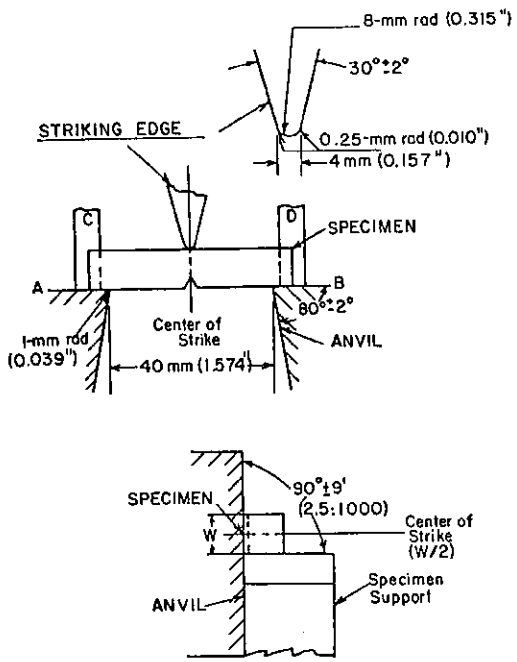

4-18. CVN test setup

NOTES:

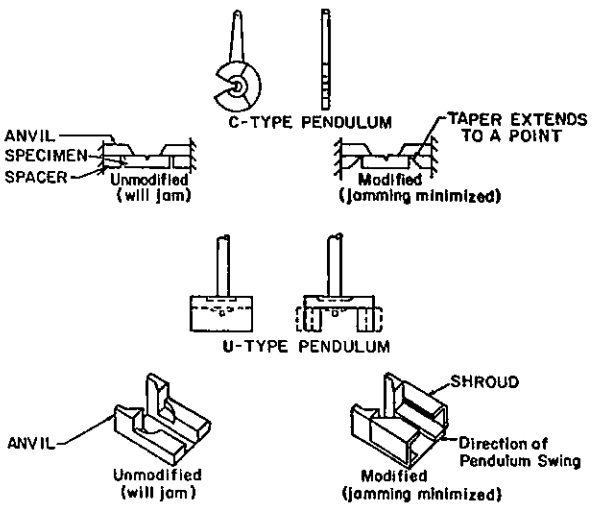

4-19. CVN test setup

NOTES:

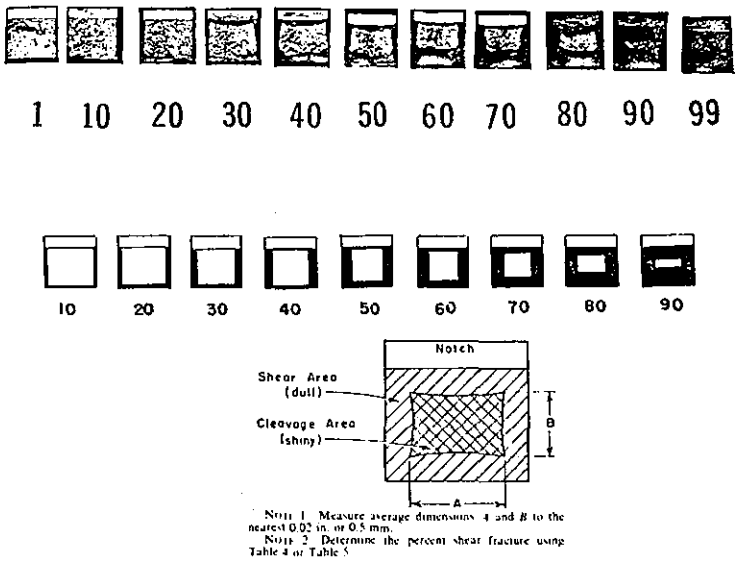

4-20. Typical rules for determining CVN fracture appearance.

NOTES:

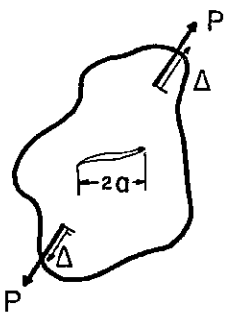

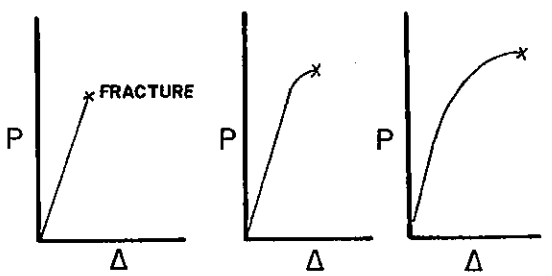

4-21. Fracture behavior can be dramatically changed by just changing the crack size in a specimen. This behavior can be

a) linear
b) slightly non-linear
c) highly non-linear

NOTES:

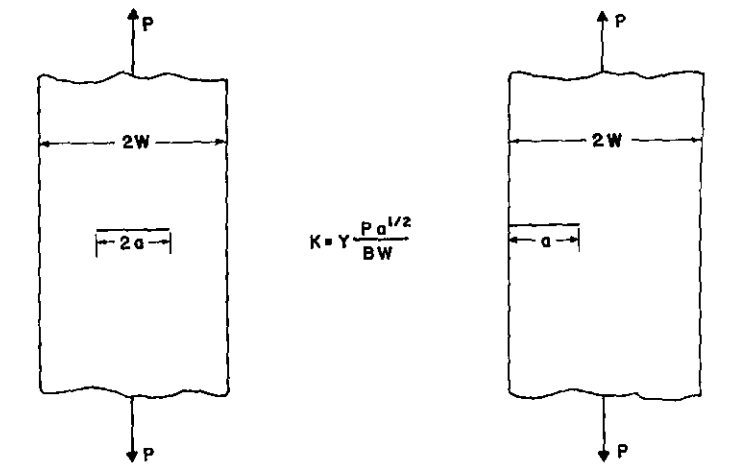

FIGURE 1a

FIGURE 1b

4-22. Typical fracture mechanics specimens.

NOTES:

THICKNESS

TEST SPEED

TEMPERATURE

4-23. Toughness depends on

a) material thickness
b) testing speed
c) test temperature

NOTES:

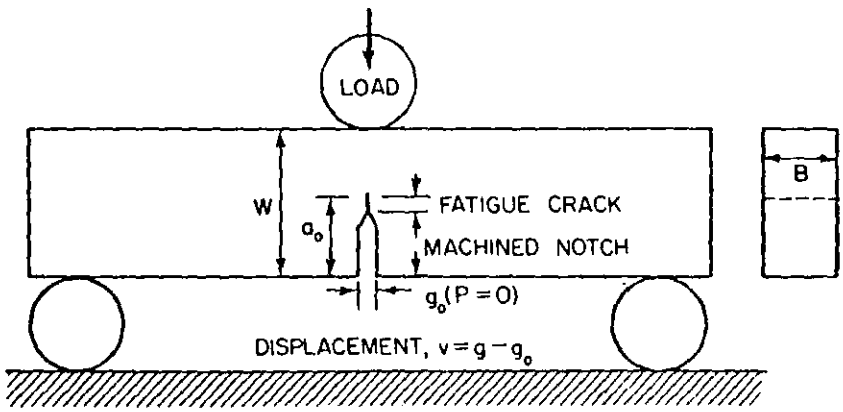

4-24. Typical E399 3 point K_{Ic} specimens

NOTES:

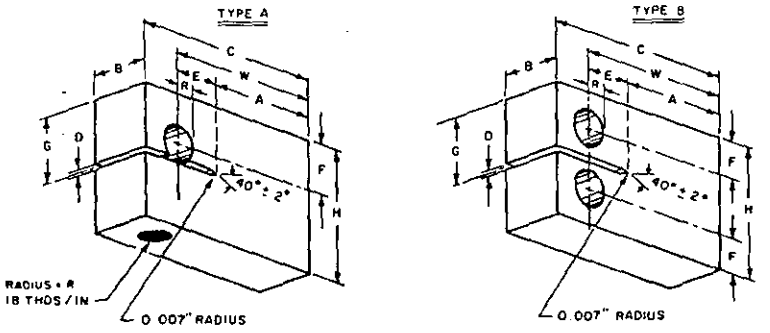

SPEC	B	W	C	A	E	H	G	D	R	F
1T-A	1.000	2.550	3.200	1.783	0.767	2.460	1.240	0.094	0.350	1.000
1T-B	1.000	2.550	3.200	1.783	0.767	2.480	1.240	0.094	0.250	0.650

4-25. Typical E399 compact tension specimen for K_{Ic} determination.

NOTES:

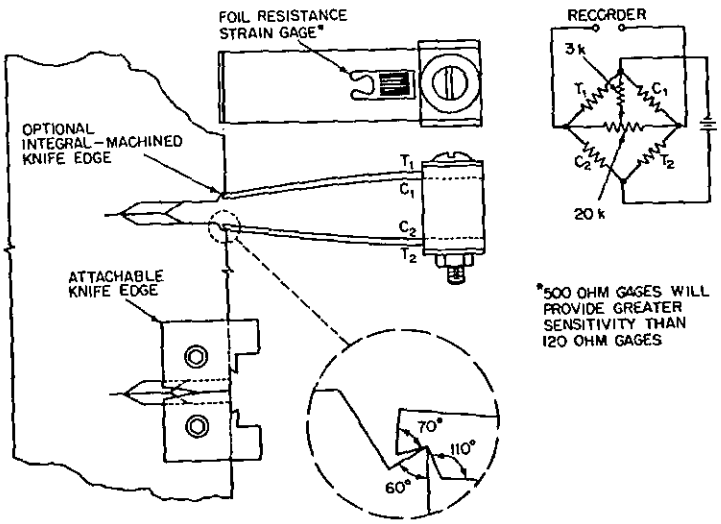

4-26. Clip gage for measuring crack opening.

NOTES:

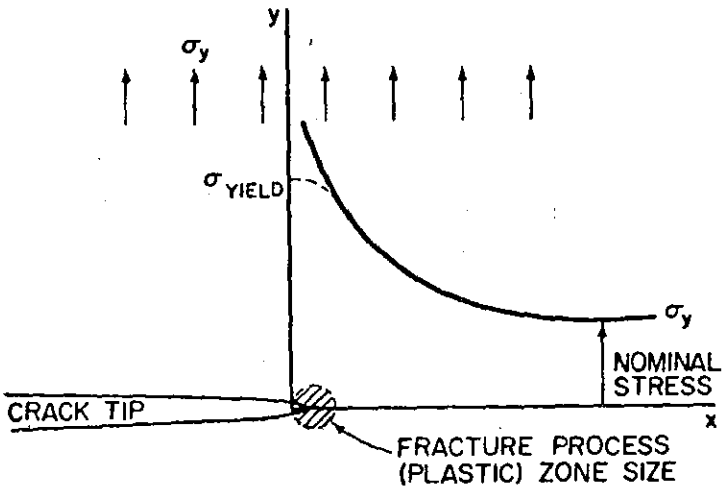

4-27. Plastic zone development in a fracture specimen.

NOTES:

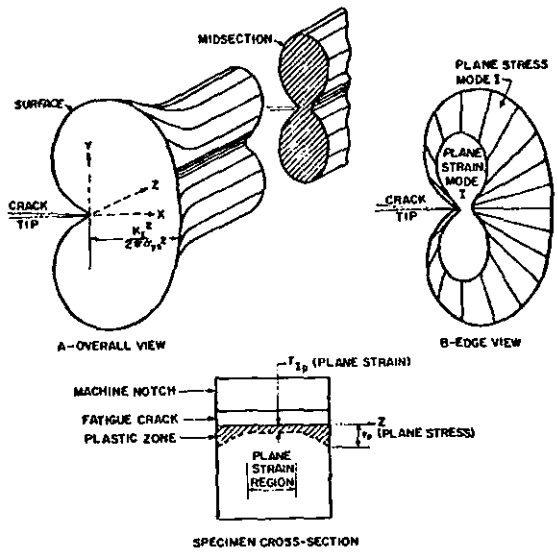

4-28. Plastic zone development in a fracture specimen.

NOTES:

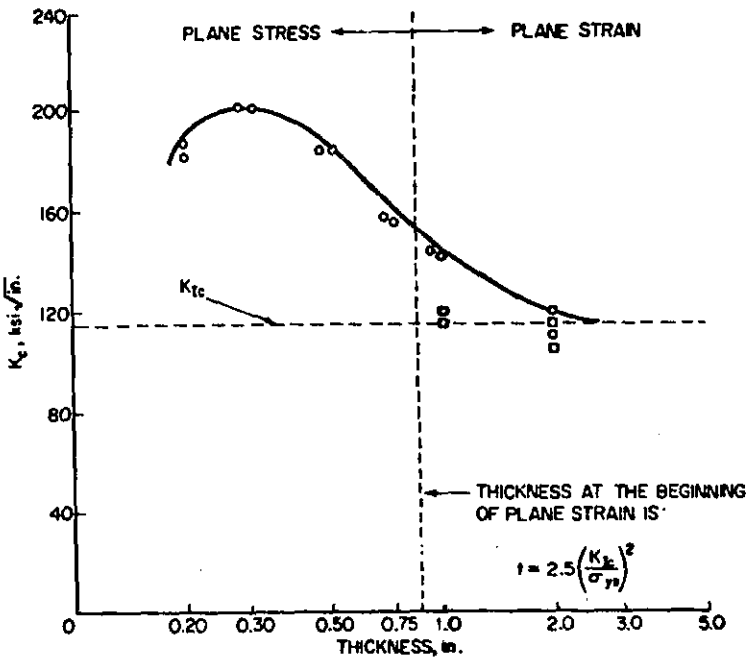

4-29. Effect of thickness of K_{Ic}

NOTES:

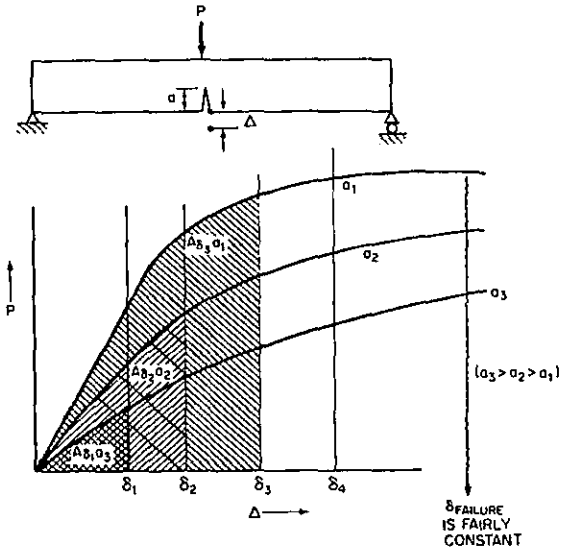

4-30. Compliance measurements

a) as crack gets large spring is weaker
b) as plasticity occurs the effective modulus is reduced

NOTES:

$$a \geq 2.5\left(\frac{K_{Ic}}{\sigma_{ys}}\right)^2$$

$$B \geq 2.5\left(\frac{K_{Ic}}{\sigma_{ys}}\right)^2$$

$$W \geq 5.0\left(\frac{K_{Ic}}{\sigma_{ys}}\right)^2$$

$$r_{y_{(\text{plane strain})}} \simeq \frac{1}{6\pi}\left(\frac{K_{Ic}}{\sigma_{ys}}\right)^2$$

$$\frac{\text{specimen thickness}}{\text{plastic-zone size}} = \frac{B}{r_y} \simeq \frac{2.5(K_{Ic}/\sigma_{ys})^2}{(1/6\pi)(K_{Ic}/\sigma_{ys})^2} \simeq 2.5(6\pi) \simeq 47$$

4-31. Specimen size requirements

NOTES:

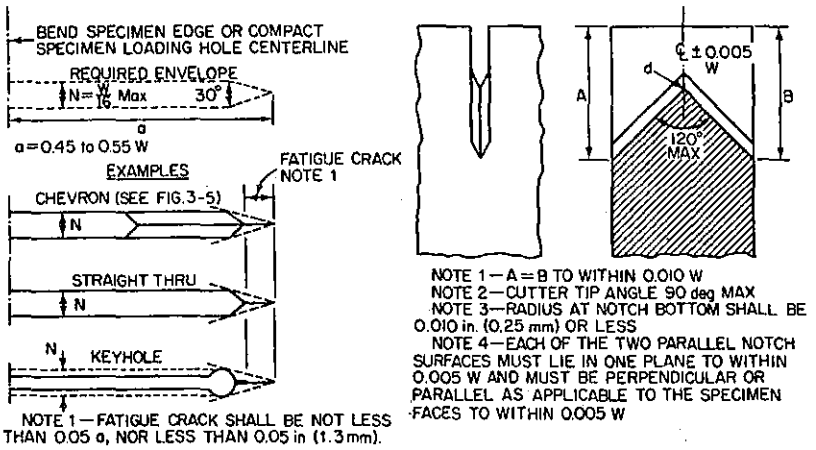

4-32. E399 Chevron notches

NOTES:

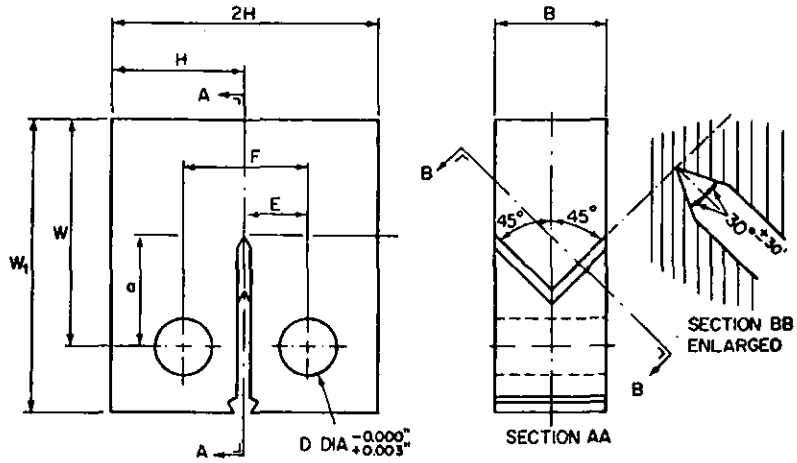

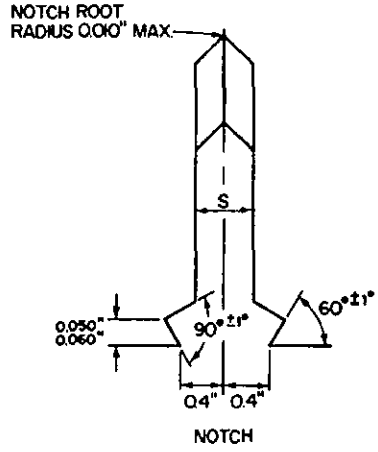

PROPORTIONS

a = NOMINAL CRACK LENGTH, INCLUDING FATIGUE CRACK

W = 2a

W_1 = 2.5a

S = 0.1a

H = 1.2a

D = 0.5a

F = 2E = 1.1a

B = THICKNESS

4-33. E399 CTS specimens.

NOTES:

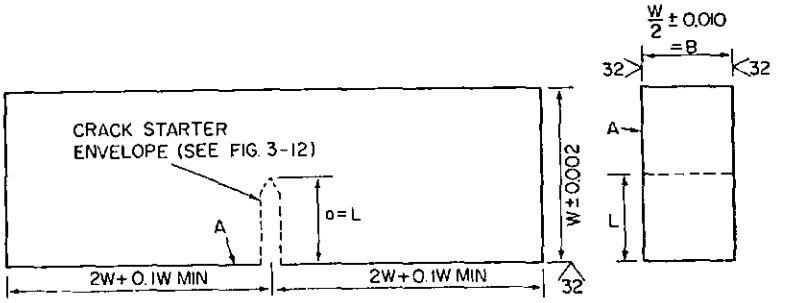

NOTE 1– DIMENSIONS AND TOLERANCES ARE IN INCHES UNLESS OTHERWISE INDICATED
NOTE 2– "A" SURFACES ARE TO BE PERPENDICULAR TO CENTER LINE OF CRACK-STARTER ENVELOPE WITHIN ±0.005-in TIR.
NOTE 3– INTEGRAL OR ATTACHABLE EDGES FOR CLIP GAGE ATTACHMENT MAY BE USED (SEE FIG. 3-16)

4-34. E399 3 point bend specimens.

NOTES:

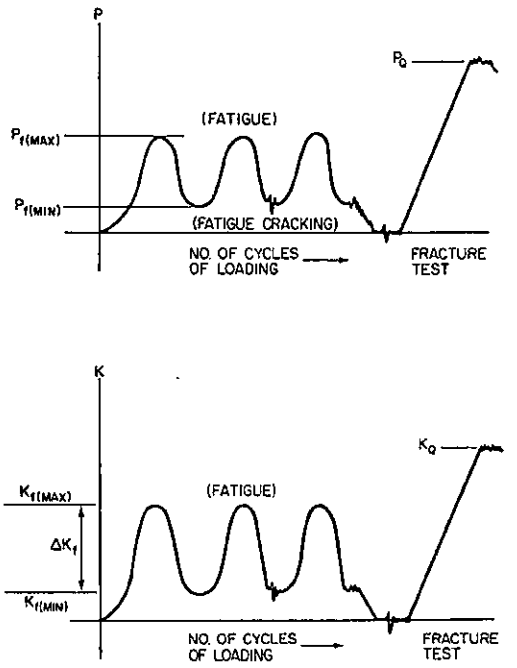

4-35. Fatigue precracking of K_{Ic} specimens.

NOTES:

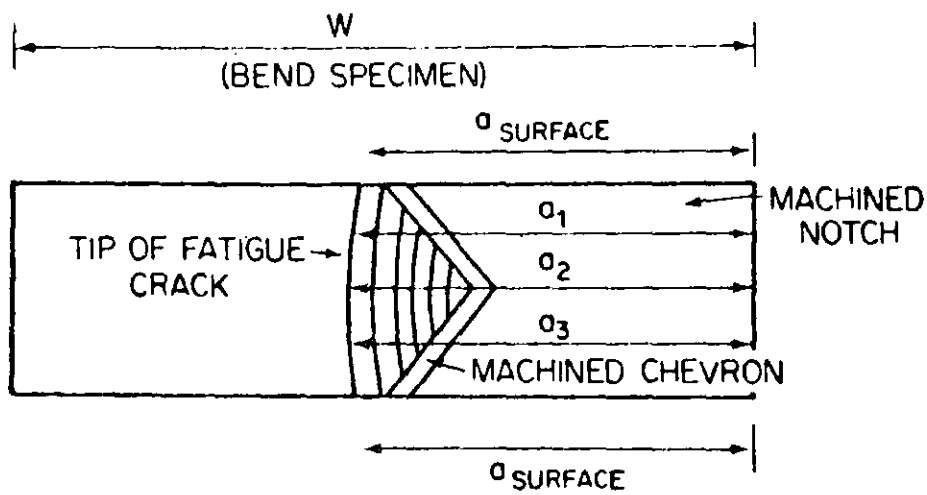

4-36. Fatigue precrack requirement

NOTES:

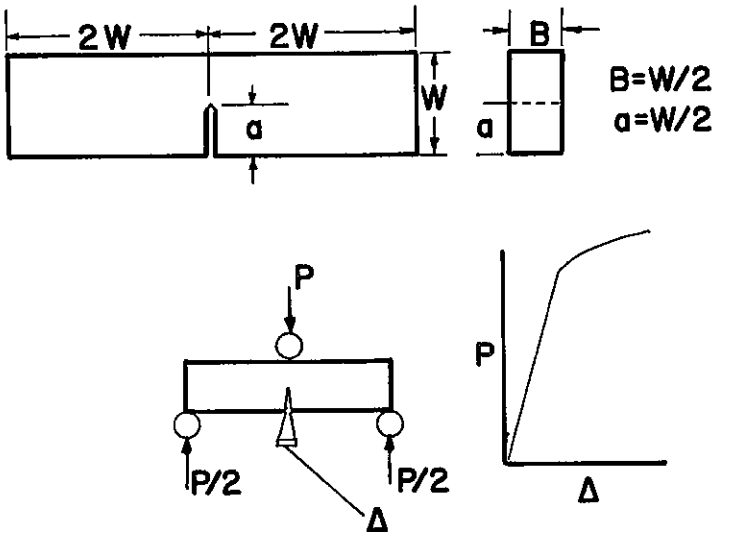

4-37. 3 point bend specimen setup for testing

NOTES:

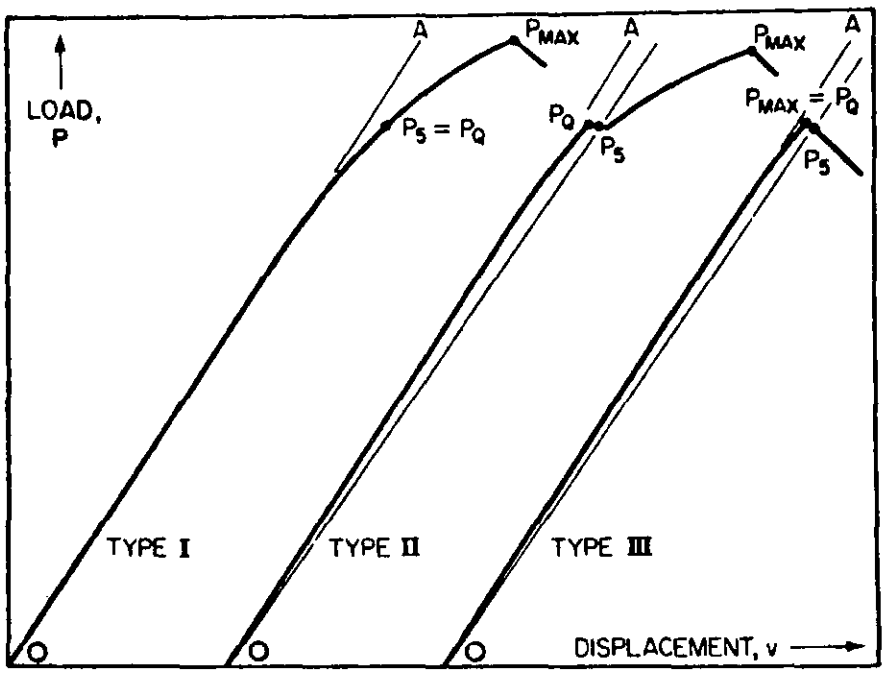

4-38. Typical load records from a K test.

NOTES:

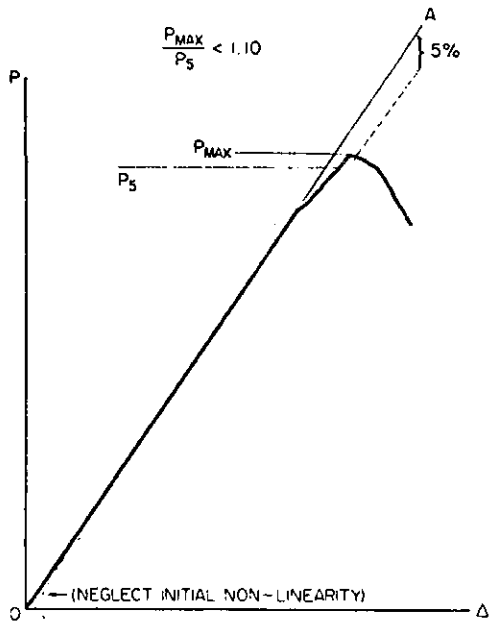

4-39. 5% secant offset.

NOTES:

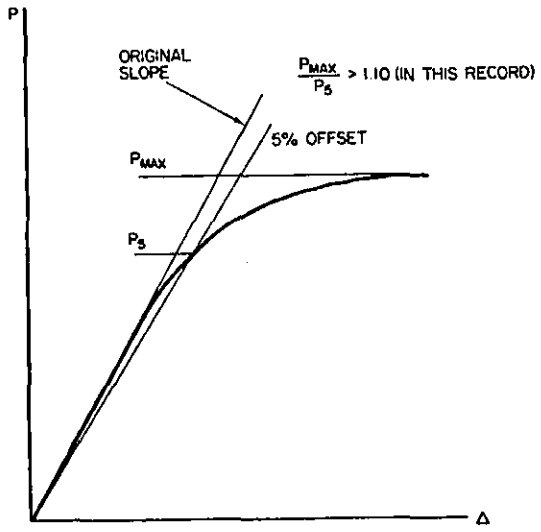

4-40. P-Δ record for a tough material.

NOTES:

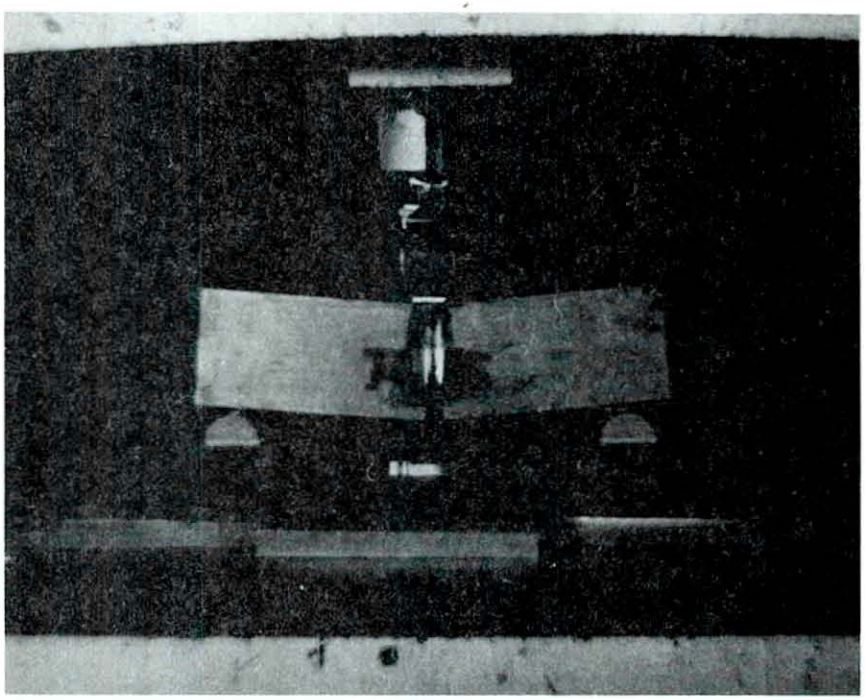

4-41. View of 3 point K_{Ic} test in progress.

NOTES:

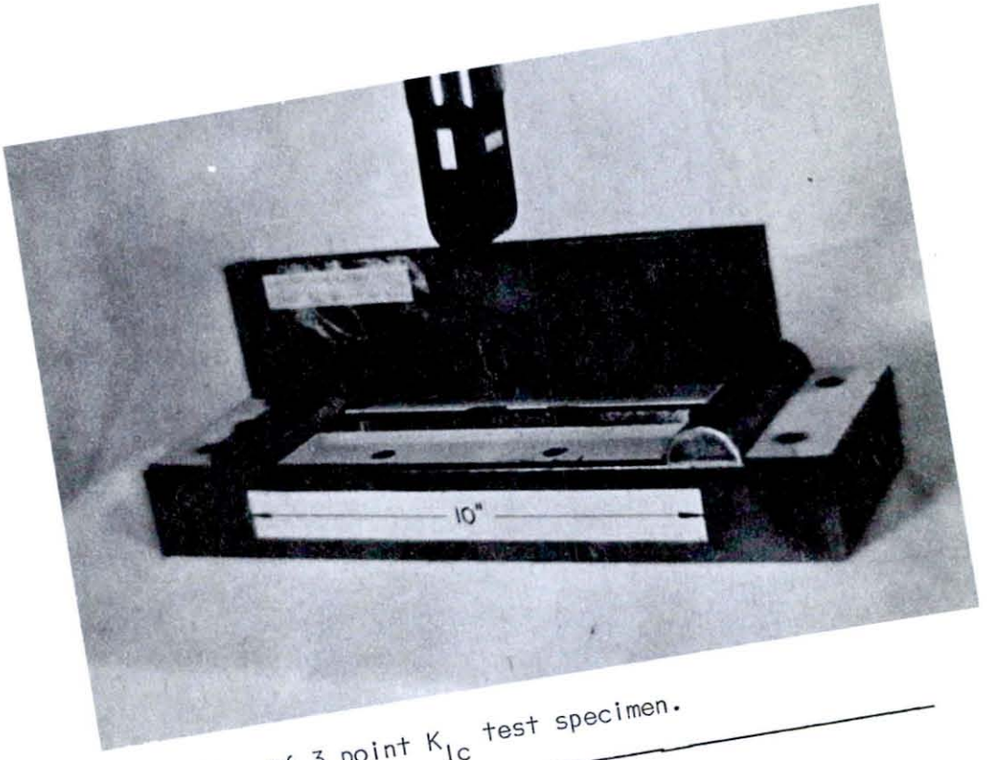

4-42. View of 3 point K_{Ic} test specimen.

NOTES:

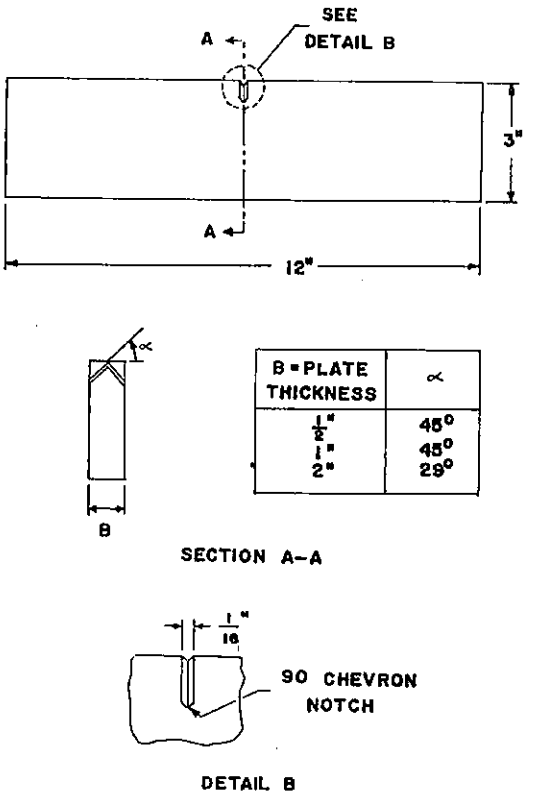

4-43. Details of Lehigh 3 point bend specimen.

NOTES:

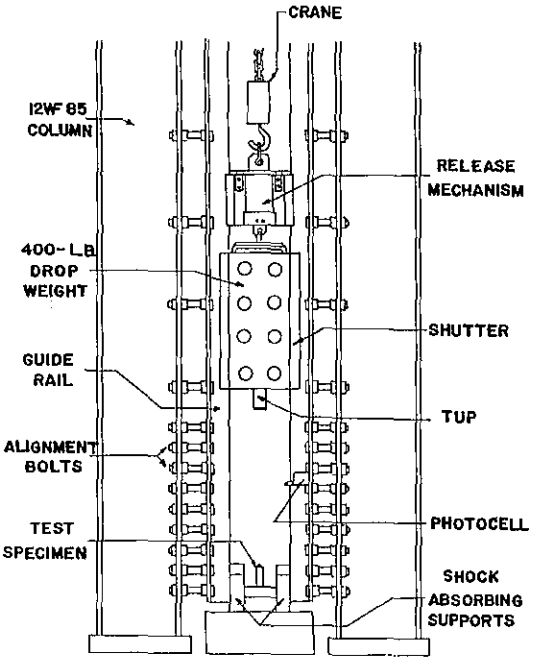

4-44. Schematic of Lehigh Drop test machine.

NOTES:

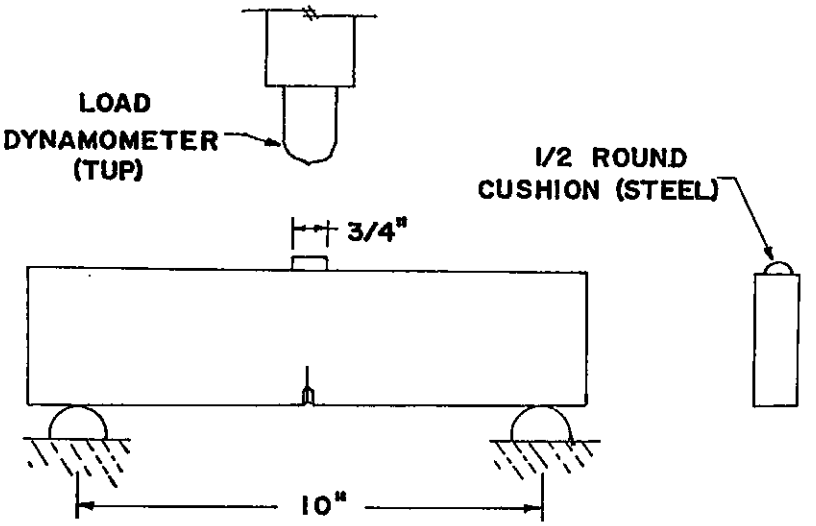

4-45. 3 point bend specimen and loading tup.

NOTES:

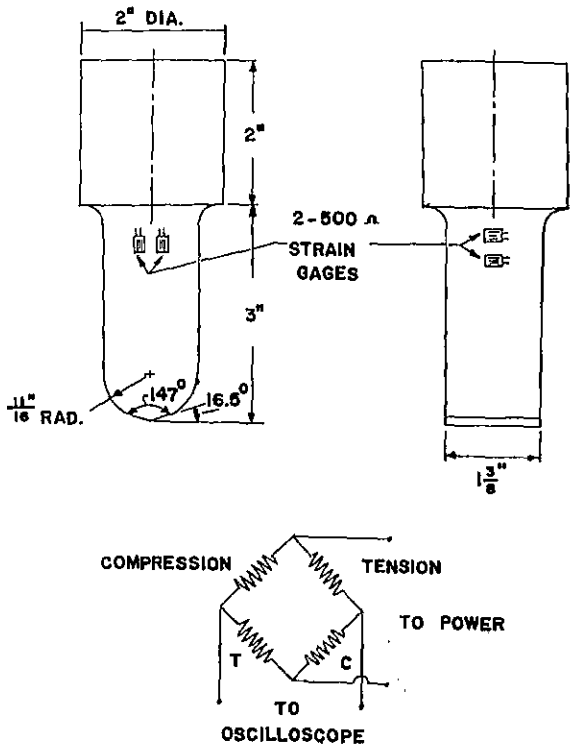

4-46. Loading tup.

NOTES:

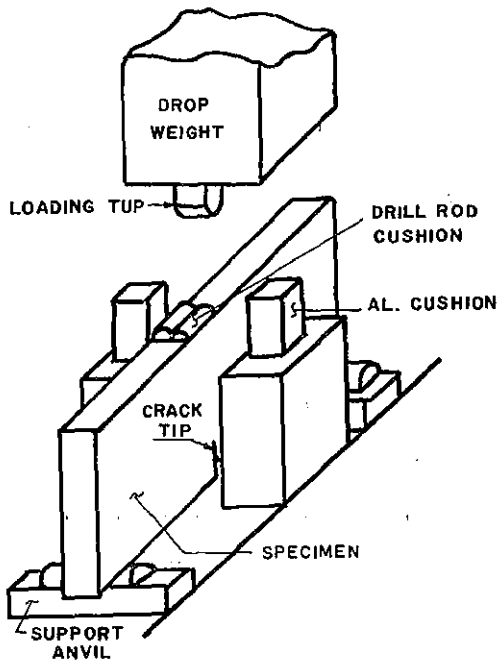

4-47. Lehigh dynamic K_{Ic} measurement system.

NOTES:

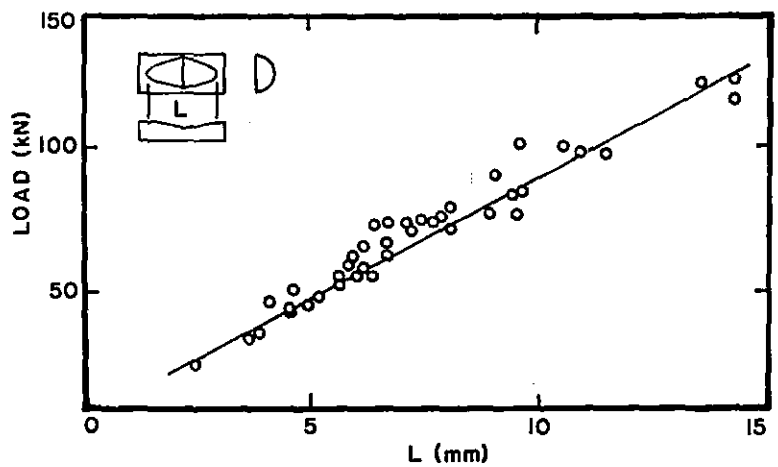

4-48. Load versus indentation length for drill rod cushions.

NOTES:

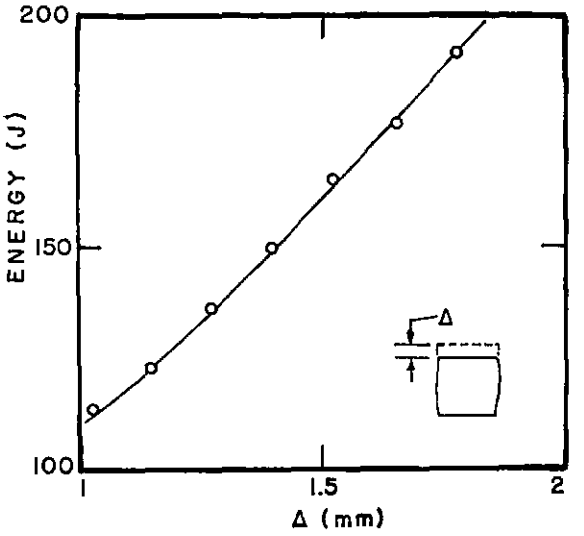

4-49. Energy versus block compression for aluminum blocks.

NOTES:

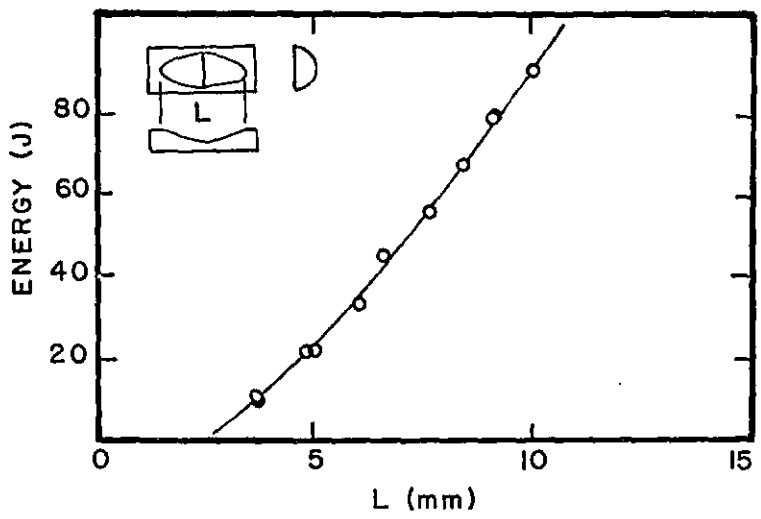

4-50. Energy versus indentation length for drill rod cushions.

NOTES:

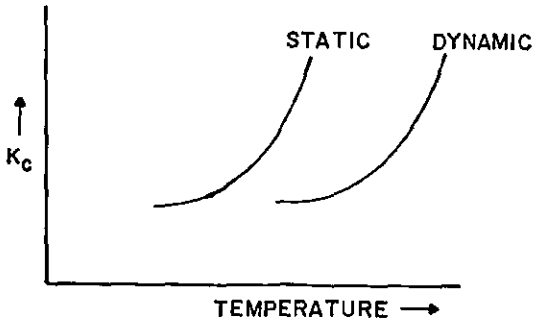

Ia.) LOADING RATE EFFECTS

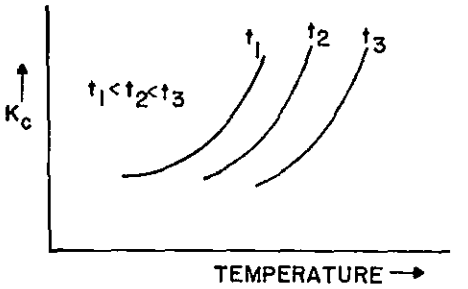

Ib.) THICKNESS EFFECTS

4-51. Effects of Temperature, Loading Rate and Thickness on K_c.

NOTES:

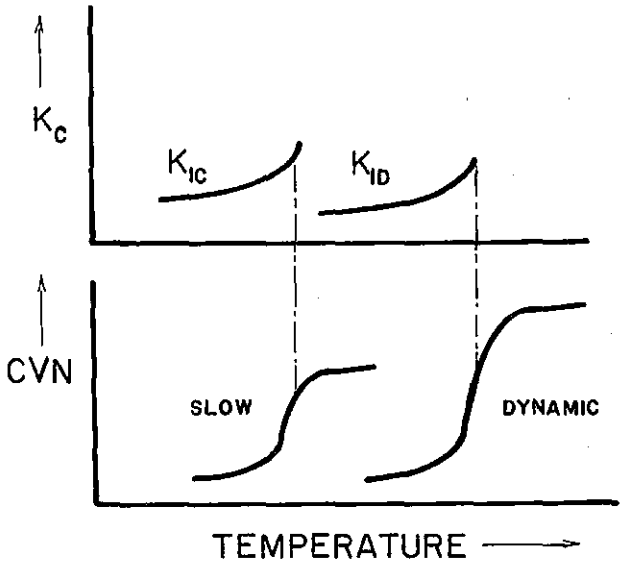

4-52. Schematic Representation of Correspondence of Temperature Transition Regions of K and CVN Curves.

NOTES:

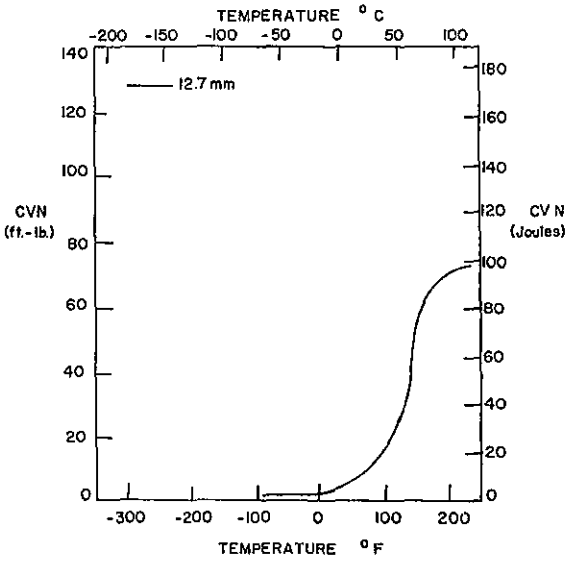

4-53. Lehigh CVN Results A7 Steel.

NOTES:

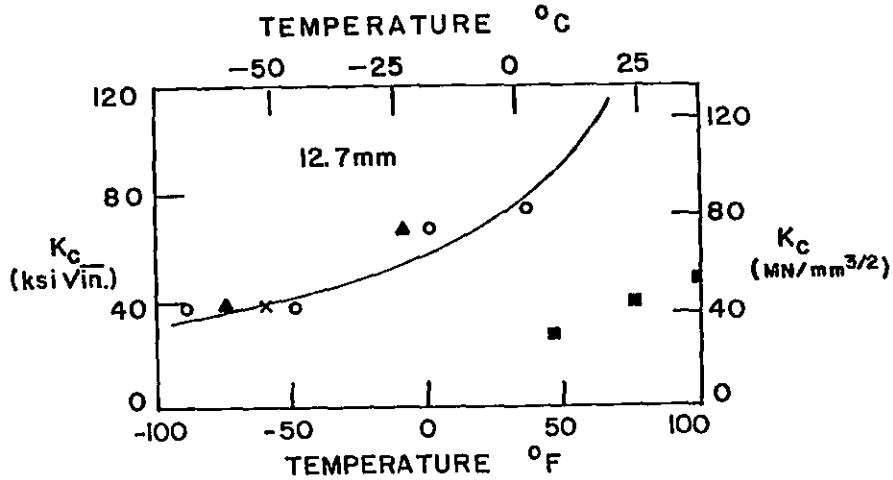

4-54. Lehigh K Data A7 Steel --- "R" Values, o Dynamic K Values, • Static K Values, ■ Estimate from Equation 4.5, x Point of Maximum Valid K.

NOTES:

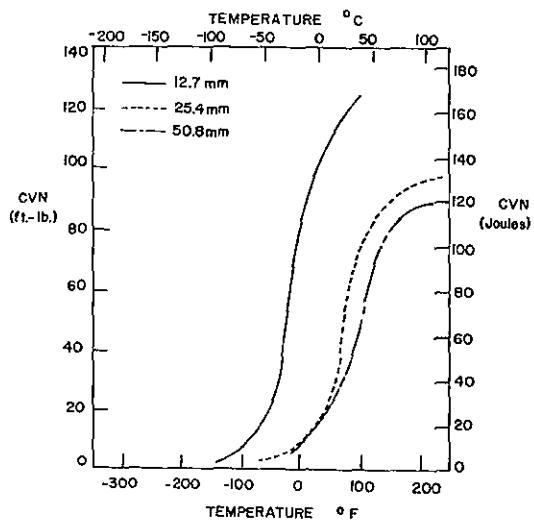

4-55. Lehigh CVN Results A242 Steel.

NOTES:

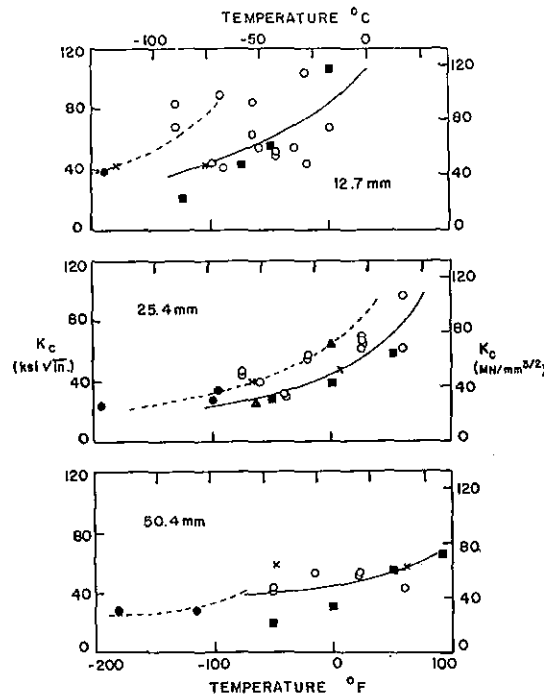

4-56. Lehigh K Data A242 Steel --- "R" Values, o Dynamic K Values, • Static K Values, ■ Estimate from Equation 4.5, x Point of Maximum Valid K.

NOTES:

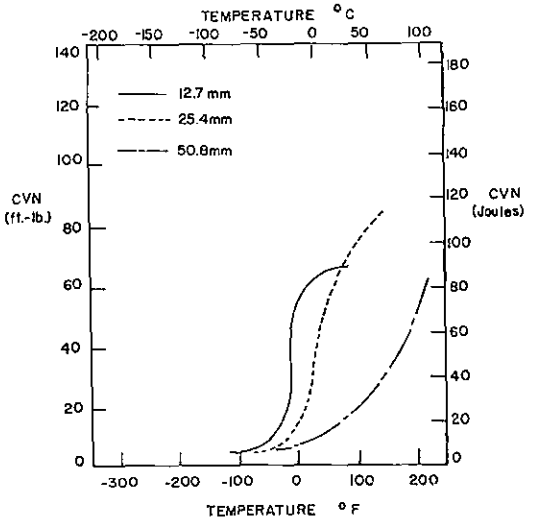

4-57. Lehigh CVN Results A440 Steel.

NOTES:

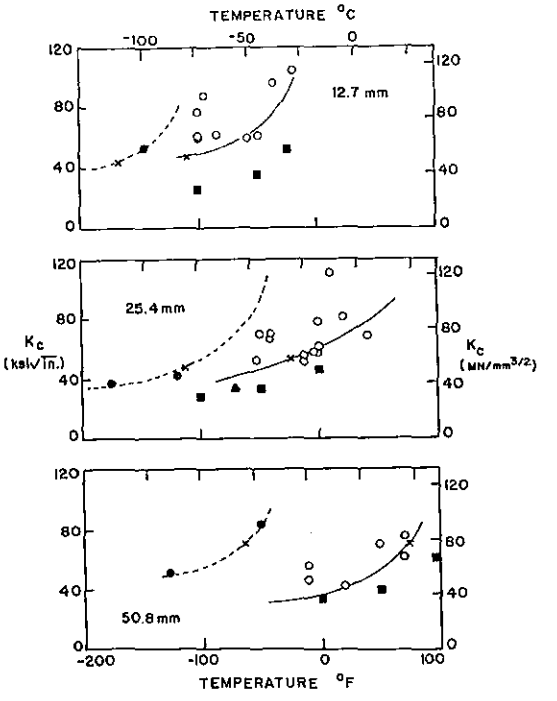

4-58. Lehigh K Data A440 Steel --- "R" Values, o Dynamic K Values, • Static K Values, ● Estimate from Equation 4.5, x Point of Maximum Valid K.

NOTES:

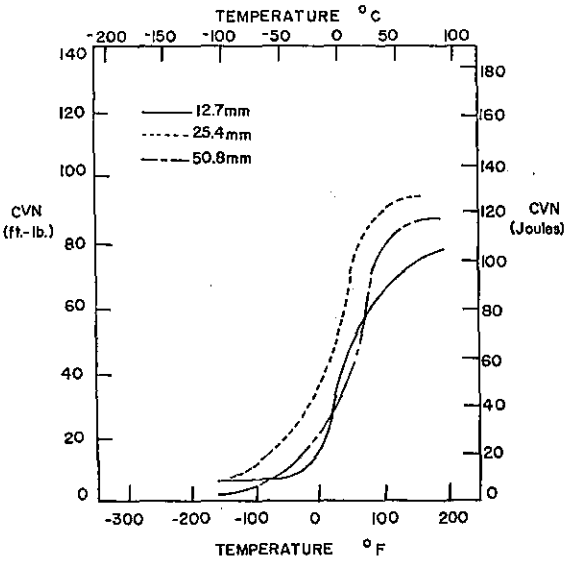

4-59. Lehigh CVN Results A588 Steel.

NOTES:

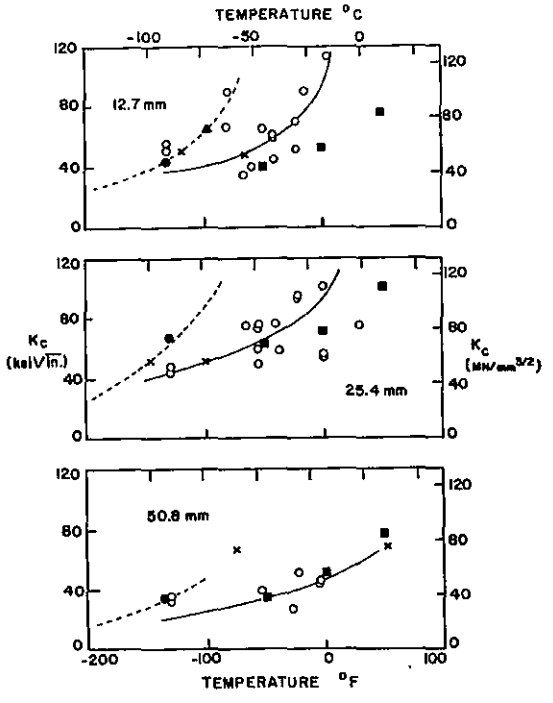

4-60. Lehigh K Data A588 Steel --- "R" Values, o Dynamic K Values, • Static K Values, ■ Estimate from Equation 4.5, x Point of Maximum Valid K.

NOTES:

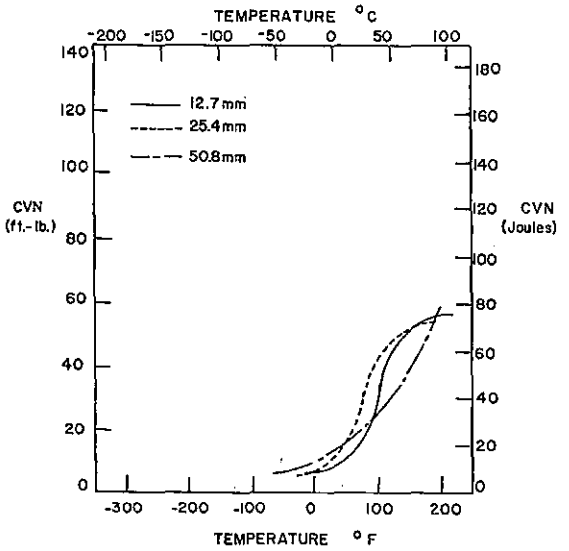

4-61. Lehigh CVN Results SAE 1035 Steel.

NOTES:

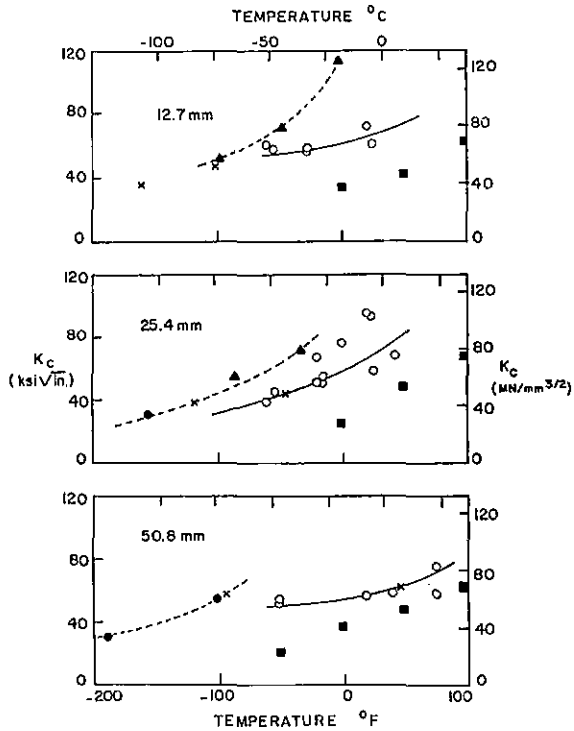

4-62. Lehigh K Data SAE1035 Steel --- "R" Values, o Dynamic K Values, • Static K Values, ■ Estimate from Equation 4.5, x Point of Maximum Valid K.

NOTES:

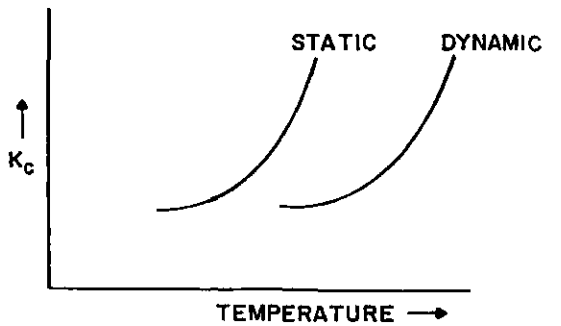

Ia.) LOADING RATE EFFECTS

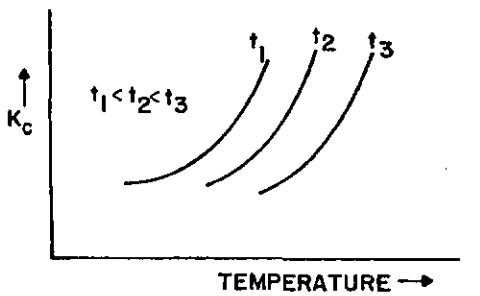

Ib.) THICKNESS EFFECTS

4-63. Effects of Temperature, Loading Rate and Thickness on K_c.

NOTES:

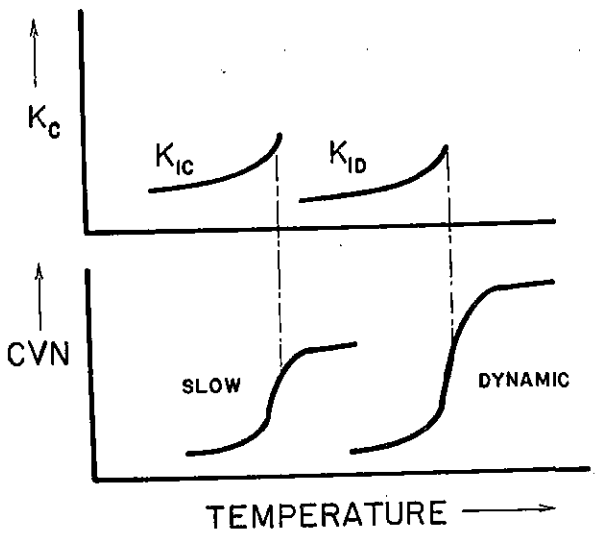

4-64. Schematic Representation of Correspondence of Temperature Transition Regions of K and CVN Curves.

NOTES:

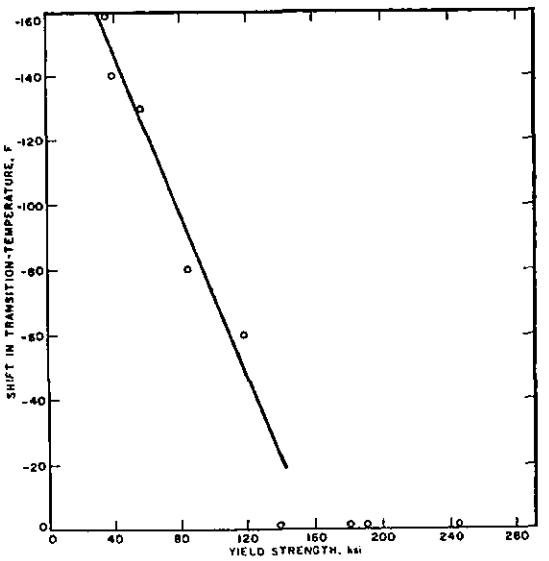

4-65. Temperature Shift versus Yield Strength.

NOTES:

ASTM Designation	*Thickness (in.)*	*CVN Impact Value, ft lb*		
		*Zone 1**	*Zone 2**	*Zone 3**
A36		15 @ 70°F	15 @ 40°F	15 @ 10°F
A572	Up to 4 in. mechanically fastened	15 @ 70°F	15 @ 40°F	15 @ 10°F
	Up to 2 in. welded	15 @ 70°F	15 @ 40°F	15 @ 10°F
A440		15 @ 70°F	15 @ 40°F	15 @ 10°F
A441		15 @ 70°F	15 @ 40°F	15 @ 10°F
A242		15 @ 70°F	15 @ 40°F	15 @ 10°F
A588**	Up to 4 in. mechanically fastened	15 @ 70°F	15 @ 40°F	15 @ 10°F
	Up to 2 in. welded	15 @ 70°F	15 @ 40°F	15 @ 10°F
	Over 2 in. welded	20 @ 70°F	20 @ 40°F	20 @ 10°F
A514	Up to 4 in. mechanically fastened	25 @ 30°F	25 @ 0°F	25 @ −30°F
	Up to 2½ in. welded	25 @ 30°F	25 @ 0°F	25 @ −30°F
	Between 2½–4 in. welded	35 @ 30°F	35 @ 0°F	35 @ −30°F

*Zone 1: minimum service temperature 0°F and above.
Zone 2: minimum service temperature from −1° to −30°F.
Zone 3: minimum service temperature from −31° to −60°F.
**If the yield point of the material exceeds 65 ksi, the temperature for the CVN value for acceptability shall be reduced by 15°F for each increment of 10 ksi above 65 ksi.

4-66. AASHTO Toughness Requirements.

NOTES:

FATIGUE LIFE

CRACK INITIATION

CRACK PROPAGATION

FINAL FAILURE

4-67. Stages of a Structures Life.

NOTES:

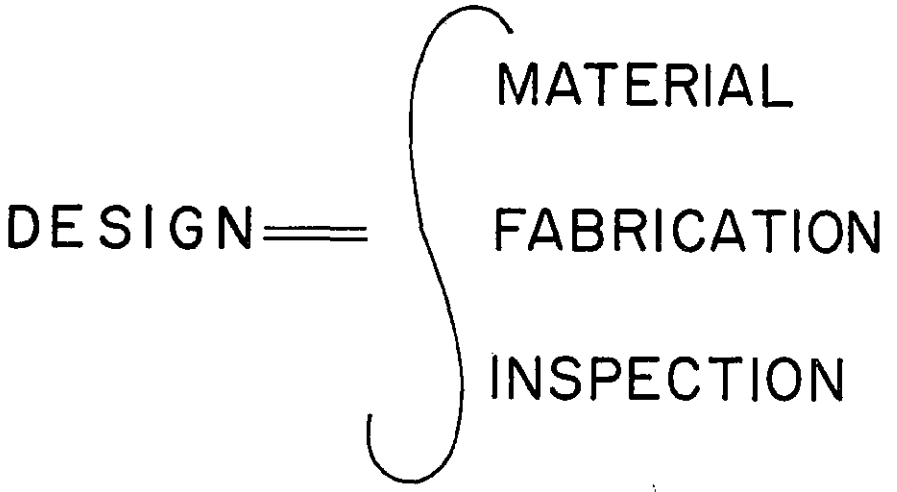

4-68. Design Requirements

NOTES:

FIGURES - SESSION 5

DISCUSSION OF FRACTURE CONTROL PLANS FOR NEW AND OLD BRIDGE STRUCTURES - PRESENTATION OF CASE STUDIES

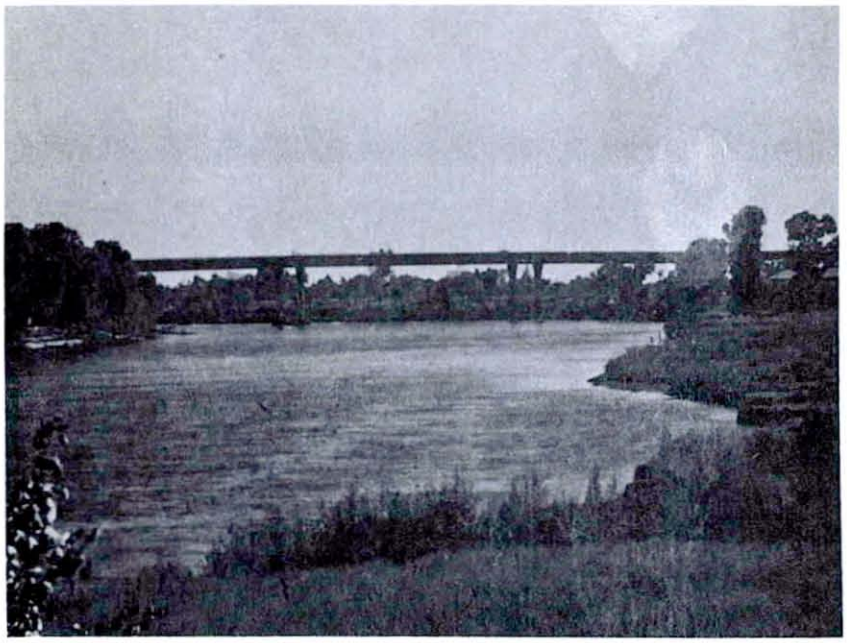

5-1 Overall View of Bryte Bend Bridge, Sacramento, California

NOTES:

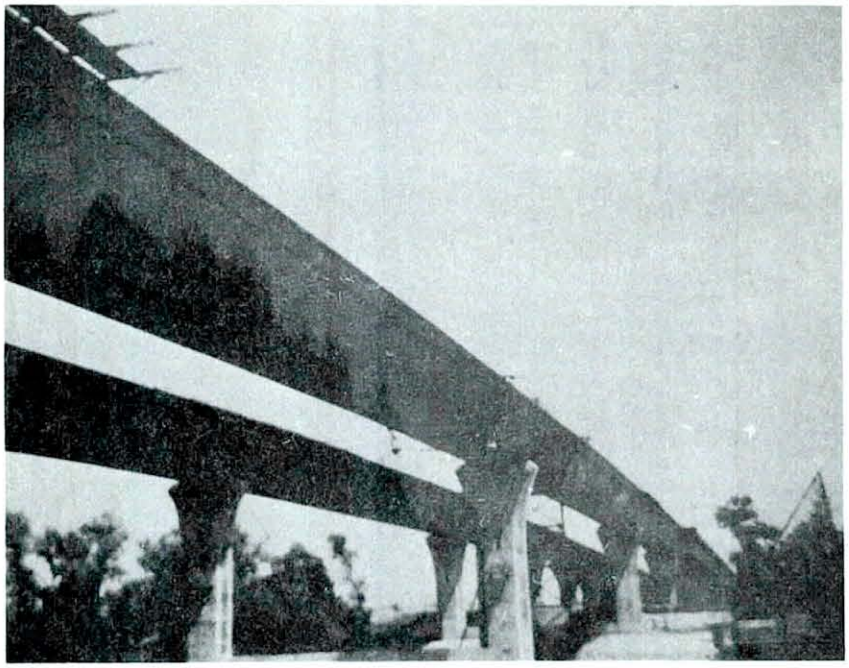

5-2. View of Twin Structures over River.

NOTES:

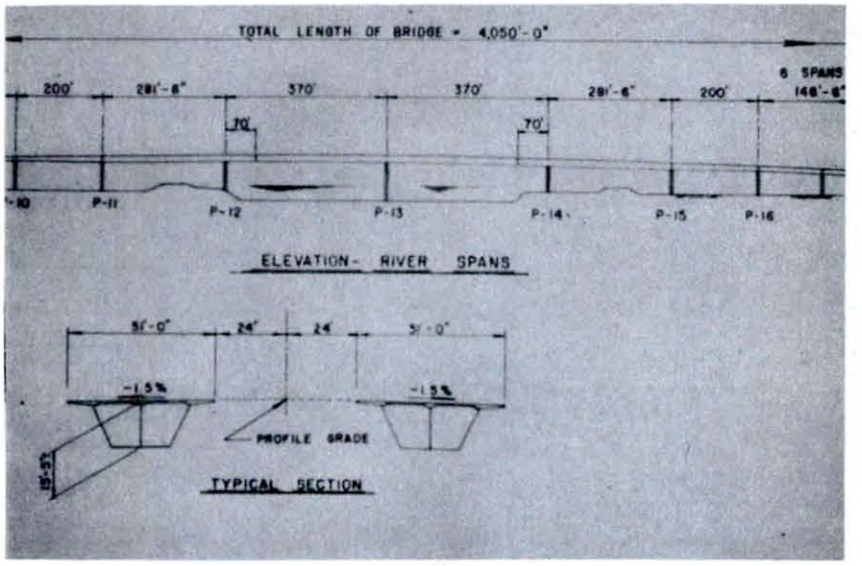

5-3. Section and Elevation of 4,050 ft. long structure.

NOTES:

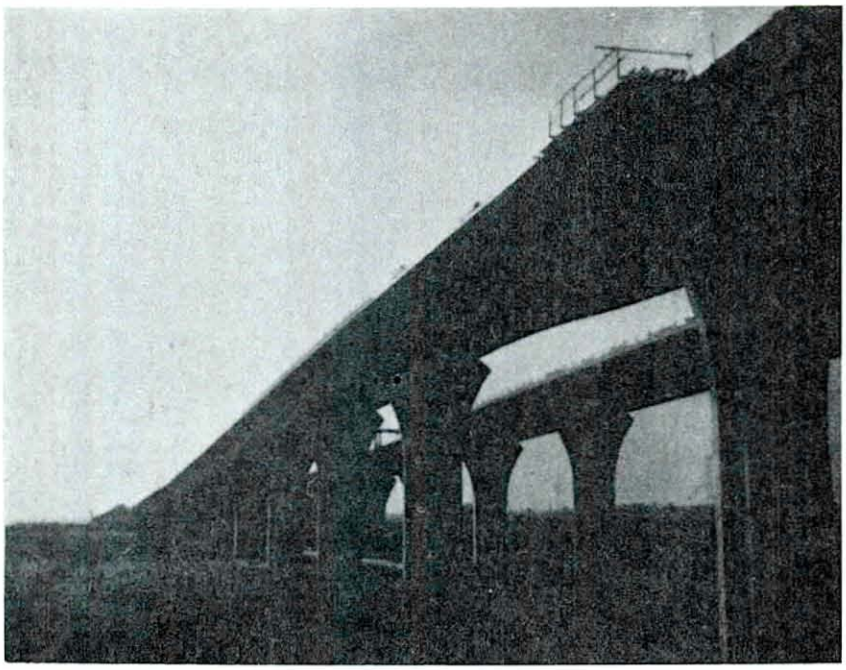

5-4. Transition Region Between Simple Approach Spans and Continuous Bridge Structure

NOTES:

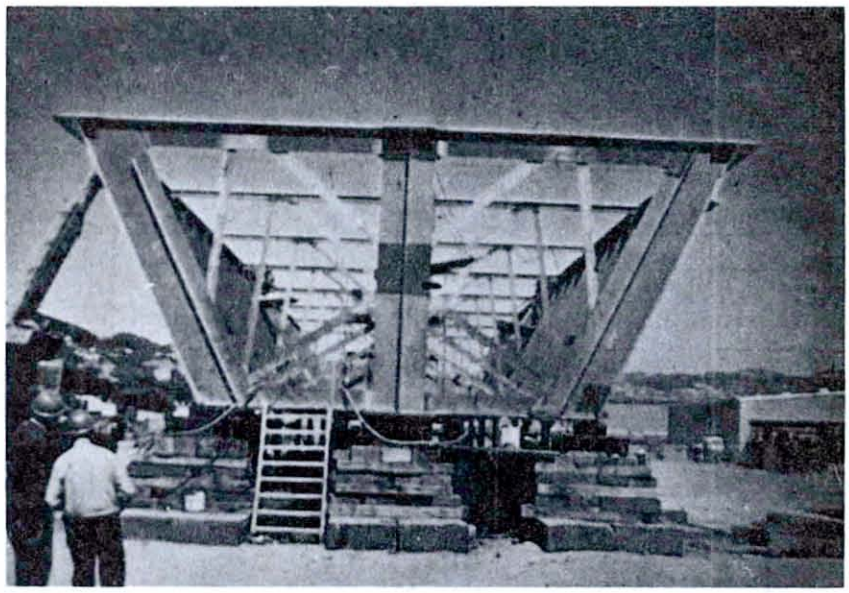

5-5. Cross-Section of Box Girder

NOTES:

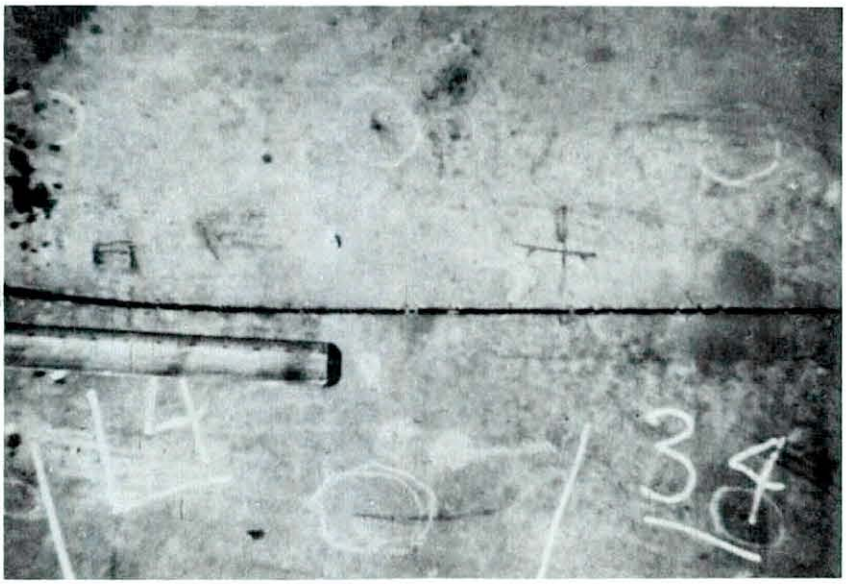

5-6. Plan View of Brittle Fracture in Flange

NOTES:

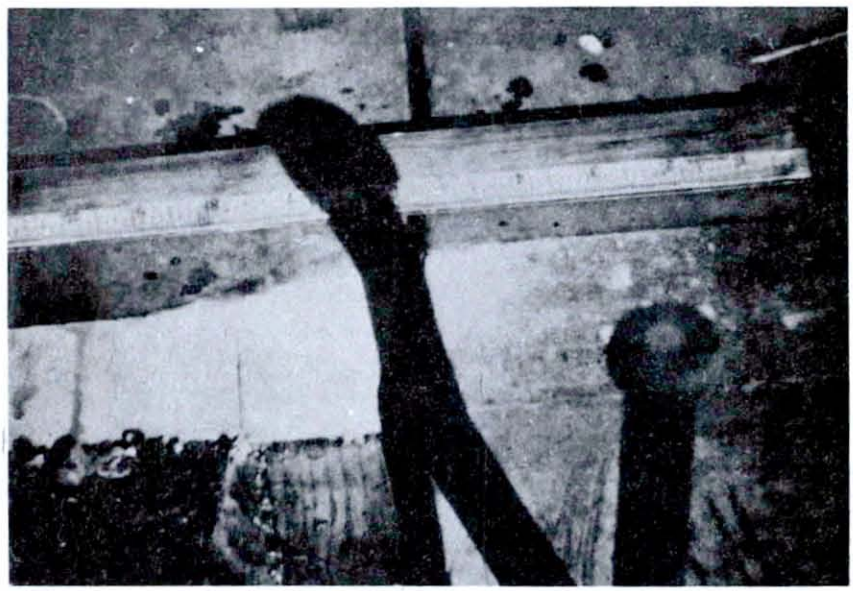

5-7. Brittle Fracture Origin at intersection of lateral attachment and flange plate

NOTES:

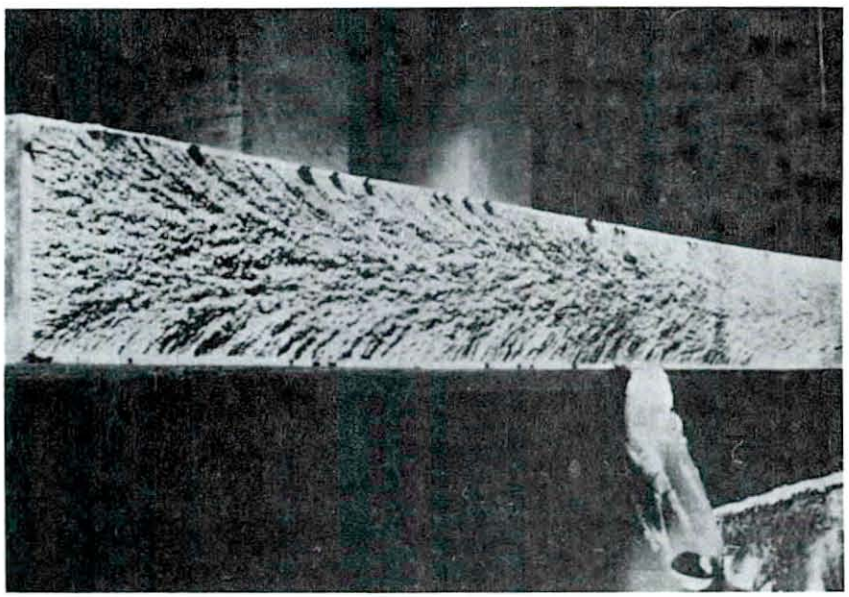

5-8. Brittle Fracture Surface Showing Classic Herringbone Pattern and Small Shear Lips.

NOTES:

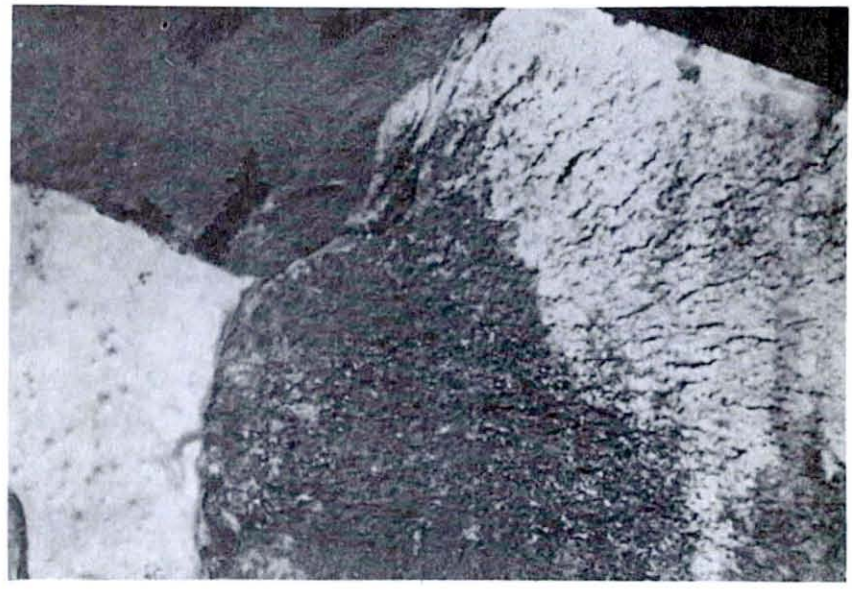

5-9. Origin of Fracture Showing 0.2-inch deep weld crack and 1.3-inch Deep Crack

NOTES:

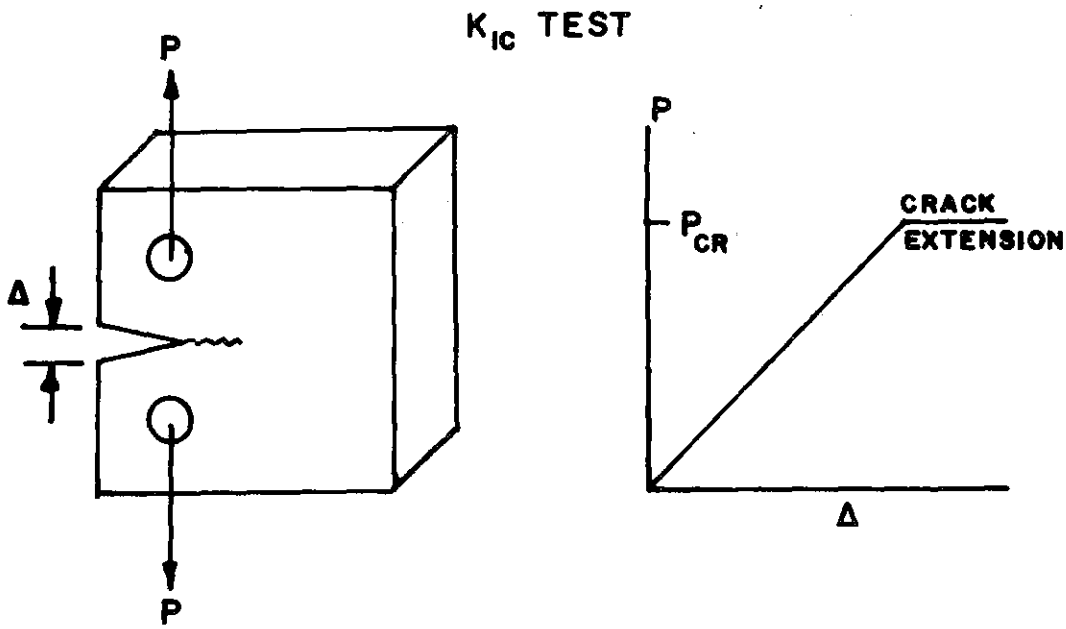

5-10. Schematic of K_{Ic} Test Specimen and P-Δ Test Record
a) fatigue cracked specimen-sharp notch
b) P_{CR} at instability

NOTES:

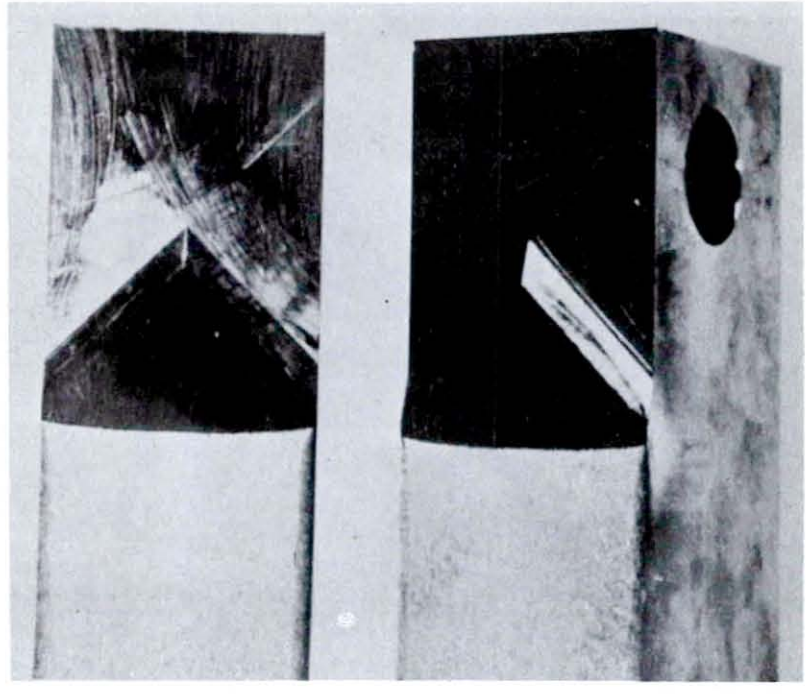

5-11. Actual Fracture Surface of K_{Ic} Test Specimen

NOTES:

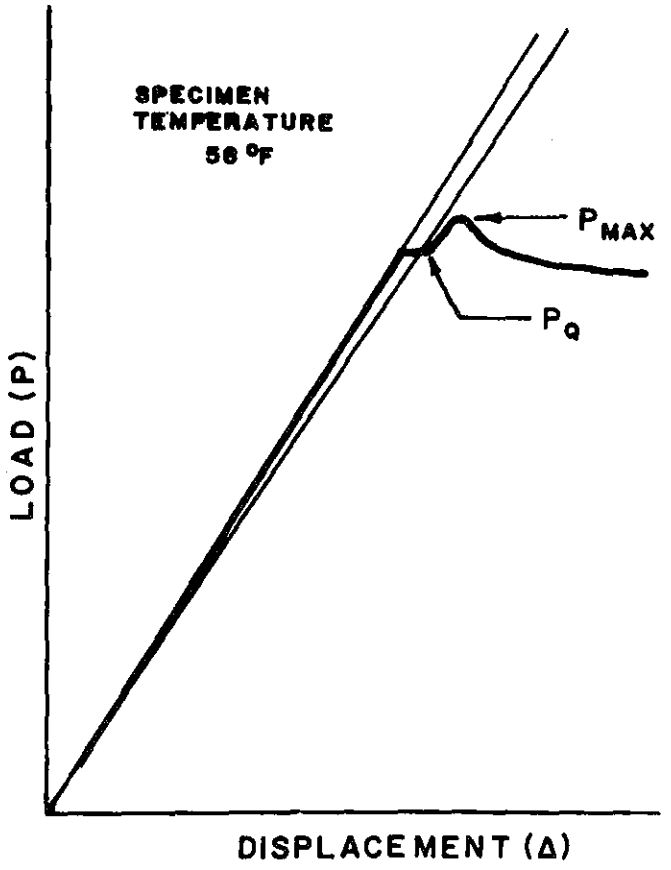

5-12. Actual P-Δ Test Record for K_{Ic} Test Specimen - K_{Ic} - 55 ksi$\sqrt{in}$. (satisfied E-399 Test Method at ^{c}+60°F)

NOTES:

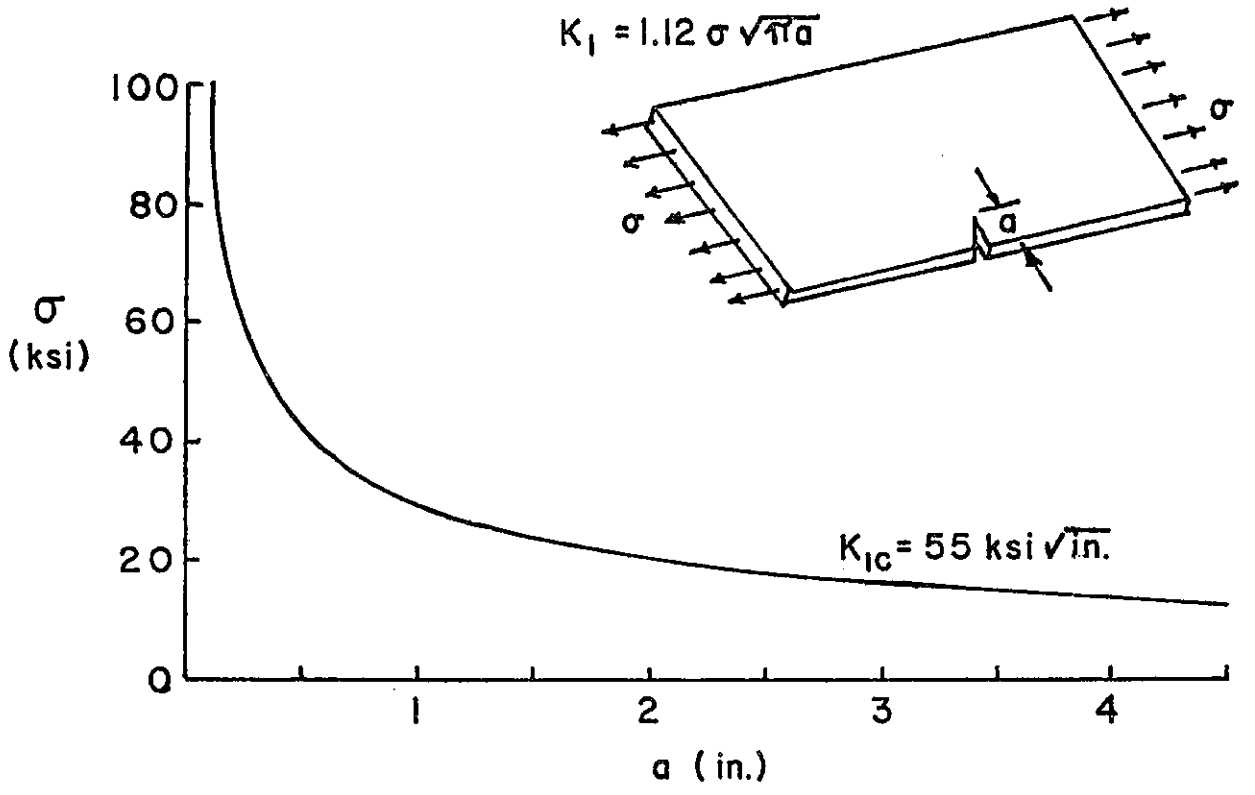

5-13. Stress-Flaw-Size Relation for Edge Crack in Steel with K_{Ic} - 55 ksi$\sqrt{in.}$

a) critical crack size for σ_{ys}
b) critical crack size for σ = 45 ksi
c) critical crack size for σ = 28 ksi

NOTES:

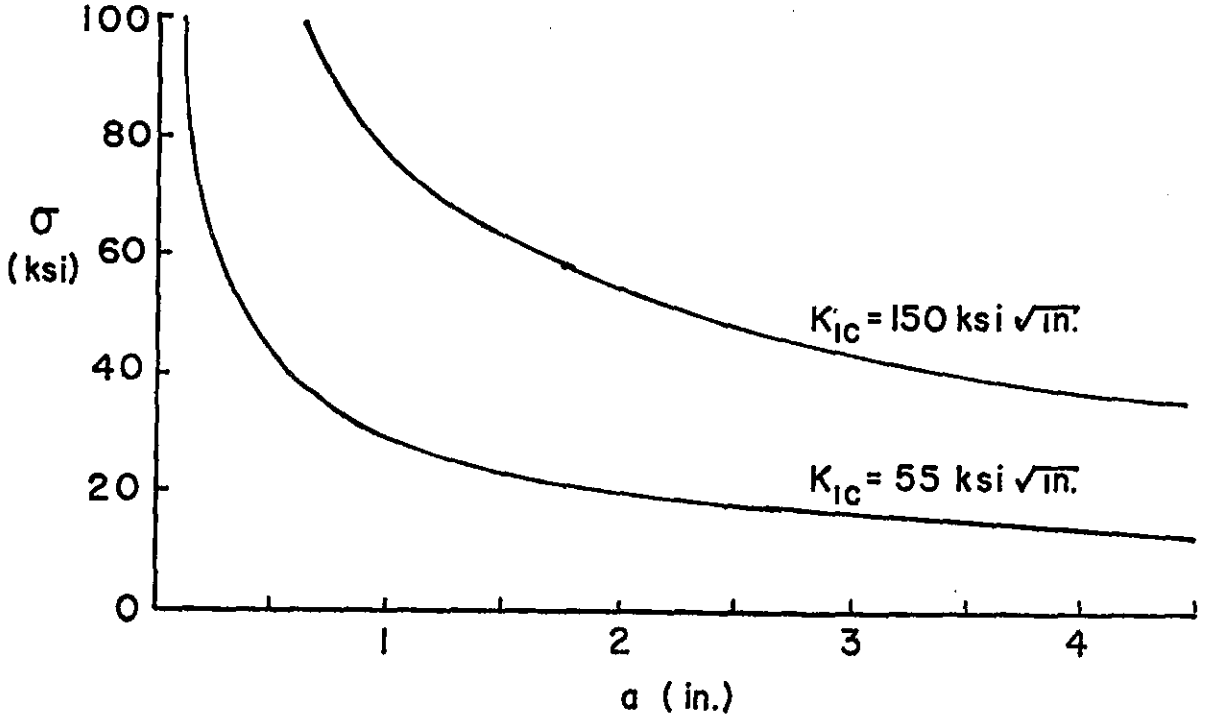

5-14. Stress-Flaw Size Relation for Edge Crack in Steel with K_{Ic} = 55 and 150 ksi$\sqrt{in.}$

a) compare a_{cr}
b) effect of toughness
c) 150 typical

NOTES:

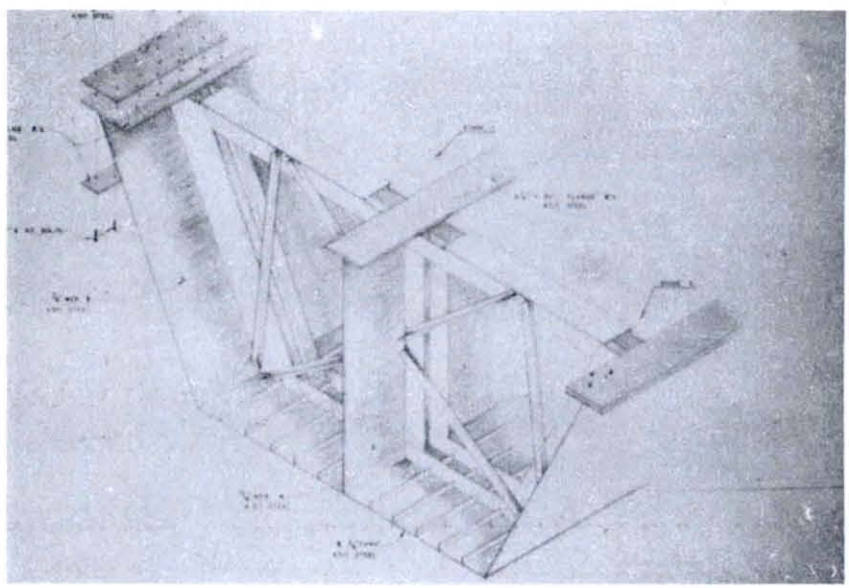

5-15. Schematic Showing Location of Additional Flange Plates.

NOTES:

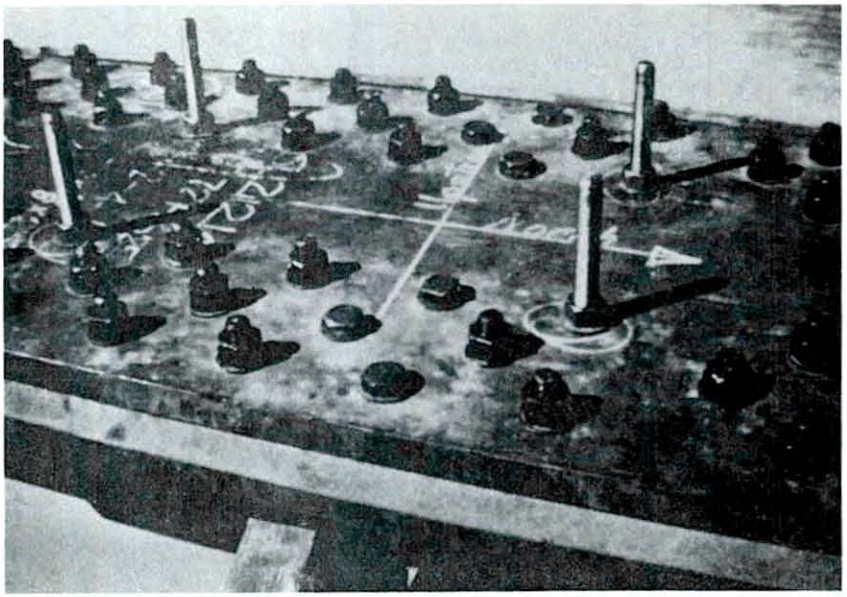

5-16. Closeup of Additional Plates Attached to Original Flange Plates

NOTES:

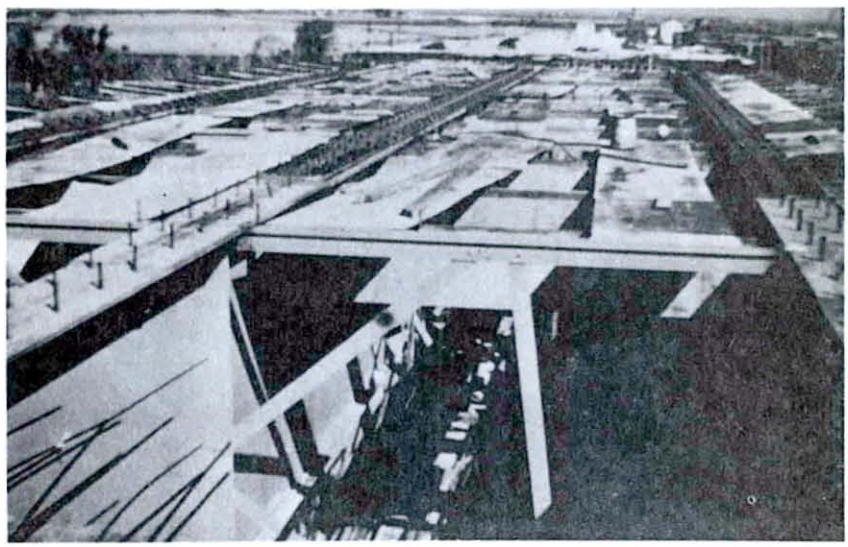

5-17. Overall View of Additional Plates Extending Back to Zero Stress Region.

NOTES:

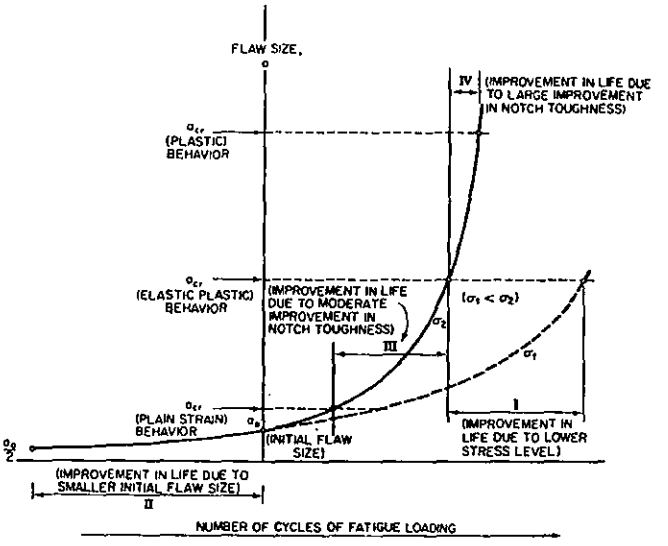

5-18. Schematic Showing flaw size- fatigue life relations for various critical crack sizes.

a) Region I
b) Region II
c) Region III
d) Region IV

NOTES:

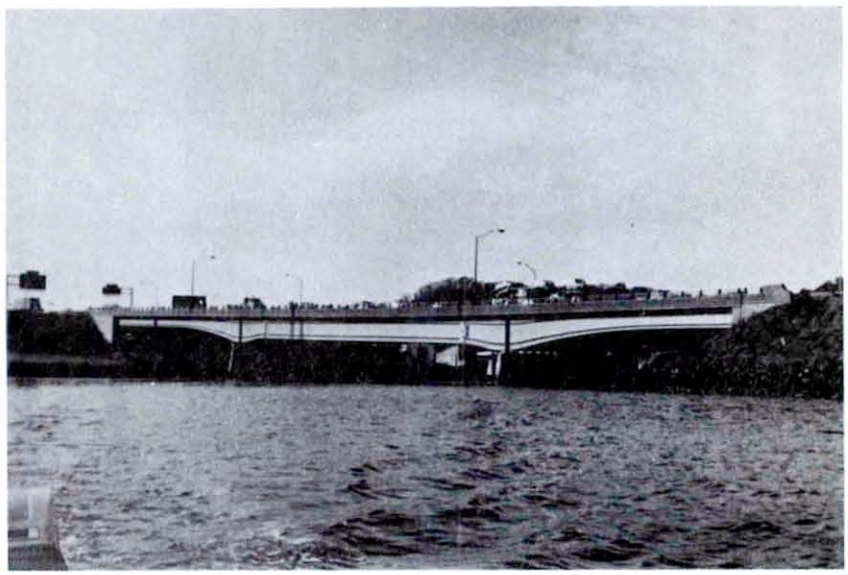

5-19. Profile of Quinnipiac River Bridge

NOTES:

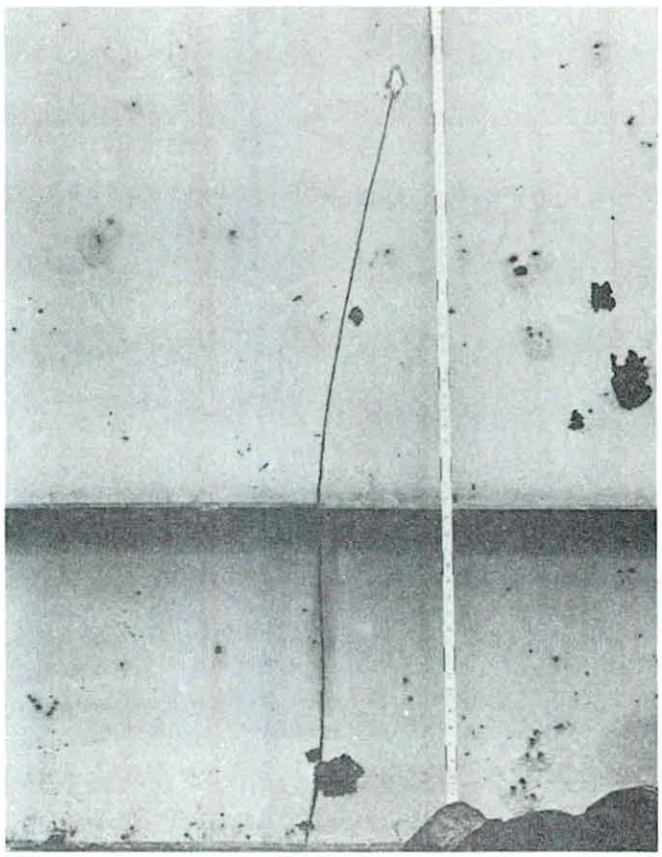

5-20. Crack in Web of Fascia Girder.

NOTES:

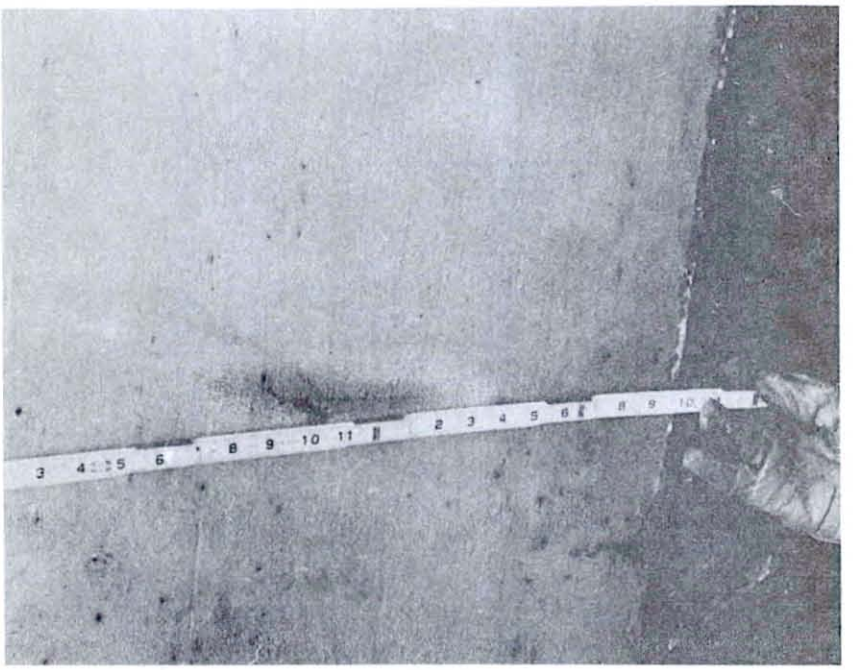

5-21. Crack on Bottom of Beam Flange.

NOTES:

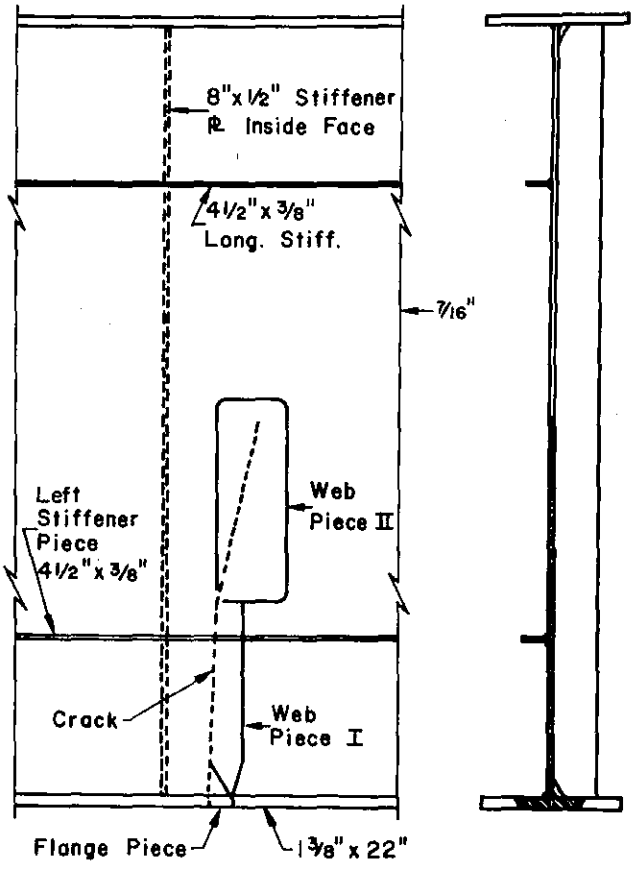

5-22. Schematic of Girder Showing Sections Removed for Examination at Crack

NOTES:

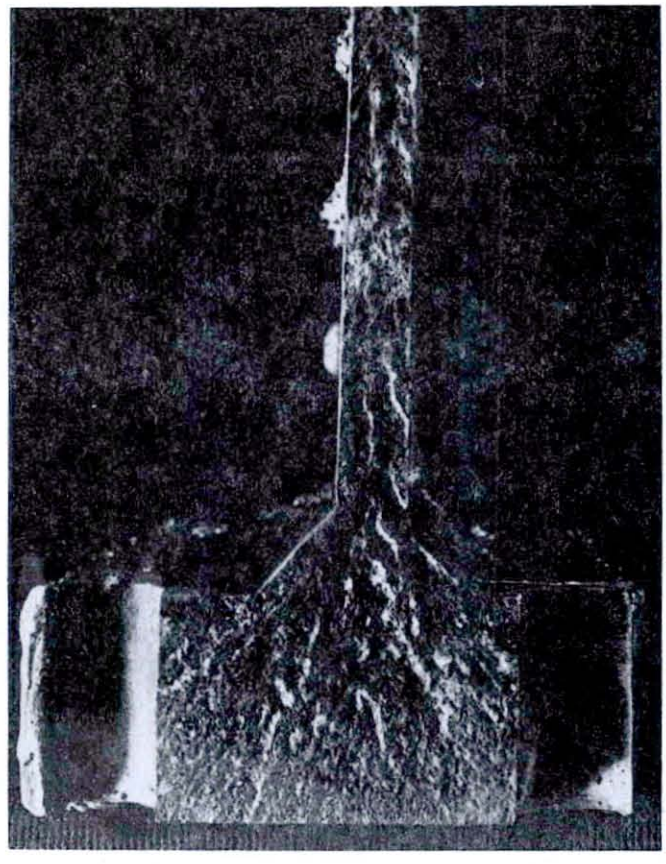

5-23. Fracture Surface at Flange-Web Junction

NOTES:

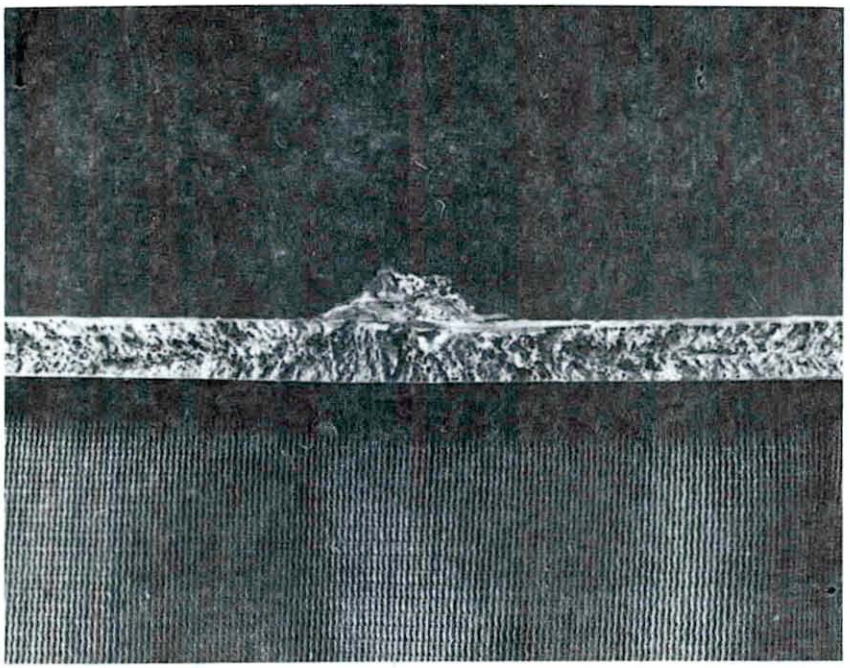

5-24. Fracture Surface of Web Near Longitudinal Stiffener

NOTES:

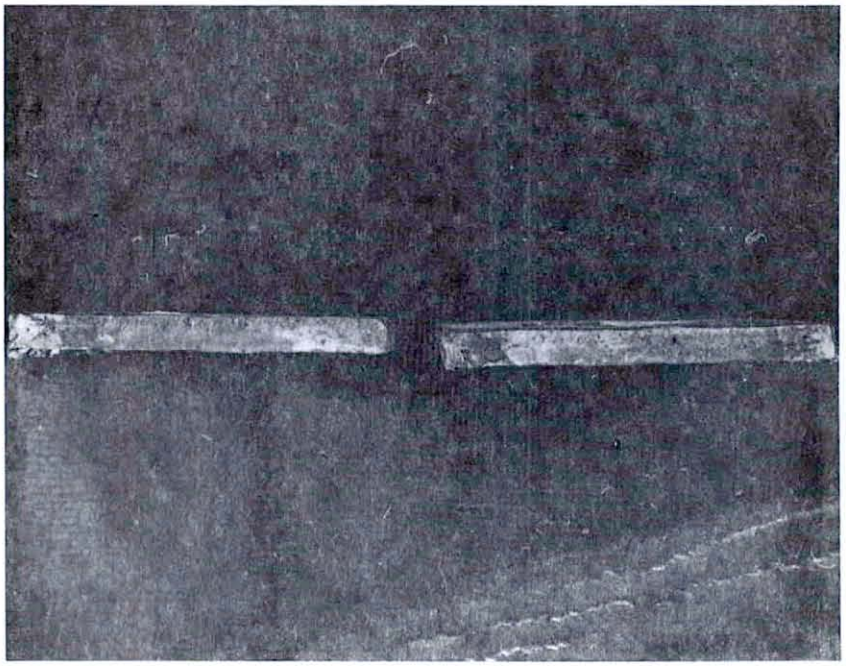

5-25. Ends of Longidudinal Stiffener at Crack

NOTES:

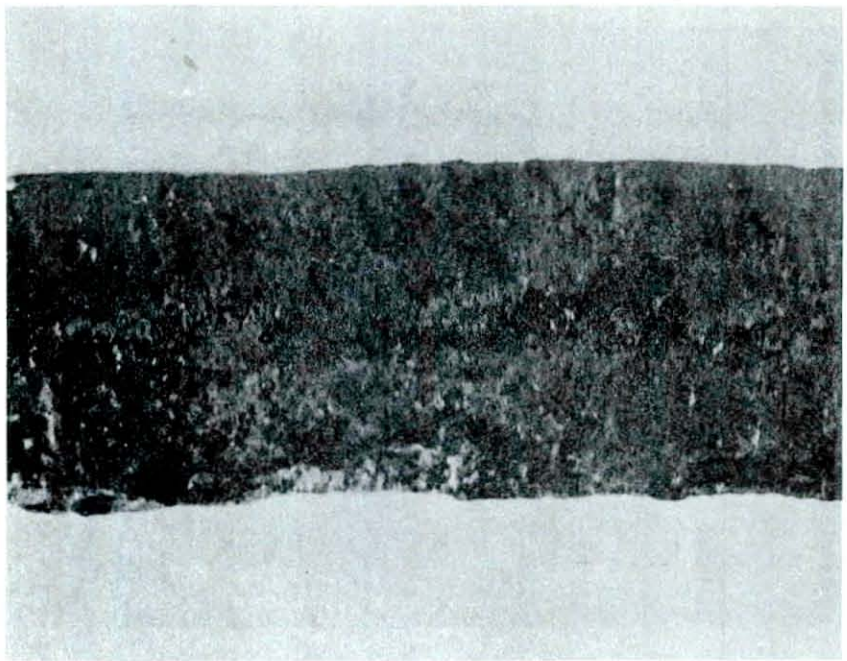

5-26. Fracture Surface of Longitudinal Stiffener Showing Lack of Penetration of Transverse Weld

NOTES:

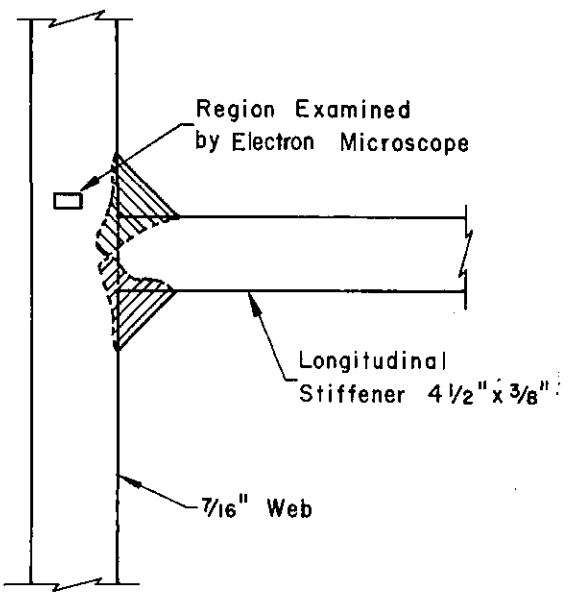

5-27. Schematic Showing Location Examined by Electron Microscope.

NOTES:

5-28. Crack Growth Striations Nearest Longitudinal Stiffener - 49125X

NOTES:

5-29. Crack Growth Striations Nearer Web Surface - 49125X

NOTES:

5-30. Cleavage in Flange Near Bottom Surface - 4300X

NOTES:

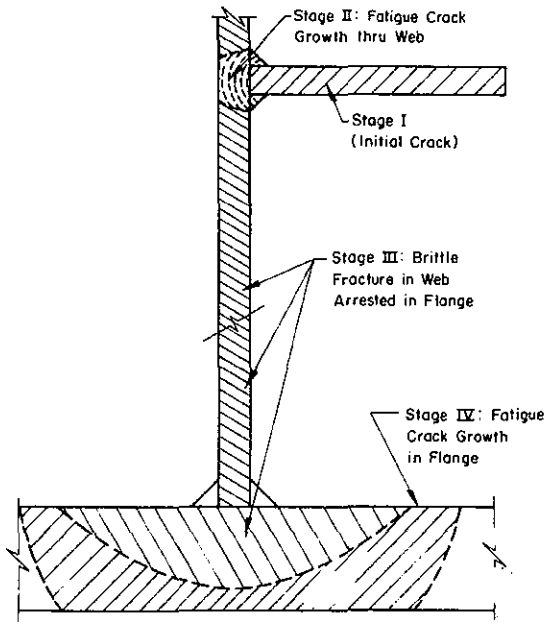

5-31. Schematic of Crack Growth Stages

NOTES:

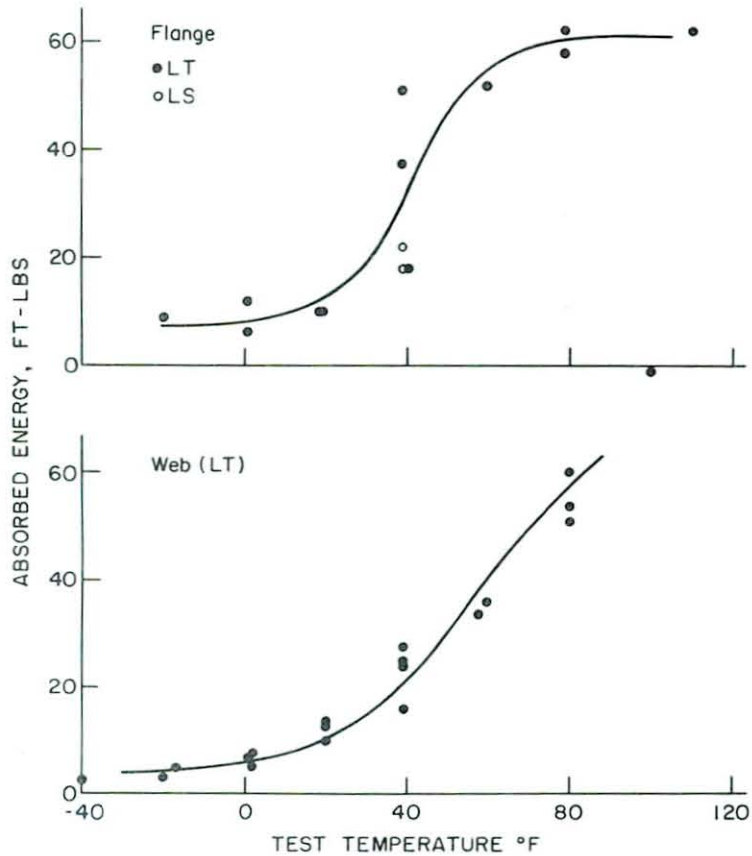

5-32. CVN Results for Web and Flange Adjacent to Crack.

NOTES:

*U.S. GOVERNMENT PRINTING OFFICE:1978 622-563/548 1-3